

THE DESIGN AND DEVELOPMENT OF A
HIGH ENTHALPY, HYPERVELOCITY EXPANSION FACILITY

A Thesis

by

EVAN KELLY MARCOTTE

Submitted to the Office of Graduate and Professional Studies of
Texas A&M University
in partial fulfillment of the requirements for the degree of

MASTER OF SCIENCE

Chair of Committee, Rodney Bowersox
Committee Members, Simon W. North
Edward B. White

Head of Department, Rodney Bowersox

December 2016

Major Subject: Aerospace Engineering

Copyright 2016 Evan Kelly Marcotte

ABSTRACT

Hypersonic vehicle development is an important problem of current national interest. Many of the key challenges, such as heat flux, are beyond our current predictive capability. Hence, experimentation is required to help build knowledge and provide validation for new modeling. Providing ground test facilities that produce realistic flight enthalpies has proven to be a major challenge. Hypervelocity expansion tunnels, which use unsteady shock and expansion processes to introduce enthalpy and kinetic energy into gaseous flows, offer a unique and brief view into true flight-like environments.

Under Navy support, Texas A&M University is developing a new large-scale (1.0 m exit diameter) hypervelocity research tunnel (HXT). The facility will be housed in the Aerospace Engineering Department National Aerothermochemistry Laboratory. The operating conditions for the facility will range between Mach 4 and 14 (1-11 MJ/kg), with a unit Reynolds number range of 10^5 - 10^8 /m. This thesis outlines the overall design of the dual mode expansion/shock tube facility. The topics to be discussed include the requirements, operating principle, gasdynamic processes, mechanical design and manufacturing, instrumentation, status of the facility construction, and the roadmap to operation.

DEDICATION

To my mother,
who has supported me unconditionally through everything I do. I wouldn't be where I
am today without her.

ACKNOWLEDGEMENTS

I would like to sincerely thank my committee chair, Dr. Rodney Bowersox, for advising me since my sophomore year. He took me on as an undergraduate at the National Aerothermochemistry Laboratory and has trusted me with more than I would've ever probably trusted myself with. I appreciate his extraordinary patience with me and the advice he has given to me throughout the years. I know for a fact that, without the opportunities and guidance he has provided, I would not be where I am today.

Additional recognition goes out to my committee members, Drs. White in the Aerospace Engineering Department and North in the Department of Chemistry. Dr. White has provided numerous resources and advice through the Oran W. Nicks Low Speed Wind Tunnel and its welding and machine shops. Dr. White has also been a sitting member of the Hypervelocity Expansion Tunnel team since its beginning and has provided a great deal of feedback throughout the project. Co-directing the lab, Dr. North has introduced me to a number of chemistry concepts and helped an extraordinary amount during my stints with laser diagnostics and the VIPER project. He and Dr. Bowersox have done an amazing job of meshing to disciplines to foster an environment of symbiotic learning that I have only witnessed at the NAL.

The Office of Naval Research gets a special thanks for providing money and other resources for the construction of this project, as well as salaries and other hidden expenses. Being such a large project and, given that this is the first project at the NAL funded by the ONR, it is appreciated that they invested time and opportunity for us to build this facility.

Special recognition goes out to my TAMU NAL colleagues, especially Chi Mai who obtained his PhD in 2014 and was a mentor to me for many years. Next to Dr. Bowersox, Chi has been and will continue to be a role model for me not only in terms of technical know-how but also in character. Without his direction and positive outlook, I would not be doing the things I am today.

Special acknowledgement goes out to the undergraduates of the HXT team: Gabriel Aguilar, Alex Pages, Cristian Sanchez, Silverio Canchola, and Chris Garcia. Gabe and Alex, I honestly don't think I did much for you as a mentor since you each already had the potential to be what you are today without me. Everything you both have done (or will do) with the Sounding Rocketry Team continues to impress me and I hope that your future holds many great things. Cristian, Chris, and Silverio, thank you all so much for your assistance this summer. There was no way HXT would be where it is today without some of the grueling work that you all did during the worst parts of the year. I hope each one of you continue to pursue your dreams whether it be grad school or industry.

Additional thanks goes out to those NAL colleagues both past and present, such as Drs. Michael Semper, Jerrod Hofferth, Alex Craig, and Rodrigo Sanchez Gonzalez. These graduates set the bar for me and the rest of the lab and their presence continues to be felt to this day. Present colleagues, such as Andrew Leidy, Ian Neel, Shanae Smith, Farhan Siddiqi, and others are appreciated for their assisted help, especially during the move of facilities when installing HXT. I know the installation interfered a lot with research but hopefully the worst has passed. Brianne McManamen gets a special mention for her assistance during the dark ages of laser diagnostics. Without her I probably would have

switched out of laser diagnostics long before I did. She kept me motivated and willing to keep tackling equipment that simply did not want to be fixed or aligned. Additionally, her facility, PHACENATE, was my first project and I am very proud to see what it has become as she put the finishing touches on it.

Cecil Rhodes also gets a special acknowledgement for his continued work at the NAL and with HXT. I have learned a lot from the advice that he gives and there is no doubt that this project wouldn't be possible without his help. He has continued to mentor me through the past couple years, and even though we may butt heads sometimes, I respect a lot of what he does and who he is.

Another major contributor to the lab is William Seward of the Chemistry Department's Machine Shop. This project would not have been possible without his selfless help in the evenings and on the weekends with tedious welding. His expertise and workmanship can be seen in every aspect of this project. He also has taught me everything I know about working on lathes, mills, and every other manner of machine at our disposal. I will surely miss the extreme patience he has with students as I transition into industry and will bring with me the appreciation and respect for machinists everywhere as I do.

In addition to Dr. White's resources he has provided from the Low Speed Wind Tunnel, support was provided by Zahir Udovicic in terms of machining. The test section and other small items were fabricated by the CNC machines that he runs and he has put in a lot of work with this project.

A final mention goes out to Colleen Leatherman, Andrea Loggins, and Rebecca Marianno for keeping the books in order. Being such a large project, a lot of purchase

orders had to go through the business office and all three of them made sure we didn't exceed the money available for the project.

NOMENCLATURE

ACE	Actively Controlled Expansion Tunnel
AIAA	American Institute of Aeronautics and Astronautics
CAD	Computer-Aided Design
CFD	Computational Fluid Dynamics
CIHI	Controls and Instrumentation Hardware Interface
CUBRC	Calspan-University at Buffalo Research Center
DAQ	Data Acquisition
FEA	Finite Element Analysis
FIRST	Four-Inch Reflecting Shock Tunnel
HSDaq	High Speed Data Acquisition
HXT	Hypervelocity Expansion Tunnel
MDS	Mylar Diaphragm System
NAL	National Aerothermochemistry Laboratory
NRST	Non-reflecting Shock Tunnel
ONR	Office of Naval Research
PHACENATE	Pulsed Hypersonic Adjustable Expansion Nozzle Facility
RST	Reflecting Shock Tunnel
ST	Shock Tunnel Mode
TAMU	Texas A&M University
VENOM	Vibrationally Excited Nitric Oxide Monitoring

TABLE OF CONTENTS

	Page
ABSTRACT	ii
DEDICATION	iii
ACKNOWLEDGEMENTS	iv
NOMENCLATURE	viii
TABLE OF CONTENTS	ix
LIST OF FIGURES	xii
LIST OF TABLES	xx
1. INTRODUCTION	1
1.1 Motivation	1
1.2 Hypersonic Impulse Facilities Overview	3
1.2.1 Generalized Overview of Shock Tube/Tunnel Design	3
1.2.2 Generalized Overview of Expansion Tunnel Design	6
1.2.3 Overview of the Hypervelocity Expansion Tunnel at Texas A&M University	10
1.3 Texas A&M University National Aerothermochemistry Laboratory	13
1.4 Manuscript Layout	16
1.5 Project Management	16
2. DRIVER, DRIVEN, ACCELERATOR SECTIONS	19
2.1 Requirements	19
2.2 Mechanical Design	21
2.2.1 General Sizing	21
2.2.2 Driver and Driven Sections	24
2.2.3 Accelerator Section	29
2.3 Shock Tunnel Mode	30
2.4 Manufacturing	34
2.4.1 Welding	34
2.4.2 Estimated Cost	35
2.5 Nozzle Option	35
3. DIAPHRAGM SYSTEM DESIGN	40

3.1	Requirements.....	40
3.2	Diaphragm Holder.....	42
3.3	Breech Diaphragm System.....	45
3.3.1	Design.....	45
3.3.2	Loading Analysis.....	58
3.3.3	Estimated Cost of Manufacture.....	65
3.4	Mylar Diaphragm System.....	66
3.5	Backup Configuration.....	71
4.	BACK ASSEMBLY DESIGN.....	74
4.1	Requirements.....	74
4.2	Design.....	76
4.2.1	Test Section.....	76
4.2.2	Tailpipe Design.....	83
4.2.3	Air Receiver Option.....	85
4.3	Load Calculations.....	88
4.3.1	Pressure Ratings.....	88
4.3.2	Forces Due to Pressures.....	93
4.3.3	Seal Design.....	95
4.4	Manufacturing.....	96
5.	SUPPORTING INFRASTRUCTURE.....	101
5.1	Stands.....	101
5.1.1	Requirements.....	101
5.1.2	Primary Stand Design.....	103
5.1.3	Secondary Stand Design.....	111
5.1.4	Roller Stand Design.....	116
5.1.5	Manufacturing.....	120
5.2	Hydraulic System.....	126
5.2.1	Requirements.....	126
5.2.2	Hydraulic System Design.....	127
5.3	Controls, Instrumentation, and Data Acquisition.....	132
5.3.1	Requirements.....	132
5.3.2	Flow Control Diagram.....	134
5.3.3	Instrumentation.....	139
5.3.4	Control and Instrumentation Hardware Interface.....	142
5.3.5	Virtual Interface.....	149
6.	CONCLUSIONS.....	156
6.1	Objectives and Requirements Summary.....	156
6.2	Construction Summary.....	159

7. FUTURE WORK AND RECOMMENDATIONS	164
7.1 Operational Roadmap.....	164
7.2 Recommendations	167
REFERENCES.....	170
APPENDIX A	175
APPENDIX B	185
APPENDIX C	230

LIST OF FIGURES

	Page
Figure 1. Indicated physical phenomena of focus for hypersonic research on a NASA X-43.	1
Figure 2. Graphical representation of generalized trends for temperature, pressure, and Mach number in a de Laval nozzle.	2
Figure 3. Time-displacement graph for a typical refelected shock tube.	4
Figure 4. Time-displacement graph of a “tailored” reflected shock tunnel.	5
Figure 5. A generalized expansion tunnel time-displacement wave diagram.	7
Figure 6. Shock placement when experimentally performed in LENS I (shock tunnel) and LENS X (expansion tunnel).....	8
Figure 7. Operating envelope for HXT as it is designed, including parameters for shock tunnel mode and the nozzle addition.	11
Figure 8. HXT layout with labeled sections. Does not show most electronics or the shock tunnel configuration.	12
Figure 9. Floor layout of the NAL with the five facilities currently performing research and the planned HXT facility.	13
Figure 10. Newly constructed gas cylinder building with additional room to house the pumps for PHACENATE.	14
Figure 11. Side-view of the Hypervelocity Expansion Tunnel with proper division of the facility representing manuscript layout.....	15
Figure 12. Representative illustration of the boundary layer as predicted in a shock or expansion tunnel.	21
Figure 13. Run-time graph using different fractions of length for the R/N/A sections and various driver/accelerator gases to determine optimum segment lengths. The dashed line is what is deemed optimal and the solid line is what is designed.	23
Figure 14. Computer aided design model for the driver and driven as they will interface with each other, the breech diaphragm system, and the support stands.	27

Figure 15. Dimensional drawing for the driver and driven section with lengths of the pipe sections and effective lengths of each section located within the breech assembly.	28
Figure 16. Computer aided design model for accelerator pipe as it appears with a 900# flange on the driven side of the segment, structural stands, and roller supports.....	30
Figure 17. The Hypervelocity Expansion Tunnel as it would appear in shock tunnel mode with the breech system reinstalled between the ST-driven and accelerator pipes.	31
Figure 18. Dimensional drawing for driven as submitted to Circle H Manufacturing. ...	32
Figure 19. ASME approved and National Board of Boilers and Pressure Vessels certified drawing as approved for manufacture.	33
Figure 20. Method of characteristics diagram used to predict the contour and length of the nozzle.	36
Figure 21. First segment of the nozzle, cut in half and displayed as it would sit in the CNC mill for machining of the contour.....	37
Figure 22. Nozzle assembly using a decagon shape and ribs that double as alignment jigs.....	38
Figure 23. Diaphragm holder exploded view with (left) male holding ring, (middle) etched diaphragm, and (right) female holding ring.	42
Figure 24. Diaphragm holder cutout with labels and locations of o-ring grooves, dowel pin alignment holes, and threaded holes.	43
Figure 25. Diaphragm etching highlighted with a blue line and its orientation relative to the pin arm holder.....	44
Figure 26. Overview of the breech diaphragm system with callouts for each major component/subassembly.	46
Figure 27. Picture of the NPL 6-inch shock tunnel main diaphragm station.	47
Figure 28. (top) Breech lock teeth dimensions for internal and external grooves and (bottom) computer aided rendering of the interlocking teeth.	48
Figure 29. Breech seat which includes the machined 20" 900# heavy barrel RTJ flange with a small section of pipe welded to it.	50

Figure 30. Breech head placed against the diaphragm holder and inserted into the breach seat.	51
Figure 31. Breech seat which includes the machined 20” 900# heavy barrel RTJ flange with a small section of pipe welded to it.	52
Figure 32. Breech nut with hydraulic mounting holes and grooves to insert teeth made out of steels with higher yield and ultimate tensile strengths.	53
Figure 33. Qualitative force diagram for the thrust plate and the center of gravity for the locking nut.	55
Figure 34. Assembly with a pair of hydraulic cylinders used to move the breech forward/back and a pair to lock the nut to seal the diaphragms.	56
Figure 35. Hydraulic pin holder placed in the breech head with four mounting arms and a blank body that can receive multiple pin configurations.	57
Figure 36. Finite element analysis of the breech head with maximum 405,000lbs of force directed on the collar.	59
Figure 37. Finite element analysis of the breech seat heavy barrel flange with forces directed on the interlocking teeth.	60
Figure 38. Von Mises stresses with iso-clippings at yields of (top) 18ksi corresponding to a factor of safety of 2 and (bottom) 12ksi corresponding to a factor of safety of 3.	61
Figure 39. Original locking nut concept with teeth machined into a single component. Iso-clipping of von Mises stresses at 12ksi (FOS 3) if made out of A36 steel.	62
Figure 40. Von Mises stress iso-clipping for values above (top) 40ksi corresponding to a factor of safety of 2, and (bottom) 26.7ksi corresponding to a factor of safety of 3.	64
Figure 41. Mylar diaphragm mechanism at the interface between the driven and accelerator sections of HXT.	66
Figure 42. Mylar diaphragm system face using threaded holes up top and clearance holes around the mid to bottom holes.	67
Figure 43. Mentionable design points for the mylar diaphragm system assembly with major components in bold.	68
Figure 44. Pneumatic panel recesses for air supply and actuator mounting.	70

Figure 45. Backup configuration using the diaphragm holder and a 20" schedule 160 pipe section.	71
Figure 46. Back assembly overview consisting of the test section and tailpipe.	74
Figure 47. Concept illustrating the test section's original design as a true octagon with toggle clamps for securing doors and the ability to separate from the front of the facility.	76
Figure 48. CAD renderings of the test section with skeleton (red), access panels (blue), and base stand (black).	77
Figure 49. The test section as it would appear at the NAL without a nozzle and with the tailpipe protruding through a wall to the outside.	78
Figure 50. Key dimensions of the test section with flat-to-flat lengths and hole diameters.	80
Figure 51. Test section door with mounting holes and flange. Inside dimensions are associated with the access hole located on the skeleton.	81
Figure 52. Cross-section detailing the mounting orientation of the roof and floor access panels with expected pressure distribution.	82
Figure 53. Full overview of the tailpipe with the 42" flange of the bottom left and the reducer and 30" flange on the top right.	83
Figure 54. Overview of the air receiver attached to the tailpipe in place of the blind flange.	85
Figure 55. Iso-clipping of von Mises stresses in the originally designed test section using (a) 18ksi corresponding to a factor of safety of 2, and (b) 9ksi corresponding to a factor of safety of 4.	89
Figure 56. Cross-section of the test section with a rib welded to the inside of the skeleton to increase support.	90
Figure 57. Iso-clipping of von Mises stresses with the addition of a rib located halfway down the length of the test section for (a) 18ksi corresponding to a factor of safety of 2, and (b) 9ksi corresponding to a factor of safety of 4.	91
Figure 58. Pressure relief plate set for approximately 1psi differential to assist with avoiding over-pressurization of the back assembly.	92
Figure 59. Test section skeleton with exploded view on the right illustrating the ten different plates machined and welded together during fabrication.	96

Figure 60. Test section pieced together and clamped just before welding.....	97
Figure 61. Tailpipe immediately before the 42” 150# slip-on flange was welded to the end of the pipe.	98
Figure 62. Tailpipe as it was installed through the wall at the NAL.....	99
Figure 63. Stands as they are expected to be located throughout the facility.	103
Figure 64. Primary stand with H-shaped central body, hole interfaces, and brace supports on both sides.....	104
Figure 65. Side view of how the threaded studs and nuts bolt into the stand. All short studs that do not fasten to the stand are omitted.	105
Figure 66. Magnified view emphasizing the difference when canting the 6-inch square tube bracing at 15 degrees.	106
Figure 67. Representation of how the stands may be shimmed to achieve proper height.	107
Figure 68. Mesh of primary stand assembly with gravitational force, force distributed over the 4 points of contact, and fixtures around concrete anchor holes.....	107
Figure 69. Von Mises stress distribution for (a) 45-degree brace positioned perpendicular to the 2-inch thick main plate and (b) 45-degree brace canted 15 degrees inward.	108
Figure 70. Von Mises stress distribution of the primary stand for (a) a total load of 81,200 lbs and (b) an iso-clipping isolating any points of the assembly that have stresses above the yield point.	109
Figure 71. Von Mises stress distribution of the primary stand for (a) a total load of 324,800 lbs to simulate a factor of safety of 4 and (b) an iso-clipping isolating any points of the assembly that have stresses above the yield point.	110
Figure 72. Secondary stand attaching to half flange welded at the second accelerator segment. The driver, where the loads originate, is located in the direction of the upper left corner.	112
Figure 73. Overhead view of the secondary stands with emphasis on the movement of the back I-beams to connect with the H-beam instead of the 2-inch thick plate.....	113

Figure 74. Mesh of the secondary stand assembly with gravitational pull, fixtures along the base plate, and locations of the design/factor of safety load.....	113
Figure 75. Von Mises stress distribution of the secondary stand for (a) a total load of 81,200 lbs and (b) an iso-clipping isolating any points of the assembly that have stresses above the yield point.....	114
Figure 76. Von Mises stress distribution of the secondary stand for (a) a total load of 324,800 lbs to simulate a factor of safety of 4 and (b) an iso-clipping isolating any points of the assembly that have stresses above the yield point.	115
Figure 77. Roller stand as it is welded to its own plate, independent of the primary or secondary stands.	117
Figure 78. Overall dimensional drawing for a roller stand. Specific individual component drawings can be found in Appendix B.....	119
Figure 79. Cross sectional cut of the roller detailing the position of the ball bearings and threads in the axle.	120
Figure 80. Example picture of the welds performed on the 2-inch thick plate to the H-shaped central body.	121
Figure 81. H-shaped central bodies welded together being prepared for the 2-inch thick main plate.....	122
Figure 82. Close up of the main gusset divided into six manufacturable pieces and welded to the stand.	122
Figure 83. Close up of the small gussets that alleviate stress buildup along the corners of the H beam and 2-inch plate.....	123
Figure 84. Driver-side primary stand fully tacked into place.	124
Figure 85. Series of 3/4” holes torched into the 1/2” thick base plate of a secondary stand.....	124
Figure 86. Schematic of the hydraulic system with power unit, pressure relief, 4-way/3-position solenoids, and cylinders.....	128
Figure 87. Haldex hydraulic power unit 2hp, 115VAC, model number 1400028.....	130
Figure 88. Location of the hydraulic cylinders for squeezing the diaphragm seals and locking the breech nut in place.	131

Figure 89. Flow diagram for HXT with pressure (blue lines), vacuum (purple lines), ball valve placement, digital regulators, and pressure relief valves.	135
Figure 90. Ball valve diagram with flows and power requirements.	136
Figure 91. Digital regulator pinout for power, command voltage, and monitor voltage.....	137
Figure 92. cDAQ unit specs and callouts [43].	142
Figure 93. (Top) Front panel and (bottom) back panel of the control and instrumentation hardware interface electronics housing.	143
Figure 94. Schematic representing the current rating amplification when using the NI solid state relays and standard relays in series.....	145
Figure 95. Circuit layout for the warning system lights and logic switches required to activate at correct time interval.....	146
Figure 96. Circuit diagram with contact switches in parallel with an override switch controlled through labview to provide power to the ball valves.	147
Figure 97. Hydraulic arming section of the CIHI electronics unit with indicators and instrumentation input.	148
Figure 98. Image detailing the progress of the CIHI electronics unit with cDAQ on the right, power supplies on the left and solid state relays on the bottom right.....	149
Figure 99. Data flow diagram of information passed between the controls and HSDaq VI programs.	151
Figure 100. Controls VI for monitoring conditions in HXT and controlling flow lines.....	152
Figure 101. High speed data acquisition virtual instrument screen.	153
Figure 102. 20” Schedule 80 pipe cut into appropriate lengths sitting at the shop waiting to be welded.....	159
Figure 103. 20” Schedule 160 pipe as it is being unloaded at Custom Fabricators to be cut.	160
Figure 104. Back assembly with test section and tailpipe running through the wall of the NAL with blind adapter plate for eventual hydrostatic pressure testing. .	161

Figure 105. Four of the five stands tacked together without the 6-inch square tube
bracings..... 162

Figure 106. Extensive roadmap laying out what actions need to be taken to reach a
point where a diaphragm can be destroyed..... 165

LIST OF TABLES

	Page
Table 1. Comparative list of parameters in the ONR proposal vs the finalized parameters [2].	10
Table 2. Select primary requirements and their respective derived requirements for the driver, driven, and accelerator sections.	19
Table 3. Schedule, pipe inner diameter, estimated core flow diameter, and price per foot for various size pipe made of 304L welded stainless steel.	22
Table 4. Maximum allowable working pressures of 20” carbon steel pipe in the temperature range of -20 to 650F [17]......	25
Table 5. Maximum allowable non-shock pressure with a working temperature between -20 and 100F [18]......	26
Table 6. Estimated cost for the pipe, flanges, and labor to manufacture the R/N/A sections.	35
Table 7. Select primary requirements and their respective derived requirements for the diaphragm changing systems.	40
Table 8. Breach overview callout list.....	46
Table 9. Estimated cost for the raw materials for construction of the breach.....	65
Table 10. Select primary requirements and their respective derived requirements for the back assembly.	75
Table 11. Volume for each section of the facility. [L]:length, [d]:diameter, [CSA]:cross-sectional area of the prism.	86
Table 12. Mass, in kg, present in each section assuming a driver pressure of 2000psia and driven pressure of 110psia for XT mode, and a driver pressure of 500psia and driven of 50psia for ST mode. The end-of-operation pressure(EoOP) is calculated using the entire volume of the facility.....	87
Table 13. Component list for the tailpipe along with pressure ratings and the source used to list the pressure rating.	93
Table 14. Dimensions and resulting forces on each access panel with minimum required bolt number using ¼”-28 Grade 8 bolts with a proof load of 4,350 lbf.	94
Table 15. Cost of test section pieces with labor. [31]	100

Table 16. Key and derived requirements as pertaining to the structural support system.	101
Table 17. Line item costs for the primary, secondary, and roller stands with labor.	125
Table 18. Key and derived requirements with regard to the design of the hydraulic system.	126
Table 19. Key and derived requirements for the hardware and software to control, monitor, and take data in HXT.	133
Table 20. Pressure ratings of pipe and tube lines with the pressure relief settings.	139
Table 21. Pressure transducer ranges and accuracies.	140
Table 22. Data acquisition modules used with the controls computer.	141

1. INTRODUCTION

1.1 Motivation

Modern aerospace systems include some of the most complex engineering marvels ever conceived, from spacecraft capable of escaping the domain of the solar system to vehicles adept to travelling several times the speed of sound. As the design challenges evolve in the 21st century, new and improved methods of testing are being developed to more accurately assist in both engineering applications and fundamental research.

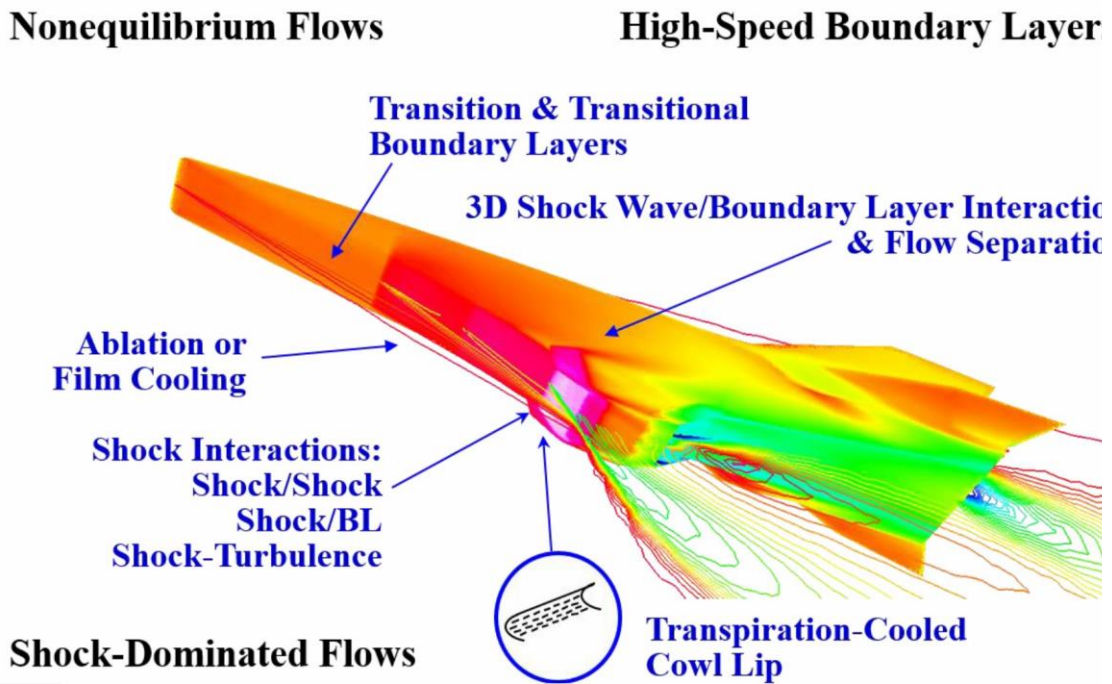


Figure 1. Indicated physical phenomena of focus for hypersonic research on a NASA X-43.

(credit: adapted from K. Lau [Boeing] and J.D. Schmisser [AFOSR] [1])

Many important areas of focus in fundamental physics for aerospace engineering are illustrated in Figure 1, one of which is in the area of turbulence prediction at hypersonic

speeds (approximately 5 times the speed of sound or greater), specifically in regard to nonequilibrium effects on turbulence behavior. These effects can be categorized into three primary definitions: mechanical, thermal, and chemical non-equilibrium. “Mechanical non-equilibrium consists of pressure gradient effects; shock waves are an example of a type of almost discontinuous mechanical nonequilibrium” [1]. Chemical and thermal nonequilibrium effects are more difficult to understand due to the inherent nature in reproducing the conditions in which accurate results can be interpreted.

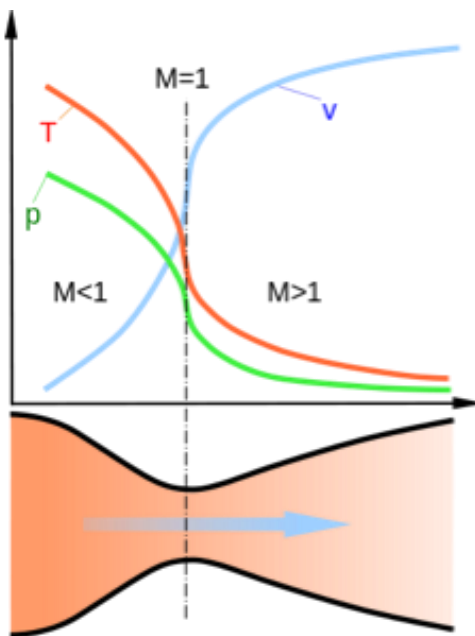


Figure 2. Graphical representation of generalized trends for temperature, pressure, and Mach number in a de Laval nozzle.

(credit:https://en.wikipedia.org/wiki/De_Laval_nozzle#/media/File:Nozzle_de_Laval_diagram.svg [public domain])

Wind tunnels have provided an advantageous way for engineers to further understand physical phenomena since before the invention of powered flight. Supersonic and hypersonic tunnels are no exception to this, with an added benefit of their use due to

the difficulty in predicting vital heat flux measurements of high speed vehicles. However, most supersonic wind tunnels operate as cold-flow, blow-down testing facilities which work by expanding preheated air through a de Laval nozzle. Figure 2 shows a de Laval nozzle with pressure, temperature, and Mach number curves depicted at the bottom. As interpreted from the figure, the pressures and temperatures at the exit of the nozzle are much lower than those experienced during flight, with most flows needing to be preheated to prevent liquefaction in the test section. With some exceptions, these conventional tunnels cannot provide the high enthalpies required (upwards of 5 MJ/kg) to properly study the physical nature of thermal nonequilibrium.

1.2 Hypersonic Impulse Facilities Overview

One solution to achieve the high enthalpies associated with hypersonic flight trajectories and better model nonequilibrium effects on turbulence at these conditions is by use of impulse facilities. There are two types of impulse facilities which provide “effective means to produce high stagnation enthalpies representative of hypersonic flight: shock tunnels and expansion tunnels” [2]. Shock tunnels and expansion tunnels are similar, with the difference being an additional section of pipe which allows the test gas to undergo an unsteady expansion and accelerate to higher speeds. A detailed description of each type is presented in the sections below.

1.2.1 Generalized Overview of Shock Tube/Tunnel Design

Both shock tunnels and expansion tunnels operate differently than that of a conventional wind tunnel in that they do not require the use of a converging-diverging nozzle to achieve supersonic flows. Both facility types can be operated in a tube mode

where the end is capped and the flow does not open into a testing cavity, though usually shock tubes are more common than expansion tubes.

Shock tubes are relatively simple facilities utilizing two sections of pipe, called the driver and driven. During operation, the driver and driven are separated by a breakable diaphragm, usually fabricated out of metal for higher pressure differentials (>300 psi), that bursts at a desired pressure ratio. This ratio, along with other parameters, determines the strength of the shockwave that propagates through the driven tube that compresses and heats the test gas, as illustrated in Figure 3. Constant reflection of this shock wave allows the test gas to be repeatedly heated to enthalpies difficult to obtain in conventional facilities [3].

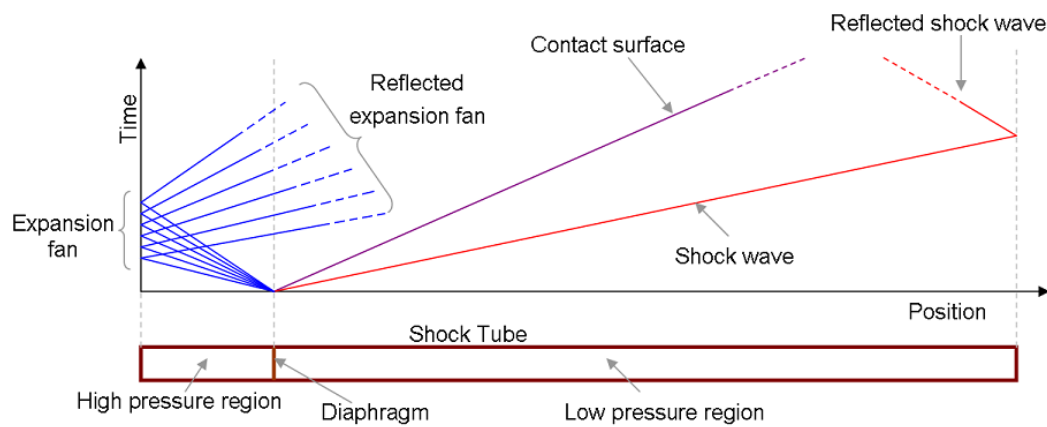


Figure 3. Time-displacement graph for a typical reflected shock tube.
 (credit: https://commons.wikimedia.org/wiki/File:Shock_tube.png [public domain])

Shock tunnels exist in three main classifications as detailed in “A Review of Shock Tubes and Shock Tunnels” by W. A. Martin: nonreflected, reflected, and tailored-interface type shock tunnels [3]. Nonreflected shock tunnels operate very similar to an expansion tunnel in that there is a second diaphragm that divides the driven from a third, vacuumed

down section. This section usually contains a diverging section of pipe used to expand the test gas after the second diaphragm has burst. This provides an increase in test Mach number while keeping the same shock Mach number (pressure ratio between driver and driven).

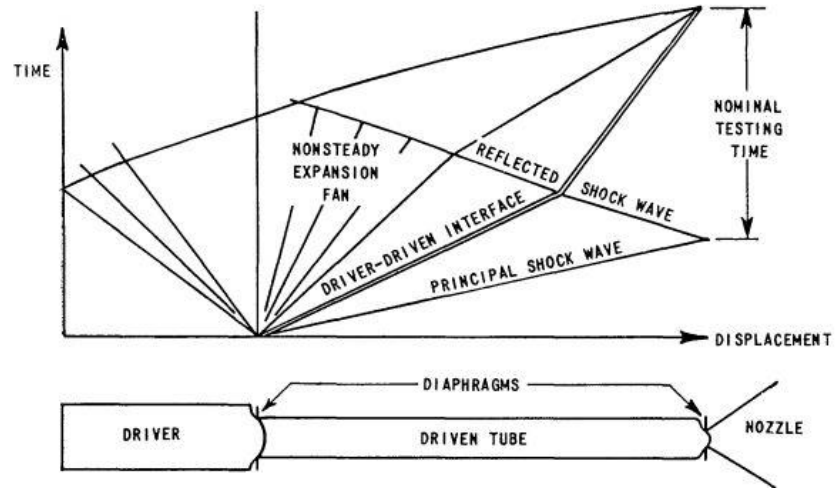


Figure 4. Time-displacement graph of a “tailored” reflected shock tunnel.
(credit: Charles E. Wittliff from Cornell Aeronautical Laboratory [6])

Reflected mode shock tunnels, such as the CUBRC LENS I and II tunnels [4] and the Caltech T5 [5], use a normal converging-diverging nozzle placed at the end of the shock tube. The tunnels hereby referenced can provide flow up to about 15MJ/kg for test times of 2-10ms [2]. As stated by W. A. Martin, “at the hypersonic Mach numbers of interest, the area ratio is so large and the throat so small that the nozzle will act as a solid plate and the initial shock wave will be completely reflected” [3]. This means that during a single operation of a reflected shock tunnel, multiple conditions can be expanded through the de Laval nozzle, reducing attenuation of the shock and increasing the test time.

In a “tailored-interface” shock tunnel, as described by Charles E. Wittliff at Cornell Aeronautical Laboratory, Inc., “the incident shock wave is reflected at the downstream end of the shock tube, and conditions of the driver and driven are matched so that no additional waves are created by the interaction of the reflected shock and the interface” [6]. Figure 4 portrays the shock and expansion wave propagation over time through a tailored shock tunnel. Advantages of this type of facility are that the test times are on the scale of 8 times longer than those facilities with untailored gases [3] [6].

A major disadvantage to shock tunnels is caused by the stagnation of the flow just upstream of the converging-diverging nozzle as described by W. A. Martin [3]. Since the throat acts as a solid plate the flows stagnates at this location where the extreme temperatures excite the molecules to a point where dissociation can occur. Once these molecules pass through the expanding section of the nozzle, some recombination occurs, but the chemical composition “freezes” out, resulting in substantial portions of unrealistic chemical and thermal states in the flow. This effect can be avoided in an expansion tunnel, since no converging section is present to stagnate the flow.

1.2.2 Generalized Overview of Expansion Tunnel Design

Expansion tunnels use a series of chambers similar to that of a shock tunnel, with sectioned off lengths of pipe by use of a diaphragm that are purposely burst at the time of operation to heat and accelerate the test gas located in the driven. The prime difference is the addition of a long, low pressure section, known as the expansion tube. Figure 5 illustrates a generalized layout of a typical expansion tunnel [7].

Three pipe lengths are identified in Figure 5: the driver and driven, similar to that of the shock tunnel, and the expansion. The expansion, sometimes referred to as the accelerator section, is typically the longest and is held under the lowest vacuum obtainable to accelerate the flow to its desired speed.

Once the shock reaches the interface between the driven and expansion sections, usually a much weaker plastic diaphragm, the diaphragm explodes and the test gas is exposed to the vacuum of the expansion pipe which accelerates the test gas. The length of the accelerator allows the driven gas to achieve a desired testing velocity.

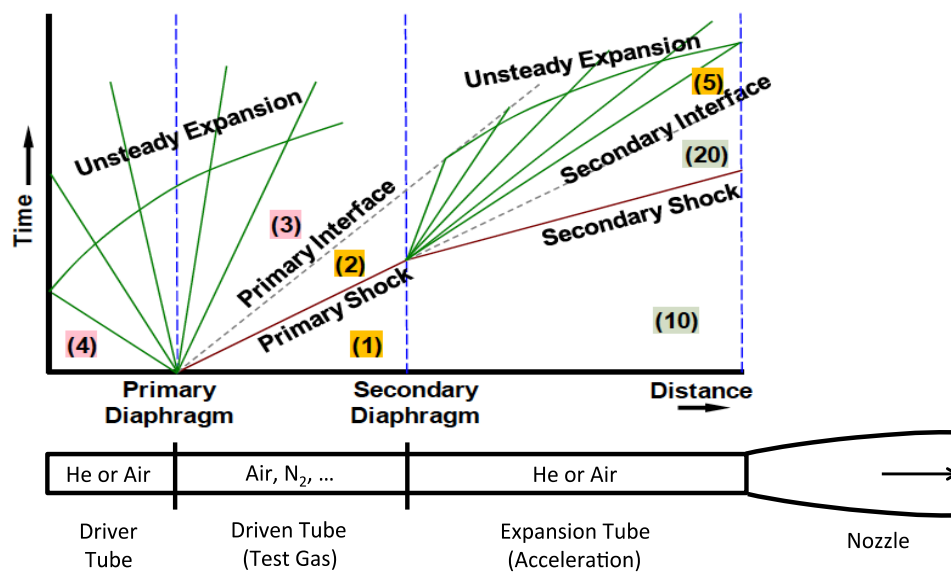


Figure 5. A generalized expansion tunnel time-displacement wave diagram.

(credit: adapted from Dufrene et al 2010)

Figure 5 shows a generalized x-t diagram for an expansion tunnel with the depicted locations and propagation paths taken by expansion and shock waves through each of the driver, driven, and accelerator sections (R/N/A). Additionally, the interfaces between each

gas are represented by grey dashed lines which indicate the boundaries between the driver/driven gases and driven/accelerator gases. The slopes of these lines indicate the inverse velocities that each is moving in its relative direction to the diaphragms.

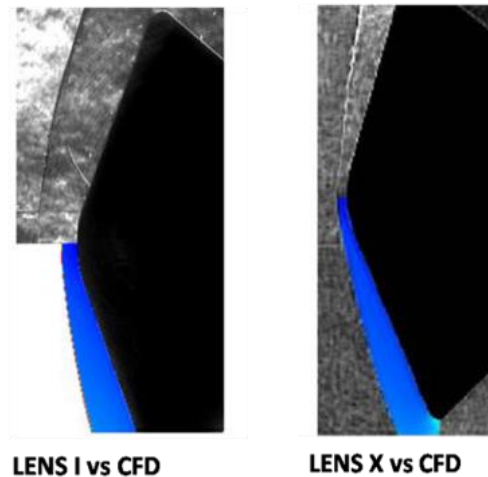


Figure 6. Shock placement when experimentally performed in LENS I (shock tunnel) and LENS X (expansion tunnel)
(credit: adopted from Holden, M. 2010 [8])

Because the flow undergoes an unsteady expansion and the driver's mechanical energy is used to heat and propel the test gas, expansion tunnels can offer a higher operating stagnation enthalpy with true-to-flight Reynolds numbers. This means that a facility such as this could be used to test subscale vehicles at high speed flight conditions with accurate heat flux measurements which are vital to hypersonic vehicle development. Furthermore, because the flow conditions accurately represent flight, shock positions match those that should be expected, such as the experiments performed at CUBRC in the LENS I and LENS X facilities, depicted in Figure 6 [8].

The disadvantage of expansion tunnels comes at their immense cost, short run times, and long turnaround between tests. Most expansion tunnels around the world are extremely large, with some capable of full vehicle testing and measuring several hundred feet in length. Larger diameter pipes are usually chosen to account for large boundary layer growth, yet even smaller facilities still require accelerator sections that occupy a high percentage of the overall length for the facility. Depending on the operating envelope, the large nature and high pressures, especially those experienced in the driver, dictate extremely thick walls which increase the base cost of an expansion tunnel.

Additionally, because an expansion tunnel acts like a huge cannon, the test gas moves through the testing region with flight-like speeds measuring in kilometers per second, limiting run times to fractions of a second. An inherent consequence of this is that the facilities also take a significant time to reload, which not only includes vacuuming and re-pressurizing of each section, but also a replacement of both diaphragms. This downtime can be minimized by proper design of a replacing mechanism, such as the ones discussed in Section 3, but, unfortunately, due to the high pressures in the driver, a cost-effective solution is still costly to engineer.

Many expansion tunnels/tubes exist throughout the world, including large facilities such as the 26-inch HYPULSE facility at GASL [9], and the 96-inch LENS X at CUBRC [8]. Smaller facilities are much more frequent due to their reduced cost and space for academic research, such as those located at the University of Queensland [10] with both an 85mm exit and 180mm exit diameter for the X2 and X3 facilities, respectively. Additional small-scale facilities are located at the University of Illinois at Urbana-

Champagne, which contains a 6-inch Mach 7 capable expansion facility [7], and Stanford which has a 3.5-inch diameter Mach 8-12 facility [11].

1.2.3 Overview of the Hypervelocity Expansion Tunnel at Texas A&M University

A proposal to the Office of Naval Research (ONR) was submitted in 2015 to request funding for the initial design and construction of an expansion tunnel at Texas A&M University, designated as the Hypervelocity Expansion Tunnel (HXT). The proposal outlined the intended operation and motivations behind building such a facility, many of which are shared in Section 1.1.

Table 1. Comparative list of parameters in the ONR proposal vs the finalized parameters [2].

	Proposed	Designed
Pipe Diameter	12"	20"
Nozzle Exit Diameter	24"	36"
Driver Length	3ft/10ft	5ft
Driven Length	7ft/20ft	15ft
Accelerator Length	60ft/40ft	50ft
Enthalpy Range	1.3-14 MJ/kg	1-10 MJ/kg
Mach Range	9-15	4-14
Reynolds Range	10^5 - 10^8 /m	10^5 - 10^8 /m

The objective parameters outlined in the ONR proposal are listed in Table 1 with the amended conditions of the finalized design presented for comparison. As stated, the initial design of the facility was to achieve a Mach range between 9-15 ($U=1.3$ - 6.0 km/s), an enthalpy generation between 1.3-14MJ/kg, and a unit Reynolds number between 10^5 /m and 10^8 /m (Bowersox, 2015) [2]. These envelopes were expanded upon during the early conceptual phases of the design to include the operating capabilities of both a shock tunnel and expansion tunnel. Figure 7 contains a graph for the operating ranges for both these

modes in terms of unit Reynolds number, freestream velocity, and stagnation enthalpy per kilogram.

One of the primary considerations when outlining the operating envelope for the facility was to design an aerodynamically “clean” freestream with correct gas and internal state distribution. For this to be true, it was assumed that an upper static temperature of 5,000F would suffice to keep diatomic oxygen from dissociating. Thus, this limit represents the upper limit for enthalpy generation of 14 MJ/kg, since anything above this would create thermal and chemical nonequilibrium in the flow upstream of the test model.

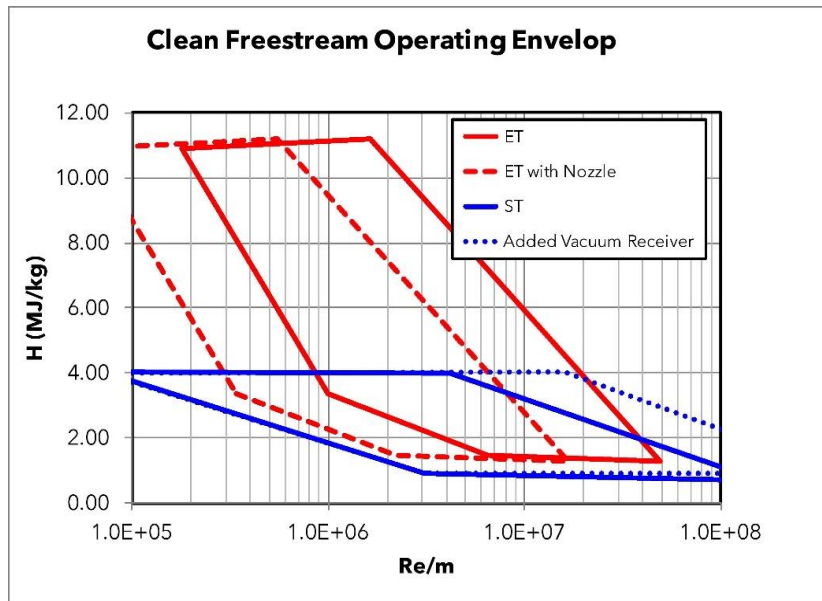


Figure 7. Operating envelope for HXT as it is designed, including parameters for shock tunnel mode and the nozzle addition.

Like all expansion tunnels, HXT consists of a driver, driven, and accelerator pipe section which opens into a large test section. A tailpipe extends past this, primarily to



Figure 8. HXT layout with labeled sections. Does not show most electronics or the shock tunnel configuration.

avoid shock reflections back into the test flow, and ends with a blind flange. Figure 8 illustrates a computer-aided design (CAD) model of the entire facility with stands, hydraulics, and diaphragm changing mechanisms installed.

1.3 Texas A&M University National Aerothermochemistry Laboratory

The Hypervelocity Expansion Tunnel will be located at the Texas A&M University Wind Tunnel Complex near Easterwood Airport and incorporated into the National Aerothermochemistry Laboratory (NAL). The NAL focuses on providing a venue for faculty, students, research associates, and visiting scientists to improve knowledge and control of non-equilibrium gaseous flows and their surface interactions.

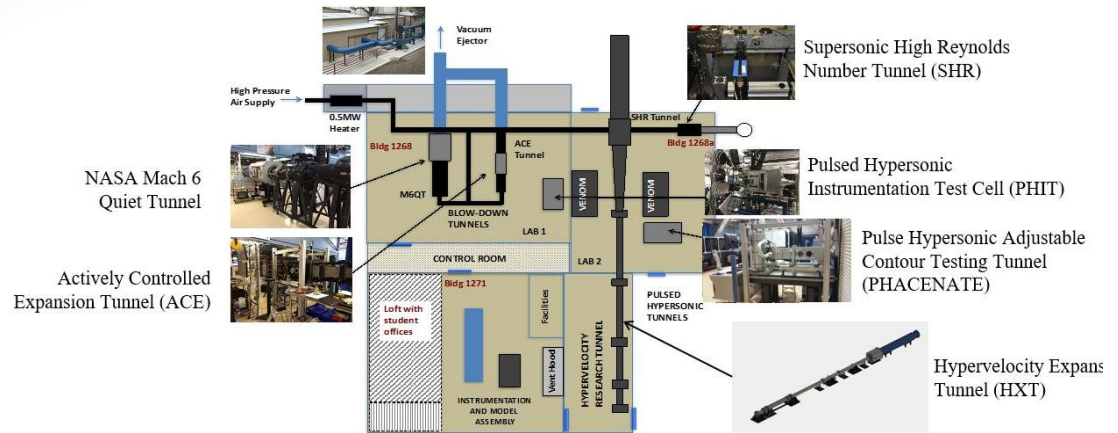


Figure 9. Floor layout of the NAL with the five facilities currently performing research and the planned HXT facility.

Housing a variety of research facilities dedicated to its overarching mission, the NAL accommodates six primary testing platforms including the Actively Controlled Expansion (ACE) tunnel, Mach 6 Quiet Tunnel (M6QT), Supersonic High Reynolds Number (SHR) tunnel, Pulsed Hypersonic Instrumentation Test (PHIT) cell, Pulsed

Hypersonic Adjustable Contour Expansion (PHACENATE) tunnel, and now the Hypervelocity Expansion Tunnel (HXT). Figure 9 depicts the layout of these six facilities at the NAL.



Figure 10. Newly constructed gas cylinder building with additional room to house the pumps for PHACENATE.

Originally, the SHR and PHACENATE facilities occupied more space than that shown in Figure 9 while the PHIT cell was positioned down the centerline of HXT between the two laser tables. These three facilities were moved at the onset of project before any construction could commence. Additionally, the vacuum pumps which control the backpressures of the two pulsed tunnels were located in the annex where the expansion pipe lengths of HXT are planned to be installed. These pumps have been relocated to a newly constructed gas cylinder bay and vacuum pump building not shown in the figure. This new location serves to shorten PHACENATE's vacuum line, increase maintenance space, and allow the movement of other facilities for the construction of HXT. Figure 10 shows the new gas cylinder building that was assembled in the back welding shop of the

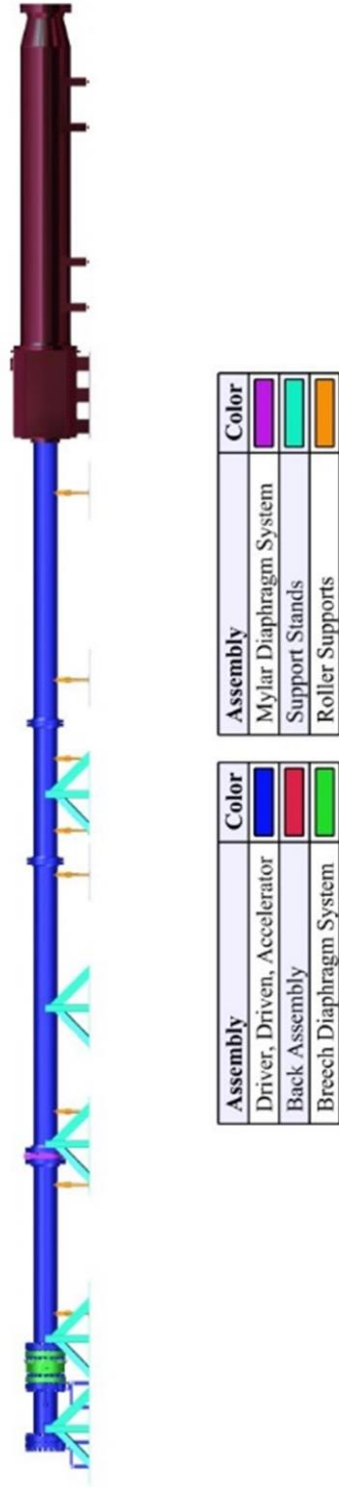


Figure 11. Side-view of the Hypervelocity Expansion Tunnel with proper division of the facility representing manuscript layout.

Wind Tunnel Complex and installed during a convenient window to minimize cutting into research time.

1.4 Manuscript Layout

The presented thesis is a summary of the overall design and the methodology behind the direction chosen for each component and the evolution leading to its final form. As such, the Hypervelocity Expansion Tunnel is divided into three primary subassemblies which are discussed in length: the driver/driven/accelerator(R/N/A), the breech diaphragm system, and the test section/tailpipe. These sections as they appear in the final CAD model are divided and illustrated in. An additional section details the supporting equipment vital to the proper operation of the facility, including the stands supporting the loads, the hydraulic system, and the electronics system which incorporates control and data acquisition equipment. The final section provides a detailed update on construction with key goals needed to make the tunnel operational and suggests a planned roadmap to shakedown and characterize the flow.

Additional appendices are located at the end of the manuscript which include the finalized requirements, the technical drawings for facility components, and schematics of the flow controls/circuit diagrams.

1.5 Project Management

The project is run by a group of approximately ten people, all of which are mentioned in the Acknowledgements section of this manuscript. Three professors wrote the proposal to the ONR and handled higher level obstacles, while a single graduate student managed the design, CAD modeling, day-to-day logistics, and the rest of the team.

Five undergraduate students made up the bulk of the workforce and assisted in construction of the facility as well as programming of the VI mentioned in Section 5.3.5. A single staff worker, Cecil Rhodes, was readily available throughout the project as well and served as a safety supervisor.

The project conception began in the fall of 2015, where many different approaches to the facility were investigated, some of which are detailed in this thesis. By the end of the fall 2015 semester the general scope and layout of the facility was cemented. During the spring of 2016 the team was able to finalize many of the subassembly designs and the material with long lead times was purchased.

During the spring of 2016, multiple preliminary design reviews were held, with each individual responsible for their assembly defending both their approach and design. For example, the primary and secondary support stands were designed by Alex Pages, so he was responsible for the organization and presentation of information regarding those items during the review process. While this was so, the graduate student reserved the right to alter certain components and drawings with the consent of the responsible engineer. This allowed for a much more error-free design process where communication and organization were held as higher priorities.

Construction of the facility began in phases, with the pipe segments being purchased first since they held the longest lead time. The summer of 2016 provided ample time to ramp up construction and, as of October 2016, fabrication of parts and assemblies are still underway.

Another major management point that was implemented from the beginning was the record of requirements and objectives for the facility. Originally, there were a multitude of objectives, most of which are not mentioned. These were narrowed to a final few which are used throughout this manuscript and serve as a primary guide when design requirements are conceived.

One of the first objectives of note is that the facility should operate in a safe and convenient manner. Sometimes these two points conflict, with safety always being held to a higher priority than convenience. Most design aspects of the facility focus on the safety of operation and these are detailed as appropriate to each subsection.

Another objective of the facility is the “aerothermally” clean nature of the flow field throughout the envelope. This is achieved through use of a 1-dimensional fluid mechanical model and validated through operation.

A third objective is to focus the test section around accessibility of laser beams from multiple directions. This will allow various laser diagnostic techniques, such as VENOM, to be implemented in the facility where heat flux measurements can be recorded.

The final objective of note focuses on the fact that HXT should be designed from the very beginning to operate in a dual mode capacity as both a shock tunnel and expansion tunnel. Doing this from the start saves money and time by ensuring that extensive redesign of the facility does not need to occur for future testing needs.

2. DRIVER, DRIVEN, ACCELERATOR SECTIONS

2.1 Requirements

In order to achieve enthalpies and velocities laid out in Section 1.2.3, the Hypervelocity Expansion tunnel utilizes the conventional driver, driven, and accelerator pipe sections, hereby abbreviated as R/N/A where appropriate. This section, as with all sections hereafter, begin by establishing a set of engineering requirements. These requirements are divided into primary and derived categories. Primary requirements are those which are either stated in the proposal, classified as required for operation, or are dictated by safety protocols. With very few exceptions, primary requirements must be fulfilled in the design.

Derived requirements are those needs that are specific to the design path in which is chosen by the HXT engineering team. These are extensions of the primary requirements, with some of them complimenting safety measures with additional factors while others simply state a suggestion for how HXT satisfied the primary requirement.

Table 2. Select primary requirements and their respective derived requirements for the driver, driven, and accelerator sections.

Primary Requirement	Derived Requirement
<u>Shall</u> achieve objective operating envelope as set out in the ONR proposal (see Section 1.2.3)	<u>Should</u> evaluate plausibility of proposed operating envelope and either expand or reduce parameters as needed
<u>Shall</u> be located in a sufficient space as allocated in the NAL	<u>Should</u> allot adequate space for the installation of a test section and tailpipe
<u>Shall</u> maintain a pressure rating of at least 2100 psi	<u>Should</u> be rated pipe with ASME certified high pressure welding

For the R/N/A pipe sectionals, Table 2 lists a select few requirements to discuss. These do not represent a full disruption of the requirements used during design, since these would crowd the manuscript with unnecessary lists of line items used to shape the design of the facility. Appendix A contains a full list of the requirements for this section and all following sections, while only those listed in Table 2 will be hereby summarized.

Overarching requirements for the facility are designated in the proposal to the Office of Naval Research and are summarized in Section 1.2.3. These conditions, however, are one of the few primary requirements with sufficient flexibility since the proposal was written as a rough estimate of what the facility is capable of. Ideally, the operating envelope presented in the proposal should be satisfied at the very least. For this reason, the engineering team's first responsibility was to either validate or expand the initial dimensions laid out in the proposal. These generalized sizing requirements are evaluated in Section 2.2.1.

The space allocation for HXT is limited to what is available at the NAL. Many different locations were investigated to reduce interference with other facilities, though in the end the original location as presented in Figure 1.9 was deemed the most practical. This space allots a total of 109ft from the entrance of the NAL, through the wall of the laser room, and to the concrete retaining wall outside. This allows additional space for the inclusion of a test section and tailpipe which will be evaluated further in Section 4.

One of the final requirements of note is in regards to safety. The proposal presents an operating pressure range for the driver up to 2,000psi, which, if not designed properly, could pose a significant danger to both people and equipment. This requires each section

of pipe chosen to be properly rated by the vendor, as discussed in Section 2.2, and all interfaces to be ASME code approved, as detailed in Section 2.4.

2.2 Mechanical Design

2.2.1 General Sizing

As summarized in Section 1 and briefly laid out in Section 2.1, engineering began with the key requirements and, from these, more specific needs were contemplated. For the driver, driven, and accelerator pipe, size is as essential aspect to design correctly, since making the pipe too small and/or short limits the test model size and run time while making the pipe too large and/or long unnecessarily increases cost.

As designated in the ONR proposal, HXT has an objective length for the R/N/A sections of 70ft. While a total available space of 109ft is present in the location illustrated in Figure 9, this provides approximately 40ft for the test section and tailpipe, which is discussed further in Section 4.

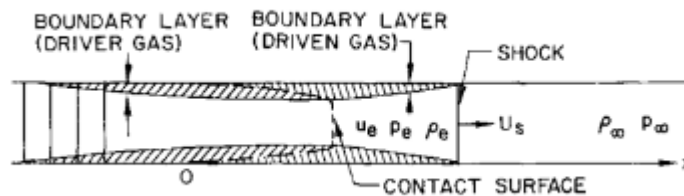


Figure 12. Representative illustration of the boundary layer as predicted in a shock or expansion tunnel.

(credit: adapted from Harold Mirels [Aerospace Corp.] [13])

While originally proposed at 12", the pipe diameter was reevaluated to minimize boundary layer effects. Under similar conditions, the boundary layer at the expansion tube exit for the CUBRC LENS XX facility, as generalized in Figure 12, was estimated at

approximately 2.7 inches for both laminar and turbulent boundary layers by Dufrene and Holden [12] following Mirels [13]. Dufrene and Holden subsequently verified this estimate experimentally in the LENS XX tunnel. Since the overall length of HXT is approximately half the length of LENS XX, the boundary layer thickness is expected to be about 2.0” under the highest Mach number condition. Numerical confirmation of the viscous effects is underway, and the tube exit flow will be characterized following Dufrene and Holden.

Using an estimated 2.0” boundary layer and a schedule 80 12” pipe, which gives a conservative estimate with an inner diameter of 11.376” [14], the effective core flow diameter is approximated at 7.376”. Due to this, various other pipe sizes were evaluated to increase the resulting core flow size, focusing on cost per foot [15] and effective core flow diameter as presented in Table 3.

Table 3. Schedule, pipe inner diameter, estimated core flow diameter, and price per foot for various size pipe made of 304L welded stainless steel.

Size, NPS	Schedule	Inner Diameter [in] [14]	Core Flow Diameter [in]	Cost per Foot [15]
12”	X.S.	11.75	7.75	\$124.00
18”	X.S./30	17.00	13.00	\$230.00
20”	X.S.	19.00	15.00	\$289.17
24”	X.S.	23.00	19.00	N/A

Based on the price per foot and total core flow available, 20” pipe presented the highest cost-benefit relationship. This diameter offers a huge advantage to the one presented in the proposal, with an exit diameter (19”) almost 80% of that proposed to ONR with a nozzle. This allows a larger nozzle to be incorporated in the facility as well, or, at the very least, a smaller inlet-to-exit ratio.

With the total length and diameter of the R/N/A sections determined, the last major element considered is the division of the 70ft into the three sections. Original requirements as set out in the proposal suggested a 3ft driver, 7ft driven, and 60ft accelerator, 3-7-60 mode, with the accelerator made up of three 20ft pipe sections. This would allow a second mode operation to convert the first 20ft accelerator into the driven and combine the 3ft and 7ft pipes to make a 10ft driver, known as the 10-20-40 mode.

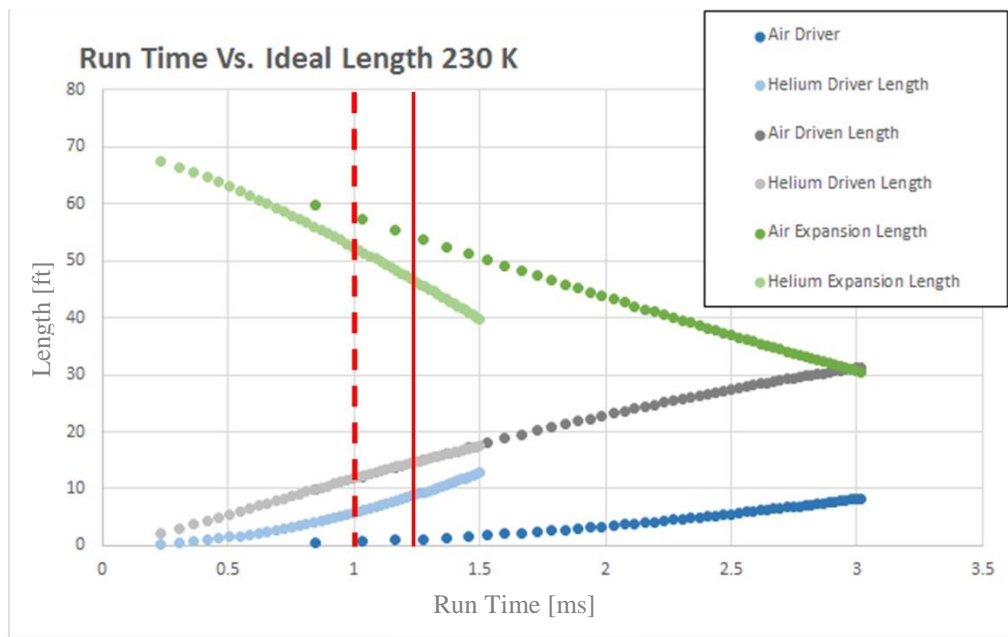


Figure 13. Run-time graph using different fractions of length for the R/N/A sections and various driver/accelerator gases to determine optimum segment lengths. The dashed line is what is deemed optimal and the solid line is what is designed.

(credit: Graph adapted from Gabriel Aguilar’s Expansion Tunnel script [16])

Once the diameter was increased to 20”, changing the sections between the 3-7-60 and 10-20-40 configurations was expected to be significantly more difficult than desired. Due to this, another simulation was performed with Gabriel Aguilar’s time-displacement

wave prediction code [16], using the 20” pipe, 70ft total length, and optimizing R/N/A lengths to have the reflected shock intersect the first reflected expansion wave.

Optimal lengths for the driver, driven, and accelerators were calculated at multiple conditions using helium and air as a driver gas. Figure 13 shows the trends in lengths vs run time for these various conditions, and an optimum R/N/A lengths were determined to be 5.7, 11.7, and 52.6ft, respectively. Due to pipe being offered in 20ft segments it was cheaper to go with a truncated 5-15-50 configuration, which is displayed as a solid red line in Figure 13. Due to pressure requirement in both the driver and driven, only one 20ft section of heavy wall pipe is required as opposed to one and a fraction of a second.

2.2.2 Driver and Driven Sections

The driver and driven sections are combined together since both sections are manufactured out of the same 20ft section of pipe. There are three major factors to consider when designing the driver and driven sections: pressure rating of the pipe, pressure rating of the interfaces welded to the pipe, and how the pipe connects to the load bearing stands.

The first concern when designing is that of the pressure rating for the 20” pipe. Pipe is measured by its schedule rating and is offered in carbon steel, as well as various alloys of stainless steel. Stainless steel was chosen to prevent rust and to avoid painting the inside of 70ft of pipe. While costing more, the stainless steel allows reduced maintenance and a cleaner flow field to reduced contaminants and oils present in and on the carbon steel. Table 4 lists the allowable working pressures for 20” seamless carbon steel pipe [17].

Even though Table 4 lists the working pressures for seamless pipe, specific vendors such as the ones used for the bidding process for HXT offer cheaper welded pipe with equivalent pressure ratings. This is beneficial since this reduction in cost slightly offsets the cost increase by going stainless. Flow field interference due to the seam along the length of the pipe was considered, but the presence of the boundary layer should mask the core flow from experiencing the weld.

Table 4. Maximum allowable working pressures of 20” carbon steel pipe in the temperature range of -20 to 650F [17].

Schedule	Wall Thickness [inches]	Allowable Working Pressure [psi]
10	0.250	435.1
20/Std	0.375	667.2
30/X.S.	0.500	884.7
40	0.594	1058.8
60	0.812	1464.9
80	1.031	1871.0
120	1.500	2770.2
160	1.969	3698.5

From the values listed in Table 4, a minimum schedule of 120 is required for the driver and driven, though after requesting quotes for a 20ft section it became evident that this was very difficult to find a manufacturer for. Due to this and the reluctance not to downgrade the maximum pressure of the facility by using schedule 80, it was determined that schedule 160 was the best option.

One of the other considerations for the design of the driver and driven is that of the interfacing flanges. These are again standardized by ANSI/ASME code and presented in terms of class size in Table 5 [18]. From this table it can be deduced that a minimum

flange size of 900lb¹ can be used to combine the driver and driven. Furthermore, due to the driver interfacing with the accelerator pipe, the first flange of the expansion utilizes a 900lb flange as well.

The final design concern for the driver and driven is how it will interface with the load bearing support stands that transfer the recoil forces to the concrete. This is exceptionally important when changing diaphragms, as the driver must be moved back from the driven to do this.

Table 5. Maximum allowable non-shock pressure with a working temperature between -20 and 100F [18].

Class Rating in lbs	Allowable Working Pressure [psi]
150	290
300	750
600	1500
900	2250
1500	3750

Section 3 details the specifics of the diaphragm mechanisms and Section 5.1 describes the design of the support stands as they appear in Figure 5. The breech is of important note because some of the effective length of the sections is located in the breech

¹ It should be noted that, if unfamiliar with flange ratings, that the “lb” designation does not correspond to the weight of the flange and is only used as a similar metric as the pipe schedule designation.

assembly, requiring the pipe lengths to be shorter than the 5 and 15ft discussed. Figure 15 details the resulting lengths of the driver and driven pipe segments needed as 49.375” and 160.125”, respectively.

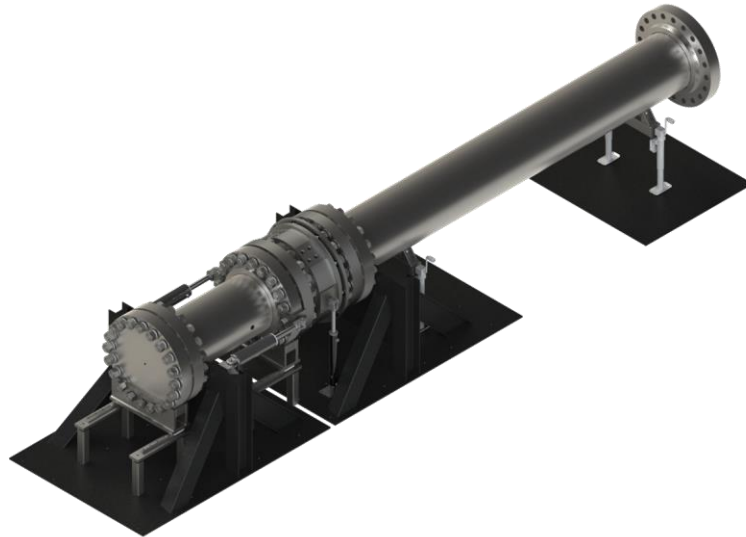


Figure 14. Computer aided design model for the driver and driven as they will interface with each other, the breech diaphragm system, and the support stands.

From a structural point of view, placing each of the flanges on the opposite side of the recoil direction would allow uniform distribution of the force along the entire bottom face of the flange. However, due to the driver requiring to move back away from the driven, this is not the case and the flange pushes up against the stand where studs can pass through alignment holes and nuts can be screwed onto the other side.

A final design point of lesser note is the plumbing connection interface. Both the driver and driven contain fill lines running into the pipe segments, though most of the primary lines used to fill and vacuum the driver run through the blind flange. One main connection point is located on the driver 16.00” from the flange opposite the blind. This

connection is a 1” NPT coupling used in case of emergency to immediately divert the high pressure gas in the driver through a pipe line and outside the lab. This emergency vent line is discussed at length in Section 5.3 with the ball valves and controls.

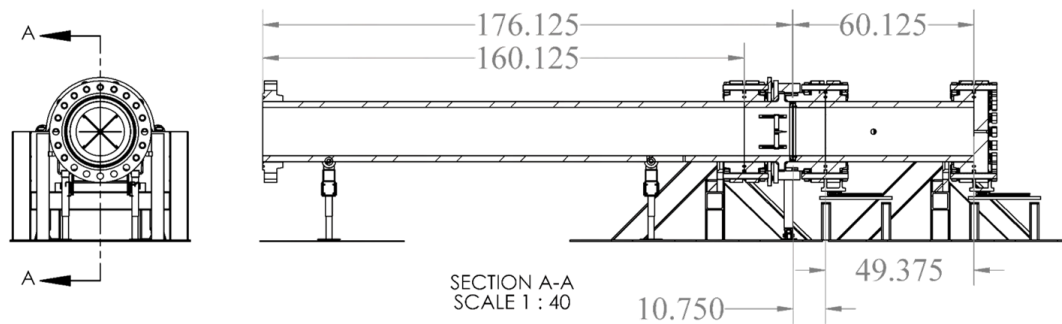


Figure 15. Dimensional drawing for the driver and driven section with lengths of the pipe sections and effective lengths of each section located within the breech assembly.

The driven contains additional interfaces, though both are ½” NPT couplings. Because the driven is sandwiched between the driver and accelerator pipes, the only interface point to fill and/or vacuum is through couplings welded into its walls. One of these couplings is used for fill/vent, while the other is a potential port for a hydraulic line to actuate the diaphragm pin assembly, discussed in Section 3. The two ports are located 20.00” and 32” from the flange that connects with the breech/driver and technical drawings can be found in Appendix B.

Both the driver and driven sections are required to be validated for pressure and temperature ratings. These are discussed thoroughly in Section 2.4 with approved drawings as submitted to the welding shop.

2.2.3 Accelerator Section

The accelerator pipe underwent a design process similar to that of the driver and driven sections with consideration to the schedule of the pipe, class of flanges, and interface with the stands. A major advantage of the accelerator pipe, however, is the lower expected pressures. During expansion tunnel mode, the accelerator is always under vacuum and, even when under pressure during shock tunnel mode as discussed in the next section, the pressures never exceed 700psi.

Overall, using the information presented in Table 4 and Table 5, the accelerator pipe requires a minimum schedule 40 pipe and class 300 flange size. This significantly cuts the price of the pipe from \$1,502.94 to \$289.17 per foot [15]. Due to the extended length of 50ft, however, the accelerator is divided into two 20ft and one 10ft pipe sections, with the 10ft pipe section located in between the two 20ft sections. For consistency, each section is labeled 1-3, with 1 being the accelerator section that connects to the driven.

The first accelerator section contains a 900# flange on the end that connects to the driver, as portrayed in Figure 16, while the third accelerator has no flange located on the end that sits inside the test section. The flange-less end of the third accelerator pipe is intended interface with the test section by use of an inflatable seal that sits around the outer diameter of the pipe.

In terms of load bearing connections, the accelerator pipe was designed differently due to the convenience that the pipe need not move. A single 150# flange is cut in half and the two pieces welded to the middles of the first and second accelerator pipe segments. The load distribution and advantages of the 150# flange are further detailed in Section 5.1.



Figure 16. Computer aided design model for accelerator pipe as it appears with a 900# flange on the driven side of the segment, structural stands, and roller supports.

Like the driver and driven, the accelerator pipe sections contain plumbing connections for fill and vacuum, located in the first accelerator pipe 48.00” downstream of the 900# flange, but also include three coupling points along the third section to allow the installation of time-of-arrival sensors. The use for these sensors are specified in Section 5.3 and are required to be spaced out at large lengths to accurately measure the shock speed. For this reason, three ½” NPT couplings are placed at 20”, 120”, and 220” downstream of the 300# flange of the third accelerator section, allowing 100” in between each sensor.

2.3 Shock Tunnel Mode

One of the major advantages of HXT is its ability to operate in shock tunnel mode by moving the metal diaphragm location from the driver-driven flanges to the driven-accelerator interface. This allows the expansion tunnel driver (XT-driver) and expansion

tunnel driven (XT-driven) to become the shock tunnel driver (ST-driver). The rest of the facility, including the test section and tailpipe become the shock tunnel driven (ST-driven).

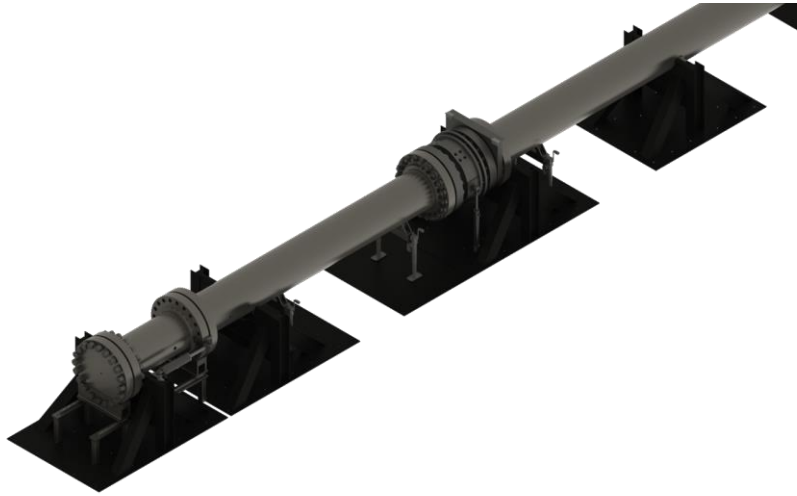


Figure 17. The Hypervelocity Expansion Tunnel as it would appear in shock tunnel mode with the breech system reinstalled between the ST-driven and accelerator pipes.

The major concerns with switching back and forth between shock tunnel and expansion tunnel modes include the end-of-operation pressure limits and the stand placement throughout the lab. The end-of-operation pressures are analyzed at length in Section 4.2.3 when describing the option of an air receiver at the end of the back assembly. This section also includes calculations for volume of each section of the facility, the operating parameters for both the shock tunnel and expansion tunnel, and how limitations for the operating envelope are influenced by the addition of an air receiver.

Because the XT-driver and XT-driven are manufactured out of the same schedule 160 pipe, use the same 900# flanges, and are welded to the same ASME standards, the pressure rating for the ST-driver is equal to that of the XT-driver.

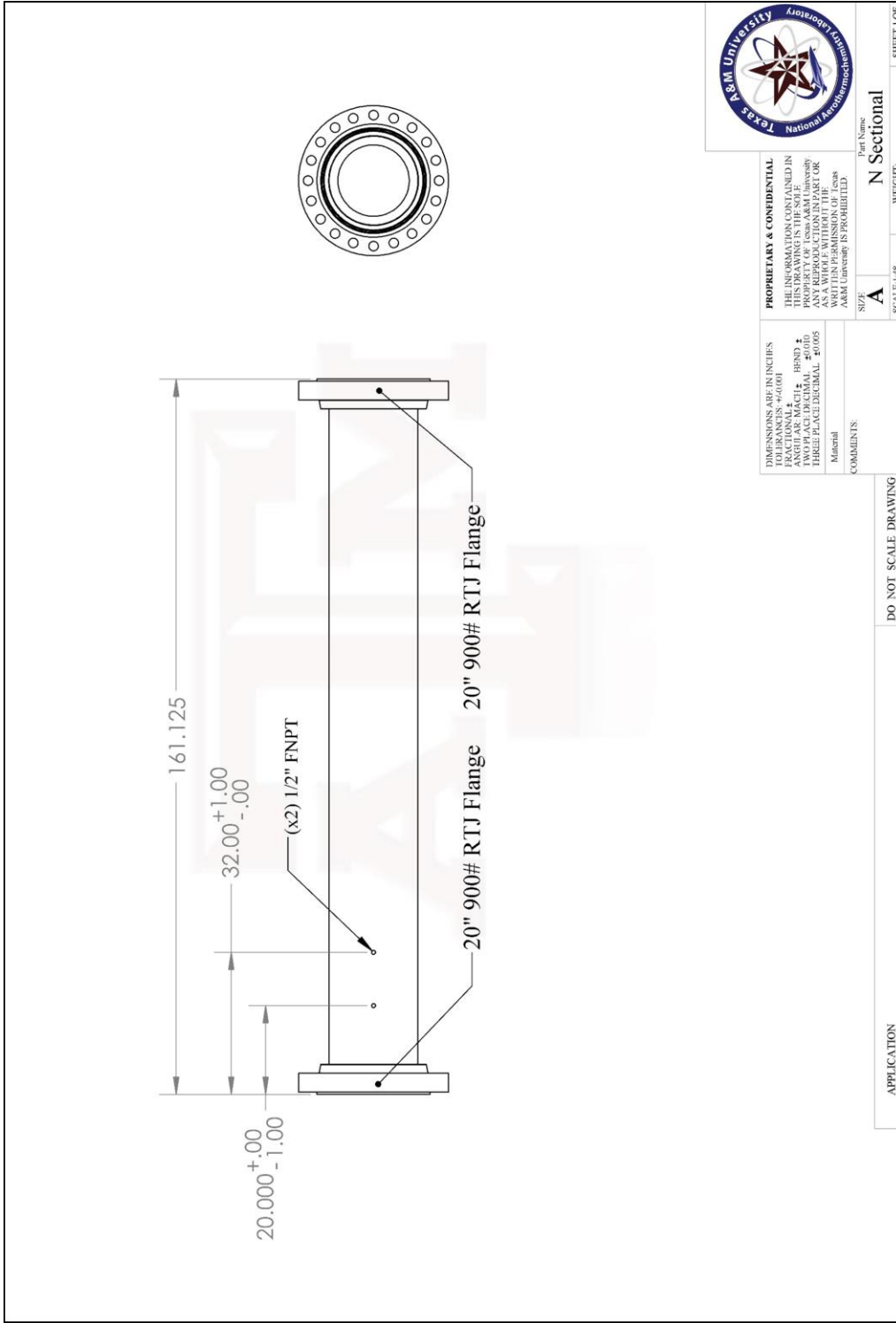


Figure 18. Dimensional drawing for driven as submitted to Circle H Manufacturing.

The main complication occurs when the breech system is installed at the XT-driven and accelerator interface since the XT-driven must move forward (towards the driver) a distance equal to the breech length. When this is done, the second primary stand that helped support the driver is too far away to be secured to the XT-driven pipe. Fortunately, during shock tunnel mode the maximum pressure of the ST-driver is drastically reduced from 2000psi to 500 psi, meaning that the recoil load is cut to a quarter of what is expected in expansion tunnel mode. Section 5.1 evaluates the rated loads for the stands and explains how the loss of one stand for shock tunnel mode is acceptable due to the reduced expected loads falling well within the factors of safety set forth in the design.

2.4 Manufacturing

2.4.1 Welding

The construction of the R/N/A sectionals are done by buying the material and welding each of the flanges to the pipe. None of this is done by employees of Texas A&M University since the extreme pipe pressures require proper ASME certified welding. Two bids were considered from Circle H Manufacturing and Refrigeration Valves and Systems with the requirement that the welds be designed, welded, tested, and registered per ASME Section VIII, Division 1. The full specification for bid are stated in Appendix A with the requirements document for the R/N/A sections. Circle H Manufacturing was ultimately chosen due to being the only one to meet all requirements set forth in the bid request.

Drawings were submitted to Circle H for each of the five segments of pipe, with example drawings of the driven section presented in Figure 18. The drawing in Figure 19 from Circle H contains signature approval from the responsible engineers on the HXT

team and is ASME code verified and checked with the National Board of Boiler and Pressure Vessel Inspectors. Drawings for all five sections can be found in Appendix B, having been properly documented since the R/N/A pipe segments cost a significant fraction of the overall budget and pose the biggest safety risk.

2.4.2 Estimated Cost

Costs are detailed in Table 6 and divided into raw materials costs for the pipe and flanges as well as the labor costs as charged by Circle H Manufacturing. As can be seen, the R/N/A sections carry a price tag over \$100,000 and do not include stands, gas/vacuum plumbing lines, or the crane system installed in the lab to be able to handle the heavy weights of the pipe.

Table 6. Estimated cost for the pipe, flanges, and labor to manufacture the R/N/A sections.

Component Name	Qty	Cost Per	Line Item
Schedule 160 20” S.S. 304L Pipe at 20ft	1	\$30,058.80	\$30,058.80
Schedule 80 20” S.S. 304L Pipe at 20ft	3	\$5,783.40	\$17,350.20
20” 900# RTJ Blind	1	\$5,214.00	\$5,214.00
20” 900# RTJ Slip-on Flange	5	\$5,064.00	\$25,320.00
20” 300# RTJ Slip-on Flange	5	\$3,174.00	\$15,870.00
Circle H Manufacturing Labor- Initial	1	N/A	\$23,650.00
Circle H Manufacturing Labor-Added	1	N/A	\$3,200.00
		Total	\$120,663.00

2.5 Nozzle Option

While the R/N/A pipe segments laid out in this section provide an exit diameter of 19.00”, the Hypervelocity Expansion Tunnel is designed to ultimately include a diverging nozzle to increase the overall Mach number and core flow for the test section. In the original ONR proposal, the nozzle was to expand the flow from a 12” pipe inner diameter to a 24” exit diameter. When the pipe size of the entire facility was increased from 12” to

20” it was suggested that the 2:1 nozzle ratio stay roughly the same, with a truncated exit diameter of 36” eventually confirmed.

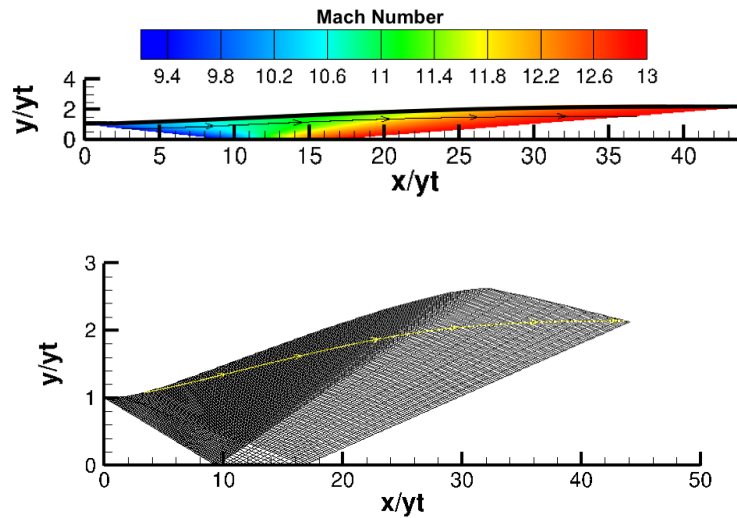


Figure 20. Method of characteristics diagram used to predict the contour and length of the nozzle.

Design of the nozzle contour was performed using an in-house, viscously corrected method of characteristics code written by Dr. Rodney Bowersox. The characteristics diagram using an inlet Mach number of 9 and outlet Mach number of 13 is shown in Figure 20 and is normalized by the inlet diameter of 19”. The method of characteristics code results in an overall length for the nozzle of approximately 23.5ft, but is truncated at 20 feet when accounting for viscous effects.

Utilizing a length of 20ft is beneficial since it only requires the replacing of the third accelerator pipe which is also 20ft in length. This is why there is no load bearing stand located along the length of the third accelerator segment, except for the roller stands, instead allowing the installation of the nozzle at a later time with no effect to the load rating of the facility.

A huge obstacle in the design of the nozzle comes in the form of manufacturing. Acquiring steel segments in excess of 24” in diameter, especially those which gradually increase to the required 36”, is extremely difficult, even in short sections. However, a 20ft long section that increases at the perfect thickness to what is required by the designed contour poses a serious challenge. For this reason, an innovative solution is proposed in terms of both machining and material fabrication.

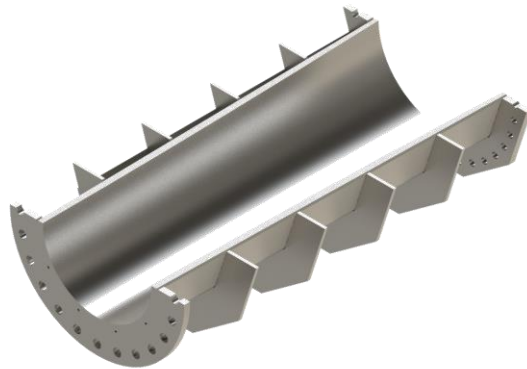


Figure 21. First segment of the nozzle, cut in half and displayed as it would sit in the CNC mill for machining of the contour.

First, the nozzle is divided into four separate sections 5ft long. This allows machining of the axisymmetric contour to be done on an accessible machine. Each section is machined in halves to further simplify the machining process and allow it to be performed on a mill rather than requiring a lathe with a 5ft travel. Ribs are located across the entire nozzle, which serve a dual use during fabrication as alignment jigs. These ribs, as portrayed in Figure 21, all sit at the same face diameter in order to sit flush on the

machining table. The CNC mill can then be programmed to machine the angle and contour required by the design.

The second major challenge to the nozzle is acquiring material capable of being machined in the proposed manner. Forging pieces of stainless steel at the required outer diameters is one solution, and one that would decrease movement of pieces during welding. However, another, cheaper solution is to weld thin bars together to create a polygon that can then be machined, especially since the machining process already requires each segment to be manufactured as a half.



Figure 22. Nozzle assembly using a decagon shape and ribs that double as alignment jigs.

Using a decagon shape and manufacturing each segment half as a welded assembly of 5 steel bars, the minimum required thickness for each individual bar is approximately 1.25”, with widths ranging from 7.5” for the first segment to 12” for the fourth segment. Each of these bars are manufactured and beveled on the sides in order to weld together

using the alignment ribs/jigs. Once five are welded together, they can be machined and combined with their other halves and once again welded.

Each segment is fastened together using a custom alignment rib with an o-ring groove placed on the face of one side. Bolt holes are also placed across these joining ribs, allowing each segment to be removed individually if required. Figure 22 depicts the nozzle assembly with all four segments. The rib thicknesses are currently designed at $\frac{1}{2}$ ", though this dimension could increase or decrease depending on the finite element analysis that should be performed. It may also be determined that four ribs are either not enough or exceed the number required by structural analysis.

Interfacing the nozzle with HXT requires the addition of a new structural support stand. While it should be designed to carry some recoil, if expected, the support stand primarily carries the enormous weight of the nozzle, estimated at 6,500lbs. Additionally, since the third accelerator pipe segment is the one designed with time-of-arrival sensor input, the nozzle will also need to accommodate coupling ports for these sensors.

3. DIAPHRAGM SYSTEM DESIGN

3.1 Requirements

After functionality and safety, ease of operation is one of the most important considerations set out when design of the facility began. Time spent altering the facility or changing diaphragms easily adds up, so reducing maintenance and maximizing research time was a main focus for the engineering team. For this purpose, a system to easily change out both diaphragms was conceived requiring a minimum of two people to operate using as little manpower as possible. Initial requirements were used to brainstorm various ideas to approach the problem. A select few of these requirements are detailed in Table 2. These requirements are listed in full in Appendix A.

Table 7. Select primary requirements and their respective derived requirements for the diaphragm changing systems.

Primary Requirement	Derived Requirement
<u>Shall</u> allow relatively easy access to the diaphragms	<u>Should</u> allow access to the diaphragms by moving the driver back away from the driven
<u>Shall</u> be able to withstand all operating temperatures and pressures as seen in the driver, driven, and accelerator sections	<u>Should</u> be manufactured with equally rated pipe and flanges already designed into the driver, driven, and expansion sections
<u>Shall</u> have a backup configuration that works without the use of any part of the diaphragm system except the diaphragm holder	<u>Should</u> use pipe spacers cut from the same Sch 160 pipe

Changing the diaphragms by interchanging a disk housed in a box was originally considered. This would allow the diaphragm to be changed by lifting the lid of the holding unit, removing the diaphragm, and putting in a new one. As far as ease of access, this was

definitely the easier of all the options weighed; however, because of the high pressures experienced around the driver and driven sections it was determined that square housings would be extremely difficult to manufacture due to large wall thicknesses. While making a circular housing would reduce the wall thicknesses, design of a lid that could easily seal around a curved surface proved to be even more difficult than the flat faces. Even so, a slip-in system is suitable for the driven/expansion interface since it can be equally rated to the schedule 80 20” pipe as discussed in Section 2.

Breech mechanisms were studied in great detail since these are very common in shock and expansion tunnels throughout the world. Originally used to close up artillery before firing, the use of a breech system allows sealing of much higher pressures but requires that the driver move away from the driven at least one foot. While not as convenient as the slip-in configuration, it does provide a workable means to quickly replace broken diaphragms that should prove to have a higher factor of safety.

In regards to pressure rating, all components of the diaphragm systems are manufactured from material with known ratings. For example, the central body of the breech is constructed out of 20” schedule 160 pipe since this has a known pressure rating of 3,698.5 as discussed in Section 2 [17].

Because both diaphragm systems will take a couple months to manufacture, cost tens of thousands of dollars, and require proper testing before use, a “backup” configuration is designed to replace the breech system for the first phase of operation. The primary purpose for this configuration was to act as alternative mode to break diaphragms in case the breech is damaged or requires maintenance. For this reason, the backup

configuration is kept as simple as possible, being designed out of leftover sections of 20” schedule 160 pipe, and is engineered with little regard to ease of operation.

3.2 Diaphragm Holder

A single “universal” diaphragm holder is designed for both the breech system and backup configuration. This simplifies manufacturing and allows multiples of the holders to be machined without limiting potential use. Technical drawings of the diaphragm holder components can be found in Appendix B.



Figure 23. Diaphragm holder exploded view with (left) male holding ring, (middle) etched diaphragm, and (right) female holding ring.

As depicted in Figure 23, the diaphragm holder consists of two holding rings clasped around the diaphragm to equal a total thickness of 2.00". Both rings are machined out of 20" schedule 160 pipe for ease of manufacturability. O-ring grooves are placed on both sides of both rings for adequate sealing as illustrated in Figure 24. Inner grooves place the o-rings against the diaphragm and are held tight using ¼" countersunk screws. One ring, called the "female" ring, has threaded holes machined into it while the other ring with through holes is labeled as the "male" ring. Due to the placement of the counter bored hole on the male ring, an o-ring groove is placed to match the inner or-ing grooves to avoid any interference, while the female ring has its dowel pin alignment holes further inside to allow for a notch on the outside.

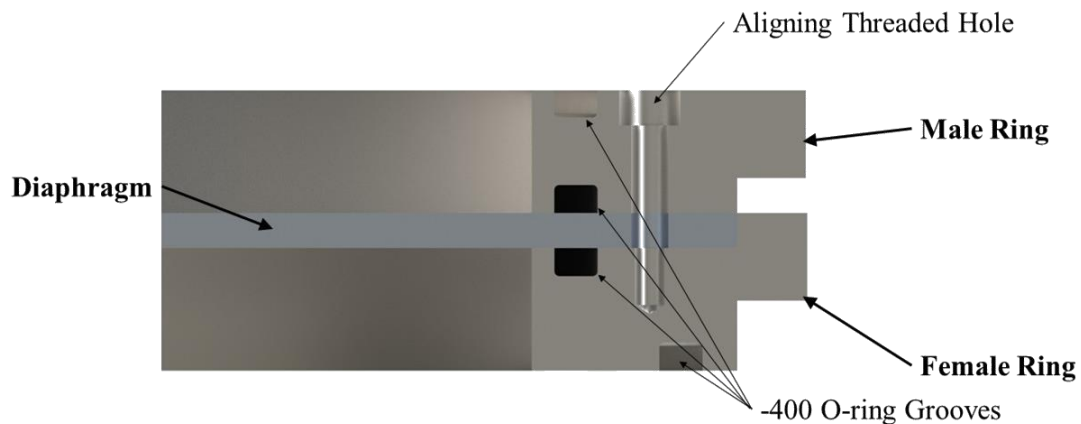


Figure 24. Diaphragm holder cutout with labels and locations of o-ring grooves, dowel pin alignment holes, and threaded holes.

For purposes of convenience, a diaphragm thickness of ¼" was chosen to be the standard for the diaphragm holder. Although variable thicknesses can be used in the diaphragm holder, it should be noted that this will greatly affect the design and seal of the

breech system. This is because the teeth carrying the loads on the breech system have very little tolerance for movement and so the breech must be redesigned to account for any deviation from a $\frac{1}{4}$ ". This will be better understood after a series of experiments are conducted which will characterize how the diaphragms break and at what pressure differential. If $\frac{1}{4}$ " diaphragms result in being too hard or too easy to break, than the correct thickness can be redesigned into the breech system.

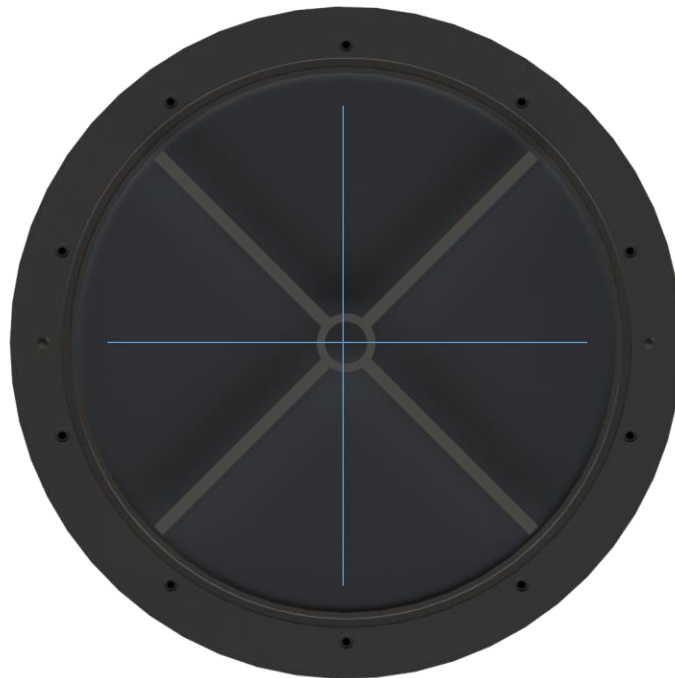


Figure 25. Diaphragm etching highlighted with a blue line and its orientation relative to the pin arm holder.

Dowel pin holes are located on the diaphragm-side faces of both holding rings in order to keep the diaphragm etch pattern in its proper orientation. This orientation was chosen to offset the pin older arms by 45 degrees, as depicted in Figure 25, so that if a petal of the diaphragm were to try and shoot down the pipe it would hit the pin arm and

reduce its maximum obtainable velocity. Additional dowel pins are located on the female holding ring to align the diaphragm holding assembly with the pin arms.

Due to the extreme pressures experienced in the driver (2000psi max), large -400 series o-rings were chosen to ensure maximum squeeze and prevent breaking with softer materials such as silicone. The -400 series groove width and depth ranges, as recommended by the Parker Handbook, are 0.309 to 0.314” and 0.201 to 0.211”, respectively [19]. A conservative depth of 0.195” was chosen to abide the 70% rule of thumb for o-ring sizing, which dictates that the groove depth should be 70% of the actual o-ring cross sectional diameter.

3.3 Breech Diaphragm System

3.3.1 Design

The breech system operates by use of a large scale locking mechanism controlled by hydraulic cylinders in two degrees of movement: horizontally back and forth along the direction of the pipe and vertical rams that rotate the nut into a locked position. Figure 26 portrays an exploded view of the breech assembly with callouts identified in Table 8. Callout 0 refers to the diaphragm assembly as discussed in Section 3.2, whereas all other callouts are discussed in the current section with a subsection of the loading analysis following the physical design.

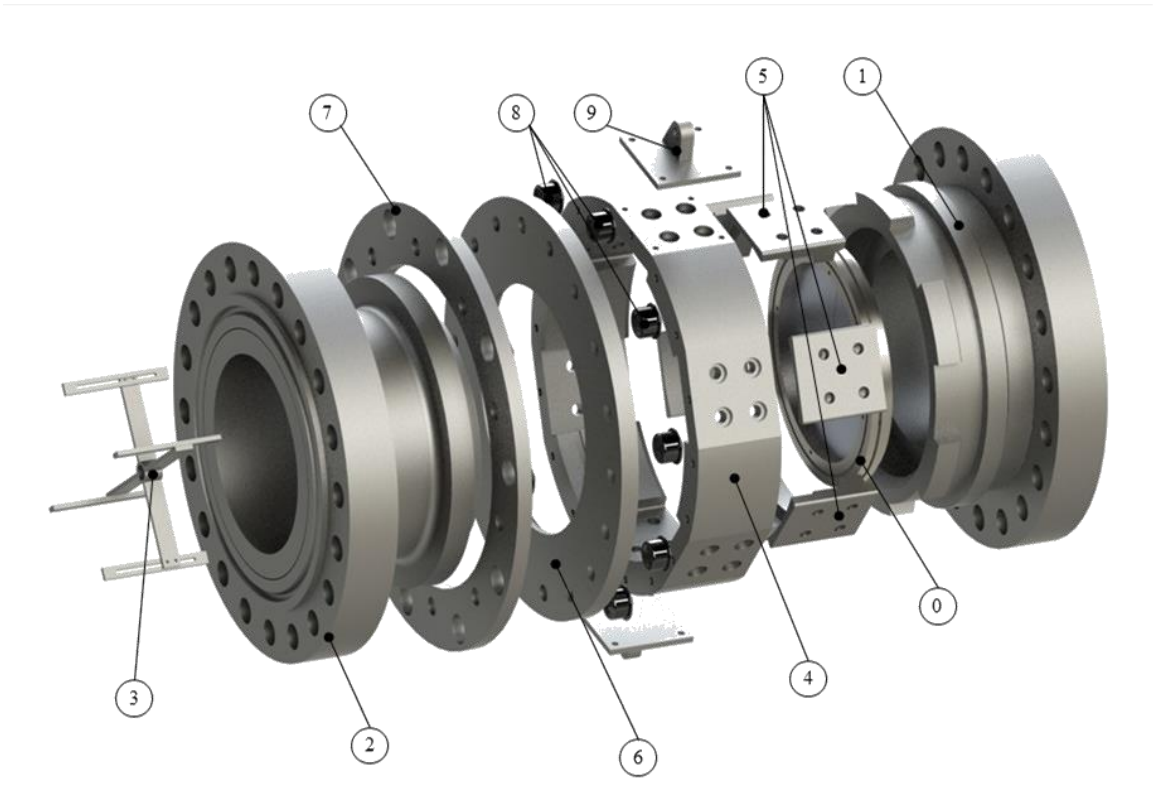


Figure 26. Overview of the breech diaphragm system with callouts for each major component/subassembly.

Table 8. Breech overview callout list.

Callout #	Component/Subassembly Name	Weight [lbs]
0	Diaphragm Holder Assembly	54.76
1	Breech Seat	1,083.10
2	Breech Head	1,293.68
3	Pin Assembly	7.98
4	Locking Nut	426.91
5	Locking Teeth Inserts	14.38 each
6	Nut Backplate	236.76 (both halves)
7	Thrust Plate	154.83
8	Thrust Plate Bearings	N/A
9	Rotation Hydraulic Mount	~10 each

Originally, the breech system was designed to have the nut screw on to the seat to increase compression of the diaphragm in between the seat and the head. Matching

standard ACME threads would be machined into both components, sealing the facility and allowing force to be distributed from the driver into the driven. However, this complicated matters in regard to screwing on the overly heavy nut which weighed several hundred pounds. Hydraulic gear motors and hand torquing the nut were the most invested designs, though after research into other large breech systems around the world it was determined that minimal rotation was the route to take.

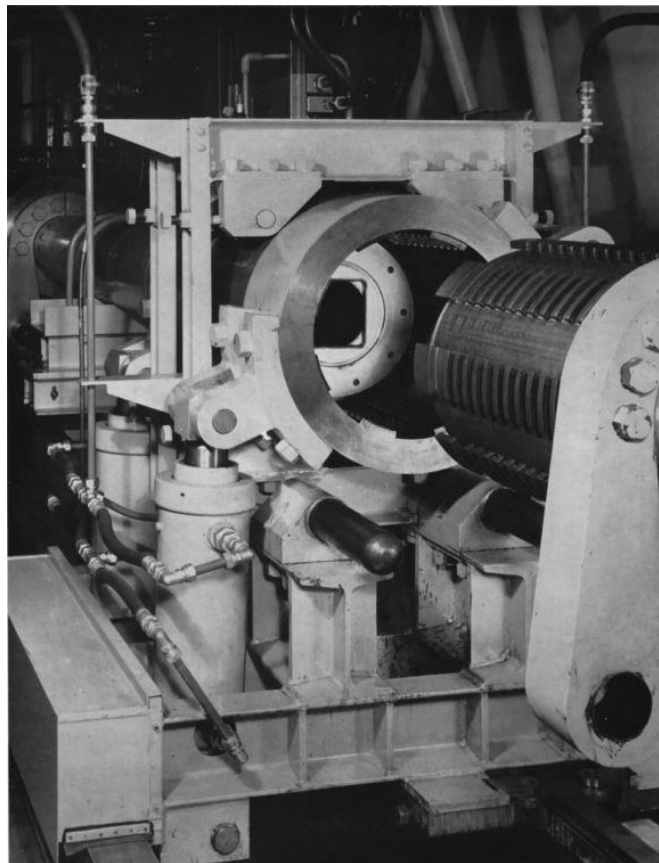


Figure 27. Picture of the NPL 6-inch shock tunnel main diaphragm station.

(credit: adopted from Pennelegion et al R&M No. 3449 [20])

The 6-inch Shock Tunnel at the National Physics Laboratory in the United Kingdom is the primary source of influence for the HXT breech system. Figure 27 presents

an image adopted from “Design and Operating Features of the N.P.L 6-inch Shock Tunnel” by Pennelegion, et al [20]. The main diaphragm station they utilize is a locking mechanism with roughly 8 columns of multiple teeth that insert into a nut. Hydraulics rams can be seen mounted to the outer diameter of the nut that allows the small angle of rotation to secure the driver in place.

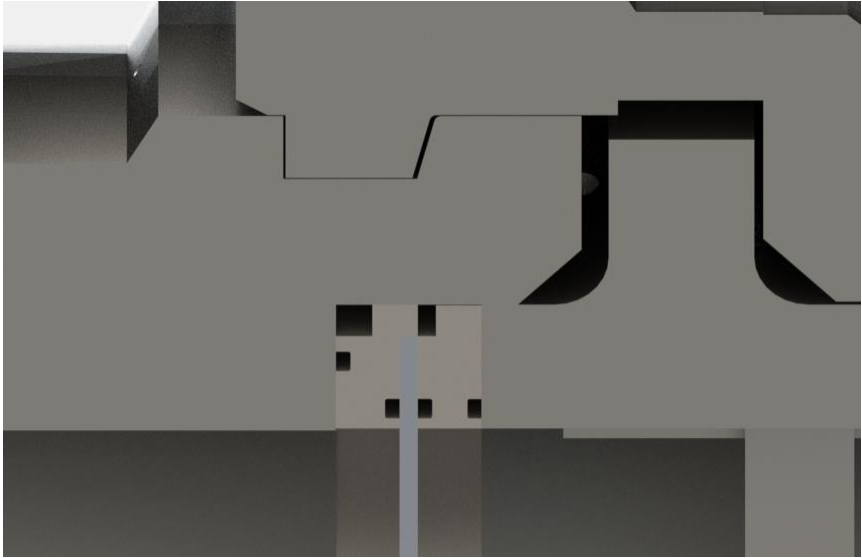
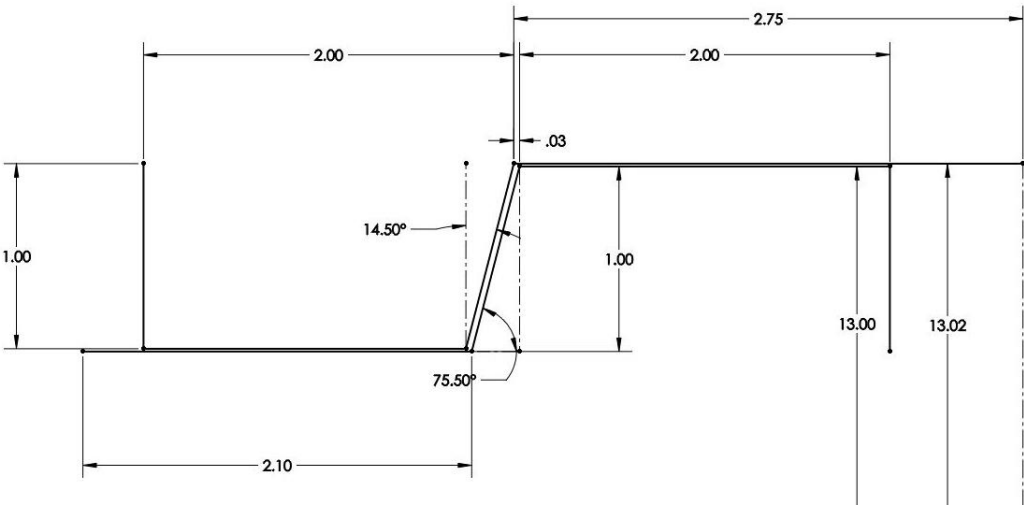


Figure 28. (top) Breech lock teeth dimensions for internal and external grooves and (bottom) computer aided rendering of the interlocking teeth.

The Hypervelocity Expansion Tunnel's breech uses a similar locking mechanism with 6 large teeth measuring 27" from end to end. Fewer, larger teeth were chosen instead of many smaller ones in order to simplify machining. These are located on both the breech seat and locking nut, with dimensions for internal and external "threads" detailed in Figure 28. The teeth angles match those present in ACME threads (29 degrees) and the tolerancing is derived from Class 2 ACME dimensions [21]. Finite element analysis was performed on the load bearing components and the results presented in Section 3.3.2 for a factor of safety over 3 for the entire system.

In order to mount the breech to both the driver and driven, the interfaces located on the head and seat as pointed out in Figure 26 are 20" 900# RTJ flanges. In order to reduce manufacturing time and overall cost, the breech seat, attached to the driver sectional, is machined out of a heavy barrel flange. The dimensions of this flange can be found in Appendix B [22] along with the mechanical drawing of the resulting seat component.

Heavy barrel flanges are similar to slip-on flanges in that they fit over the pipe they weld to, except the short stubs usually present on slip-on flanges are reinforced with thick walls of additional steel. The groove that this additional steel creates acts as a hard stop for the fastening nuts located around the flange [23]. This allows the nuts to be loosened or tightened by use of only a single wrench or driver. The additional steel found around the stub of a heavy barrel flange makes it perfect for machining deep teeth grooves without removing vital material needed to keep the pressure rating.

To keep the diaphragm holder in place, the breech seat allows the insertion of the holder into a crevice as rendered in Figure 29. This recessed face is created by welding a small section of 20" schedule 160 pipe to the heavy barrel flange, bringing the inner diameter of the seat to match the diaphragm holder and breech head diameters. This recess measures 3.375" from the far face of the HB flange, allowing the 2.00" thick holder plenty of room to sit while also allowing a small portion of the breech head to insert into the seat.



Figure 29. Breech seat which includes the machined 20" 900# heavy barrel RTJ flange with a small section of pipe welded to it.

Similarly to the seat, the breech head is designed around a 20" 900# RTJ flange and 20" schedule 160 pipe body. The role of the head is to press against the diaphragm holder and cause sufficient enough force on the o-rings to properly seal, as illustrated in

Figure 30. In order to maintain this force, however, the seat and head must be interlocked and so a collar is welded onto the outside of the 20" pipe to act as a load bearing plate. This collar is designed to keep a gap between it and the teeth of the seat by a thickness equal to that of the diaphragm, meaning that a sufficient space should always exist.

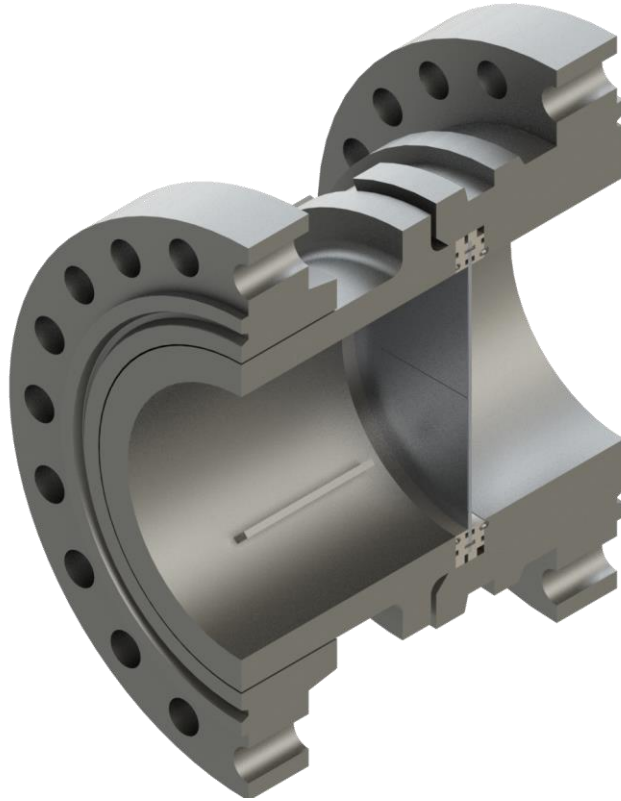


Figure 30. Breech head placed against the diaphragm holder and inserted into the breech seat.

To keep the welded collar of the breech head up against the diaphragm, a large locking nut engages with the teeth machined into the HB flange. For manufacturing purposes, however, the nut requires a removable back plate to exert the force on the collar and keep the head placed firmly into the seat as seen in Figure 31. This plate is broken into two semicircles so that it can be taken off the breech head and repaired. The back

plate and locking nut are held together by eighteen $\frac{3}{4}$ "-16 countersunk screws. Overall, the nut is 32" at its maximum outer diameter, 7.25" long, and is calculated to weigh 426 lbs.

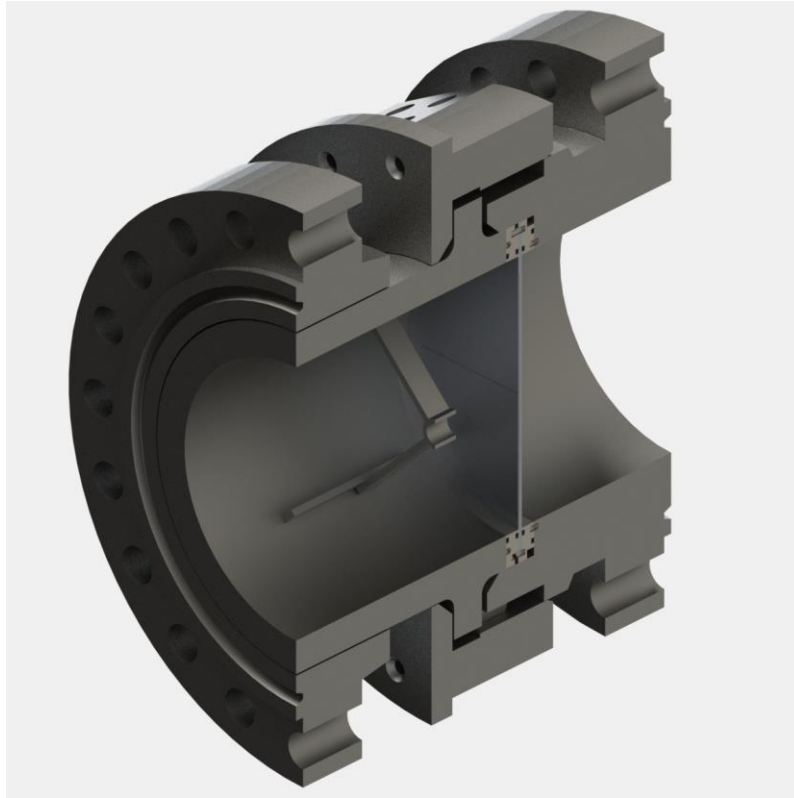


Figure 31. Breech seat which includes the machined 20" 900# heavy barrel RTJ flange with a small section of pipe welded to it.

At the start of design, the teeth were designed into the nut for structural reasons, with the original thought being that one piece was stronger than attaching smaller pieces. After many design iterations that will be discussed at length in Section 3.3.2, removable teeth were converged on due to a balance between cost and strength, allowing the teeth to be made out of extremely strong steel alloys without requiring the entire bulk of the nut to

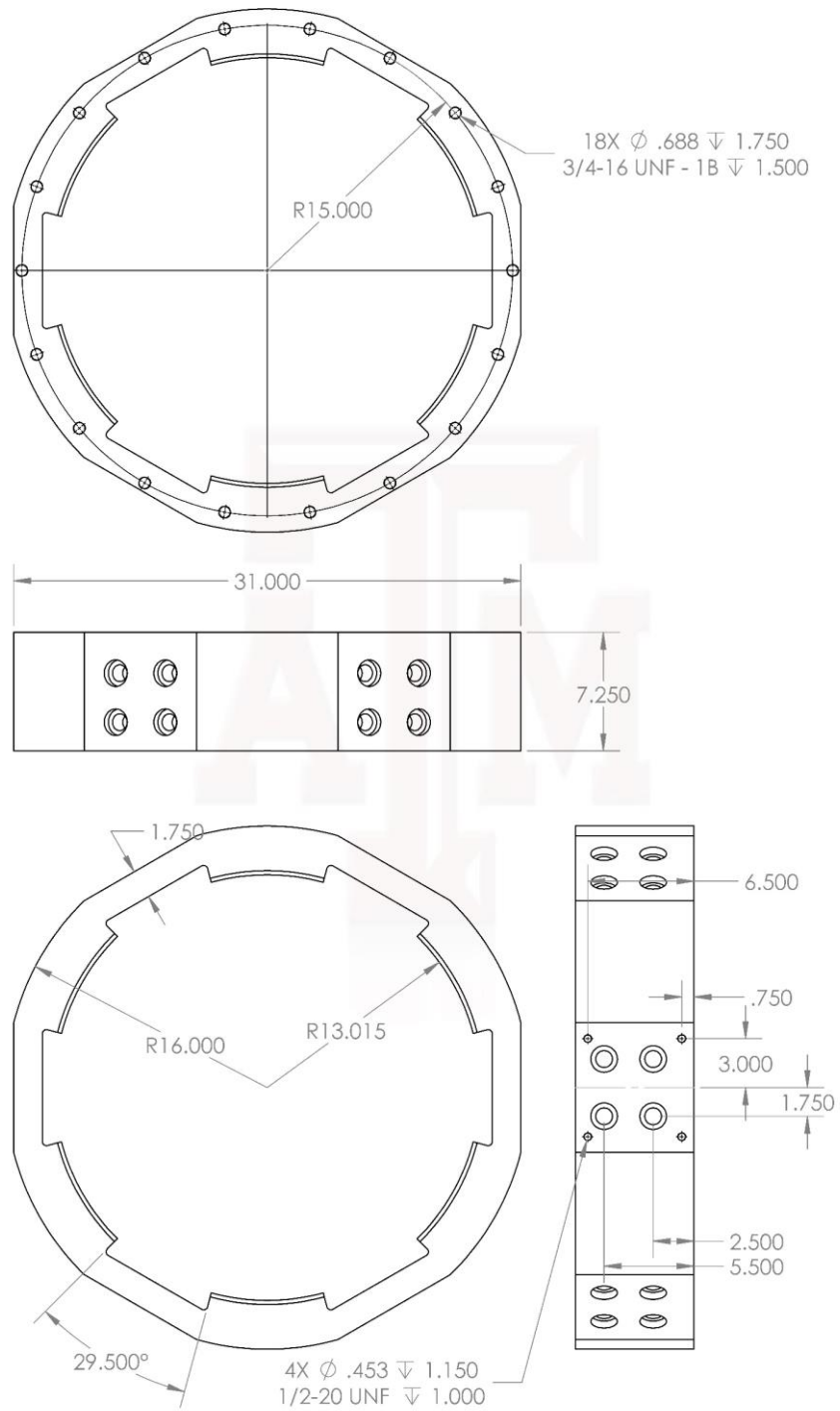


Figure 32. Breech nut with hydraulic mounting holes and grooves to insert teeth made out of steels with higher yield and ultimate tensile strengths.

be made out of such expensive material. The grooves where the teeth can be inserted, along with the rest of the locking nut body, is detailed in the drawing located in Figure 32.

A major issue with using a locking nut is that the center of mass overhangs the collar which would force the nut to “sag” depending on the tolerance given to match the outer diameter of the pipe. To counter this gravitational pull, either the bottom of the nut needs to be supported or the back plate needs to be evenly pushed forward. Holding the locking nut from the bottom while also allowing rotation proved to be difficult due to the number of degrees of freedom. The bottom support would be required to move back and forth with the driver and the force balance would have to be very accurate as to not overshoot, reversing the direction of sag.

Evenly distributing a force along the back plate, as portrayed in Figure 33, allows the no additional support since the back plate moves with the driver. The forces are exerted by 10 of the bolts used to fasten the 20” 900# slip-on flange of the breech head to the driven flange. These bolts extend out slightly further and are machined to a diameter of 1.5”. When the flanges are fastened together the bolts can be torqued to a point where a sufficient amount of force is exerted on the back plate.

Even though the forces can be generated by tightening the bolts on the flanges, rotational movement of the locking nut would cause a great deal of friction if simply pushed against the back plate. For this reason, an additional thrust bearing plate is inserted between the flange and the back plate. This plate holds 10 ball bearings capable of supporting 670lbs each for a total of 6,700lbs [24], allowing the nut to freely rotate while still experiencing a great deal of force evenly distributed by the ten studs. Shallow indented

holes are placed along the thrust plate where the 1.5” diameter stud ends should be placed, reducing movement that may occur due to any friction. While the forces on the back plate can have an upper limit of 6,700lbs, it should be noted that this force should be a magnitude above what is necessary to keep the locking nut from sagging.

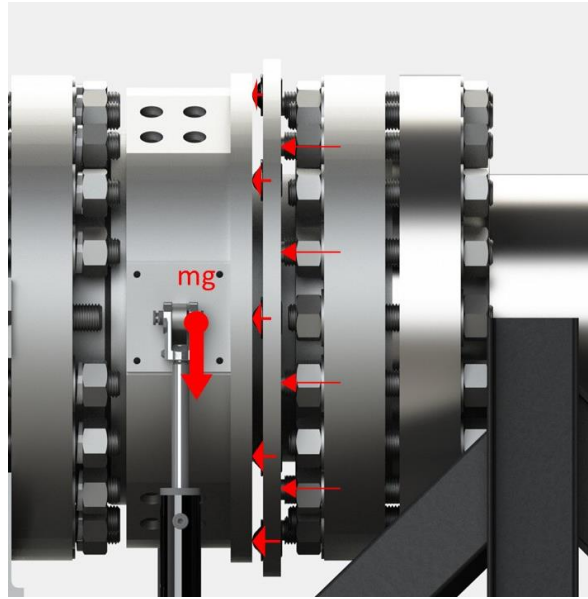


Figure 33. Qualitative force diagram for the thrust plate and the center of gravity for the locking nut.

Hydraulic rams are used for the movement of the driver back and forth and the rotation. For this purpose the hydraulics were mounted using clevis pins and custom-made mounts. For horizontal movement, the rams attach at points located along the 20”900# flange closest to the driver blind and push against the driver’s primary stand with another custom-made mount. Section 5.2 details the specific model rams used and the forces generated, while Section 3.3.2 details the loads needed to fully compress the o-rings located in the diaphragm holder.

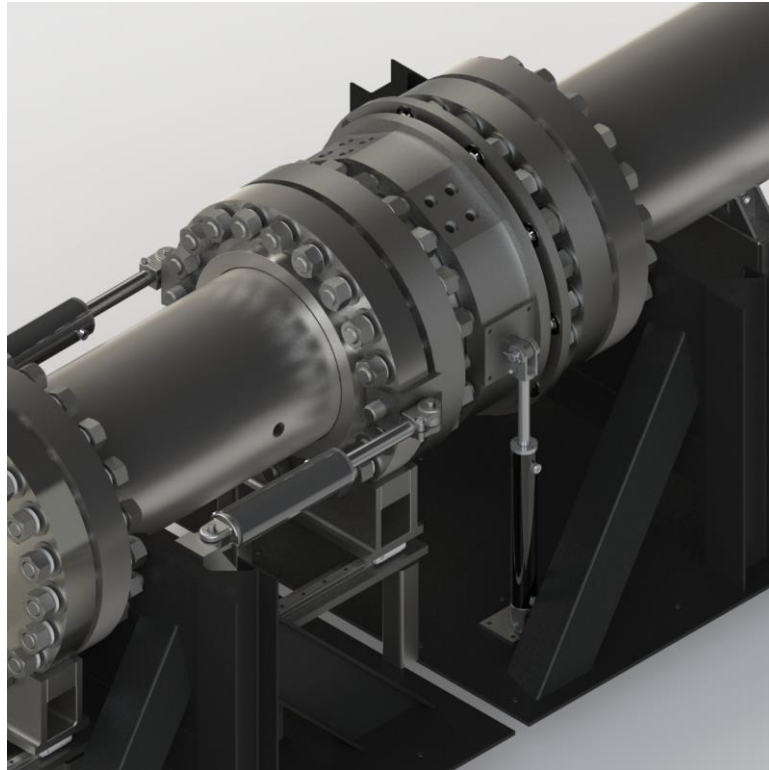


Figure 34. Assembly with a pair of hydraulic cylinders used to move the breech forward/back and a pair to lock the nut to seal the diaphragms.

Rams used to rotate the locking nut require significantly less actuated force since they should experience very little friction. Maintenance requirements will include the use of lubricating oil being injected along the teeth and any contact surfaces, such as the copper bearing sheet placed in between the collar and locking nut faces. The rotation rams should also be designed to avoid excess force in case the teeth do not interlock properly. This could potentially be caused by any type of obstruction near the diaphragms, yet, even if this were to occur, damage would be very unlikely due to the strength of the breech seat and locking nut teeth exceeding any forces that hydraulics could provide.

Figure 34 portrays the breech as it is fully expected when interfaced with HXT. Cylinders are located in the horizontal and vertical direction, with the breech depicted in the closed and locked position. To unlock and move back, the vertical rams would each move in equal and opposite directions. Afterwards, the horizontal cylinders would move the facility back and the pins attaching these hydraulics would be removed in order to pull the driver further back. This is done because the driver is relatively short and a movement of 12-14 inches is required to remove the diaphragm.



Figure 35. Hydraulic pin holder placed in the breech head with four mounting arms and a blank body that can receive multiple pin configurations.

One of the final component designs that is used in both the breech and backup configuration is that of the pin assembly. When pressurized, the diaphragms bow outward and, even though they are etched, a pin is required to penetrate and instigate breakage. For the breech system, the pin assembly, as shown in Figure 35, uses four bars of steel with

slots machined in them to mount the pin holder to the inside of the pipe. These bars are tack welded to the inside of the pipe and use socket head screws with nuts to fasten the arms of the holder in place. A circular body located at the center of the assembly is threaded to allow multiple pins to be inserted, including the option of a miniature hydraulic cylinder that can be installed to more accurately burst the diaphragms at will.

3.3.2 *Loading Analysis*

Loading requirements on the breech were of great importance for design. Like the structural support stands in Section 5.1, the breech is required to transfer much of the expected recoil when operating the facility, with an upper limit as discussed in Section 2 of 405,000 lbf at 2,000psi.

Pressure ratings are not a huge concern since properly rated pipe and flanges are used through the entire breech assembly. For instance, the breech head is manufactured by using the same 20" 900# slip-on flanges discussed in Section 2.3. Only the o-rings pose a mentionable concern since those will contain a great deal of the pressures along the lineal lengths of the diaphragm holder.

For expected loads, finite element analysis was performed on many of the individual components for the breech, the first being the collar located at the end of the head. Material used for both the pipe body and collar are A36 steel with a yield strength of roughly 36ksi and an ultimate tensile range between 58 and 80ksi [25]. Unlike the rest of the facility, stainless steels were avoided on the breech for purposes of reducing cost and adding strength.

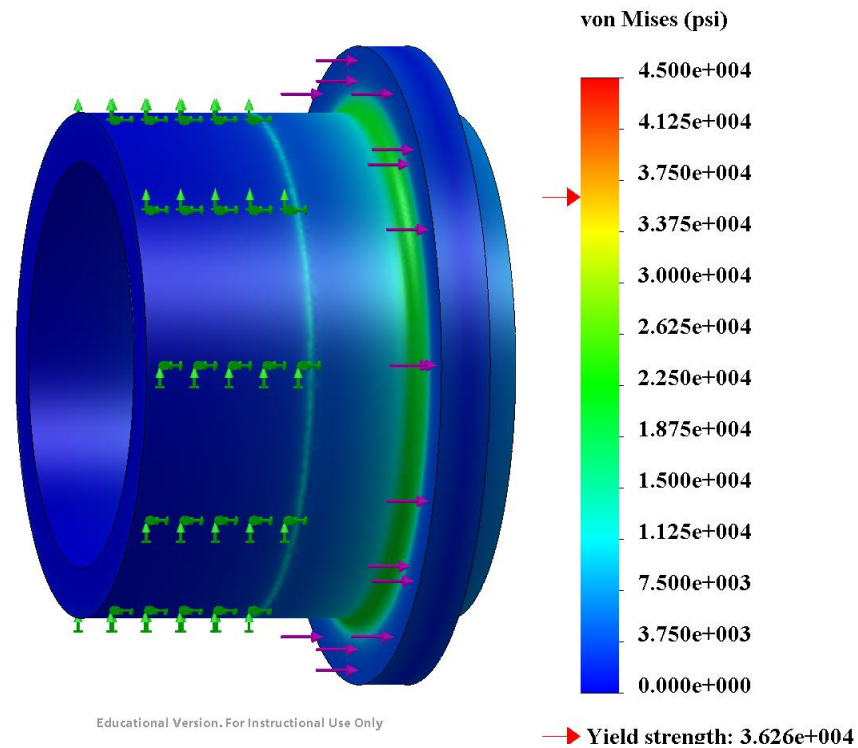


Figure 36. Finite element analysis of the breech head with maximum 405,000lbs of force directed on the collar.

For the breech head simulation, forces are distributed along the face of the collar above the weld point to give a conservative minimum acting area. While not shown in Figure 36, the fixture is modeled by use of fixing much of the outside surface around which the 900# slip-on flange will be welded. This analysis shows that sufficient stress concentrations are located along the joint between the collar and the pipe, which is to be expected. The stresses do not, however, exceed the maximum yield of the A36 shown and does not account for an increase in hardness and strength along the weld seam due to temperature hardening. Thus, the current results are assumed acceptable and can be reinforced by additional weld passes if deemed necessary.

Opposite the breech head, the teeth machined into the seat of the breech are also analyzed along with the matching teeth located in the locking nut. For the seat, 20" schedule 160 pipe is once again used as the main insert, though all forces are expected to be directed straight from the teeth and into the fasteners located on the HB flange. Consequently, only the machined HB flange is simulated using SolidWorks. While not exactly A36 steel, the heavy barrel flange is forged out of A105 steel which has a similar yield strength of 36ksi and an ultimate strength greater than or equal to 70ksi [26].

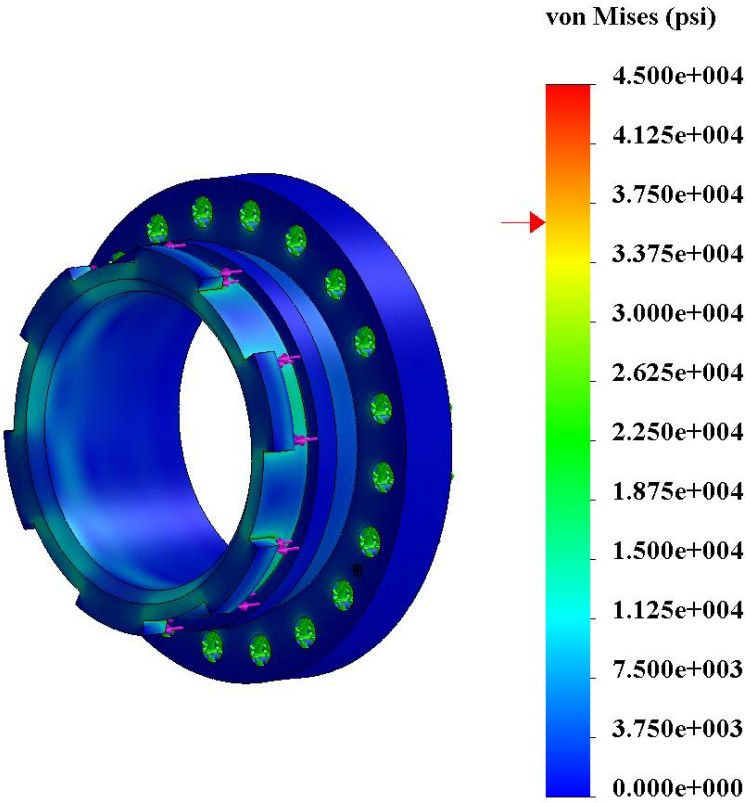


Figure 37. Finite element analysis of the breech seat heavy barrel flange with forces directed on the interlocking teeth.

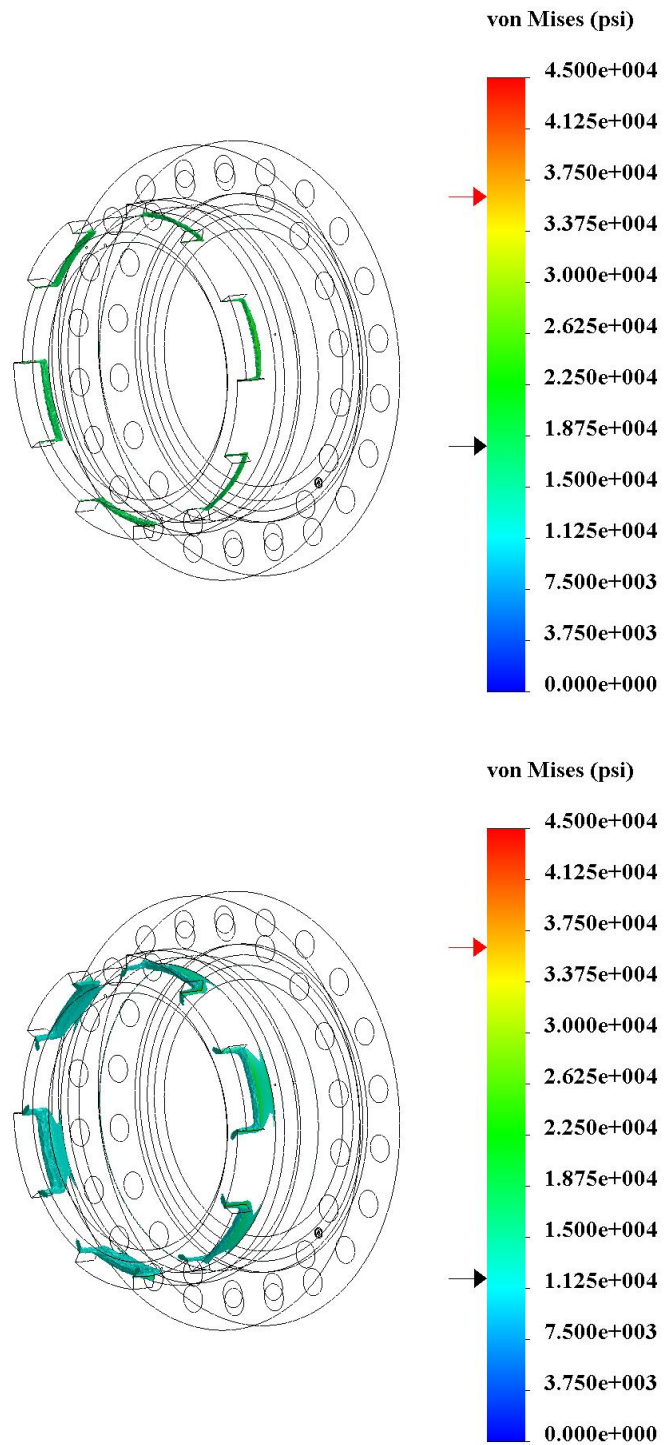


Figure 38. Von Mises stresses with iso-clippings at yields of (top) 18ksi corresponding to a factor of safety of 2 and (bottom) 12ksi corresponding to a factor of safety of 3.

Finite element von Mises stress concentrations appear primarily around the corners where the teeth meet the heavy barrel body, as highlighted in Figure 37 with the greenish hues. These concentrations are expected in this location and are reduced by the addition of a small fillet in this corner. Even so, the stress concentrations are sufficient to provide a minimum factor of safety using yield of 2, which should be sufficient considering it would be near impossible for the recoil force to exceed 810,000 lbs. Iso-clippings of the stresses in Figure 38 show a growth of the stress concentrations around the corners of the teeth when approaching a minimum of 12ksi, or a factor of 3 times lower than the yield point of A105 steel.

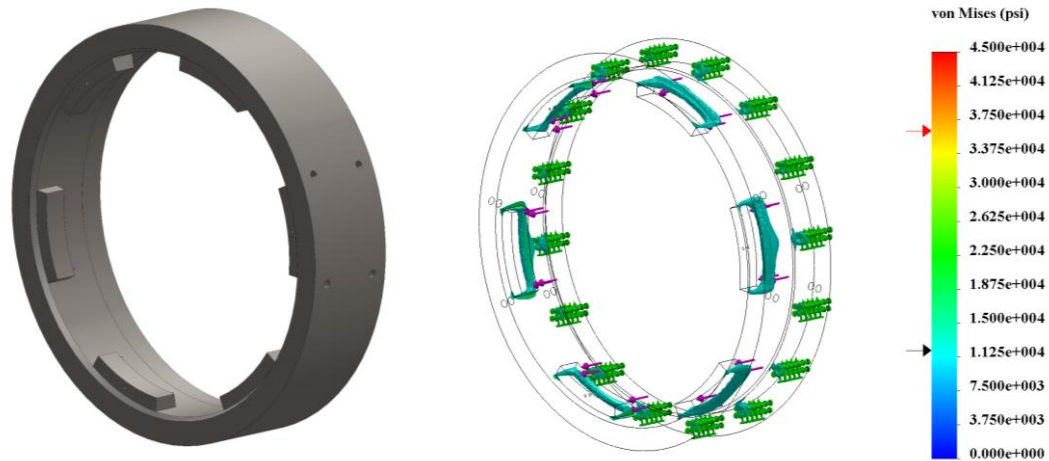


Figure 39. Original locking nut concept with teeth machined into a single component. Iso-clipping of von Mises stresses at 12ksi (FOS 3) if made out of A36 steel.

For the locking nut, a great deal of analysis was performed on the teeth present around the inner diameter. Originally, the teeth were to be made into a single unit as depicted in Figure 39. Von Mises stress distributions are shown on the right side of the

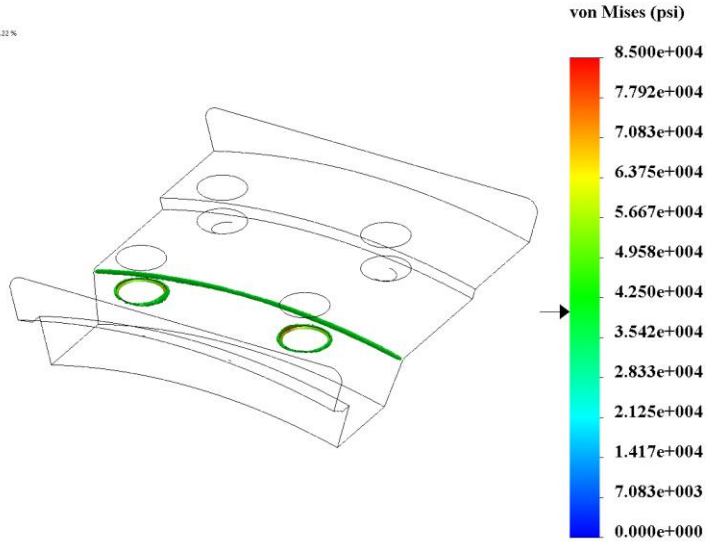
CAD model in Figure 39, with a maximum stress of roughly 15ksi, well below the yield point of A36 steel.

In terms of manufacturing, stronger steels are available to be machined for the locking nut; however, due to the size of the piece, alternate alloys become exponentially more expensive. Alloys 4130 and 4140 were investigated due to their higher yield strengths of 66.7ksi [27] and 60.2ksi [28], respectively, but each of these are difficult to use since water jetting a piece almost 7.5” thick would cause beveling in the cut and torching the shape would temperature harden the alloy, making machining impractical. Additionally, both alloys, especially 4130, are roughly 2 to 3 times more expensive per pound of material.

For this reason, it was proposed to make removable teeth that could be inserted into the locking nut body. This has multiple advantages, such as making the teeth out of much stronger steel (upwards of 80ksi yield) and being able to affordably replace the teeth if they are ever damaged. To do this, however, a way of “bonding” the teeth to the body is required, which is accomplished by use of four fasteners per tooth.

Dividing the maximum recoil load of 405,000lbs by six individual teeth, the load per tooth comes out to be 67,500lbs. For a factor of safety in shear of 3, this means that a total of 202,500lbs should be designed for. Dividing this by 4 total bolts yields a necessary proof load limit per bolt of 50,625lbs. Assuming shear strength to be approximately 0.6 of the rated tensile strength of bolts, this equates to a minimum bolt size of 1”-12 which has a minimum tensile strength for grade 8 bolts of 94,961lbs and calculated shear of 71,500lbs [29].

Model name:Brech Nut-Thread Insert
Study name:Static (3 Default)
Plot type:Static model stress (Stress1)
Volume (Element/Geometric) = 0.40 %/0.22 %



Model name:Brech Nut-Thread Insert
Study name:Static (3 Default)
Plot type:Static model stress (Stress1)
Volume (Element/Geometric) = 0.37 %/0.49 %

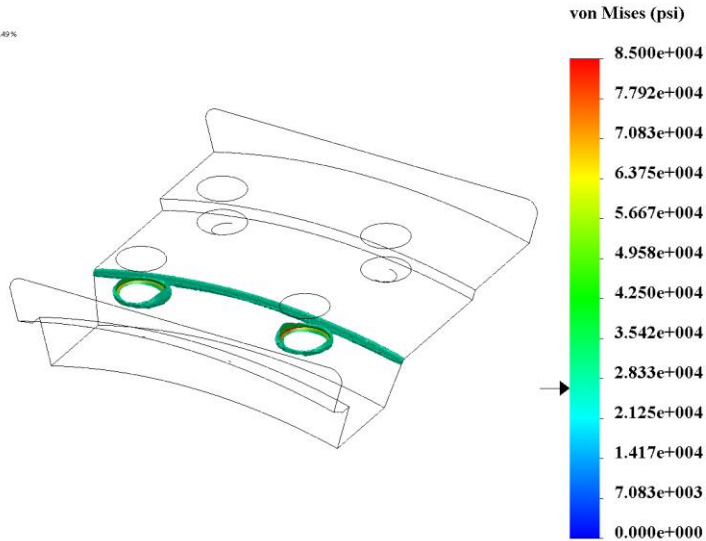


Figure 40. Von Mises stress iso-clipping for values above (top) 40ksi corresponding to a factor of safety of 2, and (bottom) 26.7ksi corresponding to a factor of safety of 3.

Knowing that reasonably sized bolts could hold the shear loads of the teeth, the teeth themselves were simulated using finite element analysis. For this purpose, it is assumed that a small 2.5”x7.5”x7.5” bar of steel with a minimum of 80ksi yield could be

obtained. This assumption is accurate since multiple alloy steels with yield strengths above 100ksi are available, such as A514 [30].

As portrayed in Figure 40, von Mises stresses do not exceed a yield point of 26.7ksi, corresponding to a factor of safety of at least 3 in each tooth. Additionally, a load of 80,000lbs was used in the simulation to yield a conservative value. Even if yielded, the ultimate tensile strength of a material such as A514 is between 110 and 130ksi which compounds the factors of safety in terms of failure [30].

3.3.3 Estimated Cost of Manufacture

Due to the sheer size of the breech and the amount of labor required, it is difficult to gauge how much a system of this magnitude will cost. This section details a rough estimate for the raw materials only and should not be taken as a comprehensive cost analysis for construction. Table 6 lists many of the component costs for the breech [31]. As noted, a final price tag not including labor is calculated just short of \$20,000, meaning sufficient review of the design should be done before construction begins. Labor costs can be expected to equal this number depending on the quality shop chosen.

Table 9. Estimated cost for the raw materials for construction of the breech.

Component Name	Raw Description	Cost
Pipe Sections	20" Sch 160 at 18" & 10" long	\$1,787.00
Breech Seat HB Flange	20" 900# RTJ HB Flange	\$7,350.00
Breech Head Flange	20" 900# RTJ Slip-on Flange	\$3,820.00
Breech Head Collar	26" OD/20"IDx2" A36 Plate	\$455.00
Locking Nut Body	32.5"OD/23"ID x 8" A36 Block	\$2,340.00
Locking Teeth Inserts	2.5"x7.5"x7.5" A514 Steel Bar	~\$400.00/pc
Nut Backplate	34"x34"x1.5" A36 Plate	\$623.00
Thrust Plate	37" OD/ 25" ID x 1" A36 Plate	\$485.00
Thrust Plate Bearings	McMaster PN: 6421K69	\$62.80/pc
	Total Raw Material Estimate	\$19,880.00

3.4 Mylar Diaphragm System

While the breech system could easily reach a price tag of \$30,000, the diaphragm placed in between the driven and expansion sections of HXT requires a much lower pressure rating due to the maximum experienced conditions after the driver. As discussed in Section 2, the accelerator pipe is rated for 700psi, so a diaphragm system being rated more than this is counterproductive. It should be noted, however, that the design presented for the mylar diaphragm system is very preliminary and further engineering work should be conducted before construction begins.

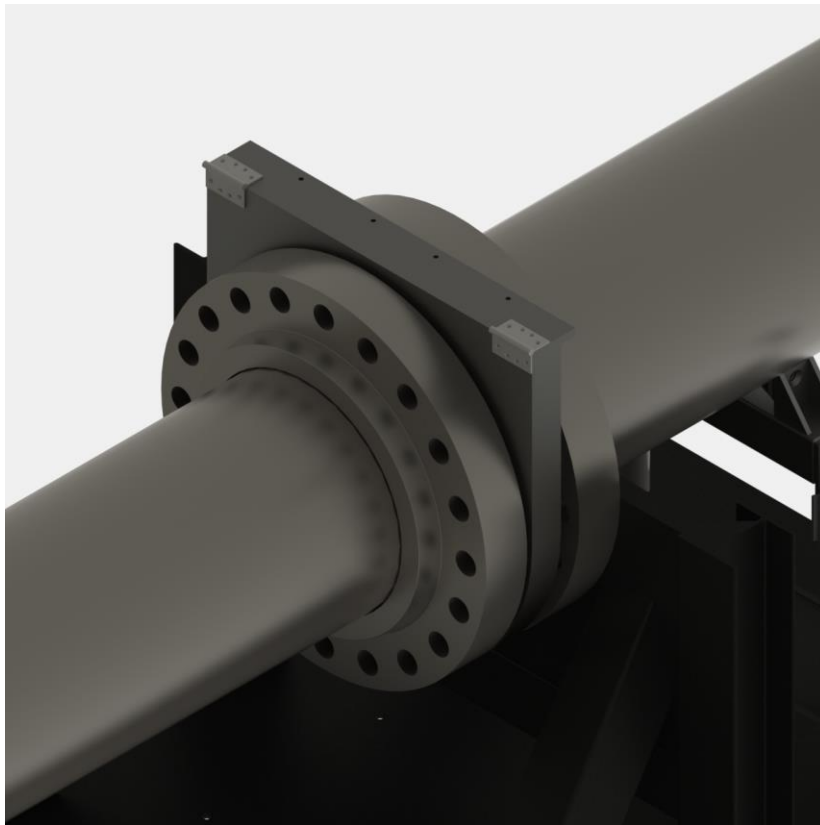


Figure 41. Mylar diaphragm mechanism at the interface between the driven and accelerator sections of HXT.

For these reasons, the mylar diaphragm system, hereby referred to by MDS, is designed using the configuration originally intended for the driver-driven diaphragms, using a slip-in mechanism to quickly replace the mylar, as shown in Figure 41. One of the main reasons this becomes practical for the MDS is the expectation that the mylar vaporizes when the primary shock hits it. Even if a portion of the plastic is still intact, the flexibility of the mylar still allows for a short, stubby diaphragm housing to be designed, whereas a slip-in mechanism for the driver-driven interface would need an opening at least 12 inches long to allow removal of the petalled diaphragm.

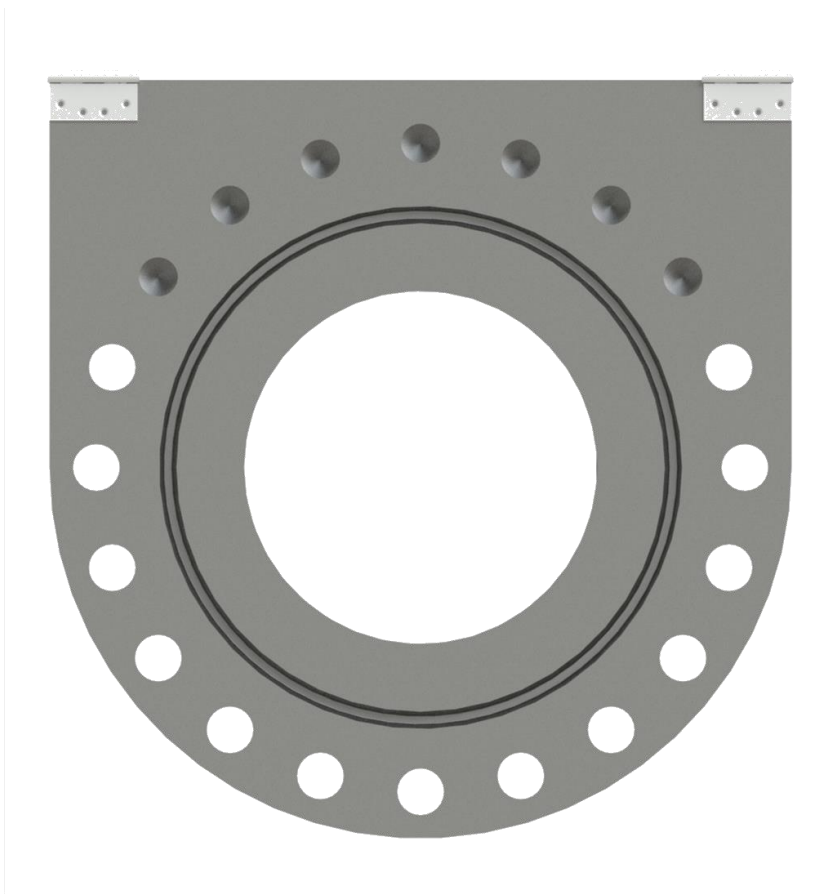


Figure 42. Mylar diaphragm system face using threaded holes up top and clearance holes around the mid to bottom holes.

The mylar diaphragm assembly must interface with the same 20" 900# flanges present in the breech system, though to avoid excess costs, welding on of additional flanges to the MDS was avoided. An alternative to this is to buy two thick plates that serve as the central body to the assembly and either tap threads or drill clearance holes into them that match the hole configuration of the 20" 900# flanges as portrayed in Figure 42 [22]. This allows the nuts and studs to press against the flanges located on the driven and accelerator pipe and screw directly into the MDS. Threaded holes are used on the top region since the diaphragm must slip-in from this direction, preventing the studs from passing through.

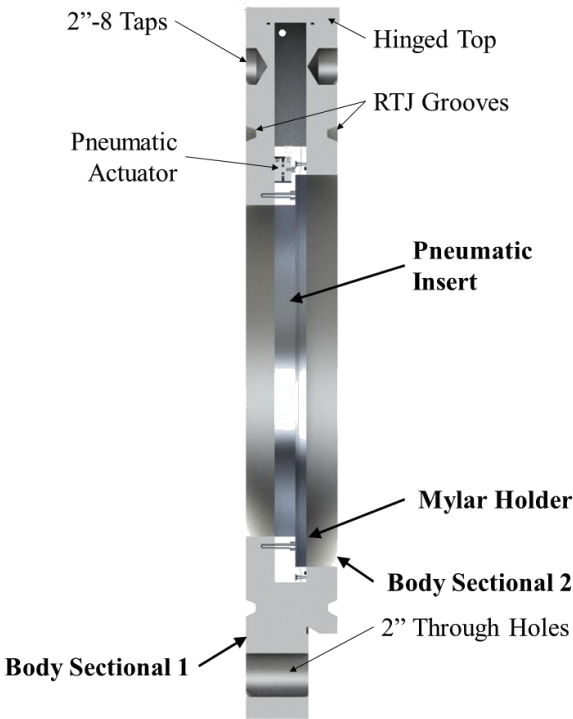


Figure 43. Mentionable design points for the mylar diaphragm system assembly with major components in bold.

Figure 43 displays some of the mentionable design aspects of the MDS, including the matching RTJ grooves to seal between the 20” 900# flanges. Additionally, the body itself made from two large plate, one welded onto the other by means of an alignment groove. This eases in manufacturing since the plates can be water jet to their rough shape and machined. It’s possible some movement will take place during the welding, so additional dowel pin alignment holes should be included which should minimize this to a tolerable amount.

Another huge problem with slip-in disks is the ability to exert enough force on the o-rings of the diaphragm holder, which usually requires the widening of the assembly housing. For the MDS, however, a number of pneumatic actuators are within the body to press against the o-ring. These pneumatics are supplied by high pressure air through a 1/8” NPT connection located near the top of the wall facing outward from the pipe.

Supply lines run through an insert panel, as depicted in Figure 43, which contains enough room for five small-scale pneumatic actuators. The panel also holds counter-bored holes that allow the panel to be fastened rigidly to the MDS main body. Socket head cap screws must be installed with the MDS removed from HXT, where the opening on the accelerator side of the assembly is made a little wider to allow these fasteners to be put in.

When installed, the diaphragm holder contains an o-ring groove that sits against the accelerator side of the MDS. Once supply pressure has been applied to the pneumatics, each of the five arms presses against the diaphragm holder, keeping the o-rings squeezed and the driven sealed off from the driver. The o-ring groove is located on the accelerator side due to the added benefit that once the driven begins to pressurize, the additional force

resulting from the pressure differential of the two sections should increase the sealing effect.

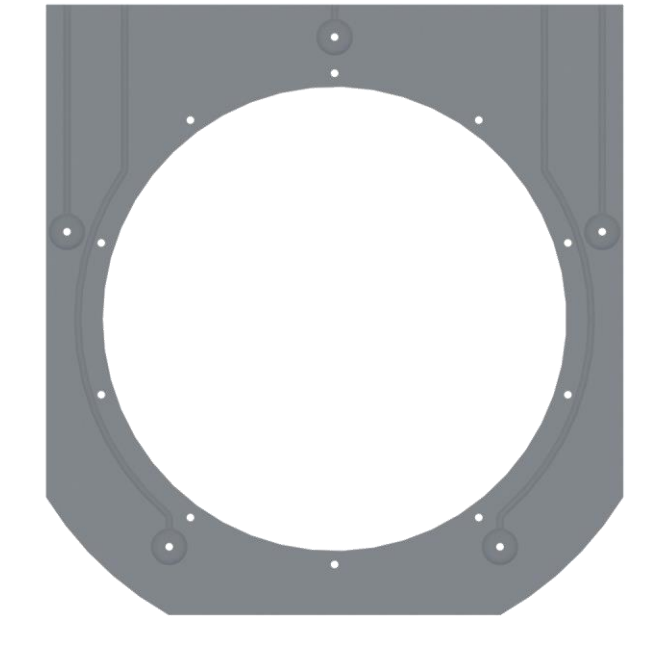


Figure 44. Pneumatic panel recesses for air supply and actuator mounting.

No initial load calculations have been performed on the MDS and no cost estimates have been compiled, reason being that there are still many options being considered along with the pneumatic seals. Another promising concept is to use a similar seal to the one used around the outer diameter of the accelerator pipe going into the test section. This uses an inflatable seal that puts an even amount of pressure across the entire face of the diaphragm holder. Even still, the least complex method would to thread the diaphragm holder into the main body and have the o-ring press against the same face. This would complicate the design, but should theoretically prove more reliable than a pneumatic solution.

3.5 Backup Configuration

For the initial phase of construction, HXT won't be outfitted with either a breech or mylar diaphragm system. Instead, a pipe spacer will act in conjunction with the diaphragm holder in place of the breech system while an even smaller pipe spacer will bridge the gap where the MDS will be mounted. This configuration also acts as a backup to the breech when it is built, allowing the facility to continue to run in case a large component needs to be replaced.

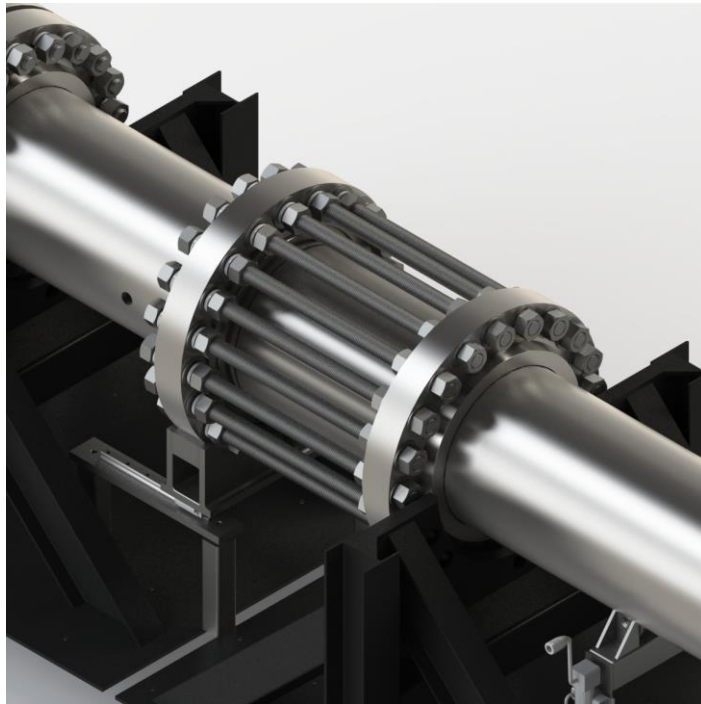


Figure 45. Backup configuration using the diaphragm holder and a 20" schedule 160 pipe section.

The backup configuration uses a 20" schedule 160 section of pipe 25" long along with the diaphragm holder with a thickness of 2", making the overall span equivalent to what the breech system would encompass. Figure 45 shows how the section of pipe and

diaphragm holder are held into place with studs that span from 900# flange to 900# flange. These studs keep a constant, uniform force along the o-rings present on each face of the flanges.

As can be inferred, changing the diaphragm in this configuration is not optimum in terms of quickly testing; however, the simplicity of the design and the access to the materials allows this to serve its primary function while costing very little. Additionally, while slow, the backup configuration has fewer moving parts so the probability of failure for any given component in the “system” is reduced.

Machining of the pipe spacer is required, though kept minimal to feed into the advantage of the configuration costing as little as possible. While primarily serving as a backup to the designed breech system, initial operation of the facility will take place in this configuration to determine the best pin assembly placement, materials, and thickness of the diaphragms that will be used from test to test. Parallel processing of the diaphragm characterization and further breech development is achieved by means of this initial configuration, especially since breaking metal diaphragms can and should be done without the use of mylar diaphragms.

The mylar diaphragm spacer is machined at ten inches, which is 5.6” longer than the proposed pneumatic mylar system. This is done to accommodate any extra space that may be needed when the MDS is built. For example, if the threaded concept is developed and requires additional space between the flanges, the extra 5.6” can extend the main body. If more than this amount of space is needed it is possible move the driver and driven back, though bolt spacers would be needed to stand the 20” 900# flanges off from the stand

faces. This would only account for a few additional inches and should not extend more than 2.5”.

4. BACK ASSEMBLY DESIGN

4.1 Requirements

Consisting of the test section and tailpipe, the back assembly houses all the test models and their instrumentation, which makes it the most important section in the facility from a research point-of-view. An overview of the assembly is depicted in Figure 46. The test section will see the most frequent day-to-day use, meaning higher wear and potentially more maintenance. Consequently, a great deal of consideration is put into the back assembly design to allow for a wide range of model types and diagnostic tools while also minimizing effort needed to access them. A list of requirements was conceived before engineering began, some of which are listed in Table 2 and the rest in Appendix A.

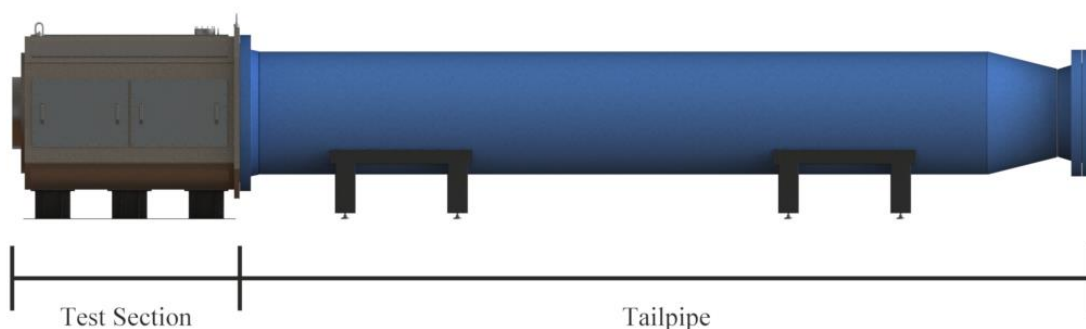


Figure 46. Back assembly overview consisting of the test section and tailpipe.

Due to safety reasons, the most vital requirement for the back assembly is the condition that it handles all operating pressures both before, during, and after a run. Before a test, the back assembly is under the presence of a full vacuum (~ 0.1 torr) and, while not usually a concern for most facilities at the NAL, vacuum begins to cause more structural

strain the larger the diameter of the pipe. Inversely, maximum pressure experienced by the back assembly is determined by the redistribution of gas in both the driver and driven to the full volume of the facility after operation. A calculation of these volumes and pressure extremes are detailed in Section 4.3.1. An additional, consequent requirement of the operating pressures is that any securing of access points, such as doors and windows, must be able to properly withstand the forces derived from those pressures.

As discussed in Section 2.2, the back assembly requires the placement of a shock delay line directly opposite the flow entrance into the test section. This tailpipe serves to allow ample space for the elongated test gas to flow into before reflecting and travelling back upstream into the test section, maximizing run time. Section 4.2.2 examines the design of the tailpipe and its interface with the test section.

Table 10. Select primary requirements and their respective derived requirements for the back assembly.

Primary Requirement	Derived Requirement
<u>Shall</u> safely operate at all expected pressures both before, during, and after a run.	<u>Should</u> utilize multiple pressure relief mechanisms to avoid the potential scenario of over-pressurization.
<u>Shall</u> have the ability to mount sensors, optics, and test models from the inside walls of the test section skeleton.	<u>Should</u> utilize multiple ¼”-28 threaded holes on all faces of the test section except the slants.
<u>Shall</u> include a pipe located behind the test section to delay the test gas from interfering with itself before the whole test time is complete.	<u>Should</u> include a 20ft pipe as the tailpipe using a standard ANSI flange interface to seal appropriately.

Another distinguishing requirement is to have versatility in mounting the models and other multiple diagnostic instruments inside the test section. For HXT this was resolved fairly simply by machining threaded holes on every surface of the skeleton. These

points allow mirrors, model stings, sensor probes, and breadboards to be placed where needed without additional machine work and down time.

4.2 Design

4.2.1 Test Section

Many of the primary requirements pertaining to the test section originally focused on the capability to easily access the test models and instrumentation from run-to-run. Some of these initial concepts included the luxury of toggle clamps to fasten access panels and pull the test section apart from the tailpipe. Figure 47 shows an early rendering of the assembly with clamps securing the doors. Another approach not depicted was to mount the test section to rails, have it secure to the tailpipe with larger toggle clamps, and allow a greater deal of access to the test model through the back.

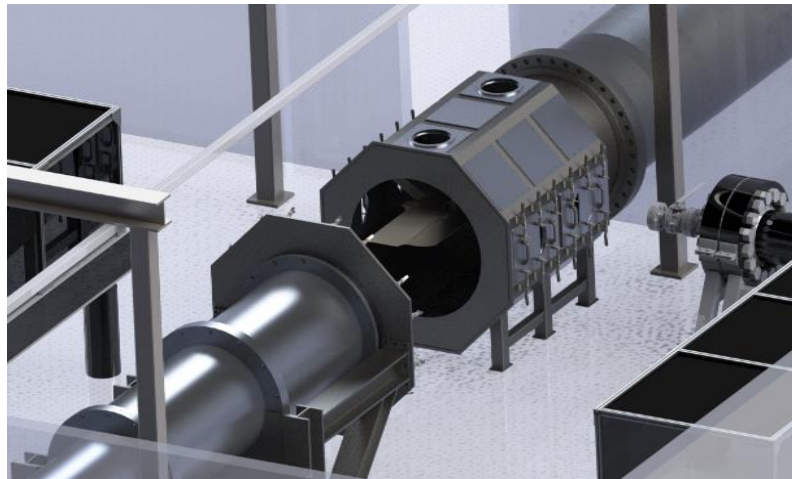


Figure 47. Concept illustrating the test section's original design as a true octagon with toggle clamps for securing doors and the ability to separate from the front of the facility.

Even though the design for toggle clamps was heavily invested in, the loading capacity of clamps is dwarfed by the huge surface areas of the doors and unbalanced pressures between the front and back plates of the test section. Section 4.3.2 details these loading requirements and the substantial advantages of using high grade conventional fasteners in place of toggle clamps. Moreover, because of this eventual change, the significant number of bolts, and the unnecessary need to maintain yet another large o-ring seal between the test section and tailpipe, it was determined that the entire back assembly be rigidly bolted into the ground for additional safety.

The final design for the test section is shown in Figure 48. As depicted, the test section consists of a welded skeleton, ten access panels, and a stand to bolt into the floor. The accelerator pipe enters the test section from the bottom left face as shown in the figure while the tailpipe interfaces with the side opposite and out of view of the rendering.

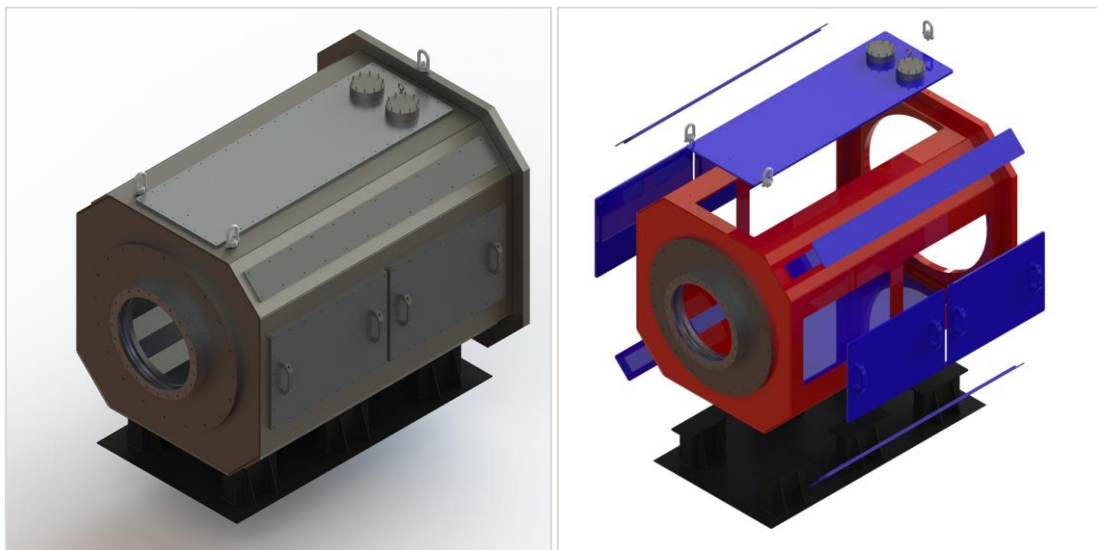


Figure 48. CAD renderings of the test section with skeleton (red), access panels (blue), and base stand (black).

Because rectangular prisms have increased stress concentrations on their corners when under pressure, the main skeleton has an octagonal cross-section. While not as advantageous as a round face which distributes stress uniformly, the flats associated with the octagon allow the placement of windows and doors to access the test model. The test section measures 70" long inside from face to face, with two flat-to-flat lengths of the octagon at 60.75" and 52" as illustrated in Figure 50. Each lateral face was designed to have a wall thickness of 0.5", which was increased to 0.6" to reduce face-off machine time for each plate.

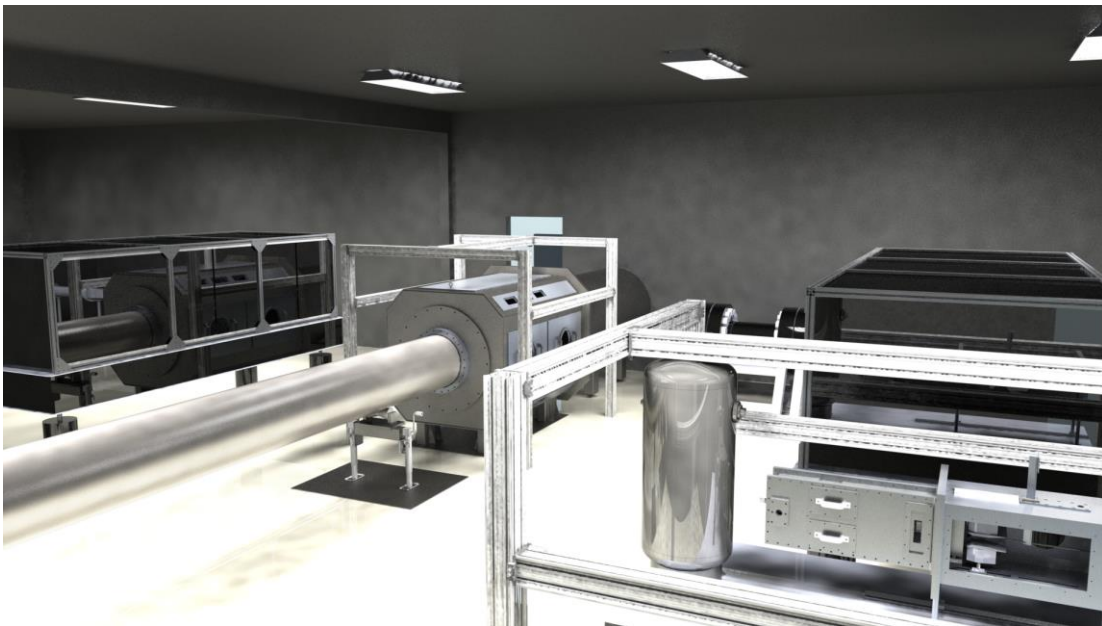


Figure 49. The test section as it would appear at the NAL without a nozzle and with the tailpipe protruding through a wall to the outside.

The diagonal faces of the octagon are made shorter to maximize access through the sides and are specifically designed so that the length of one horizontal/vertical face and one diagonal face are equal to just under 48". This is chiefly done from a

manufacturing standpoint, as standard plate sizes plateau at 4'x8'. Section 4.4 further discusses the process of manufacturing the test section skeleton.

Each lateral face of the skeleton, minus the diagonals, also contains two series of ¼"-28 threaded holes for mounting. In total, each plate has sixteen of these holes in order to mount optics, test models, pitot probes, or any other sensors that may be needed.

Both the front and back plates of the skeleton are significantly thicker than the lateral plates, at 1.25" and 1.9" respectively. The front plate is machined with a diameter of 37.00" to accept the planned nozzle mentioned in section 2.4, which has an exit diameter of 36". While a nozzle is not in use the current configuration of the facility, as is pictured in Figure 49, it does include an adapter plate to reduce this opening to 20.5" and allow the installation of an inflatable seal. The adapter plate mounts to the skeleton using twenty 3/8"-24 bolts and a 300 series o-ring groove. Mechanical Research and Design, Inc. manufactures the seal and housing that is detailed in Section 4.3.3 with full technical drawings presented in Appendix B [32].

The back plate wall thickness (1.9") is calculated by adding the expected wall thickness of 0.50" to the minimum threading distance acceptable for a 1 ½". This bolt hole size is used to secure the tailpipe to the test section and patterned based off the matching 42" 150# flange that it mates with. Because the test section must maintain a seal, the bolts could not go all the way through the back plate. Similarly, the width and height of the back plate was determined by the mating tailpipe flange which possesses a hub diameter of 53". Figure 50 depicts how the back plate dimensions rely heavily on the tailpipe flange, increasing its overall size and weight.

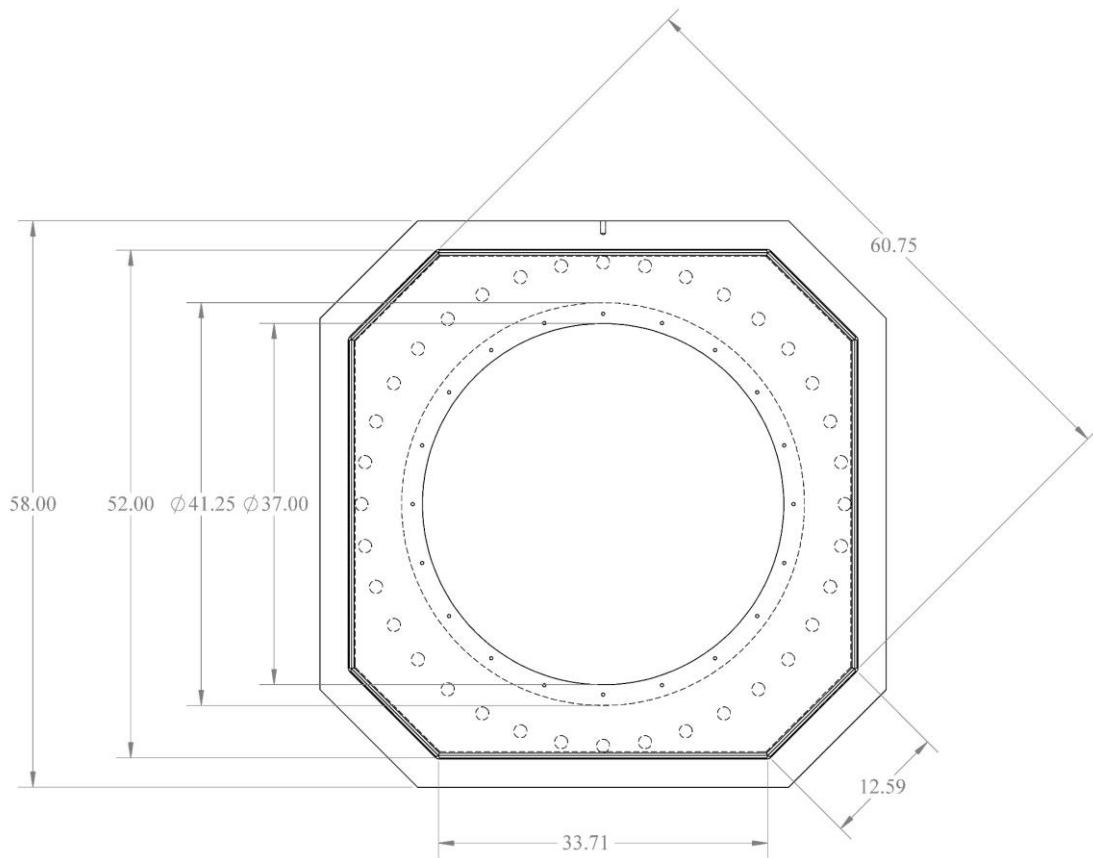


Figure 50. Key dimensions of the test section with flat-to-flat lengths and hole diameters.

Overall there are ten access panels: four general purpose doors along the sides, four slant panels, a roof access panel, and a floor access panel. Because the entire side face need not usually be accessed from run-to-run, typical access through the sides was split into two door access holes measuring 29.5" wide by 20" in height, as detailed in Figure 51. Furthermore, each door is fastened with twenty-four 1/4"-28 socket head cap screws, whereas a single panel would require approximately forty, reducing panel removal time. Two handles, rated for 100lbs each, accompany each door for additional ease of removal,

leaving an approximate square area of 24"x20" between the handles and cap screws for the placement of windows or mounting of probes.

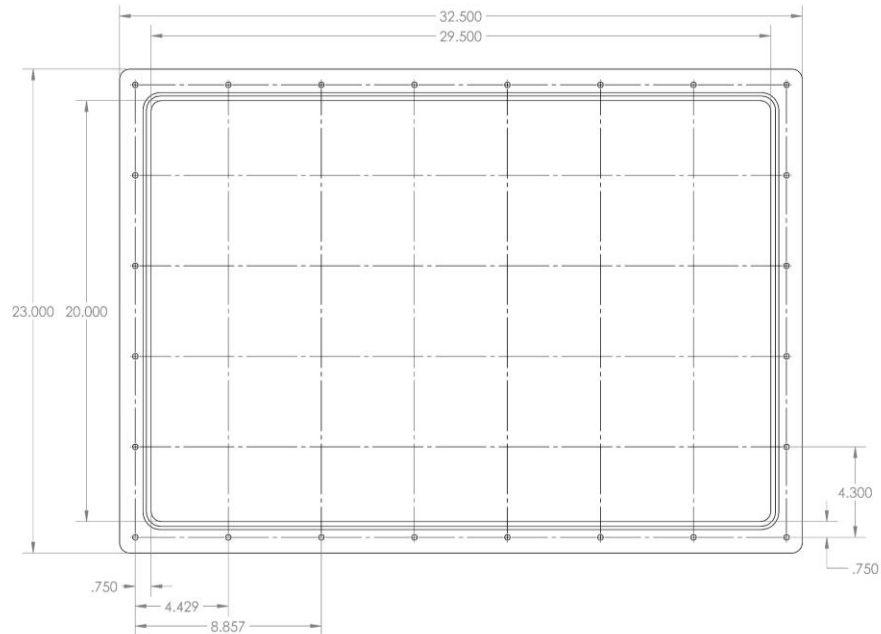


Figure 51. Test section door with mounting holes and flange. Inside dimensions are associated with the access hole located on the skeleton.

The slant, roof access, and floor access panels serve a much more passive role since none are expected to be used from run-to-run. Instead, these panels serve primarily to allow laser beam access to the test model. The roof access panel is the exception, with an additional use of allowing test models to be inserted or removed when too large to use the side doors. Additionally, the roof has two pressure relief plates for safety which lift when the test section experiences a slight positive pressure. These are discussed more fully in Section 4.3.

To avoid mounting holes around the test section stand, the floor access panel was specially designed to be inserted from the inside, whereas all other panels mount into

threaded holes on the outside of the skeleton, as presented in Figure 52. Because of this, the roof access hole measures at 22” wide by 64” long and the floor access hole measures at 18” wide by 64” long, allowing the floor access panel to be lowered from above with the use of a crane. The test section bolts into the stand using twenty-four 3/8”-24 bolts that are machined into the underside of the skeleton.

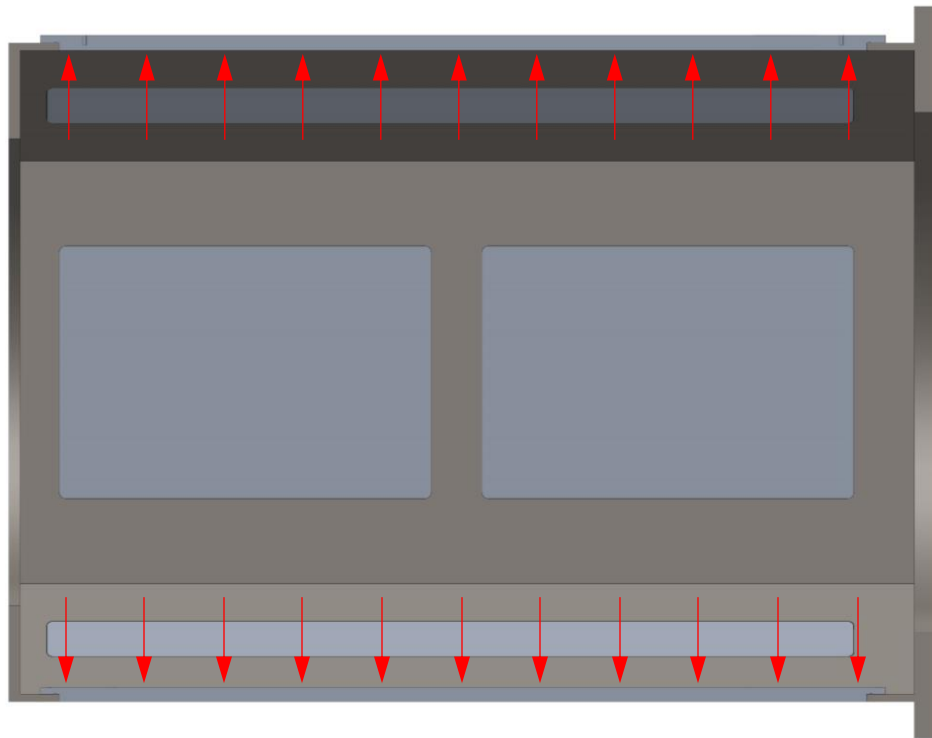


Figure 52. Cross-section detailing the mounting orientation of the roof and floor access panels with expected pressure distribution.

All access panels for the test section contain the interface seals so that if any grooves are machined incorrectly or designed improperly they can be fixed relatively easy. Any machining of the test section skeleton would require shipment to a specialized shop resulting in unnecessary downtime, so all dimensional uncertainties such as o-ring grooves

and pressure taps are designed into access panels. O-ring sizing is discussed at length in Section 4.3.3.

4.2.2 Tailpipe Design

In order for the flow to pass over the model uninterrupted, the tailpipe is fastened directly to the back plate of the test section skeleton to allow the test gas to expand into the vacant space of the tailpipe. [Include paragraph detailing wave reflection graph to determine minimum tailpipe length]

A final length of 20ft was accepted due to standard available pipe, which adds an additional 6ft of travel (3ft down the pipe and 3ft back up) to account for any uncertainties in shock or test gas travel speeds.

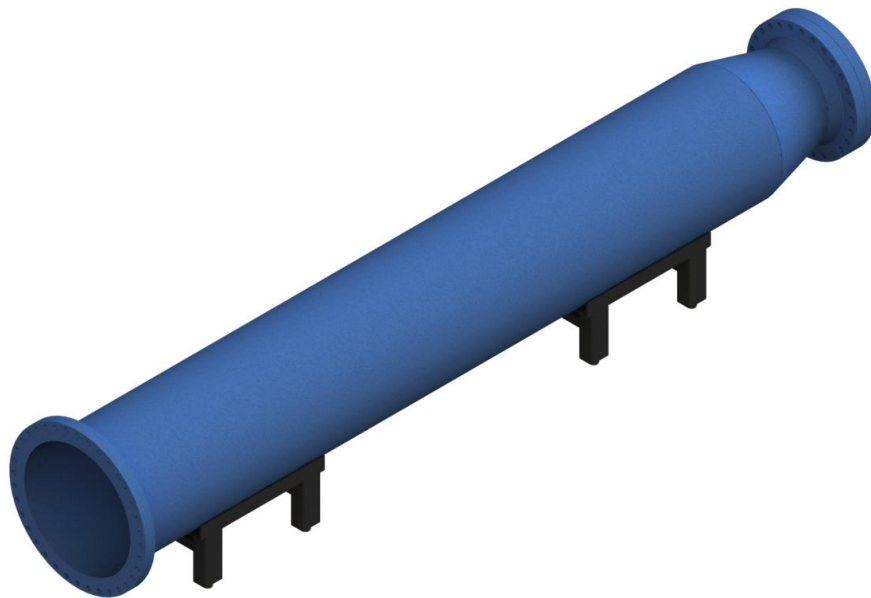


Figure 53. Full overview of the tailpipe with the 42" flange of the bottom left and the reducer and 30" flange on the top right.

The diameter and schedule of the tailpipe are similarly vital in that these two parameters greatly influence the pressure rating, end-of-operation pressure, and cost of manufacturing. Initially, a diameter of 54" was investigated to maximize total volume and reduce the end-of-operation pressure. In the end, the cost for pipe and matching flanges outweighed the benefit of slightly larger volumes and lower pressures. A final size of 42" was accepted due to its ample expansion margin for a 36" nozzle exit and overall cost of \$112/ft. The standard schedule (0.375" w.t.) for a 42" pipe, which is the largest schedule for a pipe this large that does not need special fabrication, is rated for 189psig [17].

For both ends of the tailpipe, interfacing flanges were dictated by standard ANSI/ASME flange class ratings. Figure 53 depicts the whole tailpipe assembly in its planned initial configuration. The end of the tailpipe which connects to the test section has a 42" 150# raised face slip-on flange welded to the end of the pipe. A technical drawing of this flange can be found in Appendix B. This flange is rated for 285psig [18] and bolts directly into the back plate of the test section skeleton using thirty-six 1 1/2"-6 grade 5 bolts at a length of 4" long each. A 1/8" thick, full face gasket is used to seal between the raised face of the flange and the flat face of the test section. Silicone was chosen due to its low cost and chemical resistance for the potential use of corrosives such as nitric oxide in diagnostics.

Opposite the test section, the tailpipe necks down to a 30" OD with a 300# raised face weld neck flange. This flange then bolts into a 300# raised face blind as depicted in Figure 53. A 30" 300# flange is rated at 750 psig [18], which is significantly more than that of the 42" flange because of the uncertain stagnation pressures associated with this

section of the facility. Ideally, the flow would expand as it enters the larger diameter of the tailpipe and the stagnation pressure would decrease; however, due to the extreme difficulty in predicting the flow behavior in a facility such as this, a decision was made to increase the pressure rating at this end for safety purposes.

4.2.3 Air Receiver Option

The reasoning behind reducing the tailpipe diameter to 30” was not only influenced by the reduced cost when increasing to a 300# flange and blind, which would roughly double, but also by the potential benefit in attaching an air receiver tank directly to the weld neck flange in place of the blind as illustrated in Figure 54. An air receiver tank acts as a dead volume to decrease the end-of-operation pressure, which does not affect the operational range of the facility in expansion mode but does significantly widen the Reynolds number testing envelope for shock tunnel mode.

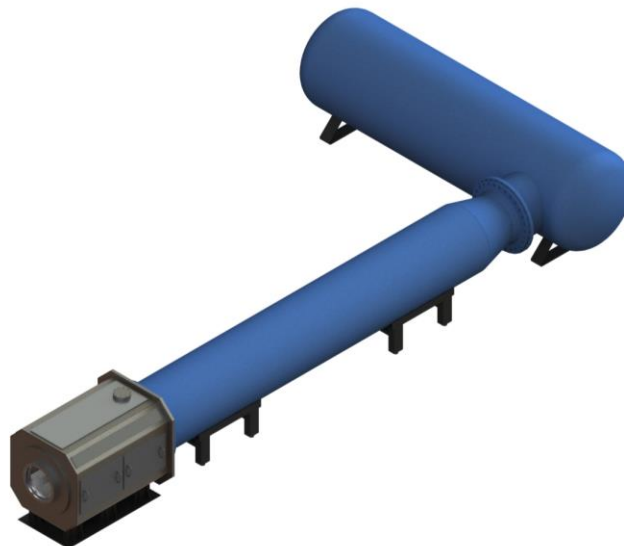


Figure 54. Overview of the air receiver attached to the tailpipe in place of the blind flange.

Physically, the air receiver is a large, custom order pressure vessel oriented horizontally and perpendicularly to the direction of flow. The outer diameter of the main vessel is 60” and contains stiffening rings to prevent implosion under vacuum. The rated volumetric space of the tank is 2,520 gallons (582,120 in³) and is rated for a pressure of 137 psig [33]. A single flange is located at its end with a short section of standard schedule 30” pipe and a 30” 300# raised face slip-on flange. It is important to note that if this option is executed then the hole alignment must match that of the 300# flange welded to the tailpipe. This orientation was random for convenience when welding at the NAL. Figure 7 details a modification to the operational envelope of the facility both with and without the use of the air receiver tank and an increase in maximum pressure for the ST mode driver up to 930psi.

Table 11. Volume for each section of the facility. [L]:length, [d]:diameter, [CSA]:cross-sectional area of the prism.

Section	Dimensions [in]	Volume [in³]	Volume [gallons]
Driver	60”[L]x16.064”[d]	12,160.42	52.64
Driven	180”[L]x16.064”[d]	36,481.26	157.93
Accelerator	600”[L]x19.00”[d]	170,117.24	294.58
Test Section	2,447.875 in ² [CSA]	171,351.25	741.78
Tailpipe	252”[L]x41.25”[d]	336,773.82	1457.89
	Total w/o Receiver	726,884.00	3,146.68
Air Receiver [33]	220”[L]x60”[d]	582,120.00	2520.00
	Total with Receiver	1,309,004.00	5,666.68

Table 11 lists the total volumes for each individual section of HXT. As noted, the tailpipe provided almost half of the total volume available while the back assembly as a

whole, without the air receiver, makes up over 75%. With an air receiver at 2,520 gallons, the total volume of the facility almost doubles.

Table 12. Mass, in kg, present in each section assuming a driver pressure of 2000psia and driven pressure of 110psia for XT mode, and a driver pressure of 500psia and driven of 50psia for ST mode. The end-of-operation pressure(EoOP) is calculated using the entire volume of the facility.

	Driver	Driven	Acc.	Test Sect.	Tailpipe	EoOP [psia]
XT	32.25	5.32	~0.00	~0.00	~0.00	38.12
ST	32.25	N/A	2.26	2.27	4.47	42.79
ST-AR	32.25	N/A	2.26	2.27	4.47	23.76

Expansion tunnel mode, as detailed in Section 2.2, operates with a maximum driver pressure of 2000 psia and a driven pressure not to exceed 110 psia. Table 12 calculates the mass in each section assuming the ideal gas law and an ambient temperature of 297K (75F) both before and after a run. The far right column lists the pressure when using the same equation but with all the masses distributed between the sum of all the volumes expressed in Table 11.

Shock tunnel mode differs in that the ST-driver is the sum of both the XT-driver and XT-driven pipe lengths. Because this combined volume of 210.57 gallons would quadruple the mass if operated at 2000psi, the operating pressure of the shock tunnel mode was reduced to 500psi. Table 12 lists the difference in end-of-operation pressure with multiple ST-driver pressures and an across-the-board ST-driven pressure of 10psi. Limiting the ST-driver pressure to 500psia forces the end-of-operation pressure of 42.79psia to be comparable with expansion tunnel mode.

The addition of an air receiver allows the shock tunnel mode to increase its driver pressure to approximately 1000psia, and, though not as high as the expansion tunnel driver

setting, increase the operational Reynolds number range of the mode as depicted in Figure 7.

4.3 Load Calculations

A significant amount of effort was exhausted insuring the test section and tailpipe would hold expected loads. These forces are analyzed in two subsequent sections: pressure ratings and access panel forces as a result of those pressures. An additional subsection briefly discusses the design of the o-ring grooves present throughout the entire back assembly.

4.3.1 Pressure Ratings

All forces in the back assembly, neglecting gravity, originate from either the presence (internal pressure) or absence (external pressure) of mass contained within the facility. Preceding operation, the back assembly is pumped down to the lowest achievable pressure, which is optimistically expected to be around 0.1 torr. Conversely, the extreme for positive pressure is determined by the redistribution of mass in both the driver and driven to the entire volume of the facility after operation. These pressures are calculated and presented in Section 4.2.3 when discussing the optional air receiver.

With a consistent expected pressure not to exceed 43psia between expansion tunnel and shock tunnel modes, design of the back assembly could proceed. Original design of the test section, as discussed in section 4.2.1, called for an octagonal prism made of A36 carbon steel with eventual wall thicknesses of 0.60". Finite element analysis was performed on this design using a pressure of 40 psig, a yield strength for A36 steel of

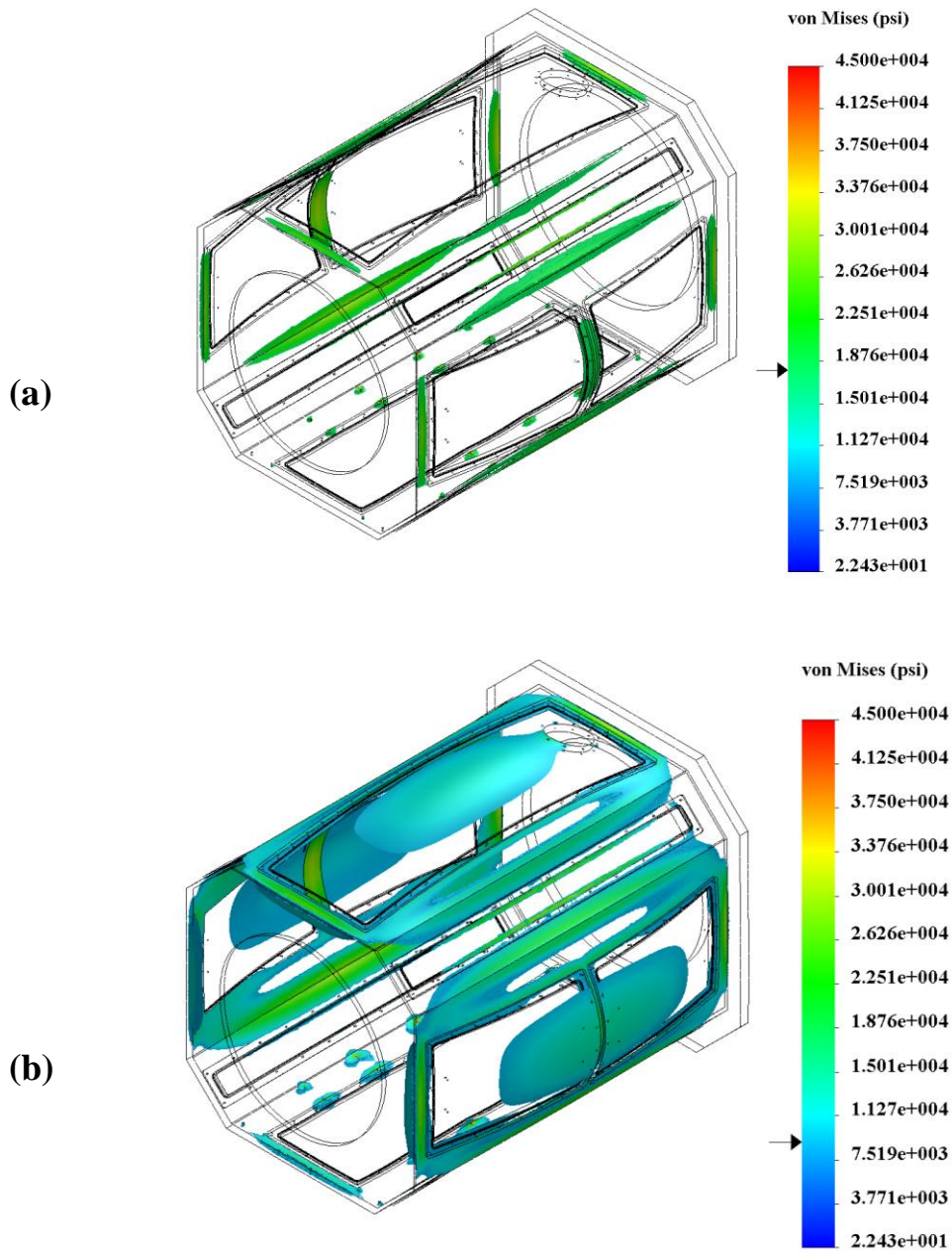


Figure 55. Iso-clipping of von Mises stresses in the originally designed test section using (a) 18ksi corresponding to a factor of safety of 2, and (b) 9ksi corresponding to a factor of safety of 4.

36ksi [25], and a yield strength of aluminum 6061-T651 of 35ksi (low side). Figure 55 illustrates an iso-clipping of 18ksi and 9ksi for the assembly's von Mises stresses.

Because the original design does not meet the requirement that that test section have at least a factor of safety of 2, modifications were made. The first addition was the welding of a rib through the middle of the skeleton to prevent bowing, as depicted in Figure 56. The rib runs between the two door cutouts and spans across the roof access where a series of screws can be fastened from the inside, through the rib, and into the access panel. The rib ends at the floor access plate since the support stands prevent excess bowing along the bottom of the skeleton.

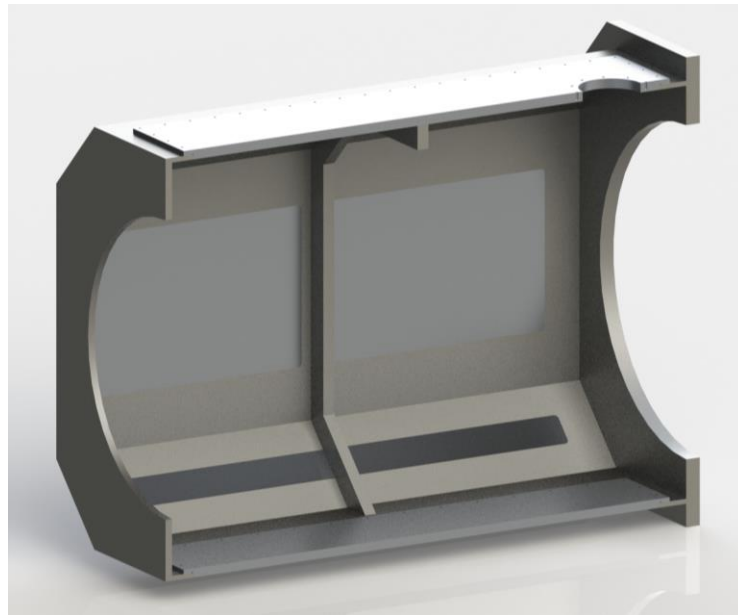


Figure 56. Cross-section of the test section with a rib welded to the inside of the skeleton to increase support.

Finite element analysis was once again performed on the test section with the rib welded to the skeleton. These results are presented in Figure 57 with isolated von Mises

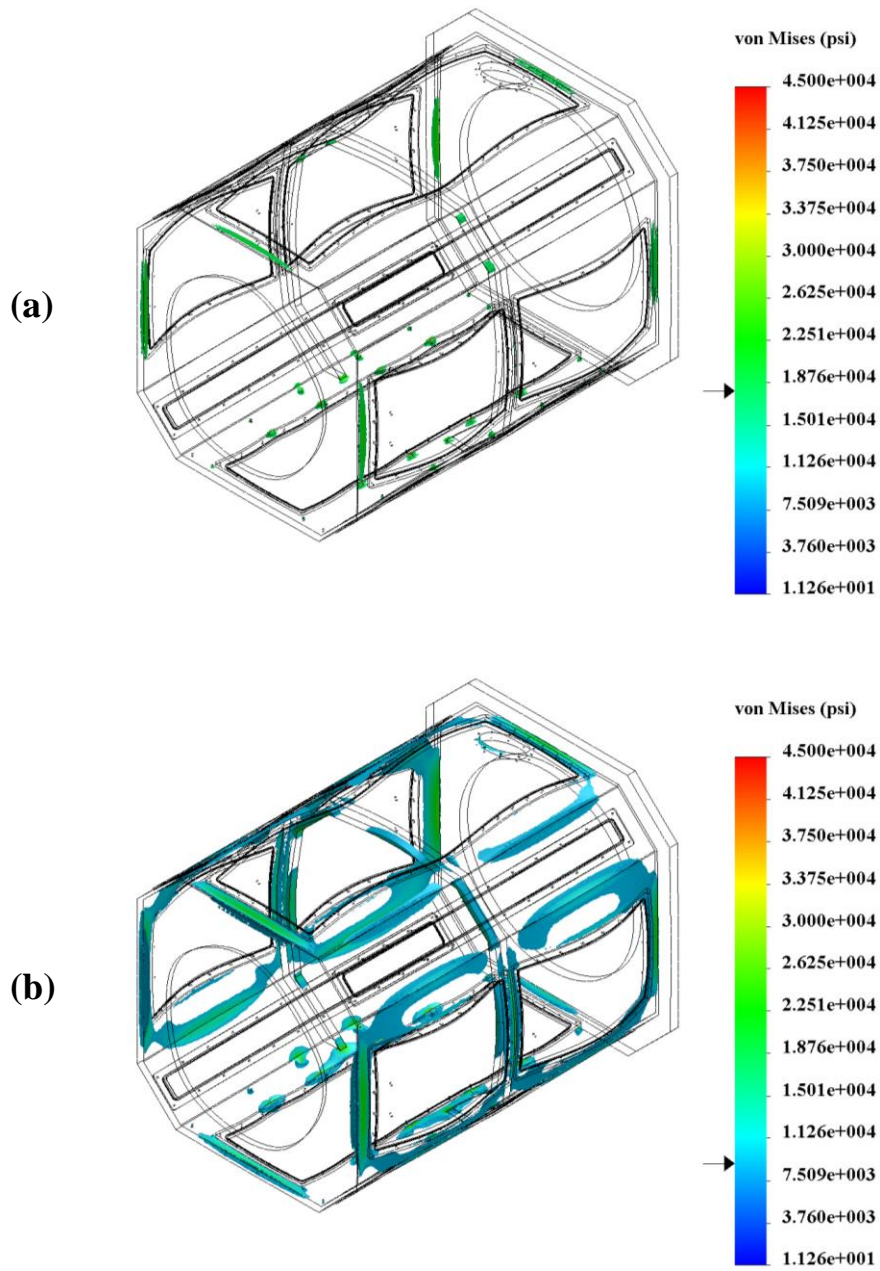


Figure 57. Iso-clipping of von Mises stresses with the addition of a rib located halfway down the length of the test section for (a) 18ksi corresponding to a factor of safety of 2, and (b) 9ksi corresponding to a factor of safety of 4.

stresses corresponding to a yield FOS of 2 and 4, reducing the bowing experienced around the midsection and decreasing the maximum experienced stresses.

A limitation to the finite element analysis performed is that SolidWorks assumes all coincident surfaces to be perfectly bonded, whereas usually the surfaces are welded or fastened. FEA also does not account for variations in the weld, such as addition of weld or locations where weld may still sit underneath the beveled surface. Overall, however, the pressure rating of the test section does not solely depend on FEA, as hydrostatic testing will certify the structural integrity of the entire back assembly up to 80 psig.

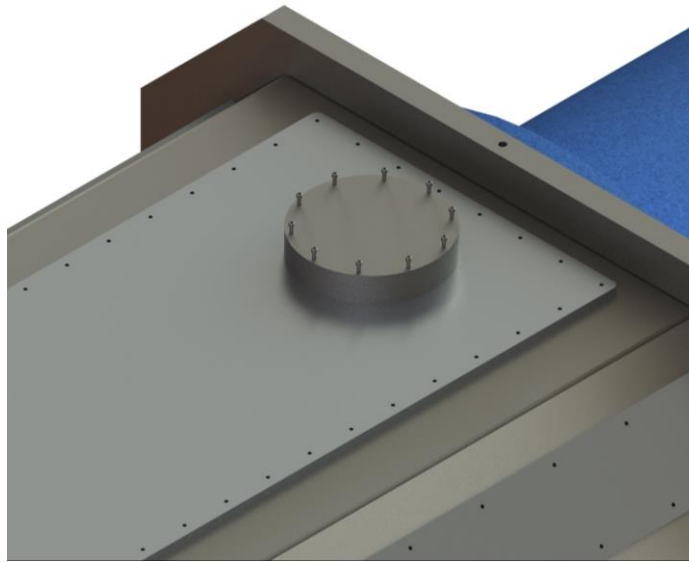


Figure 58. Pressure relief plate set for approximately 1psi differential to assist with avoiding over-pressurization of the back assembly.

A further safety measure designed into the test section is the addition of a pressure relief plate. This plate simply seals against the top face of the roof access panel using the force of gravity. When under vacuum the relief plate has additional force due to atmospheric pressure which assists in sealing, whereas an internal positive gauge pressure

begins to act against the weight of the plate. Made out of stainless steel with a diameter of 10.25”, thickness of 2.00”, and weight of 46.5lbs, the relief plate sits above an 8.00” diameter hole with an area of 50.27 in². Using a simple free body diagram with the weight of the plate and the pressure across the hole with a result of 0.925 psig. Figure 58 illustrates the position and orientation of the relief plate as it should appear on the facility.

Pressure rating of the tailpipe, as briefed in Section 4.2.2, is evaluated using the lowest common pressure rating of the components welded together. Table 13 lists each component with its verified pressure rating. Since the 42” 150# flange contains the lowest workable pressure, the tailpipe is listed as having a 189psig pressure rating which far exceeds that designed into the test section. Because of this, the tailpipe is not hydrostatically tested past the limits of the test section at 100psig.

Table 13. Component list for the tailpipe along with pressure ratings and the source used to list the pressure rating.

Tailpipe Component	Pressure Rating (psig)	Source for Rating
42” Std Sch Pipe (0.375” w.t.)	189	[17]
42” 150# RF Slip-on Flange	285	[18]
30” 300# RF Weld-Neck Flange	750	[18]
30” 300# RF Blind	750	[18]

4.3.2 Forces Due to Pressures

As mentioned in Section 4.2, there was a brief investigation into the use of toggle clamps during the brainstorming of ideas at the onset of the project. These would allow quick and convenient access into the test section, reducing time to adjust instruments or change models through the side doors. These were abandoned when the forces due to the maximum pressures were calculated for each panel.

Using a maximum end-of-operation pressure of 42.8psig (28.1psia), the force exerted on each panel was calculated and is recapped in Table 14. The main concern when designing the fastening of the access panels is that the force due to the pressures may overwhelm the proof load ratings of the combined bolts that hold them to the skeleton. Assuming a grade 8 bolt with a minimum tensile strength of 150ksi, minimum yield of 130ksi, and minimum proof strength of 120ksi, the minimum number of bolts for each panel is listed with the maximum force. These values are accompanied by the actual number of bolts used. All calculations were done using a proof load of a ¼”-28 bolt of 4,350lbf [34] as is rated for a grade 8 bolt.

Table 14. Dimensions and resulting forces on each access panel with minimum required bolt number using ¼”-28 Grade 8 bolts with a proof load of 4,350 lb_f.

Access Panel	Dimensions	Area [in ²]	Max Force [lb _f]	Min. Bolt	Bolt #
Door	29.5”x20”	590	16,570.84	4	24
Slant	64”x4”	256	7,190.06	2	24
Roof	64”x22”	1408	39,545.32	10	36
Floor	64”x18”	1152	32,355.26	8	36

The number of bolts used to secure each panel was quadrupled for a factor of safety of four with the exception of the roof access panel, which was designed with approximately 48 bolts but was reduced to 36 during manufacturing due to an error. Additional fasteners serve a dual purpose since the o-rings require constant, uniform pressure along the groove to maintain proper squeeze and seal. This cannot be accomplished using 2 or 4 bolts along the entire perimeter of the slant or door, respectively.

4.3.3 Seal Design

O-rings are the primary type of seal used throughout the back assembly, of which contains the largest number of sealing interfaces in the entire facility. There are many o-ring sizes that could be used, though all access panels located along the lateral faces of the test section use -200 series o-rings with actual cross-sectional diameters of 0.139 ± 0.004 [19]. Besides these lateral seals, the only other o-ring in use is with the pip-to-test section adapter plate, which uses a -300 series o-ring with a cross-sectional area of 0.210 ± 0.005 " [19]. All o-rings and gaskets used in the facility are silicone unless otherwise noted.

For a -200 series o-ring, the Parker Handbook recommends a gland width of 0.158" to 0.164" for vacuum and gases and a gland depth of 0.101" to 0.107" [19]. Common rule of thumb also usually dictates that the groove depth be roughly 70% of the actual o-ring cross-sectional diameter which would equal 0.0973", shallower than what the handbook suggests. Because it would increase squeeze, a final gland width of 0.160" and gland depth of 0.098" was used for the panel seals, with the thought that if the o-rings were to slip out or wear too quickly than the grooves could be machined to depths within the range that the Parker Handbook suggests.

The -300 series o-ring was designed in a similar fashion, with a suggested groove width of 0.239" to 0.244" and depth of 0.152" to 0.162" [19]. The finalized dimensions using the rule of thumb of 70% are 0.239" for the width and 0.147" for the depth.

Because all the grooves for the adapter and access panels have linear lengths longer than any commercial o-ring manufactured, stock o-ring had to be used and glued together

to make custom sizes. This is not preferred since one-piece o-rings are the strongest and the point that is glued presents a weak joint in the seal.

4.4 Manufacturing

Construction of the back assembly was the first to begin, starting in May of 2016, with material and machining cost estimates being done while other sections of the facility were still under design review. This section discusses the designed manufacturing methods and estimated total cost for the test section, tailpipe, and air receiver.

The test section skeleton was engineered to be welded together as ten individually machined plates as illustrated in Figure 59. Each of the plates were purchased and waterjet to the appropriate material dimensions from QMF Steel. The water jetting included all large access points and the general outline of each plate with a tolerance of $\pm 0.010''$. Drawings submitted to QMF Steel for this work can be found in Appendix B.

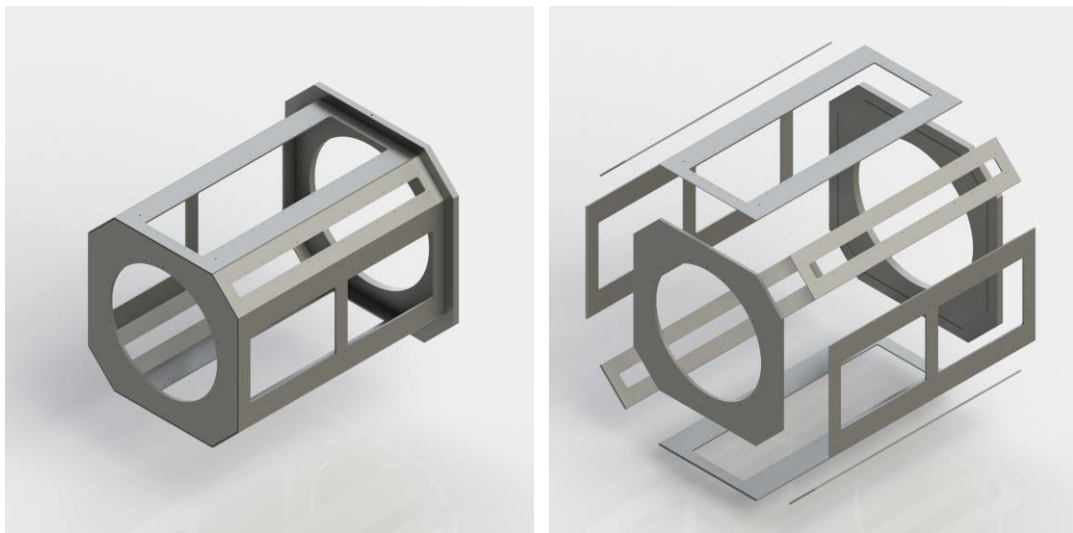


Figure 59. Test section skeleton with exploded view on the right illustrating the ten different plates machined and welded together during fabrication.

In order to prepare for welding, the ten plates of the skeleton were machined down to thickness, tapped, and beveled. With the exception of the front and back plates, which were sent to Machine Works for their final cuts, all plates were machined at the shop located at the Low Speed Wind Tunnel Complex and welded at the Texas A&M University Cyclotron Lab. An alignment groove was engineered into the back plate as seen in Figure 59 in order to ease assembly before welding while the front plate was designed to slide between the lateral faces. For purposes of alignment, the skeleton is assembled on its back and clamped to reduce bowing as shown in Figure 60. This configuration minimizes movement of the plates during welding and creates a more accurate final product.



Figure 60. Test section pieced together and clamped just before welding.

Each access panel is machined out of 1 1/8" thick 6061-T651 aluminum plates, which was done at the LSWT shop. The access panels and skeleton plates are all too long

to have been machined in one pass on the CNC mill located at the LSWT, so each was done using two or more passes and aligning at a common point. All finalized drawings for the access panels, plates, and the support stand for the test section can be found in Appendix B.

The tailpipe was manufactured with the components listed in Section 2.2.2 and 2.3.1 and welded together by William Seward of the Department of Chemistry Machine Shop. While not certified for high pressure welding, Will used to be authorized for such and performed the labor on the tailpipe as if he were certifying it. This involved making a smooth raised face on the 42” 150# slip-on flange after beveling the front and welding both sides of the flange. This flange can be seen in Figure 61 and Figure 61 right before being aligned flush with the end and welded permanently in place. The 30” 300# weld neck flange used multiple passes and all was certified by hydrostatically testing the tailpipe to an operating pressure of 80psig.



Figure 61. Tailpipe immediately before the 42” 150# slip-on flange was welded to the end of the pipe.

Alignment of the back assembly proved to be the most difficult because the 30” 300# flange and 42” 150# of the pipe were not welded with holes aligned vertically. This

means that when one side of the pipe is lifted using a flange hole that there is a torsional force that wants to rotate the pipe. This hardship was magnified by the fact that the tailpipe had to be installed through the wall of the NAL as pictured in Figure 62. Once attached to the test section inside, however, the rotational degree of freedom was constrained and the back assembly was easier to align with proposed centerline of the facility.



Figure 62. Tailpipe as it was installed through the wall at the NAL.

Budgeted estimates for the back assembly, minus the tailpipe, were assumed to be roughly \$10,000 in total; however, changes to 300# flanges on the end of the tailpipe drastically raised the cost of the facility. Table 15 lists a relatively thorough cost for the back assembly as it is divided into the test section and tailpipe. The air receiver option was quoted from Hanson Tanks and is also listed; though, if approved, this money would be pulled from a separate proposal and account.

Table 15. Cost of test section pieces with labor. [31]

Test Section				
Item	Description	Price Per	Qty	Cost
Door Plate	34"x71"x5/8" CS	\$550.00	2	\$1,100.00
Top Plate	34"x71"x5/8" CS	\$530.00	1	\$255.00
Bottom Plate	34"x71"x5/8" CS	\$527.00	1	\$527.00
Slant Plate	13"x71"x5/8" CS	\$321.50	4	\$1,286.00
Front Oct.	51"x51"x1" CS	\$785.00	1	\$785.00
	-Machine Works Labor	\$1,750.00	1	\$1,750.00
Back Oct.	60"x60"x2" CS	\$1,993.50	1	\$1,993.50
	-Machine Works Labor	\$2,500.00	1	\$2,500.00
Slant Panel	1 1/8"x7.5"x67.5" Al 6061	\$181.75	4	\$727.00
Door Panel	1 1/8"x23.5"x33.5" Al 6061	\$282.50	4	\$1,130.00
Roof Panel	1 1/8"x25.5"x67.5" Al 6061	\$646.00	1	\$646.00
Floor Panel	1 1/8"x25.5"x67.5" Al 6061	\$646.00	1	\$646.00
Stand Baseplate	1/4"x40"x72" A36 Plate	\$120.00	1	\$120.00
Stand Tube	12"x4"x3/8"x60" RectTube	\$153.00	1	\$153.00
		Total Sub Cost		\$13,618.00
Tailpipe				
42" Pipe		\$2,240.00	1	\$2,240.00
42" Flange		\$1,000.00	1	\$1,000.00
30" Flange		\$1,800.00	1	\$1,800.00
30" Blind		\$2,498.00	1	\$2,498.00
Reducer		\$1,406.71	1	\$1,406.71
Labor	William Seward	\$56.50	8	\$452.00
		Total Sub Cost		\$9,396.70
Air Receiver	2,520 gallon tank	\$24,345.00	1	\$24,345.00
		Total Cost w/o Air Receiver		\$23,014.70
		Total Cost w/Air Receiver		\$47,359.70

5. SUPPORTING INFRASTRUCTURE

5.1 Stands

5.1.1 Requirements

The primary purpose of the structural support system is to transmit the horizontal recoil loadings of the facility into the ground. Additionally, the structures serve in the ease of alignment for the entire facility through the inclusion of rails and hydraulics. To best address the engineering requirements and design, the support stands are broken into three separate designs: the primary, secondary, and roller stands. Table 16 lists some of the key requirements set forth during the conceptual phase of the project. A full list of these requirements can be found in Appendix A.

Table 16. Key and derived requirements as pertaining to the structural support system.

Key Requirements	Derived Requirements
<u>Shall</u> be able to handle design recoil load of 406k pounds	-Each structure <u>should</u> have a safety factor of 4 -Safety factor <u>should</u> be defined as yield stress
<u>Shall</u> provide a nominal facility height	-Supports <u>should</u> provide a nominal centerline height of 36inches -Supports <u>should</u> use crank jack roller stands to support all weight loads and assist with height adjustment
<u>Shall</u> support facility weight	-Roller supports <u>should</u> be rated for twice the weight of the supported section
<u>Shall</u> be able to interface with existing facility components	-Structural supports <u>should</u> interface with 20” diameter pipe -Primary stands <u>should</u> interface with 20” 900# flanges -Secondary stands <u>should</u> interface with 20” 150# flanges

Before discussing some of the requirements and the reasoning behind them, it is important to note the assumptions of the load distribution system. As discussed in Section 3, the recoil force is calculated using an unbalanced pressure located at the blind end of the driver. This maximum loading due to a conservative pressure differential of 2000psi acting upon an area of 202.67 in² was computed to be 405,347.28 lbf.

Furthermore, the loading distribution is assumed to be a rigid system, which is true to within tolerance considering the thickness of the pipe, especially along the driver and driven lengths. The thick walls allow one to assume that the overall displacement from one stand to the next remains very minimal. Under this rigid body assumption, the horizontal design load of each support (five total) is set to 81,200 lbf. To account for discrepancies in this assumption, the safety of factor for each support stand was set at 4 times the design load, resulting in a failure criterion of 324,800 lbf. Additionally, since the support stands are of no use when in a permanently deformed position, failure was defined as the yield point of the material chosen to construct each member.

Upon the start of the design process, the facility was agreed to be supported in two separate regards: support in the horizontal direction and support in the vertical direction. This was gravely important due to the orders of magnitude difference in each loading and the ability to align the facility in the long run. In order to manufacture stands capable of handling 324,800 lbs, many structural calculations relied on the ability to weld large steel components into place. This, in turn, limited the ability to adjust the height of the facility after manufacture. For this, separate roller stands were fabricated to specifically support the sheer weight of each pipe section. These supports were placed two on each section in

order to keep the center of mass in between two points of contact. Moreover, the roller stands would not inhibit movement in the horizontal direction, allowing the sliding of pipe sections apart from each other for either cleaning or inspecting. These roller stands, as a pair, were determined to be rated for twice the weight of the heaviest section of pipe: the driven at 9,450 lbs.

The final requirement of note is that the stands be able to properly fasten to parts of the facility. While the roller stands need not do this, the primary stands are designed to bolt through the 20" 900# flanges welded to the ends of the driver and driven while the secondary stands push against two halves of a 150# stainless steel flange welded to the middle of the first and second accelerator pipe sections.

Figure 63 illustrates the position for each type of stand, for a total of three primary stands, two secondary stands, and eight roller stands.



Figure 63. Stands as they are expected to be located throughout the facility.

5.1.2 Primary Stand Design

There are three primary support stands, as shown in Figure 64: one which attaches to the blind end of the driver, one which attaches to the driver end of the driven section, and one that attaches to the accelerator end of the driven section. All of these interfaces are with 20" 900# flanges which fasten with the use of four 2" threaded studs and a nut.



Figure 64. Primary stand with H-shaped central body, hole interfaces, and brace supports on both sides.

The general design of the primary supports relies on a central 2-inch-thick A36 steel plate. Four of the 2 inch threaded studs are cut longer than the other sixteen found on the 900# flange interfaces. These four studs run through holes located on the 2-inch-thick plate where a nut fastens to the opposite side as seen in Figure 65.

The steel plate sits atop a 6" square tube at 0.5" wall thickness and is supported along its sides by two vertical W6x25# H beams, all of which are welded together. The square tube is milled down along the edges to fit inside the webbing of the H beam, which, when welded, creates an H-shaped support that the 2-inch plate slips into. Gussets are engineered in multiple locations between the H beam webbing and steel plate, as well as between the steel plate and the 6-inch square tube. These alleviate stress concentrations along the weld seams from building past the point of yield.

For bracing, two S8x23# I-beams are located on the back end and welded at a 45-degree angle from the base to the 2-inch thick plate. Two additional 6-inch square tubes at $\frac{1}{2}$ " thick wall are placed on the front to directly oppose the recoiling force (compression). These square tubes are placed at a 45-degree angle similar to the I-beam except with an additional cant of 15 degrees pointing toward the center of the stand as portrayed in Figure 66.



Figure 65. Side view of how the threaded studs and nuts bolt into the stand. All short studs that do not fasten to the stand are omitted.

The H-shaped central body and bracing members are welded directly to a $\frac{1}{2}$ " thick A36 steel plate. A series of twenty-two $\frac{3}{4}$ " holes are placed along each stand base in order to bolt into the concrete. The floor strength has a rating of 6ksi and, while each stand is placed in a location in the lab with a unique floor height, the stands are “shimmed” with thick bars that span the undersection of the base plate as laid out in Figure 67.

With an extreme load of 81,200 lbs, it was deemed necessary to perform extensive finite element analysis using SolidWorks Simulation on each stand. For each primary

stand the total design load is distributed over the area of the four washers that the fastening nuts sit over, as shown in Figure 65. The baseplate is fixed along the twenty-two holes where the concrete anchors are located and the entire underside of stand is constrained as a roller fixture in order to provide a no penetration condition that simulates the existence of a floor. Additionally, the entire support stand assembly is assumed to have all its components perfectly bonded to each other and, while all parts are welded together, this is not entirely accurate. Welding does not provide perfect penetration into both metals, yet also adds metal that otherwise doesn't exist in the assembly in the form of fillets. Because of this, the assumption of perfect bonding is only approximately accurate and is compensated for in the factors of safety.

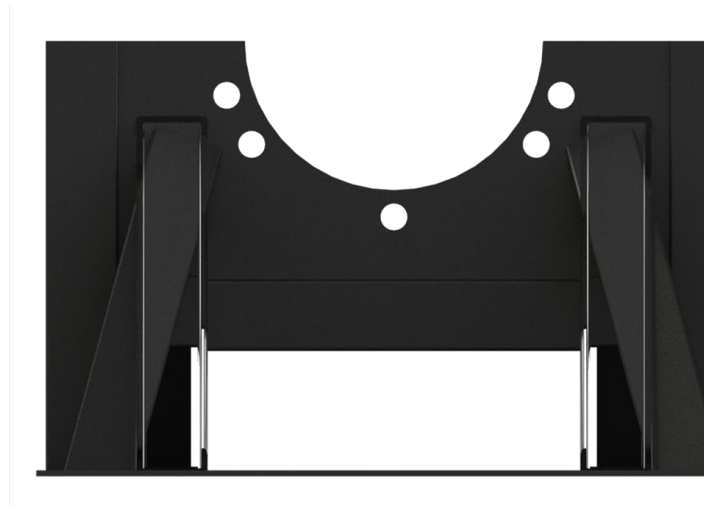


Figure 66. Magnified view emphasizing the difference when canting the 6-inch square tube bracing at 15 degrees.



Figure 67. Representation of how the stands may be shimmed to achieve proper height.

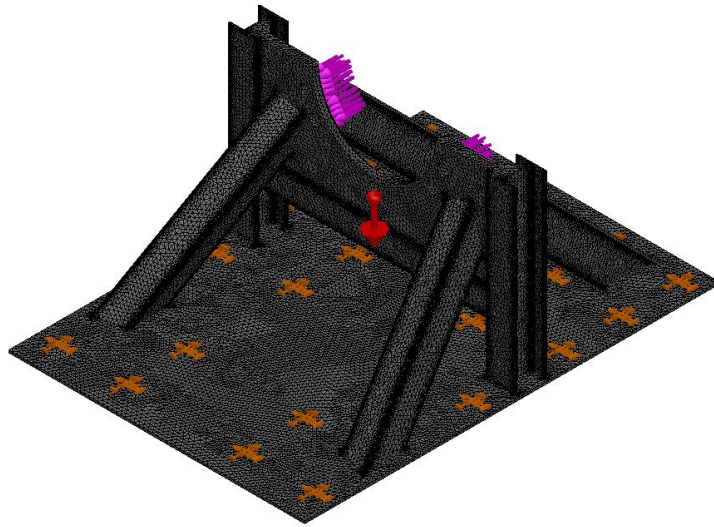


Figure 68. Mesh of primary stand assembly with gravitational force, force distributed over the 4 points of contact, and fixtures around concrete anchor holes.

The material used in the simulation was conservatively chosen as A36 because it is on the lower end of the yield and ultimate tensile strength rating, at 36ksi and 58ksi respectively [25]. While most components are, in fact, made of A36, some of the structural

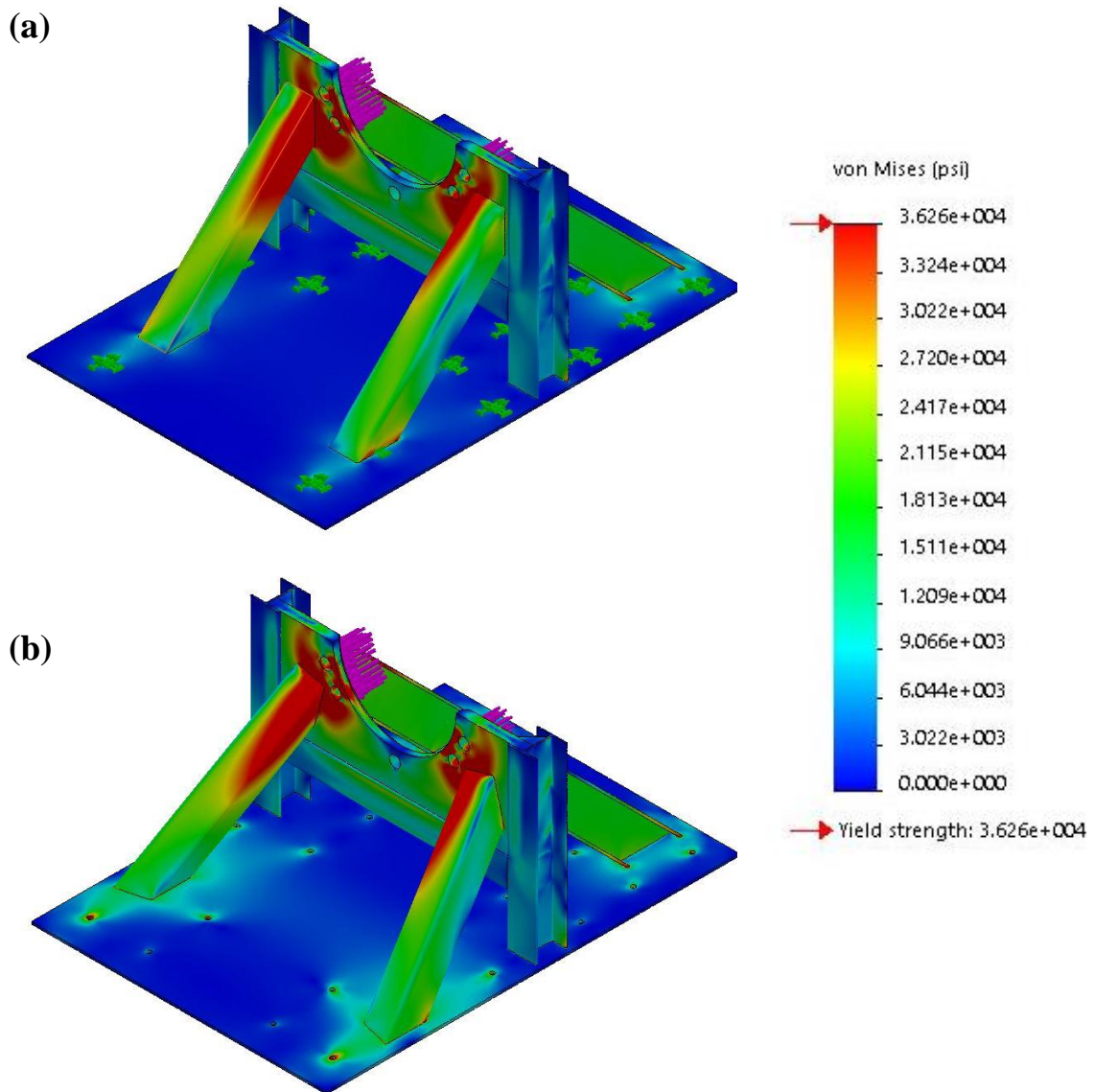


Figure 69. Von Mises stress distribution for (a) 45-degree brace positioned perpendicular to the 2-inch thick main plate and (b) 45-degree brace canted 15 degrees inward.

members such as the I-beam, H-beam, and square tubing have material properties that are slightly higher in strength.

Originally, the design of the primary stands called for 45-degree square tube braces without a cant pointing them into the center of the body. Figure 69 illustrates the difference

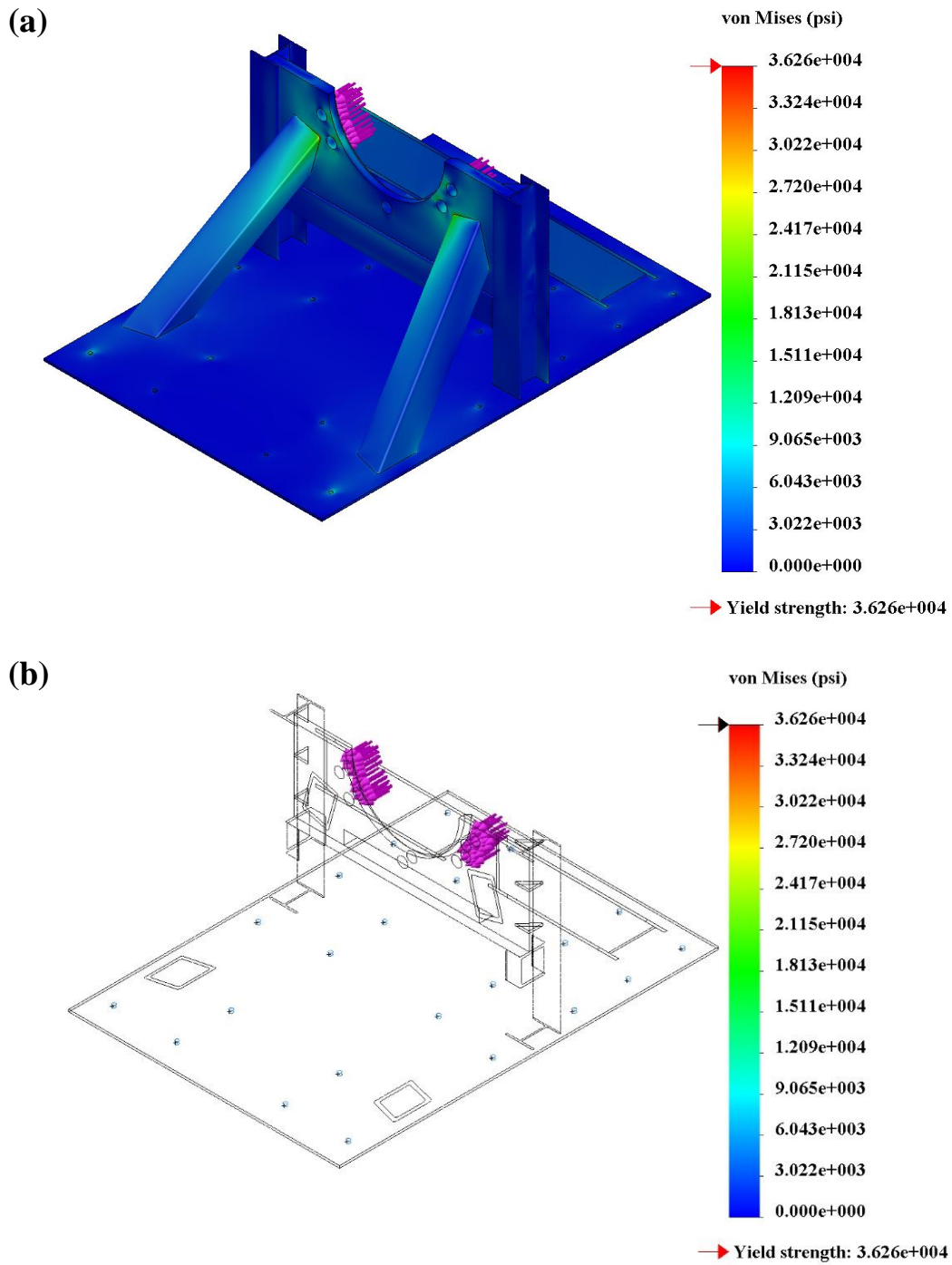
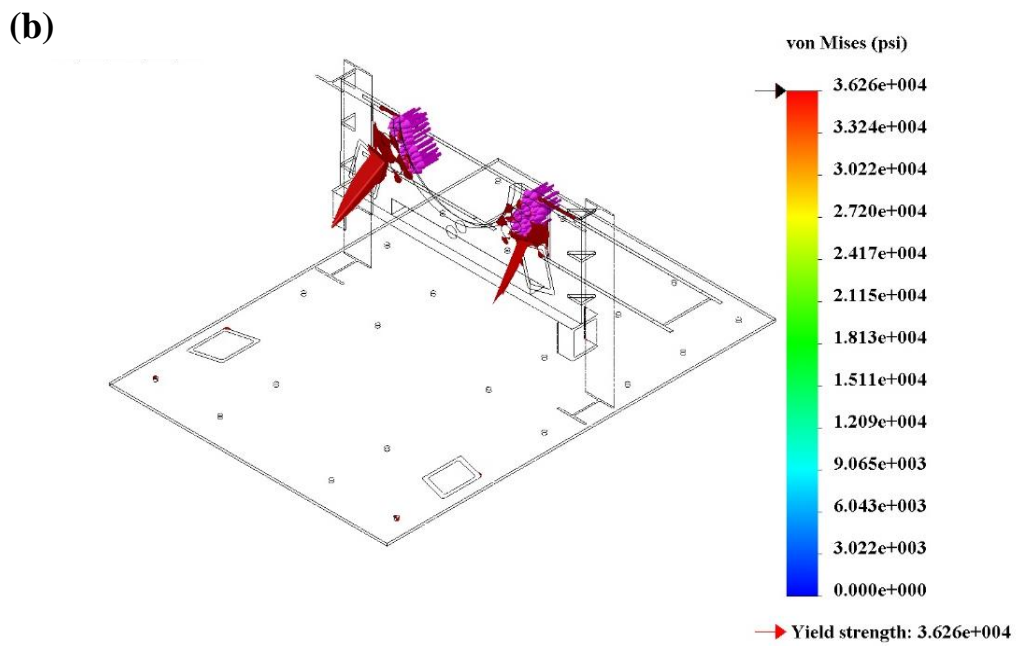
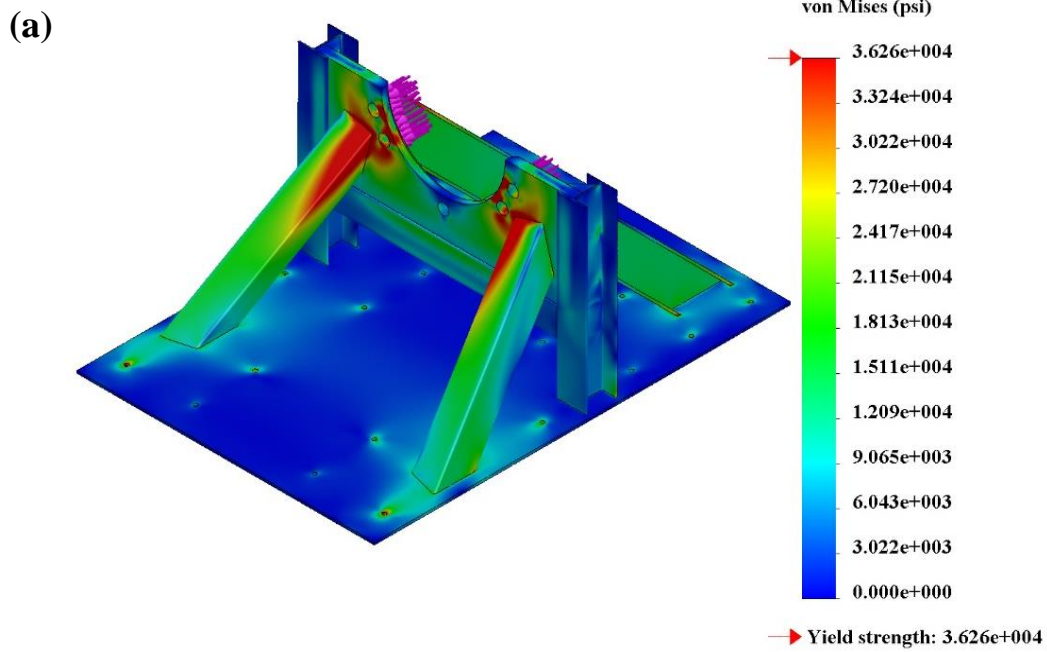


Figure 70. Von Mises stress distribution of the primary stand for (a) a total load of 81,200 lbs and (b) an iso-clipping isolating any points of the assembly that have stresses above the yield point.



Educational Version, For Instructional Use Only

Figure 71. Von Mises stress distribution of the primary stand for (a) a total load of 324,800 lbs to simulate a factor of safety of 4 and (b) an iso-clipping isolating any points of the assembly that have stresses above the yield point.

in stress distribution both with and without the cant. These angles were added due to stress concentrations occurring along the entire inner edge of the 6-inch square tubing, possibly leading to yield.

Figure 70 shows the von Mises stress distribution on the primary stands. Under the design load of 81,200 lbs, an iso-clipping of these von Mises stresses simulate that no point of the assembly passes the point of yield. Figure 71 (b) is a representation of the stand under an experienced load of 324,800 lbs, which is 4 times the expected load for a given stand. There are points above the yield point under this condition, specifically around the tip of the square tube that connects with the 2-inch thick plate, but these are expected to be reduced by the significant amount of weld that is built up along the edges. Multiple passes along the edges that contact the 2-in plate required in order to provide deep enough penetration without the need for heating up the entire stand when being manufactured. The process behind manufacturing is further discussed in Section 5.1.5.

5.1.3 Secondary Stand Design

The secondary stands are derivatives of the primary stands, with key differences being that they interface with the facility at 150# stainless steel half flanges welded to two of the three accelerator pipe segments. Figure 72 portrays one of the secondary stands as it connects to the second accelerator pipe section. The other stand is located at a similar flange welded at the midpoint of the first accelerator pipe section.

The main advantage in switching to the secondary stand configuration is that the entire face of the half flange resists the recoiling force, whereas the primary stands rely on

the threaded studs to undergo tension while the nuts carry all of the directed load. Because these half flanges are permanently welded to the pipe, the stands distribute the load easier.

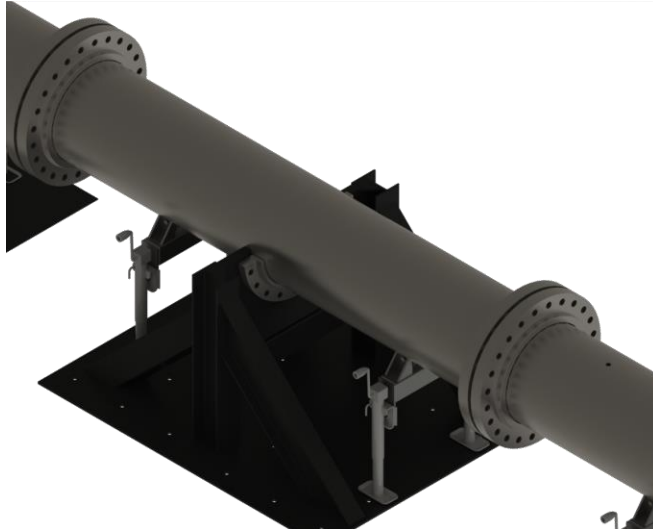


Figure 72. Secondary stand attaching to half flange welded at the second accelerator segment. The driver, where the loads originate, is located in the direction of the upper left corner.

An additional advantage of the secondary stands is that, because the flange has a smaller diameter compared to the 900# flange (27.5" outer diameter versus a 33.75" diameter), the 2-inch thick plate can be made narrower than the primary stands. The primary stand holds a plate that is 52"x20", whereas the secondary stand has a 40"x18" plate, saving money in both material and water jetting. A side effect of the narrower body is that the I-beam braces had to be relocated to the H-beam vertical supports that are part of the H-frame, as illustrated in Figure 73.



Figure 73. Overhead view of the secondary stands with emphasis on the movement of the back I-beams to connect with the H-beam instead of the 2-inch thick plate.

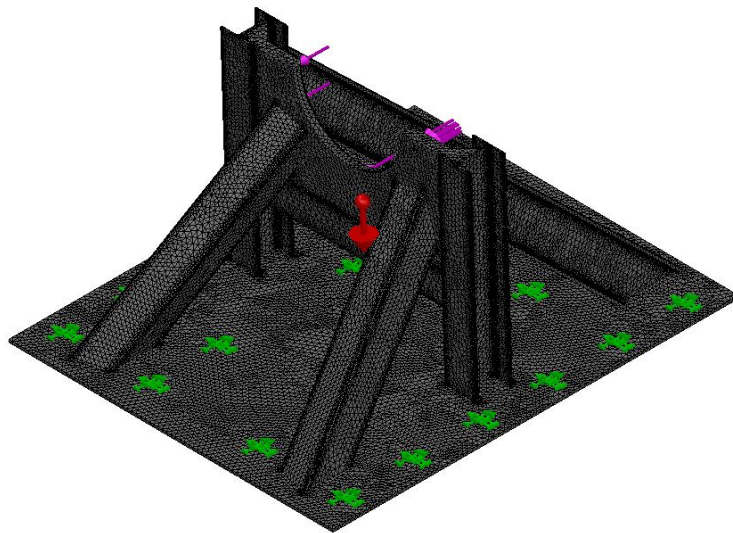


Figure 74. Mesh of the secondary stand assembly with gravitational pull, fixtures along the base plate, and locations of the design/factor of safety load.

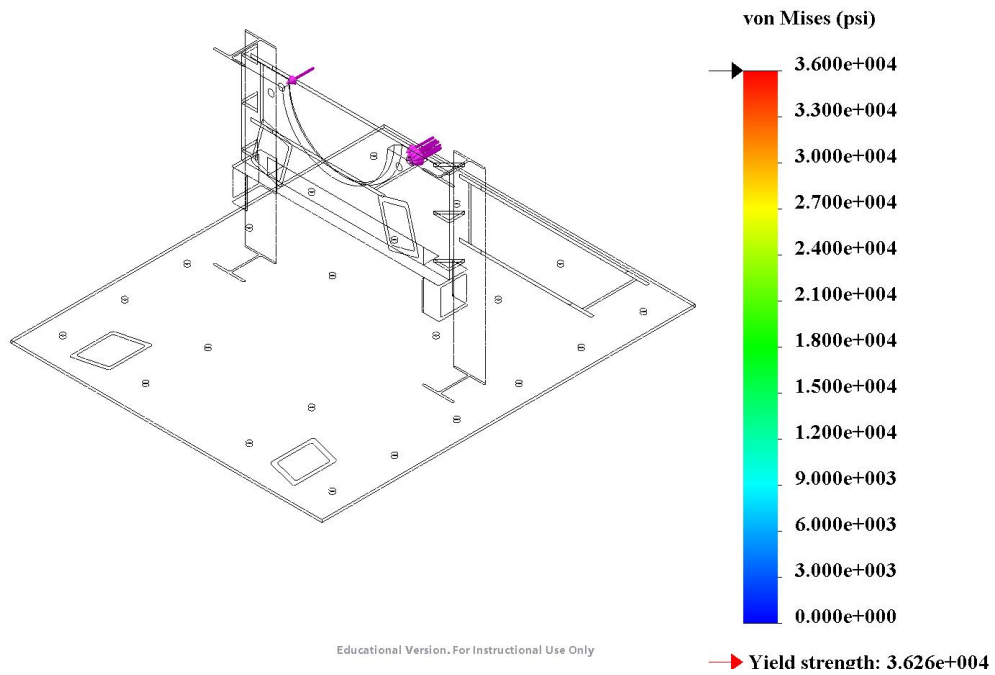
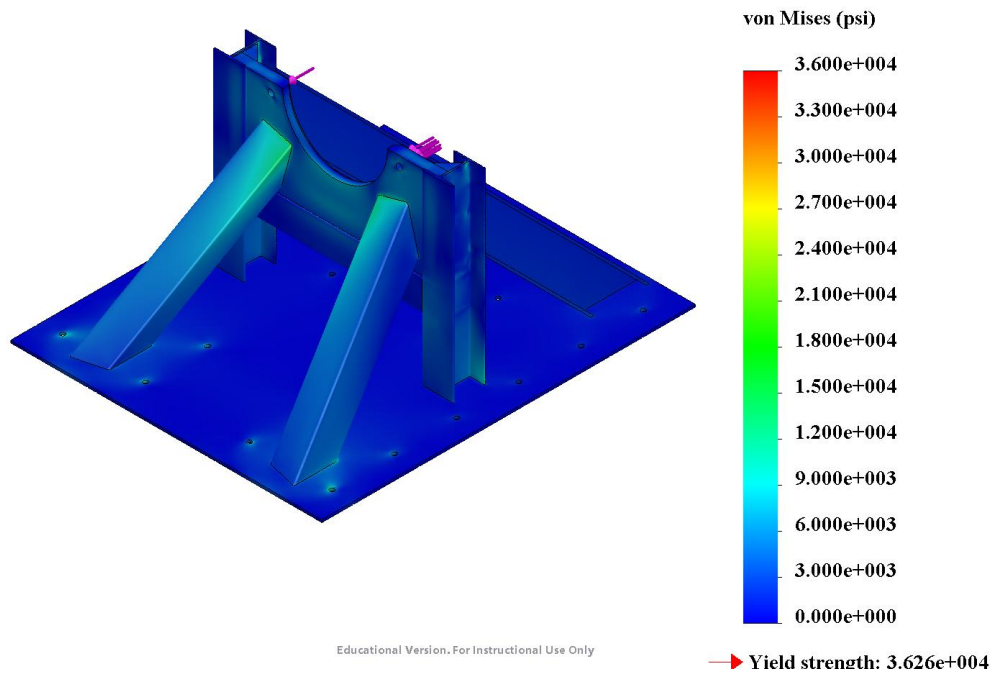


Figure 75. Von Mises stress distribution of the secondary stand for (a) a total load of 81,200 lbs and (b) an iso-clipping isolating any points of the assembly that have stresses above the yield point.

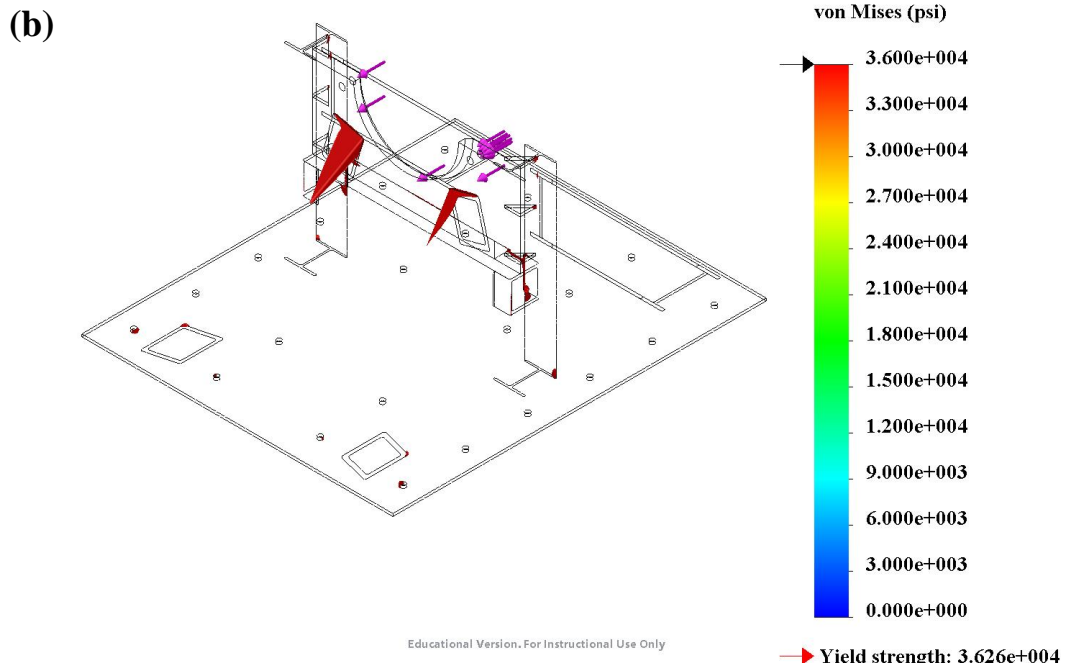
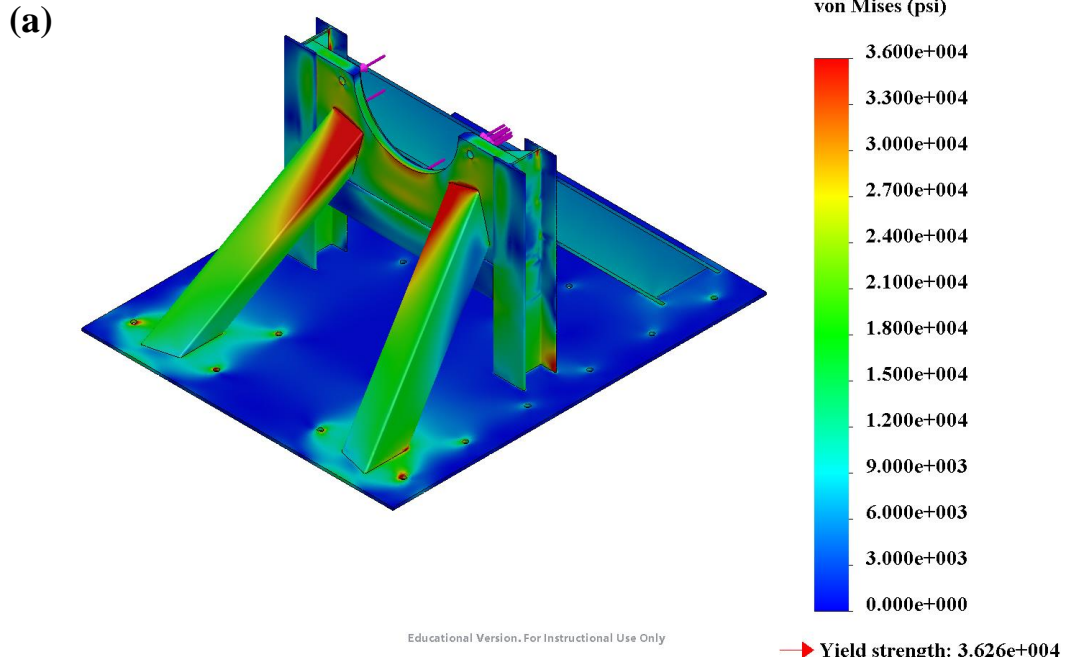


Figure 76. Von Mises stress distribution of the secondary stand for (a) a total load of 324,800 lbs to simulate a factor of safety of 4 and (b) an iso-clipping isolating any points of the assembly that have stresses above the yield point.

Separate finite element analyses were performed on the secondary stands to insure a similar factor of safety of 4. Figure 74 illustrates the mesh of the assembly and the applied forces/fixtures used for simulation. All assumptions discussed for the primary stands still apply for the second stands, including the use of A36 steel for all components and perfect bonding between all connected faces. The secondary stands, while smaller, are designed to be rated at the same 81,200 lbs of force as the primary stands, with a factor of safety of 4 yielding a load of 324,800 lbs.

Figure 75 shows the first simulation using the design load and an iso-lipping of the yield stress of 36ksi. Like the primary stands, no point of the assembly ever exceeds the yield point for this load, whereas for the load of 324,800lbs in Figure 76, a great deal of stress can be seen along the tips of the 6-inch square tubes.

For similar reasons as the primary stands, the excess stress seen in the tips of the 6-inch square tube is determined to be adequate enough when considering the presence of abundant weld beads that overlap. Additionally, the welds possess much higher strength than the chosen A36, though it should also be noted that the heat affected zone around the weld is significantly weaker.

5.1.4 Roller Stand Design

For supporting the weight for the facility, roller stands were incorporated at two points along each pipe segment as can be recalled in Figure 63. Even though there are five sections of pipe there are only eight roller stands, with the driver being absent the traditional roller stands in lieu of two flange mounts that attach to rail carriages.



Figure 77. Roller stand as it is welded to its own plate, independent of the primary or secondary stands.

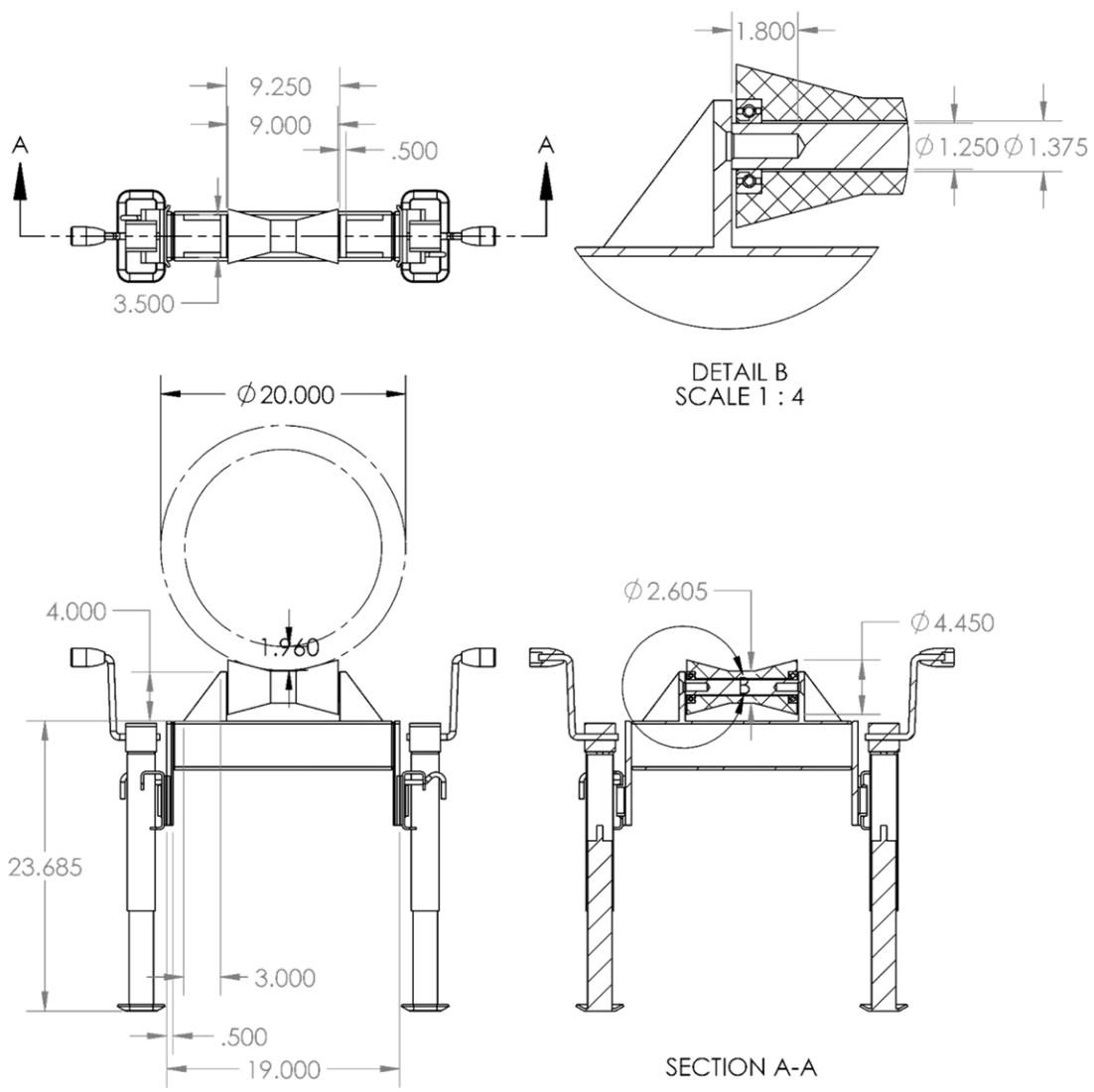
The roller stand is designed first and foremost to fasten into an adjustable height crank shaft. For convenience, two crank shafts straddle the main body of the roller stand as is portrayed in Figure 77. These leveling jacks have a vertical adjustment of 10” and a weight capacity of 5,000lbs. At its minimum height, the jack sits at 16 ¾” with mounting holes located at 9” and 12” above the ground. These mounting holes are sized at 3/8” free clear and are equally spaced at 3”x3” at the heights previously listed.

For durability, the main body of the roller stand is made from 4-inch square tube with 3/8” thick walls. Two 4” wide by 8.5” long steel bars ¾” thick are welded to each end of the square tub. These bars extend underneath the main body where matching holes are machined to interface with the crank jacks. This additional height is not only required to achieve the proper centerline height of 36” for the facility but also allow the bolts to be tightened against the nuts located on the opposite side of the jacks.

Sitting atop the central body are two $\frac{3}{4}$ " thick plates 3" wide by 4" tall. These raise the axis that the roller sits on to a position where the roller will avoid hitting the central body. Two gussets are located on each side of the vertical axle supports in order to prevent a bending moment in that direction and increase the weld linear length for attachment. These plates fasten to the main axle by screwing a $\frac{3}{4}$ "-10 bolt through the outside and into the axle. An example drawing is showing in Figure 78 and all other drawings for the roller stand can be found in Appendix B.

The axle is not designed to rotate, as this would cause friction against the vertical supports. Instead, the roller relies on two ball bearings located at each end of the roller as depicted in Figure 79. These ball bearings are rated for 5,000lbs each to match the two leveling jacks. Due to this and the overdesign of the central body and roller, each roller stand is appropriately rated for 10,000lbs of vertical force.

In order to best accommodate the 20" outer diameter of the pipe that it supports, the rollers were custom designed for this diameter. Originally, the roller was to be bought from a commercial source; however, when one was bought the lead time was deemed too long so a similar model was manufactured in the Low Speed Wind Tunnel Machine Shop for a similar price. The slope in the roller connects at two locations along the pipe as represented in Figure 78.



DIMENSIONS ARE IN INCHES TOLERANCES: ± 0.001 FRACTIONAL \pm ANGULAR: MACH \pm BFND \pm TWO PLACE DECIMAL ± 0.010 THREE PLACE DECIMAL ± 0.005		PROPRIETARY & CONFIDENTIAL THE INFORMATION CONTAINED IN THIS DRAWING IS THE SOLE PROPERTY OF Texas A&M University. ANY REPRODUCTION IN PART OR AS A WHOLE WITHOUT THE WRITTEN PERMISSION OF Texas A&M University IS PROHIBITED.	
COMMENTS:			
APPLICATION	DO NOT SCALE DRAWING	SIZE: Part Name A Roller Stand Overview Drawing SCALE: 1:12 WEIGHT:	SHEET 1 OF 1

Figure 78. Overall dimensional drawing for a roller stand. Specific individual component drawings can be found in Appendix B.



Figure 79. Cross sectional cut of the roller detailing the position of the ball bearings and threads in the axle.

5.1.5 Manufacturing

Construction of the stands took approximately three months due to excessive welding labor. While tedious and time consuming, the welding process takes time because of the number of passes needed to penetrate sufficiently into the steel, especially for the 2-inch thick plate. Welding efficiency depends heavily on the overall temperature of the pieces being joined, so the thicker the part the more thermal mass capable of absorbing the heat generated by the arc. Overlapping weld beads allows additional material not simulated in the finite element analysis and heats the steel with each pass, avoiding the need to preheat the parts with a torch. Figure 80 shows a picture of the resulting weld beads with several passes.



Figure 80. Example picture of the welds performed on the 2-inch thick plate to the H-shaped central body.

The stands were constructed as a batch, with each being welded to a certain point to streamline the process of manufacturing. First, each 6-inch square tube was milled along the edges to fit between the W6x25# H beam webbing where they were aligned and tack welded into position. At this point the structures created an H shape central body, as depicted in Figure 81 that could have the 2-inch thick plate slid into. Using gravity, the large plate was held against the webs of the H-beam, tacked, and then fully welded into place.



Figure 81. H-shaped central bodies welded together being prepared for the 2-inch thick main plate.



Figure 82. Close up of the main gusset divided into six manufacturable pieces and welded to the stand.

Next, the large gusset located at the bottom between the 2-inch plate and the 6-inch square tube was welded into place as exhibited in Figure 82. While the gusset is simulated as a single part in all the FEA that was performed, finding a vendor for a triangular prism bar at 30" long proved to be more difficult than anticipated. A solution

for this was to take 3” square bar, cut it into 5” long segments, and then shop saw these along their diagonal, producing two right triangular prism pieces that are needed. Six of these are beveled and welded together as seen in the figure.

The smaller gussets were then saw cut out of 3” wide by ¾” thick steel bar. Figure 83 illustrates the positioning of the gussets against the web of the H beam and, like the main gusset, required a bevel along the tip of the triangle in order to press it into the edge with an already present weld.

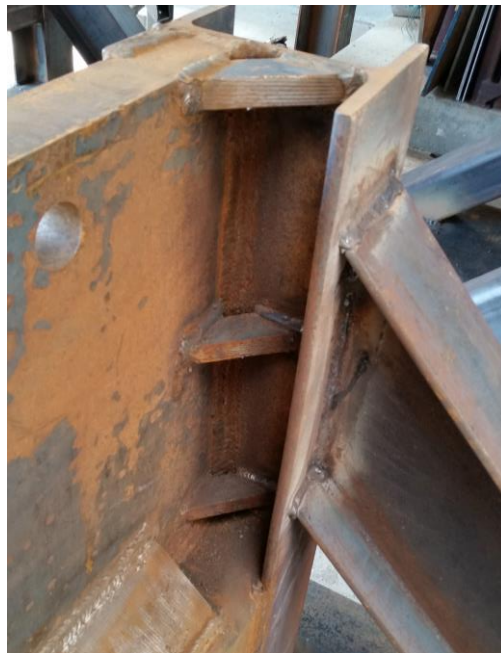


Figure 83. Close up of the small gussets that alleviate stress buildup along the corners of the H beam and 2-inch plate.

Once the H-body was complete, it were tacked into position with the two front and two back braces against the base plate. This was done in order to minimize movement

during the welding process. Figure 84 portrays the first primary stand, specifically the driver stand, to be tacked together and welded.



Figure 84. Driver-side primary stand fully tacked into place.

Finally, once the stand was fully welded together, the base plate was marked in the twenty-two locations for the $\frac{3}{4}$ " holes. These were torched, as opposed to drilled, due to the sheer number of holes and the availability of an acetylene-oxygen setup in the weld shop of the Low Speed Wind Tunnel. A representation of these torched holes can be seen in Figure 85.



Figure 85. Series of $\frac{3}{4}$ " holes torched into the $\frac{1}{2}$ " thick base plate of a secondary stand.

Following all the stands being fully welded together, each was coated with a single coat of primer and 3-4 coats of black paint in order to protect the steel from rusting, even though they are located inside and away from most moisture. The stands were then installed in the lab in rough locations where they could be aligned, shimmed to height, and bolted into the concrete.

Financially, the stands were budgeted to cost around \$10,000 in material and approximately \$10,000 in labor. Unfortunately, when ordering material there was some mix up between the I-beam and H-beam specifications. This increased material costs slightly from what was planned, but, overall, the stands came in at a relatively acceptable price of \$22,171.50 as is explained in Table 17.

Table 17. Line item costs for the primary, secondary, and roller stands with labor.

Primary & Secondary Stands				
Item	Description	Price Per	Qty	Cost
2-inch Plate	2"x20"x52" A36 Waterjet	\$865.00	3	\$2,595.00
2-inch Plate	2"x18"x40" A36 Waterjet	\$775.00	2	\$1,550.00
6" Squ. Tube	6" Squ. Tubex1/2"w.t. \$/ft	\$19.50	40	\$798.00
1/4" Base	1/4"x60"x72" A36 Plate	\$210.00	2	\$420.00
1/4" Base	1/4"x60"x72" A36 Plate	\$245.00	3	\$735.00
1/2" Base	1/2"x60"x72" A36 Plate	\$368.00	2	\$736.00
1/2" Base	1/2"x60"x72" A36 Plate	\$429.00	3	\$1,287.00
H-Beam	W6x25#x20' A36 Steel	\$260.00	1	\$260.00
H-Beam	W8x24#x20' A36 Steel	\$248.00	1	\$248.00
H-Beam	W10x33#x20' A36 Steel	\$339.50	2	\$679.00
3" Squares	3" Squ. Traingles x 5"L	\$19.50	30	\$585.00
H-Beam	W6x25#x13' A36 Steel	\$221.50	1	\$221.50
I-Beam	S8x23#x105" L A 36 Steel	\$177.00	5	\$885.00
6" Squ. Tube	6" Squ. Tubex1/2"w.t. x44"	\$102.00	7	\$714.00
Labor	William Seward	\$58.00	150	\$8,700
			Total Sub Cost	\$20,413.50
Roller Stands				
4 1/2" Roller	4 1/2" x84" 1018 Rod	\$455.00	1	\$455.00
1/4" Base	1/4"x40"x72" A36 Base	\$120.00	1	\$120.00

Table 17 (cont'd)

Roller Stands (cont'd)				
Item	Description	Price Per	Qty	Cost
¼" Bar	¼" x3"x20' HR A36 Bar	\$39.50	1	\$39.50
5/8"Bar	5/8"x6"x12' 1018 Flat Bar	\$252.50	1	\$252.50
Labor	LSWT Machining	\$45.00	19.8	\$891.00
		Total Sub Cost		\$1,758.00
		Total Cost		\$22,171.50

5.2 Hydraulic System

5.2.1 Requirements

In order to ascertain movement of the driver, hydraulic cylinders are used to provide ample force against the breech head. Hydraulics are the only mechanisms capable of providing an ample force to seal the o-rings along the breech, as explained in Section 3. The required force was calculated to not exceed 45,000 lbs and is included as a set of requirement laid out during design. Some of these requirements are listed in Table 18, while a full list of requirements can be found in Appendix A.

Table 18. Key and derived requirements with regard to the design of the hydraulic system.

Key Requirements	Derived Requirements
<u>Shall</u> be rated for pressures above the maximum rating of the hydraulic pump	-Should have a pump with maximum pressure of no more than needed to prevent excess force or damage to the cylinder
<u>Shall</u> have pressure relief valves	-Should have manually controlled relief valves
<u>Shall</u> not be allowed to operate without public notification	-Should utilize a multicolor warning light system with sirens to alert when armed and when locked

For safety purposes, all pressure ratings for fittings, tubing, hoses, and cylinders are required to have maximum pressure ratings greater than what can be provided by the

pump unit. Thus, the design stemmed from the overall force required and the size of the cylinder (and thus the cylinder's pressure rating).

Furthermore, pressure relief valves are placed throughout the system in order to prevent over pressurization, which should only occur if the pump somehow maintains a higher motor torque than what it is rated for. These are joined by a number of manual pressure relief ball valves that simply redirect the pressurized side of the hydraulic lines back into the reservoir.

A final safety measure is one for the public notification of operation. Because the forces generated by the hydraulics are sufficient to easily harm people, it was deemed imperative that no one be allowed near the driver or driven during operation. A warning light is installed above the breech and driver where most forces will be generated which flashes a myriad of different colors to transmit different states of the hydraulic system. The warning light includes two distinct sirens: one for initial warning that the hydraulics are armed and another that sounds when the facility is locked.

5.2.2 Hydraulic System Design

Two ram systems are required to operate the breech diaphragm system: one to exert force on the breech in order to seal the diaphragm and another to rotate the breech nut and lock it into place. Design first began by creating a general layout for the overall hydraulic system. A schematic with component layout is identified in Figure 86.

For the ram system required to seal the diaphragms, dividing the force between two cylinders serves to provide a symmetric force on the breech, as well as reduce the bore

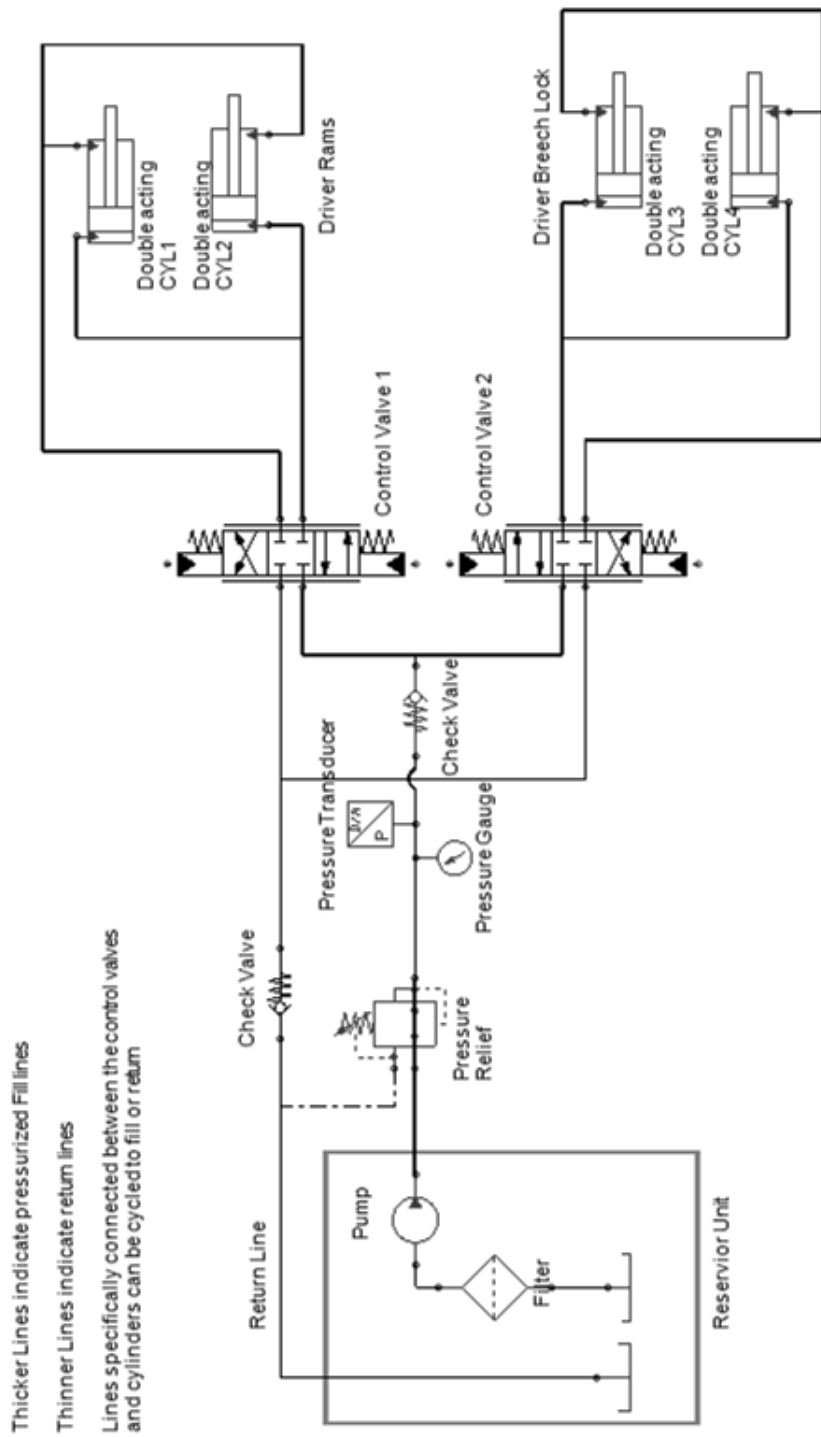


Figure 86. Schematic of the hydraulic system with power unit, pressure relief, 4-way/3-position solenoids, and cylinders.

size of the chosen cylinders. As is mentioned in Section 3, a minimum force of [45,000 lbs] is needed to properly maintain the o-ring seals along the diaphragm holding unit.

In order to choose proper cylinders, however, a hydraulic power unit had to be selected to ascertain the operating supply line pressure. Figure 87 provides an image of this power unit, which is manufactured by Haldex and provides a maximum line pressure of 2,000psi [35]. This unit includes a filter, motor, reservoir, relief line, transducer ports, pressure gauge, and sight fill gauge in a compact system that can be installed near the driver or driven sections.

The cylinders chosen for the horizontal movement are dual acting, 3,000 psi, 4-inch bore Tie-Rod Line cylinders from Prince. Prince hydraulic cylinders were investigated due to their reliable nature and abundance of literature. The 4-inch bore size with a 12" stroke length (as determined was needed in Section 3.3) at 3,000 psi can support a column load of 37,700 lbf which, when reduced to the 2,000 psi pressure that can be provided by the Haldex power unit, equals 25,130 lbf per cylinder for the HXT system design [36].

For the purposes of rotating the breech nut to lock the threads, large amounts of force aren't necessarily required since the angular movement should have minimal friction between the threads. Because of this, small 2.5-inch bore cylinders with much larger stroke lengths are chosen with the same operating pressures. Two cylinders are once again used for symmetry, though it should be noted that only one required and would not necessarily put asymmetric stress on the breech nut.

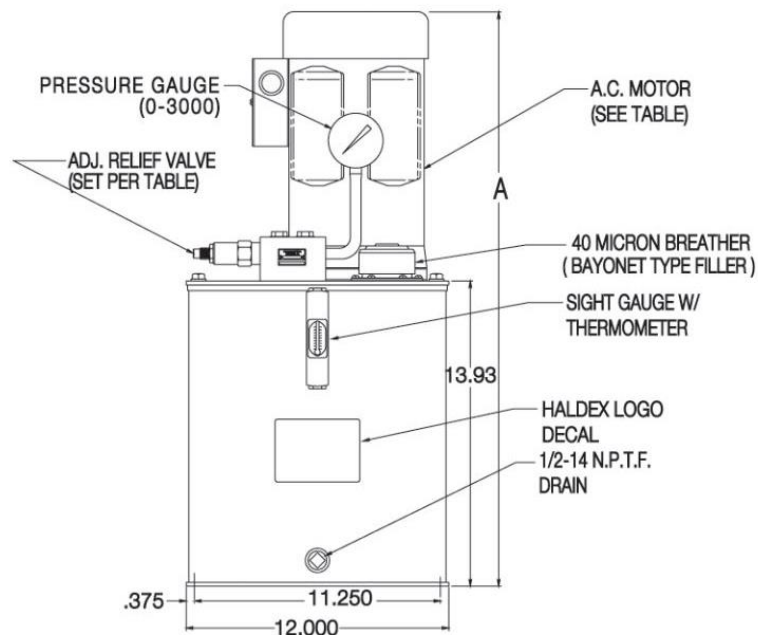
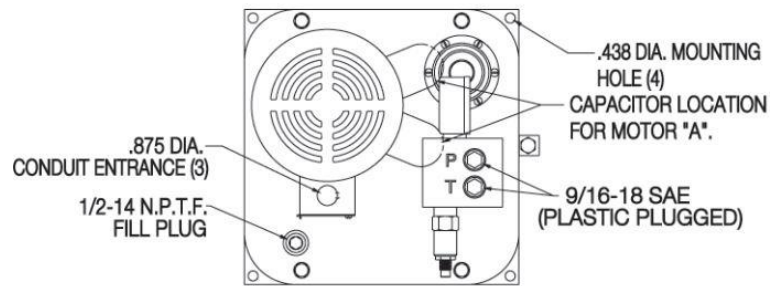


Figure 87. Haldex hydraulic power unit 2hp, 115VAC, model number 1400028.
 (credit: Northern Tool + Equipment) [35]

Similar rams to the Prince 3,000 psi Tie-Rod Line cylinders are chosen for consistency during maintenance. Unlike the large 4-inch bore, however, a 2.5-inch bore cylinder with a total stroke length of 16" and column load rating of 11,520lb_f at 3,000psi provides the lower force requirements [36]. At the supply pressure of 2,000 psi, each cylinder is capable of providing 9,800lb_f.

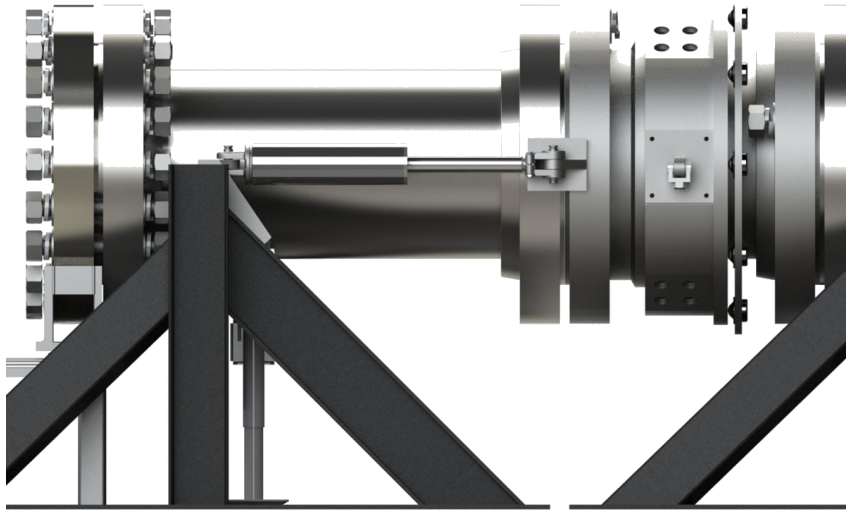


Figure 88. Location of the hydraulic cylinders for squeezing the diaphragm seals and locking the breech nut in place.

The two 4-inch bore cylinders are designed to mount on the driver-side primary stand and the 900# flange interface between the driver and breech. Rotation of the nut is provided by the 2.5-inch bore cylinders by mounting one end of the clevis rod to the base plate of the breech primary stand and the other end of the clevis rod to a point on the nut flats. Figure 88 portrays how the cylinders mount to the stand on the 45-degree I-beam brace by use of a custom-made mount. The drawings for these mounts can be found in Appendix B.

Figure 86 details many of the components required for the hydraulic system, including the control solenoids, check valves, and flow dividers. Control solenoids for double-acting hydraulic systems are typically 4-way, 3-position valves. These are labeled in Figure 86 as Control Valve 1 and Control Valve 2 and represented by a symbol including two crossing arrows on top and two parallel arrows on the bottom. Four positions refers

to the number of inlet and outlet ports located on the solenoid, while 3-position means that there are 3 different states that the valve can be in. For these valves, the natural position is for all ports to be closed to each other and are reverted to this state by spring-return. One of the two controlled states takes the inlet ports and opens them to one outlet port each, while the second state switches the inlets to the other outlet port. This allows hydraulic fluid to run way while draining the other, extending the arm of the cylinder. When necessary, the second state energizes and the flow reverses course, retracting the arm.

One 4-way, 3-position valve controls a single pair of hydraulic cylinders to move, requiring a total of two solenoids: one to operate the rotation rams and one to operate the horizontal rams. Each pair of cylinders is simultaneously controlled through the use of a flow divider, which proportions the fluid supply to each arm equally. This avoids one arm moving before or faster than the other.

All controls of the hydraulics are performed by an electronics pendant that ties into the electrical system described in Section 5.3.4. This, in turn, is tied into the safety system that controls warning lights, sirens, and interlocks.

5.3 Controls, Instrumentation, and Data Acquisition

5.3.1 Requirements

Facility control, instrumentation, and data acquisition refers to the peripheral equipment used to operate the facility, from vacuuming/pressurizing each section to the sensors installed to monitor states throughout fill/vacuum lines and supply reservoirs. Controls have two main points of design: one in regards to the flow diagram and another in terms of the virtual interface of the computer. Instrumentation details all the monitoring

equipment, with locations and interface specifications that tie into the data acquisition. Select engineering requirements of note for both the hardware and software design are listed in Table 19.

Because of the danger posed by operating the facility, all the control and monitoring equipment must be administered remotely through the use of LabVIEW. Two primary computer systems are used to operate the facility: one dedicated to high sampling data acquisition for pitot probes and time-of-arrival sensors and the other dedicated to the monitoring of fill lines and control of ball valves to divert flow. These two computers are incorporated into a hardwired system that was custom built to interface specifically with the instruments and safety equipment of HXT.

Table 19. Key and derived requirements for the hardware and software to control, monitor, and take data in HXT.

Key Requirements	Derived Requirements
<u>Shall</u> remotely open and close fill/vac lines as well as regulate pressures	-Should utilize two separate computers for high sampling data acquisition and relay control/status monitor
<u>Shall</u> monitor pressure and temperature in 4 locations of the facility	-Should be additional TC in each location port and have one additional pressure transducer in the back assembly
<u>Shall</u> contain safety relief valves in all pressure lines	-N/A

Knowing the states of the driver, driven, and accelerator gases is important in predicting the test conditions generated during operation. Due to this, at least one pressure transducer and thermocouple are installed in each section to feed directly back into the controls computer. An additional pressure transducer and thermocouple are placed in the hydraulic pressure line and similarly processed. Because thermocouples will often drift or break before pressure transducers and their cost is relatively low, it was determined to pair

an additional thermocouple at each R/N/A segment. One additional pressure transducer is located in the back assembly to verify the pressure reading from the accelerator section.

A final requirement of note is the inclusion of pressure relief valves located in each pressure line. As will be explained in the following subsection (Section 5.3.2), pressure relief valves are not only included in the primary fill lines, but also in any section of the line that will be closed due to a ball valve or solenoid.

5.3.2 Flow Control Diagram

Before the instrumentation, hardware interface, or VI could be built, an overall flow diagram of the facility was drawn out. This diagram provides a general locations of the components involved during the operation and monitor of the facility. Figure 89 details the schematic with standard engineering symbols.

The high pressure air (skinny lighter blue line) is supplied from the compressors and run through a ½” pipe into the Annex of the NAL. This line is then split and regulated into two pressures: one line is controlled by the high pressure digital regulator (PRA) that goes to the driver, and the other lines goes to a manual regulator that reduces the pressure to the maximum input for the low pressure digital regulator (QPV1) for the driven.

The vacuum lines run from the shed outside near the tailpipe and emergency exit of the building along the length of the facility and split in three locations. Because the pressure in the accelerator and back assembly section never need to be pressurized unless running in shock tunnel mode, only a vacuum line is run to the accelerator interface. A

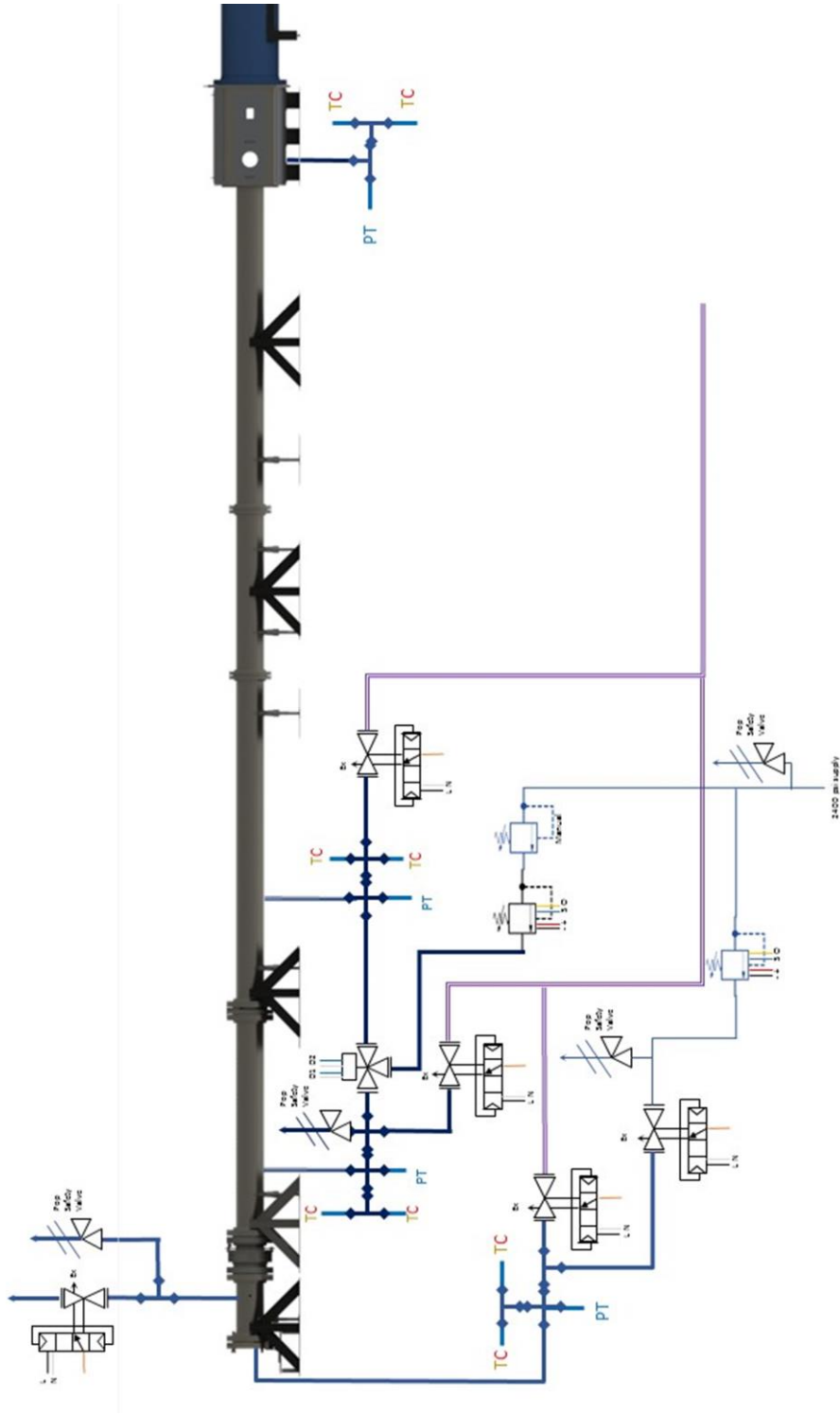


Figure 89. Flow diagram for HXT with pressure (blue lines), vacuum (purple lines), ball valve placement, digital regulators, and pressure relief valves.

separate vacuum line for each of the driver and driven sections are run in order to allow easy control when vacuuming down the segments.

For shock tunnel mode, it was devised that, since the XT-driver and XT-driven become the ST-driver, a three way ball valve can be used to switch filling from the driven to the accelerator, which becomes the ST-driven along with the back assembly. The 3-way ball valve also is designed to accept a custom-built position sensor with two switches: one which closes a circuit when in ST mode and the other which closes when in XT mode.

All fill lines run through a minimum size tubing of 3/8" with a wall thickness of 0.028" rated to 2,300psi [37]. Along the length of the facility, depending on what obstacles arise, these tubes may alternate to pipe or hose rated for similar pressures. For quick venting, the emergency relief line for the driver flows through a 1" stainless steel schedule 80 pipe rated for 2,601psi between -20F and 650F [17].

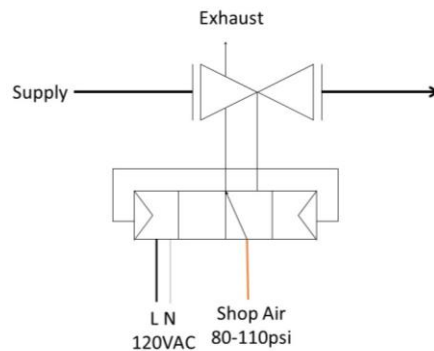


Figure 90. Ball valve diagram with flows and power requirements.

For control purposes, ball valves are chosen over solenoids or butterfly valves due to their high flow rates, high pressure ratings, and low cost. Large volumes, as are present in HXT, require large flow rates through the lines in order to minimize operation time. For

all ball valves minus the emergency relief and driver fill valves, a Dynaquip Controls 3/8” NPT spring return-fail close pneumatic ball valve are used. These are rated for 1,000psi and utilize a pneumatic supply pressure between 80-110psi controlled by a solenoid powered by 120VAC [38]. Figure 90 illustrates the diagram for the ball valves. The ball valves going into the driver will be a different model yet to be decided.

Two digital regulators are used: one with a lower, more accurate pressure range, and another with a higher, error-prone pressure range. Both digital regulators are bought from Equilibar and are operated by sending a 0-10V signal to the regulator which scales linearly with its total pressure range. Each regulator also includes a pressure monitor which can feed back directly to the controls computer. The signal control diagram is pictured in Figure 91, which shows the power and signal inputs along with the pressure transducer signal outputs.

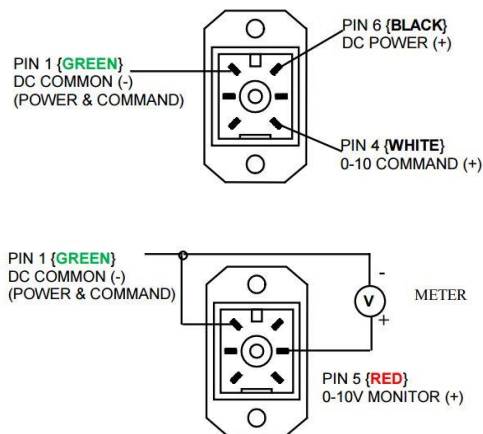


Figure 91. Digital regulator pinout for power, command voltage, and monitor voltage.

(credit: Equilibar QBT manual [39])

For the driven segments of the facility, a lower pressure digital regulator is used to provide a higher accuracy when filling the test gas. An Equilibar QPV1 High Resolution Pressure Control Valve with a custom upper pressure range of 105psia is powered by a supply voltage ranging from 15-24VDC and has an accuracy of less than $\pm 0.2\%$ full scale (0.21psi) and resolution up to $\pm 0.005\%$ (0.005psi) [39].

Due to the maximum pressure of the driver being 2,000psia, a different digital regulator had to be chosen. The PRA-45-2500-E works similar to the QPV1 since the PRA utilizes a QB2 pneumatic pilot regulator, which then controls the outlet pressure with a 45:1 ratio diaphragm. With a maximum pressure of 2,500psi and a similar command signal of 0-10V, the overall accuracy of the PRA is 2.5% of full scale (62.5psi) [40]. This accuracy is tolerable since the driver is the last section to be pressurized which, in turn, bursts the diaphragm. Fine control of the driver pressure is not necessary because the burst pressure should be designed into the thickness and etching depth of the diaphragm. Additional pressure transducers with higher accuracies are also located in the driver which will allow the maximum pressure to be recorded before the diaphragm breaks. This recording is more important to know than it is to control since it allows the prediction of the test conditions.

Pressure relief valves are required due to the extremely high pressures being used to fill lines. The driver maximum pressure is 2,000psi and, even though the driven section pressure does not exceed 105psia, it is important to include pressure relief valves to avoid even the possibility of over-pressurization. Pop safety valves pop open and provide

immediate pressure relief of the line over the set pressure. Various relief valves are located throughout HXT, with a summary listed in Table 20.

When discussing fire safety in the lab it was pointed out that the driver is located next to an emergency egress. If the condition ever may arise that a fire originate in a section of the lab that requires access through this exit, safety protocol dictates that a “more hazardous” line of egress is not allowed. Thus, if a fire were to occur during operation of the facility, the emergency exit located next to the driver would not be allowed. For this reason, an emergency vent line is installed that plumbs directly into the driver volume and connected to an emergency switch in the control room. This switch, when activated, opens a 1” NPT ball valve that vents high pressures in the driver through a pipe that runs through the roof of the annex. Having a larger diameter pipe venting up and out of the building allows this emergency exit to be used at any point by removing the hazard of a pressurized vessel.

Table 20. Pressure ratings of pipe and tube lines with the pressure relief settings.

Section	Size Line	Line Pressure Rating (psi)	Relief Valve Setting (psi)
Driver Fill Line	3/8” Tube (0.028”wt)	2,300 [37]	
Driven Fill Line	3/8” Tube (0.028”wt)	2,300 [37]	
Vacuum Line	½” Sch 40 PVC	358 [43]	50
Supply Line (2500psi)		2,601 [17]	N/A
Shop Air Line (130psi)	¼” Tube (0.02”wt)	2,500 [44]	N/A
Emergency Vent Line			

5.3.3 Instrumentation

The Hypervelocity Expansion Tunnel has various types of pressure transducers located throughout its sections. For simplicity, only the pressure transducers used for

monitoring the fill and vent lines is hereby discussed, with only a brief description of the PCB time-of-arrival sensors that will be sampled from the data acquisition computer.

Each of the driver, driven, and accelerator sections have one monitoring pressure transducer. All of these are bought from Omega and customized to appropriate pressure ranges as can be interpreted from Table 21. Absolute pressure ranges are chosen (except for supply and shop air lines) in order to monitor each section when under both vacuum and pressure, granting the ability to leak test each section individually.

Table 21. Pressure transducer ranges and accuracies.

(credit: Omega website specifications [41])

Pressure Transducer Location	Pressure Range (psi)	Accuracy ($\pm\%$)	Pressure Accuracy (psi)
Driver	2,500	0.05	1.25
Driven	150	0.03	0.045
Accelerator	100	0.05	0.05
Test Section	100	0.05	0.05
Hydraulic	2,500	0.08	2
Supply (2500psi)	2,500 (gauge)	0.05	1.25
Shop Air (130psi)	200 (gauge)	0.25	0.5

All pressure transducers are amplified to either a 0-5V or 0-10V scale for signal measurement. To do this, each transducer is powered by 24VDC from a common source through a cable connected to its end with a custom connector for the four wires: red as positive power, white as positive signal out, black as common (-), and (if used) green as shunt [41]. Connector details are further discussed in Section 5.3.4.

Thermocouples exist in various types with multiple ranges. For simplicity, Type K thermocouples are the most commonly used at the NAL and are optimally suited to temperatures expected (rated for -454F to 2,300F). Type K thermocouples have yellow

(+) and red (-) wires made of nickel-chromium and nickel-alumel metals that provide a range of $\pm 2.2C$ [42].

Because of the multiple functions that have to be tied into the controls computer, a multi-use cDAQ (9184) [43] from National Instruments uses pic-and-choose task modules that conform to the instrumentation needs of the facility. Table 22 details specifications for the four modules being used in the cDAQ as well as a fifth standalone module (NI-6525). Figure 92 provides a drawings with details about the cDAQ 9184.

Table 22. Data acquisition modules used with the controls computer.

(credit: National Instruments website [44])

Module	Description	Sample Rate	Resolution	Connection
9205	32 SE/16D $\pm 10V$ AI	250 kS/s	16-bit	DSUB 39 pin
9213	16Ch $\pm 78mV$ TC	75 S/s	24-bit	Screw Terminals
9263	4 AO, $\pm 10V$	100 kS/s/ch	16-bit	Spring Terminals
9485	8ch $\pm 60V$ SSR output	N/A	N/A	Screw Terminals
6525 (USB)	8ch $\pm 60V$ SSR output 8ch $\pm 60V$ digital I/O	N/A	N/A	Screw Terminals

The cDAQ is powered by the common 24VDC supply voltage that also powers the pressure transducers. Ethernet is used to communicate to the device because it is located in the annex (approximately 80ft from the control room) and USB deteriorates in signal strength with distance. This also allows the placement of Ethernet ports in the annex for permanent wiring and connecting of the cDAQ system [43].

Until characterization of the flow field begins, the data acquisition computer will only be sampling PCB time-of-arrival sensors located along the accelerator pipe. These sensors were used in the Four-Inch Reciprocating Shock Tube (FIRST), the precursor to HXT at the NAL, to predict the arrival of the shock wave as it travelled through the pipe.

They produce mV ranges that are amplified and sense the almost-discontinuous increase in pressure due to the shock wave preceding the test gas. For the time being, the specific DAQ card that will be sampling these sensors has not been chosen for the computer. One specification that should be noted though is the minimum sampling rate of the card should be determined to produce a sufficient number of data points during a single run. This will minimize the total number of runs needed to produce proper averages in run conditions and their errors.

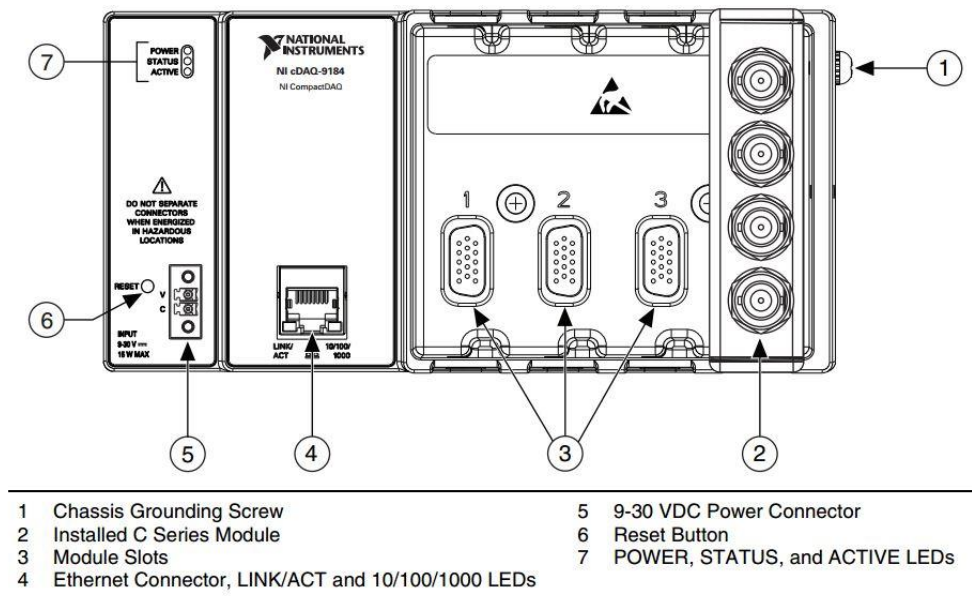


Figure 92. cDAQ unit specs and callouts [43].

5.3.4 Control and Instrumentation Hardware Interface

For purposes of convenience and efficiency, all instruments and relay controls are housed in a single electronics unit called the Control and Instrumentation Hardware Interface, hereby known as CIHI. The cDAQ system, power supplies, and common wiring

for the safety system are all run through this unit. The front and back panels of the box are shown and labeled in Figure 93.

The voltage inputs of the NI-9205 [44] are distributed through Lumberg 4-pin KFV connectors, which mate to compatible male connectors that are soldered to the cables of sensors, such as pressure transducers. The pinouts are as follows: 1-24VDC positive (red), 2-DC ground (black), data positive (blue), data ground (grey). Depending on wiring, these port scan be used exclusively for power or data transmission if the other is not needed by omitting connections to the other pins.

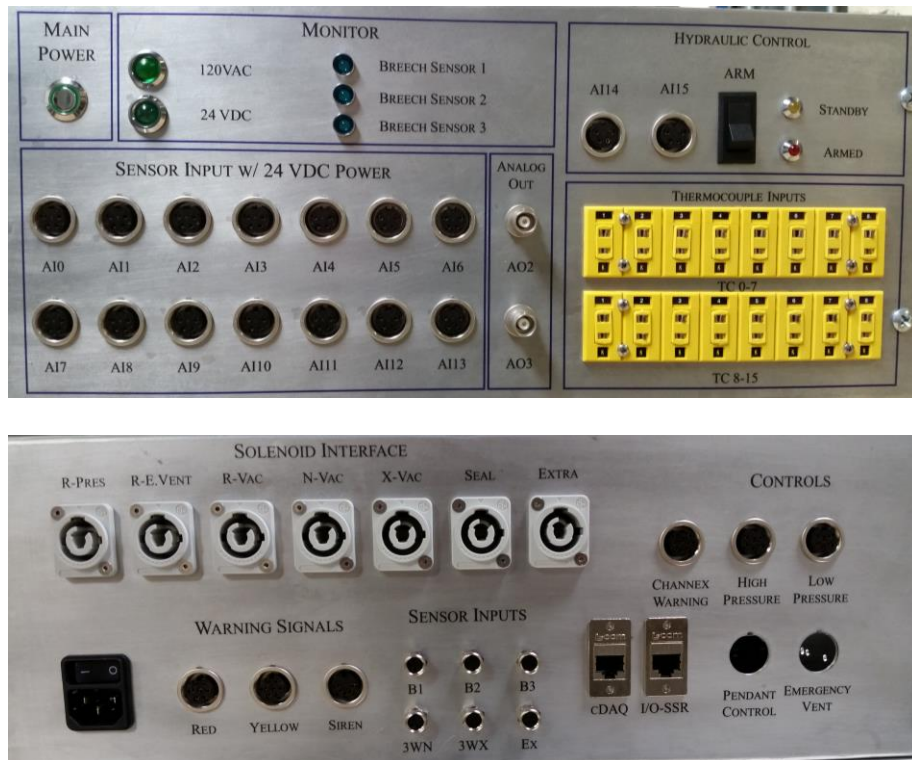


Figure 93. (Top) Front panel and (bottom) back panel of the control and instrumentation hardware interface electronics housing.

Due to variable needs in power, CIHI runs on 120 VAC, 24VDC, and 12 VDC. The 24VDC power comes from a transformer with a maximum current supply of 4A and supplies voltage to the sensor inputs, all of the solid state relay (separate from the cDAQ relays) except one, the warning lights, and digital pressure regulators.

Two rows of Type K thermocouple connectors are wired directly into the thermocouple module of the cDAQ. No power is required to run these. Two analog outputs are provided through use of standard BNC connectors on the front panel. These are labeled AO2 and AO 3 (number 3 and 4 out of the four provided by the module) because AO0 and AO1 wired directly into the connectors for the QBV1 and PAR regulators.

Connecting through the back panel, solenoid interfaces run through and are controlled through the use of solid state relays. Figure 94 displays a circuit diagram of how the solid state relays control each of the ball valves and the resulting current rating increase by using a second solid state relay not part of the cDAQ module. This allows the NI relays, which can pass no more than 500mA per channel, to pass up to 5A rated at 280VAC. While nowhere near the current that the ball valves draw, this increased rating helps further protect the cDAQ module. Additionally, warning lights and other numerous safety protocols are controlled by use of the NI relays which helps lock circuits out by using them in tandem with the virtual interface.

Warning notifications are designed to be controlled through the CIHI to make the system more integrated when operating. There are two different warning systems: one for facility status during fill/vacuum and the other for hydraulic operation. Facility status employs the use of two warning light colors and a siren. Yellow flashing begins at the

onset of operation and indicates the vacuuming down of all sections. When this light flashes it is important to note that people can travel around the facility if need be but it should be avoided. Red flashing implies that no person should be around any part of the facility, including the back assembly. Before this light can be turned on the siren must fire and the operated must verify no individuals are anywhere in the lab except the control room or the loft.

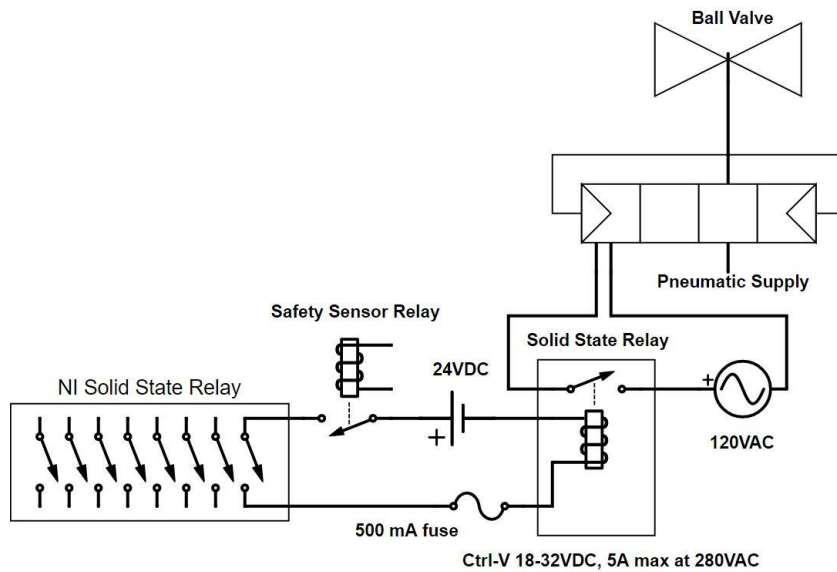


Figure 94. Schematic representing the current rating amplification when using the NI solid state relays and standard relays in series.

There are three locations for the facility status warning lights: two pairs outside both entrances to the annex (one outside and one inside) and a single pair located on the plate that the tailpipe runs through. These are all wired as “red” and “yellow” on the back panel since all signals of a signal are either on or off. The siren is only located on the

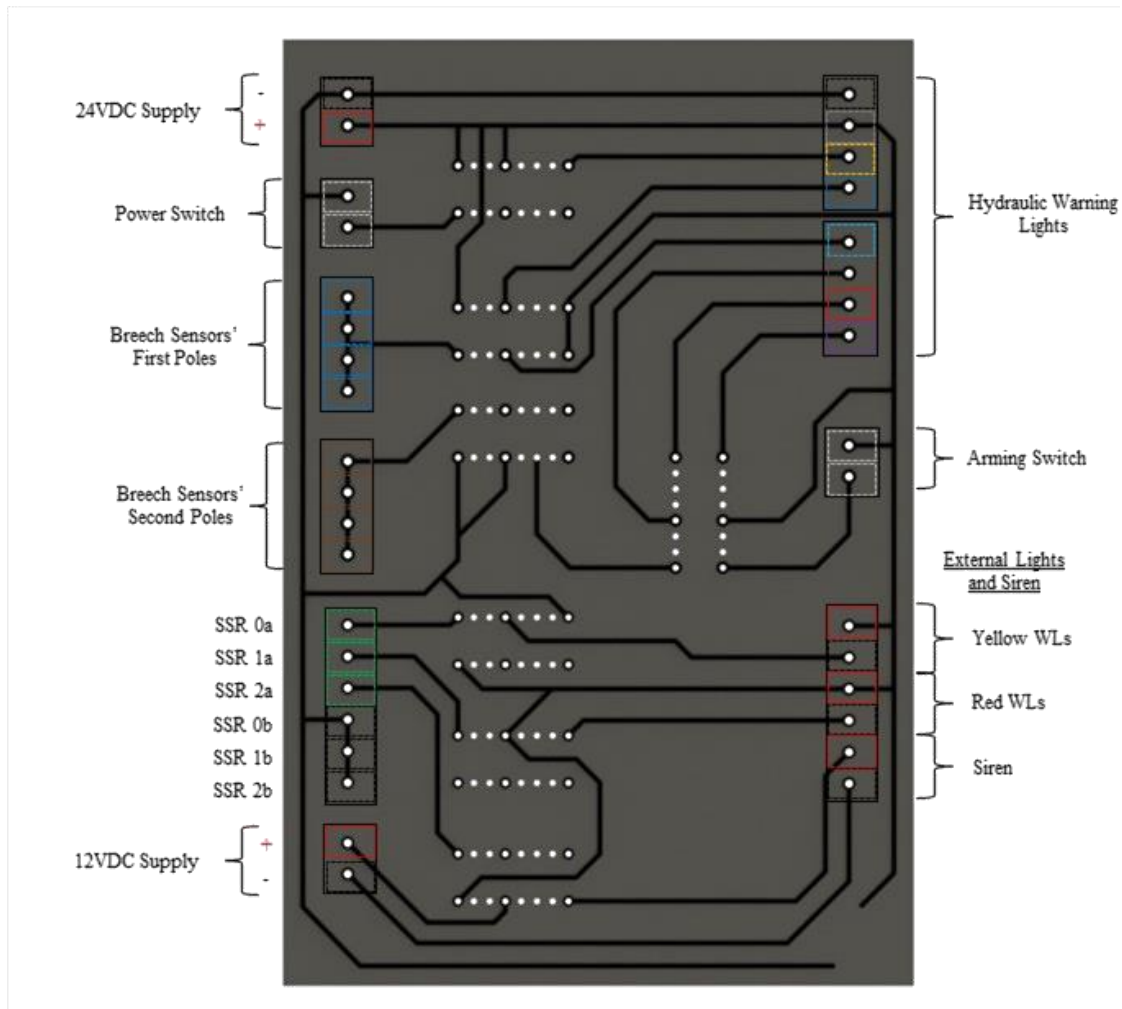


Figure 95. Circuit layout for the warning system lights and logic switches required to activate at correct time interval.

tailpipe plate in order to signal to those outside to come inside or stay away. It is the responsibility of the operators to clear the inside of the lab.

Hydraulic operation warning lights are located in the annex on the wall above the driven. These indicate the status of the hydraulic units and notify people to avoid moving pipes or pressure lines. Three colors of lights and two sirens are used in the unit. A steady yellow light turns on when CIHI is turned on. This light stays on the entire time and turns

off when shut down for the day. Flashing red, along with a short pulse of the first buzzer, occurs when the hydraulics are armed on the front panel of the CIHI and turns a steady blue when the facility is locked at the breech. Blue indicates that the facility is ready to be pressurized and is accompanied by another short pulse of the second buzzer.

All of the warning lights tie into a small, compact, custom-built circuit board as identified in Figure 95. Power and relay switches are run to this circuit board in order to minimize the number of wires that have to be used for the amount of logic switches being used in the warning light system.

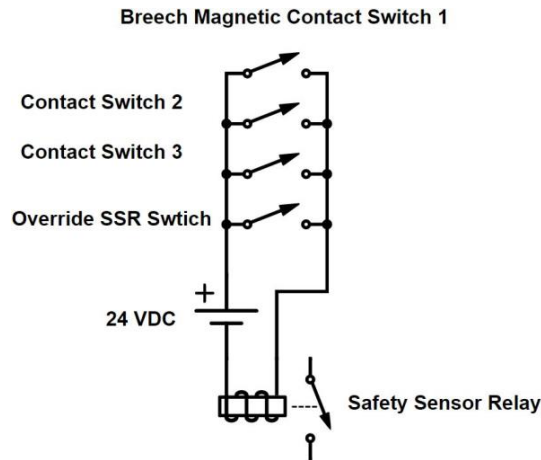


Figure 96. Circuit diagram with contact switches in parallel with an override switch controlled through labview to provide power to the ball valves.

A primary safety mechanism built into the facility, and specifically the CIHI, is the use of breech locking sensors. As described in Section 3, three magnetic contact switches are built into the breech nut and head flange. The sensor diagram is pictured in Figure 96 and incorporates the switches into the ball valve power lines to prevent vacuum or filling while all sensors are open. Only one sensor needs to work since they are small,

inexpensive and may not last long, which would increase downtime if all were required to be closed.

Hydraulics are armed using a separate switch located on the front of the CIHI, as portrayed in Figure 97, with two lights that indicate standby mode or armed. Arming of the hydraulics should only be done when movement of the pipe or sealing forces are ready to be implemented on the facility. Hydraulics pose a large safety risk when around individuals not familiar with their operation. Since lab personnel are not required training for such systems it was determined to invest a great deal into as much public notification as possible.



Figure 97. Hydraulic arming section of the CIHI electronics unit with indicators and instrumentation input.

The hydraulics system is operated by use of a customized pendant that controls various movements in the facility. This pendant is programmed to control the 4-way solenoids that redirect flow as shown in Figure 86 of Section 5.2. Each button on the pendant lights when appropriate to use. For instance, if the breech is locked than the only button that will light is the UNLOCK button since this is the only movement that can be

made. When just unlocked, the LOCK and BACK buttons light because, at this stage in movement, those are the only two options available. All other button circuits are closed as to avoid damage when, for instance, an individual presses the BACK button when the breech is locked.

The CIHI is currently under construction and an updated image is presented in Figure 98. Currently, all data wires are run to the cDAQ with the thermocouple (NI 9213) and analog input (NI 9205) modules being completely connected. Many components still need to be incorporated, such as the warning light circuit board and safety lockout relays.



Figure 98. Image detailing the progress of the CIHI electronics unit with cDAQ on the right, power supplies on the left and solid state relays on the bottom right.

5.3.5 Virtual Interface

As described earlier in this section, two computers are used to control HXT: a controls computer and a high sampling data acquisition computer (HSDaq). This is done

in order to devote full resources to the DAQ card present in the HSDaq computer without the need to monitor fill/vac conditions or control. Even so, both computers share a degree of information with each other as laid out in Figure 99. While limited, the information serves to split the responsibilities of running the facility to a certain degree as will be explained. Before operation, the communication between the computers is terminated, allowing the HSDaq computer to fulling focus on data sampling.

Operation of HXT begins with the input of two of three variables: Reynolds number, Mach number, or the driver/driven pressure ratio. These are input into the HSDaq computer, computed for initial pressures for each of the R/N/A sections, and forwarded to the controls VI. Based on the initial parameters it receives, the controls computer calculates the required voltage signals needed to be generated through the analog out ports and sent to the digital regulators. Once the controls computer receives this information, the communication pathway collapses and each computer runs individually. This prevents the re-typing in of information which could lead to human error and consume useful time.

Each VI utilizes two monitors for additional space to represent ample information. Representations of the planned VI for the controls computer is portrayed in Figure 100. A control flow diagram is overlaid on the first monitor screen with the pressure and temperature monitors of each section labeled as (1), including the set point pressures relayed from the HSDaq computer. Pressure transducer and thermocouple statuses are indicated in (2) and (10), with each indicator lighting green when the pressures and temperatures are within nominal limits. Ball valve indicators (3) light when the solenoids are energized and turn off when the circuit is open.

For control, fill and vent switches (4) are accompanied by additional lights that flash when appropriate to operate. For instance, all the vacuum lights flash yellow when the facility needs to vacuum down and stay yellow when a sufficient vacuum has been achieved. Digital regulators (5) are not directly controlled but do signal when power is going to them. These indicators do not determine whether the analog out ports are working correctly, only that power is being sent to them. An option for vacuuming all lines is offered for initial pumping down of the facility (6) and to minimize the pressure differential on the diaphragm during this process.

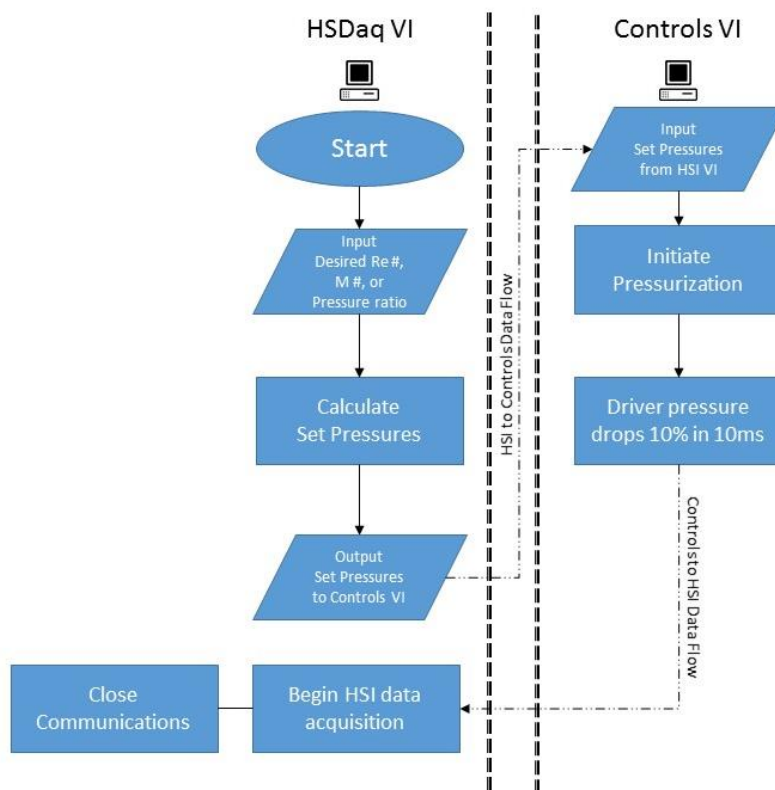
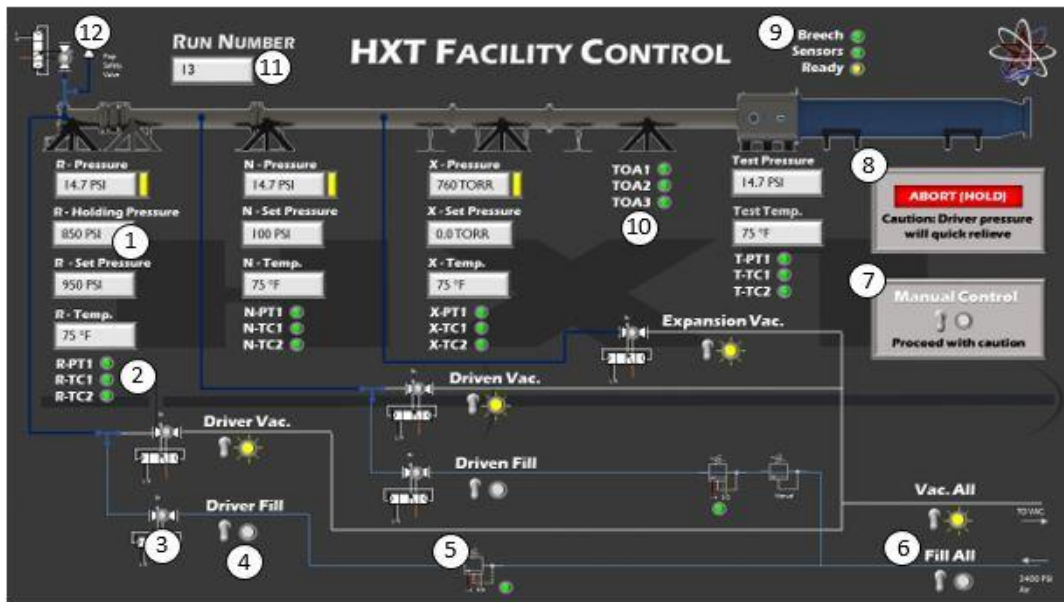


Figure 99. Data flow diagram of information passed between the controls and HSDaq VI programs.



Control Screen (Left): HXT Facility Control

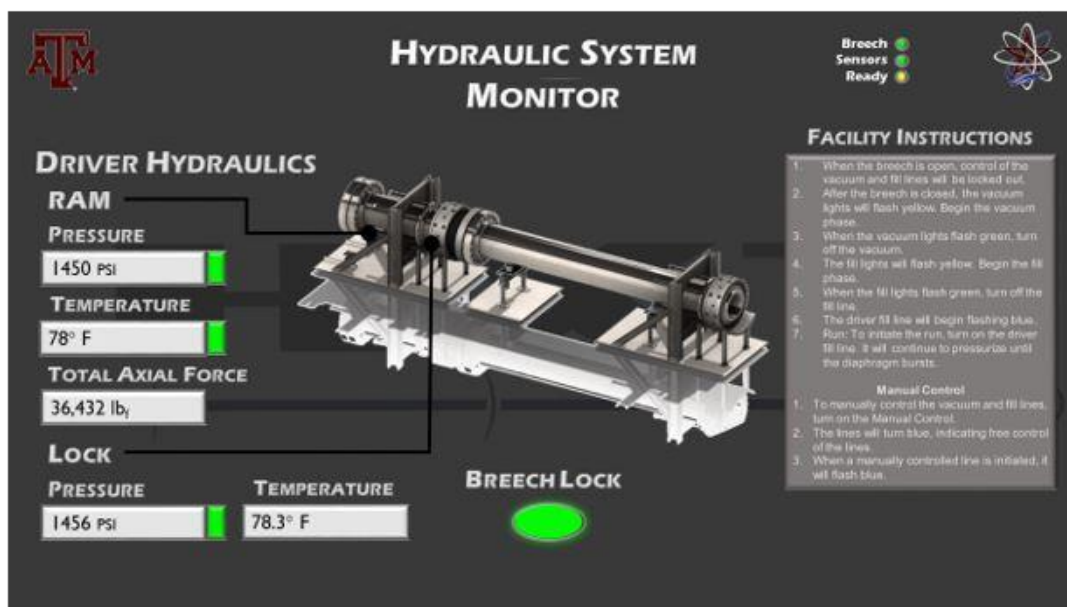


Figure 100. Controls VI for monitoring conditions in HXT and controlling flow lines.

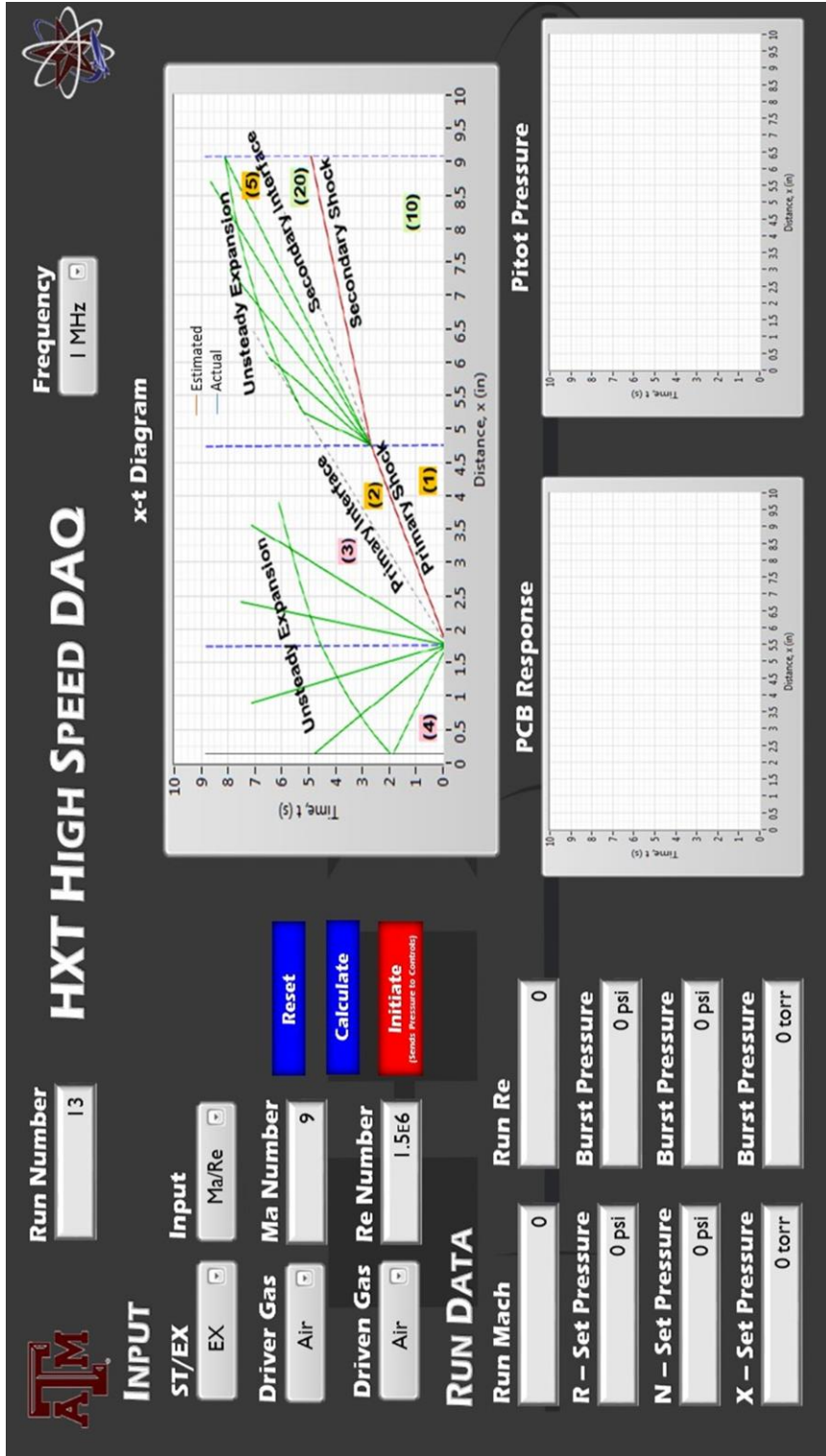


Figure 101. High speed data acquisition virtual instrument screen.

Manual override is an optional control only to be used when absolutely necessary, usually for troubleshooting ball valve controls or leak testing specific lines. This override disables all lockouts in the VI, allowing the user to hit any control switch at will.

Finally, run number count and operational status are represented in (11) and (9), respectively. Run count automatically populates at the run of the program and can only be reset manually in the programming. Operational status indicates breech sensor feedback through the use of the I/O ports integrated into the NI 6525 unit.

The second monitor of the controls computer represents the hydraulic pressures, temperatures, and resulting forces on each cylinder. This monitor is dually displayed in both the control room and near the hydraulics control pendant in order to monitor the status of the system while operating the rams. A facility instruction protocol is also displayed to the right of the 3D representation of the driver which will explain the options at each step during the operating procedures.

For high sampling data acquisition for both the time-of-arrival sensors and the pitot probes used in the test section, a separate VI, presented in Figure 101, is used so that the computers do not interrupt each other. This is extremely important so that the analog-to-digital converter can be dedicated the data stream coming from these instruments, maximizing the sample size for a single run.

The HSDaq system also calculates the 1-dimensional fluid mechanical modelling code that converts desired inputs of Reynolds number, altitude, Mach number, etc using the driver, driven, and accelerator gases into set pressures for the controls computer. This is not explicitly required, though due to the congestion of the controls VI it was suggested

to distribute this role to the HSDaq system. Since a minimum of two people are required to operate the facility, one for each computer system, this also reduces the responsibility of the controls operator and allows redundancy for insuring the settings are correct.

6. CONCLUSIONS

The following section details a summary of the construction efforts thus far in the project as well as a brief synopsis of the four primary objectives as stated in Section 1.5 and how these objectives were accomplished.

6.1 Objectives and Requirements Summary

As stated in Section 1.5, the Hypervelocity Expansion Tunnel is designed around four top-level objectives. These are accompanied by an extensive list of primary and derived design requirements, all of which can be found in Appendix A.

The first and most important objective was that the facility should operate in a safe and convenient manner. As stated in each section, all items are designed using a factor of safety based on the yield point of the material. This gives a significant buffer region when compared to ultimate strength, especially in regards to A36 steel that has almost twice the ultimate strength as its yield (50ksi against 36ksi) [25].

Additionally, when each component was analyzed using finite element analysis, a minimum factor of safety of 2 was always achieved, with most components designed to achieve factors of 4 or higher. For the pipe segments, each ASME rating already has these factors of safety built in, meaning that the facility should ultimately have no weak pressure points. The test section, which is a custom built pressure vessel, will be hydrostatically tested up to pressure, which is still a conservative action considering that the pressure relief plate located on its roof pops when the test section is under any positive pressure whatsoever.

For convenience, multiple action items are included in the design of the facility, with the largest and most time-saving being the breech and mylar diaphragm systems. These two assemblies should allow the duty cycle of the facility to fall from around one test a day to upwards of three a day, significantly increasing data generation and morale of the operators.

Another primary objective for HXT is that it have an “aerothermally” clean flow. While not explicitly achieved since the facility has yet to fire, the predicted flow field using the 1-dimensional fluid mechanical model should properly achieve these conditions. Utilizing an expansion tunnel from the beginning prevents stagnation points along the accelerator section, preventing the high energies that can dissociate or vibrationally excite the molecules in the flow.

Furthermore, while an “aerothermally” clean flow was the top-level objective, a side point designated by the team was to maximize the operating parameters of the flow itself, including run-time, core flow diameter, and Reynolds number range. Run-time was maximized by the calculated reflection distance required for the tailpipe in order to prevent the shock from re-entering the test section as discussed in Section 4.2.2. Core flow diameter was increased by upping the pipe size from the 12” NPS proposed in the ONR proposal to a 20” NPS. This almost doubles the core flow size without a nozzle, as detailed in Table 3 of Section 2.2.1. Finally, Reynolds number range increase is accomplished by the optional air receiver tank positioned at the end of the tailpipe. While not effecting the expansion tunnel mode of the facility, the increase in volume significantly expands the shock tunnel operating envelope as depicted in Figure 7.

The third objective stated in the Introduction is that the facility be optimally suited for laser diagnostics in its test section. Section 4 details the dimensional sizing of the test section with its multiple access panels and spacious interior. This large cell allows laser beam access from any direction with the use of optical mounts fastened to the inside of the walls. Models can also be inserted from both the sides and top of the test section, allowing models up to 60” long (diameter is significantly smaller).

The final objective mentioned is the inclusion of a shock tunnel mode in addition to the expansion tunnel operation. This includes the movement of the breech system and allowing a great deal of flexibility for stand placement. The biggest issue with designing a shock tunnel mode was the pressure limitations of the test section and tailpipe, since the ST-driver has four times more volume than the XT-driver, increasing the end-of-operation pressure. This was dually accomplished by reducing the driver pressure of the facility, as detailed in Section 4.3.1, and adding a future phase where an air receiver would be connected to the facility to increase the overall volume. The air receiver is discussed in Section 4.2.3 and the end-of-operation pressures are summarized in Table 12.

These objectives have been accomplished to the best ability of the engineering team and, while the facility is being built at present, will be tested in a safe and reliable manner. Records of test will be recorded and this manuscript, along with others, will be compiled for the future students assisting with the project. Given the approximate year from fall of 2015 to fall of 2016, a great deal of work has been accomplished, primarily by students who are also juggling classes and other extracurricular activities. With a price tag of approximately \$350,000, it is extremely impressive that a group of 5 undergraduates

and a single graduate student have been able to design, develop, and build this facility in that time span.

6.2 Construction Summary

Construction of HXT began in April of 2016, which started with ordering material for the test section and tailpipe. The following is a summary of the progress made up until late September 2016. For more in-depth details on the timeline of fabrication for each part please refer to each components devoted subsection titled “Manufacturing.”



Figure 102. 20” Schedule 80 pipe cut into appropriate lengths sitting at the shop waiting to be welded.

The driver, driven, and accelerator pipe sections were ordered during the month of February 2016, however, due to complications with purchasing and the cost of the pipe, delays occurred that consumed the entire summer and beginning of fall. The schedule 80 20” stainless steel pipe was cut and delivered to the welders at the beginning of August 2016, as pictured in Figure 4, along with all five of the 20” 300# slip-on flanges and all five of the 20” 900# slip-on flanges.

Postponement of welding was caused primarily due to the delay in the schedule 160 20” pipe, which took several weeks longer to fabricate as a consequence of the walls

being too thick (~2”) and the manufacturer’s rolling machine breaking down multiple times. When delivered to Custom Fabricators as depicted in Figure 103, additional delays were caused by the shop not being able to plasma or saw cut the walls because they were too thick, so the pipe had to once again be loaded up, shipped to Houston for cutting to length, and then delivered to the welding shop.



Figure 103. 20” Schedule 160 pipe as it is being unloaded at Custom Fabricators to be cut.

Final drawings were finalized at the end of September 2016 for the welders at Circle H Manufacturing. These drawings were signed off and copies are presented in Appendix B. Welding and pressure testing is expected to take 13-15 business days and delivery is expected by mid to late October.

The diaphragm systems, while fully designed for the breach, are on hold for manufacturing due cost and other pressing matters regarding the operation of the facility. As of September, all resources and personnel are devoted to making HXT operational by use of the backup diaphragm configuration. While not ideal, this system will allow

diaphragms to be broken in the facility while construction of the breech and MDS, which is expected to last many months, simultaneously takes place.



Figure 104. Back assembly with test section and tailpipe running through the wall of the NAL with blind adapter plate for eventual hydrostatic pressure testing.

Additionally, while the breech system is detailed in full in Section 3.2, the mylar diaphragm system presented in this thesis is only one option being considered as the final design. Further engineering of the MDS should take place before construction even begins on the breech system. These two mechanisms are inherently tied together since the shock tunnel and expansion tunnel modes depend on the same overall length of the facility with these two mechanisms, thus the use of a spacer in the backup configuration. Ideally, the tunnel, when in the backup configuration, needs to have an additional spacer for the MDS. This means that the maximum allowable size of the MDS should be determined prior to the bolting down of the stands, since the primary and secondary stands, once bolted, cannot be moved by less than a foot due to interference and structural weakening of the concrete.

The back assembly, as of September, is fully constructed and installed as pictured in Figure 104. The test section pictured does not have a rib or any brackets welded to the skeleton, so this is to be done before proceeding any further. The front pipe-to-test section adapter is machined as a blind to allow the test section to be hydro-statically tested to 100 psig. An additional blind will be manufactured to be placed at the tailpipe end of the test section to fully enclose it. Besides the modifications to the test section and slight alignment still necessary for the tailpipe, the back assembly is the most complete section of HXT as of September.



Figure 105. Four of the five stands tacked together without the 6-inch square tube bracings.

As discussed in Section 5.1, the support stands took approximately three months to complete and, as of September, are fully constructed but not painted or installed. Figure 105 displays four of the five stands tacked together without the canted 6-inch square tube bracings. Since the picture was taken, all stands have been fully welded together and mounting holes torched into the baseplates.

Alignment of the facility will take place once the test section modifications are complete and the support stands are installed. The driver stand, being the furthest from the back assembly, will be installed first and the tailpipe aligned with it. Shimming of the support stands will take the longest time but should hopefully be complete shortly after the delivery of the pipe sections.

The controls and instrumentation hardware interface (CIHI) electronics unit's progress is detailed fully in Section 5.3.4. Significant wiring still needs to be done with regards to the relay units and circuit boards need to be etched for the control of the warning lights. Figure 5.36 displays the current condition of manufacture for the CIHI.

7. FUTURE WORK AND RECOMMENDATIONS

7.1 Operational Roadmap

The following section details in length the action items necessary to get HXT running. Figure 106 maps out what actions need to be taken and the order in which they should be executed to break a diaphragm in the facility.

Moving left to right on Figure 106, the stands are more than likely the easiest to finish. All five major stands along with the eight roller stands have to be painted and installed in their rough location in the lab. Alignment with the tailpipe and the walls of the annex will need to be done in order to attain proper height with the stands and test section located in the laser lab.

The driver, driven, and accelerator pipe sections, once welded and delivered, will be installed on the roller stands to be leveled with the test section. No adjustment in height should need to occur with the back assembly, though some lateral movement may be needed to square up with the annex walls.

The vacuum pumps which will pull down the accelerator and back assembly will need to be installed in their location yet to be determined before the test section can be moved. This is done so that any o-rings can be fixed and/or modified before hydrostatic pressure testing is done. Even before then, however, modifications must be made to the test section to add the central rib and the seam brackets. These will increase the pressure rating of the test section as discussed in Section 4.3. Once the test section is hydrostatically

tested, it will be repositioned in its designated location as pictured in Figure 104 and alignment of the pipes can begin.

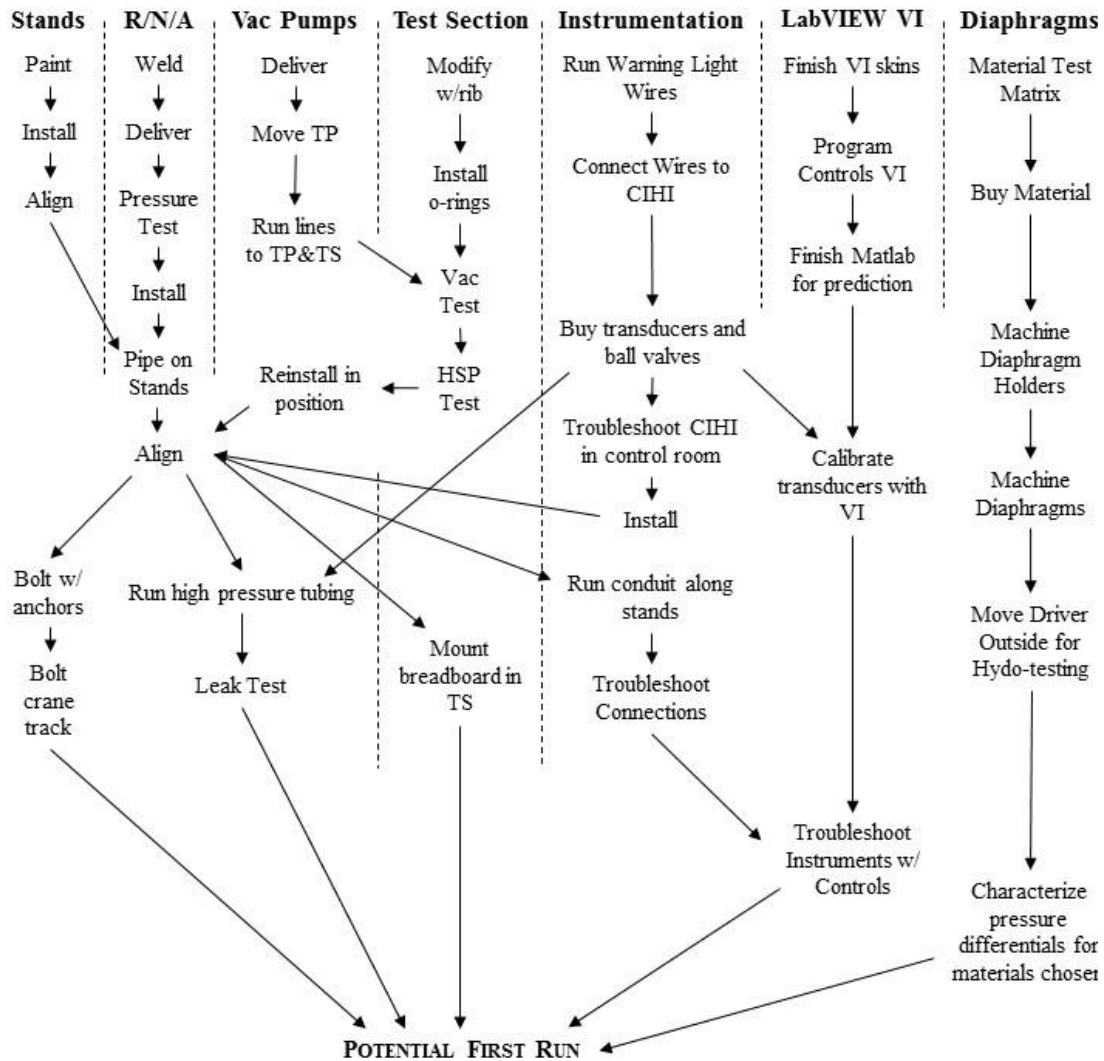


Figure 106. Extensive roadmap laying out what actions need to be taken to reach a point where a diaphragm can be destroyed.

Tweaks to the alignment of the sections along HXT should take a relatively short amount of time, with most of the legwork being done during the alignment of the primary and secondary stands. Once all sections are in their desired locations, anchors can be

placed by hammer drilling into the concrete along the torched holes at each stand's baseplate. The crane track, which runs immediately along the edge of the stands, can then be bolted down in a similar manner using smaller concrete anchors.

After alignment of the facility is complete, the high pressure, shop air, fill, and vacuum lines can be run along the length of the pipe, mounting to each stand for a clean look when running the facility. Ball valves also will be placed in their proper location at this point in time, along with transducers and other additional wiring in a conduit line running parallel to the rest of the lines. All pressure and vacuum lines will need to be leak tested individually before full operation of the facility can occur.

The CIHI will be installed along with the ball valves and other warning lights. Troubleshooting of the electronics unit can occur even before the entire unit is completely wired, allowing data channels to be checked and calibrated before being fully incorporated. Transducers should be separately calibrated on the NAL calibration cart and the data input into the virtual interfaces being used in the controls computer.

Before a full run can begin, the entire facility should test each section individually for leaks and data interference. A "dry run" should occur prior to the first fire and a set of initial conditions, discussed at length in Section 6.3, should be conducted before a test at the highest pressure conditions obtainable.

Additionally, while the roadmap presented in Figure 106 describes many of the items necessary for a first run, it should not be taken as a comprehensive list. For instance, the process to manufacture diaphragms is not stated, nor is the course needed to be taken in order to properly machine the spacer or diaphragm holder as described in Section 3.4.

Unexpected needs are inevitable in a project this large and Figure 106 is a generalized plan for accomplishing a first test.

7.2 Recommendations

After a first successful test of the Hypervelocity Expansion Tunnel, four additional projects are already in the works: characterization of the diaphragms, construction of the diaphragm mechanisms, characterization of the flow field, and the manufacturing/installation of the 36” diameter diverging nozzle.

In order to fully understand how to operate the facilities at pre-determined conditions, the diaphragm burst pressures must be recorded for different thicknesses and etching depths. This process can take many months depending on the desired resolution of pressure differentials for a given diaphragm between the driver and driven. For example, if the resolution is only chosen at every 100psi between 100 and 2000psi, than 20 different diaphragms must be characterized. If a finer resolution of 50psi is required, than 40 different etching depths and thicknesses must be specified.

Characterizing the diaphragms is extremely tedious, but vital to the predictability of the facility since the burst differential dictates the pressure ratio between the driver and driven and, thus, the shock strength and all subsequent events thereafter. Controlling the diaphragms burst point allows finer control of the conditions being tested in the facility and will allow proper flow characterization by creating a more repeatable environment.

For diaphragm testing, however, the backup configuration of the diaphragm system will be utilized which, while slow, will allow simultaneous construction of the breech and mylar diaphragm mechanisms. These two systems will most likely be

manufactured by Machine Works due to their large nature and tight tolerance requirements. The breech unit can be pressure tested remotely from the rest of the facility, as can the mylar diaphragm system when it is finished being designed.

Installation of the breech can occur either before, during, or after diaphragm characterization, but after seems to be the more likely scenario due to unexpected problems arising either during manufacture or pressure testing. While these should be surmountable issues in the long run, timelines for custom-made mechanisms of this size and pressure rating should expect to run longer than expected.

After characterization of the diaphragm mechanisms and, preferably, after the installation of the diaphragm systems, full radius pitot rakes can properly measure the flow coming out of the 20" pipe. Characterization of the flow field is important for many reasons, including predictability for operation and noise level measurements. Pitot rake measurements will also be able to determine the size of the boundary layer at the exit of the accelerator tube and permit proper sizing of test models to fit inside the core flow. Error measurements are derived from these experiments and present a baseline that all future experiments will follow.

As described in Section 2.6, a diverging nozzle has been preliminarily designed and included in a proposal written to the Air Force Research Laboratory (AFRL). This nozzle will expand the Mach number range of the facility and increase the core flow size during testing. Similar to configuration without the nozzle, the flow field will need to be characterized and error measurements recorded along with the estimates of boundary layer thickness at varying conditions.

Overall, the design and development of the Hypervelocity Expansion Tunnel should reach ultimate conclusion by the end of 2016. The few loose ends that have been discussed in this thesis should either be resolved or handed off in proper fashion to those taking over responsibility by the end of the calendar year. Construction of the facility will still progress through the concluding revisions of this manuscript and final examination defense. The ultimate goal is to have HXT break a diaphragm before the beginning of January 2017, though plans are firmly in place for the next generation of graduate students if this is not to happen.

Either way, the Hypervelocity Expansion Tunnel should prove to be one of the most productive facilities at the National Aerothermochemistry Laboratory in terms of research within the near future. It is optimally suited for thermal nonequilibrium testing at flight-light conditions at Mach numbers between 4 and 14. Its dual shock tunnel mode should make HXT a facility capable of research not yet achievable in many accessible wind tunnels around the world.

REFERENCES

- [1] C. L. N. Mai, "Near-Region Modification of Total Pressure Fluctuations by a Normal Shock Wave in a Low-Density Hypersonic Wind Tunnel," Ph. D. Dissertation, Department of Aerospace Engineering, Texas A&M University, College Station, TX, 2014.
- [2] R. Bowersox, S. North and E. White, "Hypersonic Expansion Facility for Fundamental High-Enthalpy Research," Research Project Proposal to the Office of Naval Research, 2015.
- [3] W. A. Martin, "A Review of Shock Tubes and Shock Tunnels," Convair Aeronautics Engineering Department, 1958.
- [4] T. Albrechtinski, D. Boyer, K. Chadwick and J. Lordi, "Calspan's Upgraded 96-inch Hypersonic Shock Tunnel: Its Development and Application in Performance of Research Testing at Higher Enthalpies," 33rd Aerospace Sciences Meeting and Exhibit, Aerospace Sciences Meeting, 1995.
- [5] H. Hornung, "Performance Data for the New Free-Piston Shock Tunnel at GALCIT," Proceedings of the 18th International Symposium on Shock Waves, Sendai, Japan, 1991.
- [6] C. Wittliff, M. Wilson and A. Hertzberg, "The Tailored-Interface Hypersonic Shock Tunnel," *AIAA Journal of Aerospace Sciences*, Vol. 26, No. 4, pp. 219-226, 1959.
- [7] A. Dufrene, M. Sharma and J. Austin, "Design and Characterization of a Hypervelocity Expansion Tube Facility," *Journal of Propulsion and Power*, Vol. 23, No. 6, 2007.
- [8] M. Holden, "The LENS Facilities and Experimental Studies to Evaluate the Modeling of Boundary Layer Transition, Shock/Boundary Interaction, Real Gas, Radiation, and Plasma Phenomena on Contemporary CFD Codes," CUBRC Internal Report and Presentation, 2010.
- [9] J. Erdos, R. Bakos, A. Castrogiovanni and R. Rpgers, "Dual Mode Shock Expansion/Reflected Shock Tunnel," NASA Technical Report, 1997.

- [10] A. Neely and R. G. Morgan, "The Superorbital Expansion Tube Concept, Experiment and Analysis," *Aeronautical Journal*, Vol. 98, No. 973, pp. 97-105, 1997.
- [11] A. Ben-Yakar and R. K. Hasnon, "Characterization of Expansion Tube Flows for Hypervelocity Combustion Studies," *Journal of Propulsion and Power*, Vol. 18, No. 4, pp. 943-952, 1992.
- [12] A. Dufrene, M. MacLean, R. Parker, T. Wadhams and M. Holden, "Characterization of the New LENS Expansion Tunnel Facility," *48th AIAA Aerospace Sciences Meeting*, Paper #2010-1564, Orlando, FL, 2010.
- [13] H. Mirels, "Shock Tube Test Time Limitation Due to Turbulent-Wall Boundary Layer," *AIAA Journal*, Vol. 2, No. 1, pp. 84-89, 1964.
- [14] "Pipe Schedules," Engineers Edge, LLC, [Online]. Available: http://www.engineersedge.com/pipe_schedules.htm. [Accessed 7 10 2016].
- [15] Texas Pipe and Supply, "Quote Request for 18",20", and 24" Pipe," Houston, TX, 2016.
- [16] G. Aguilar, "Expansion Tunnel Script Code", unpublished computer script, National Aerothermochemistry Laboratory, Texas A&M University, College Station, TX, 2016.
- [17] Atlas Specialty Metals, "Carbon Grade B Pipes-ASTM A53M, A106M, API5L, Seamless," [Online]. Available: <http://www.atlassteels.com.au/documents/Carbon%20steel%20pipe%20pressure%20rating%20chart.pdf>. [Accessed 7 10 2016].
- [18] The Engineering Toolbox, "ANSI B16.5 Flanges Pressure and Temperature," [Online]. Available: http://www.engineeringtoolbox.com/ansi-flanges-pressure-temperature-d_342.html. [Accessed 7 10 2016].
- [19] Parker Hannifin Corporation, "ORD 5700 Parker_O-Ring_Handbook," 14 September 2016. [Online]. Available: https://www.parker.com/literature/ORD%205700%20Parker_O-Ring_Handbook.pdf.
- [20] L. Pennelegion, R. F. Cash and D. F. Bedder, "Design and Operating Features of the N.P.L. 6 in. Shock Tunnel," Aeronautical Research Council, London, 1967.

- [21] Engineers Edge, "ACME General Purpose Thread Design Calculator-Derived from ASME/ANSI B1.8.," [Online]. Available: <http://www.engineersedge.com/hardware/acme-threads-calculator.htm>. [Accessed 7 October 2016].
- [22] Texas Flange, "Texas Flange CAD/3D Flange Drawings," 1 February 2010. [Online]. Available: <http://www.texasflange.com/index.php/flange-drawings-models>. [Accessed 7 October 2016].
- [23] FCI: Forged Components Inc., "Connection Types and Nomenclature," 2015. [Online]. Available: <https://forgedcomponents.com/fci-asme-pressure-vessels-connections/connection-types-and-nomenclature/>. [Accessed 4 October 2016].
- [24] McMaster-Carr, "Press-Fit Ball Transfer 6421K69," [Online]. Available: <http://www.mcmaster.com/#6421k69/=14hui5x>. [Accessed 29 September 2016].
- [25] AZO Materials, "ASTM A36 Mild/Low Carbon Steel Mechanical Properties," 28 June 2012. [Online]. Available: <http://www.azom.com/article.aspx?ArticleID=6117>. [Accessed 7 October 2016].
- [26] PHIONE Limited, "ASME/ASTM A105," [Online]. Available: <http://www.phione.co.uk/specialised-steel-products/flanges/a-105>. [Accessed 7 October 2016].
- [27] AZO Materials, "AISI 4130 Alloy Steel (UNS G41300)," 6 September 2012. [Online]. Available: <http://www.azom.com/article.aspx?ArticleID=6742>. [Accessed 7 October 2016].
- [28] AZO Materials, "AISI 4140 Alloy Steel (UNS G41400)," 7 September 2012. [Online]. Available: <http://www.azom.com/article.aspx?ArticleID=6769>. [Accessed 7 October 2016].
- [29] TineLok, "Grade 5 vs Grade 8 Fasteners," Permanent Technologies, Inc., 2013. [Online]. Available: <http://tinelok.com/grade-5-vs-grade-8-fasteners/>. [Accessed 7 October 2016].
- [30] AZO Materials, "AISI A514 Grade B Alloy Steel (UNS K11630)," 6 September 2012. [Online]. Available: <http://www.azom.com/article.aspx?ArticleID=6737>. [Accessed 7 October 2016].

- [31] QMF Steel, "Individual Quote for Custom Cut Pieces of A36 Steel," Campbell, TX, 2016.
- [32] Mechanical Research and Design, *Dimensional Drawing for Inflatable Seal MPL-22.500-SC*, Mechanical Research and Design, 2016.
- [33] Ro E. Hanson Jr. Manufacturing, "60-HG-2520-W Air Receiver Specifications," 22 August 2011. [Online]. Available: <http://hansontank.com/airreceivers/horizontal/60HG2520W/60HG2520W.pdf>. [Accessed 7 October 2016].
- [34] Alma Bolt Company, "Proof Load Tensile Strength for Grade 2, 5, & 8," 2006. [Online]. Available: <http://www.almabolt.com/pages/catalog/bolts/proofloadtensile.htm>. [Accessed 7 October 2016].
- [35] Haldex Hydraulic Power Unit, "1-5HP AC Hydraulic Power Units Operating Instructions and Parts Manual," [Online]. Available: <http://www.northerntool.com/images/downloads/manuals/10591.pdf>. [Accessed 7 October 2016].
- [36] Prince Hydraulics, "3000psi Tie-Rod Line-Royal Series," Prince Manufacturing Corporation, 2008. [Online]. Available: <http://www.princehyd.com/Products/Hydraulic-Cylinders/Tie-Rod/3000-PSI-2-5-Bore>. [Accessed 7 October 2016].
- [37] McMaster-Carr, "Smooth-Bore Seamless 304 Stainless Steel Tubing 3/8" OD at 0.028" Wall Thickness," McMaster-Carr, [Online]. Available: <http://www.mcmaster.com/#89895k736/=14hvmqf>. [Accessed 7 October 2016].
- [38] Grainger, "3/8" Spring Return-Fail Close Pneumatic Actuated Ball Valve, 3-Piece," Dynaquip Controls, [Online]. Available: <https://www.grainger.com/product/DYNAQUIP-CONTROLS-3-8-Spring-Return-Fail-Close-1AWR2>. [Accessed 7 October 2016].
- [39] Equilibar, "QB1T & QB2T Installation and Maintenance Instructions," 22 March 2016. [Online]. Available: <http://www.proportionair.com/literature/installation-guides/QBT-Installation.pdf>. [Accessed 8 August 2016].
- [40] Equilibar, "PRA Proportional Ratio Assembly: High Pressure Electronic Pressure Controller," [Online]. Available:

- <https://www.equilibar.com/PDF/PRA-Ratio-Reader.pdf>. [Accessed 8 August 2016].
- [41] Omega Engineering Inc., "Pressure Transducers," Omega, 2016. [Online]. Available: <http://www.omega.com/section/pressure-transducers.html>. [Accessed 7 October 2016].
- [42] REOTEMP Instrument Corporation, "Types of Thermocouples," Thermocouple Info, [Online]. Available: <http://www.thermocoupleinfo.com/>. [Accessed 7 October 2016].
- [43] National Instruments, "User Manual NI cDAQ-918x/919x," May 2014. [Online]. Available: <http://www.ni.com/pdf/manuals/372780h.pdf>. [Accessed 7 October 2016].
- [44] National Instruments, "Datasheet NI 9205," 15 October 2015. [Online]. Available: http://www.ni.com/pdf/manuals/374188a_02.pdf. [Accessed 7 October 2016].
- [46] The Engineering ToolBox, "Maximum Operating and Required Burst Pressure of PVC Pipe," [Online]. Available: http://www.engineeringtoolbox.com/pvc-cpvc-pipes-pressures-d_796.html. [Accessed 7 October 2016].
- [47] McMaster-Carr, "Smooth-Bore Seamless 304 Stainless Steel Tubing 1/4" OD at 0.02" Wall Thickness," [Online]. Available: <http://www.mcmaster.com/#89895k722/=14hw4uh>. [Accessed 7 October 2016].
- [48] National Instruments, "Datasheet NI 9213," January 2016. [Online]. Available: http://www.ni.com/pdf/manuals/374916a_02.pdf. [Accessed 7 October 2016].

APPENDIX A
REQUIREMENTS DOCUMENTS

This section lists each requirements document in order of manuscript presentation. The requirements are a series of design points needing to be achieved in order for proper and safe operation. These requirements are listed as primary and contain the word ‘shall’ in bold letters for each point. Derived requirements are additional conditions imposed by the specific nature of the design route taken and the location at the NAL. The following documents will be presented in this Appendix:

- Driver, Driven, Accelerator
- Diaphragm System
- Test Section
- Stands
- Hydraulic System
- Instrumentation and Electronics

Driver, Driven, and Accelerator Pipe Design Requirements

Primary Engineering and Safety Requirements

- Pipe shall be able to achieve the operating conditions equal to or greater than those presented in the ONR proposal
 - 2000 psi max pressure in driver
 - 100 psi max pressure in driven
 - 10^5 - 10^8 /m in Reynolds number range
 - Mach 5-15 with nozzle addition
- Pipe shall allow the installation of a nozzle at a later time as part of the accelerator section
- Pipe shall be reconfigurable as to operate in a shock tunnel mode
- Pipe, flanges, and fittings shall safely maintain pressures and temperatures as set out in the ONR proposal and abide by ASME codes
- Pipe shall have ports capable of filling and vacuuming each section independently
- Pipe shall fit in space allocated at the NAL as to not require extensive construction of additional lab space
- Pipe costs shall lie within the allotted budget set out, potentially increasing pipe size and core flow diameter

Derived Requirements

- Pipe should have multiple ports located along the accelerator for mounting time-of-arrival sensors
- Pipe should expand on the core flow parameters set out in the ONR proposal and investigate improving/expanding upon the predicted operating envelope of the facility
- Accelerator pipe should be dividing into 20/10/20ft segments to allow the replacement of the third segment with the future nozzle
- Pipe should be located along the length of the support structures in a configuration that allows 4 of the 5 stands to be used while in shock tunnel mode
- Pipe should be welded and approved by board certified inspectors according to ASME Section VIII, Division 1

Diaphragm System Design Requirements

Primary Engineering and Safety Requirements

- System shall allow easy access to diaphragms
- System shall align diaphragms in a specific orientation in regard to the bursting pin
- System shall interface appropriately with the driver, driven, and accelerator sections
- System shall be able to withstand operating temperatures and pressures
- System shall be able to transmit any recoil force from the driver to the driven and not yield
- System shall be removable from the facility in case of malfunction, maintenance, or further testing
- System shall seal at all operating pressures and temperatures
- System shall have a backup configuration that works without any use of any part of the diaphragm system except the diaphragm holder

Derived Requirements

- System should allow access to diaphragms by moving the driver back away from the breech
- System should align the diaphragm using dowel pins located in the diaphragm holder and alignment grooves with the backup configuration
- System should interface with the 900# flanges that are already welded on the driver and driven sections of the facility
- System should be manufactured with equally rated flanges and wall thicknesses as are used in the design for the rest of the driver, driven, and accelerators
- System should be able to handle at least 3 times the recoil force designated at 404,540 lbf, but preferably 4 times
- System should be removable at the 900# interfaces, meaning it shall too have 900# flange interfaces
- System should utilize o-rings in order to seal at the necessary interfaces, especially in regard to the diaphragm holder
- System should use spacers as a backup configuration using leftover sections of pipe cut from the 20ft schedule 160 stainless piece
- System should use two separate systems for the driver/driven and driven/accelerator diaphragms since the pressures seen by these two diaphragms vary drastically

- System should use a breech mechanism to seal the high pressure driver/driven diaphragm since these are known to be able to the expected forces as noted in 2 different papers [4,5]
- System should utilize a slip-disk system for the lower pressure mylar diaphragm to reduce cost and manufacturing time

Test Section Design Requirements

Engineering Requirements

- The Test Section shall hold models capable of being placed wholly in the flow both with and without a nozzle
 - 19" diameter without a nozzle
 - 36" diameter with a nozzle
- The Test Section shall have the access to remove and/or replace test models
- The Test Section shall have convenient run-to-run access of the models
- The Test Section shall have model and optics mounting capabilities
- The Test Section shall have laser diagnostic access through multiple lines of sight (LOS)
- The Test Section shall maintain operating pressures without loss to structural integrity of the facility
 - Pressure after 2000 psi R expansion fire: 36.5psia
 - Pressure after 1000psi R/N shock tunnel fire: 72.75psia
- The Test Section shall resist pressures on all access points into the facility
- The Test Section shall include a shock delay line for maximum operating runtime
 - Calculated at approximately 17ft
- The Test Section shall not be larger or longer than the space available at the NAL
- The Test Section shall be simple and cost-effective to manufacture
- The Test Section shall seal completely with the use of o-rings at each access point and on the front face with the 20" pipe and in the back with the tailpipe

Derived Requirements

- The Test Section should be roughly 4' in diameter (or slants) or larger to accommodate models and prevent blockage
- The Test Section should have door(s) on each side for multiple access points to the models

- The Test Section should split the door access on each side into two doors to reduce the loads on each individual door, reducing the number of fasteners needing to be removed
- The Test Section should have an upper access panel to allow larger models to be inserted into the facility
- The Test Section should have a lower access panel to allow for window access points to be machined if need be
- The Test Section should be at least 5 ft long to allow plenty of room both in front of and behind the model for sensor equipment and optical mirrors
- The Test Section should be made into an octagonal prism in order to reduce the loads on the walls when the test section acts as a pressure vessel
- The Test Section should minimize the surface area of the additional four walls and make them access points in case window access needs to be machined into those locations
- The access panels and doors should have approximately twice as many fasteners as theoretically needed and the exact number needed to maintain proper squeeze on the o-rings
- The Test Section and Tailpipe should not exceed a length of 28ft and width of 7ft to accommodate the space available at the NAL
- The Tailpipe should be approximately 20ft in length to conform to standard pipe lengths available for purchase in industry
- The Tailpipe should have a diameter of roughly 40” to accommodate residual expansion of the flow field through the test section at maximum flow area

Support Stands Design Requirements

Engineering Requirements

- Structural support system shall be able to handle 408k lbf of instantaneous load
- Structural support system shall be able to support facility weight
- Structural support system shall provide a nominal facility height
- Structural support system shall be easy to operate and maintain
- Each structural support shall be aligned to specification
 - Horizontal alignment offset shall not exceed ± 1 deg.
 - Center line of pipe between supports shall not exceed 0.25 in.
- Each structural support shall be able to interface with existing location layout

Derived Requirements

- Each structure should have a safety factor of 4x design load
- Failure criterion should be defined as the yield stress
- Primary and Secondary stands should have available space allocated for vertical load supports
- Material should be weldable and machineable.
 - Material should be ATSM-A36-Steel
- All structural supports should interface with 20 in. OD pipe
- Primary supports should interface with 20 in. – 900 flanges
- Secondary supports should interface with 20 in. – 150 flanges
- Supports should provide a centered and level mounting interface
 - Steel plate base
- Supports should provide a nominal pipe centerline of 36 in from the base plate
- Roller supports should facilitate installation
 - Crank jacks
- Roller supports should be rated for two time the weight of the facility
- Roller supports should minimize friction in the horizontal direction
- Supports should minimize stress concentrations throughout the structure

Hydraulic System Design Requirements

Engineering and safety Requirements

- System shall consist of all hydraulic components (see Figure HS-1)
 - Hydraulic Fluid Reservoir
 - Suction Line
 - Pressure Relief Line
 - Oil Strainer (Filter)
 - Pump
 - Relief Valve (Solenoid)
 - Pressure Line
 - Control Valve (Solenoid)
 - Hydraulic Cylinder
 - Return Line
- System shall consist of the following hydraulics, but be run on a common system (i.e. common reservoir and pump)
 - Hydraulic Driver Ram to maintain proper squeeze on sealing O-Rings

- Hydraulic Driver Cylinders for Breech Head and Nut Locking
- Hydraulic Fluid Lines shall be rated for appropriate pressures above the maximum rating of the hydraulic pump
- Hydraulics shall not exceed required forces
- Hydraulic cylinders shall be double-acting
- System shall not expose operators to forces (no gaps for fingers, arms, other extremities)
- System shall minimize hydraulic fluid leakage (minimum # of fittings)
- Lines to hydraulic cylinders shall be flexible as to allow movement
- hydraulic forces should be variable up to required force
- Hydraulic pressure lines should be run as far away from compressed air lines as possible
- System cost should be kept to a minimum with the knowledge that more expensive equipment may reduce maintenance cycle/down-time

Operational Requirements

- System shall have back-up manual pressure relief valves in cases of digital controls failure
- System components shall not interfere with common run-to-run operation of the tunnel
- system shall not be allowed to operate without public notification light (no flashing/must be distinct from tunnel warning light)
- System shall include both an Operational Manual and Maintenance Manual/schedule
- System should be easy to operate (control system is simple as possible)

Derived Requirements:

- System should use solenoid valves for remote actuation of valves
- System should integrate with pendant or Labview for solenoid on/off and expected sealing force of O-rings and feedback lights
- System should be easy to maintain (overall is as system simple as possible)
- System should incorporate magnetic contact switches with controls for operational feedback

Instrumentation and Electronics Design Requirements

Engineering Requirements

- The Controls **shall** monitor real-time temperature in 4 locations:
 - 1 in the Driver
 - 1 in the Driven
 - 1 in the Expansion
 - 1 in the Hydraulics (return line)
- The Controls shall monitor real-time pressure in 4 locations:
 - 1 in the Driver
 - 1 in the Driven
 - 1 in the Expansion
 - 1 in the Hydraulics (fill line)
- The temperature range of the tunnel shall be between 70°F – 400°F
- The temperature range of the hydraulic system shall be between 70°F – 180°F
- The Controls shall remotely set the pressures to the Driver, Driven, and Expansion:
 - Driver: 0 – 2100 psia
 - Driven: 0 – 150 psia
 - Expansion: 0 – 760 torr
- The Controls shall remotely open and close the Driver and Driven fill lines
- The Controls shall monitor the open and close status of the breach
- The Controls shall require the breach to report “closed” status before allowing pressurization
- The Controls shall incorporate a remotely controlled emergency vent line for the Driver section
- The system shall include an operational manual, circuitry diagrams, and operational algorithms

Derived Requirements

Pressure

- The Driver, Driven, and Expansion pressures should be controlled via digital pressure regulators with the following requirements:
 - Driver pressure range: 20 – 2,500 psia
 - Driven pressure range: 0 – 200 psia
 - Expansion pressure range: 0 – 760 torr
- There should be a protective *manual* pressure regulator before the Driven *digital* pressure regulator (see diagram)

- An additional pressure transducer should be placed in the Nozzle Exit or Test Section to fully define the state of the HXT facility
- The pressure transducers should
 - Range between zero to twice the hydraulic pressure
 - Be protected or rated against pressure spikes
 - Be shielded against EMF and routed to avoid high EMF areas
 - Be sealed against dust and fluids
- Pressure input should be an analog to digital converter (ADC) input with the following requirements:
 - At least 12-bit resolution
 - Enough channels for pressure regulators *and* pressure transducers

Temperature

- The temperatures should be monitored via K-type thermocouples
- There should be an additional thermocouple in the Nozzle Exit or Test Section to fully define the state of the HXT facility
- There should be one redundant thermocouple for every thermocouple
- The thermocouple input should be a dedicated thermocouple module with the following requirements:
 - At least 12-bit resolution
 - Enough channels for thermocouples and redundant thermocouples

Remote Controls and Relays

- The breach open/close monitoring should:
 - Utilize magnetic proximity sensors
 - Have at least 2 redundant proximity sensors (3 total)
- All pressure lines should be open or closed with ball valves
- Remotely actuated ball valves should be used wherever possible (especially if manual actuation compromises safety)
- Solid state relays should be used to control and monitor the ball valves and proximity sensors, respectively, with the following requirements
 - Enough channels for Driver fill and vacuum, Driven fill and vacuum, Expansion vacuum, Driven vent, and proximity sensors
 - Enough current output to actuate any ball valves
 - Compatible switching voltage for circuit requirements
- The pressure inputs (regulators and transducers) should be consolidated on a single module with at least 12 bit resolution and enough channels

- The pressure regulation output **should** be controlled via a digital-to-analog converter (DAC) module with enough channels for the two digital pressure regulators (see diagram)

Computers

- The Controls **should** utilize computers currently owned by the NAL
- The following programs **should** be installed on the Controls computer:
 - NI LabVIEW
 - NI DAQmx
 - NI MAX
 - Microsoft Office Suite
- The Controls computer **should** have the following specifications:
 - Minimum 16 GB of RAM
 - Quad core CPU
 - Minimum 500 GB Hard Drive Disk, SATA 6.0 GB/s, 7200 RPM
 - Windows 7 or later
 - VGA or DisplayPort ports for compatibility with currently owned NAL monitors

APPENDIX B

TECHNICAL DRAWINGS

This section provides technical drawings for each of the components designed and manufactured for the facility. The drawings are organized following the format of the thesis and presented below.

- Driver, Driven, and Expansion Pipe Drawings
 - Engineering Drawings
 - Figure B-1: Driver(R) Sectional Drawing
 - Figure B-2: Driven(N) Sectional Drawing
 - Figure B-3: Accelerator 1(A1) Sectional Drawing
 - Figure B-4: Accelerator 1(A2) Sectional Drawing
 - Figure B-5: Accelerator 1(A3) Sectional Drawing
 - Welder-Approved Drawings
 - Figure B-6: Driver(R) Sectional Drawing 1
 - Figure B-7: Driver(R) Sectional Drawing 2
 - Figure B-8: Driven(N) Sectional Drawing 1
 - Figure B-9: Driven(N) Sectional Drawing 2
 - Figure B-10: Accelerator 1(A1) Sectional Drawing 1
 - Figure B-11: Accelerator 1(A1) Sectional Drawing 2
 - Figure B-12: Accelerator 1(A2) Sectional Drawing 1
 - Figure B-13: Accelerator 1(A2) Sectional Drawing 2
 - Figure B-14: Accelerator 1(A3) Sectional Drawing 1

- Figure B-15: Accelerator 1(A3) Sectional Drawing 2
 - Figure B-16: Hole Alignment Drawing
 - Figure B-17: R/N/A Overall Drawing
- Component Drawings
 - Figure B-18: 20” 900# RTJ Blind
 - Figure B-19: 20” 900#RTJ Slip-on Flange
 - Figure B-20: 20” 300# RTJ Slip-on Flange
- Breech Diaphragm Mechanism Drawings
 - Figure B-21: Female Diaphragm Holder Component
 - Figure B-22: Male Diaphragm Holder Component
 - Figure B-23: Breech Seat
 - Figure B-24: Breech Head
 - Figure B-25: Pin Assembly
 - Figure B-26: Locking Nut
 - Figure B-27: Locking Tooth
 - Figure B-28: Nut Back Plate
 - Figure B-29: Thrust Plate
- Mylar Diaphragm Mechanism Drawings
 - Figure B-30: Driver-Side Plate
 - Figure B-31: Accelerator-Side Plate

- Test Section Drawings
 - Figure B-32: Bottom Access (BA)
 - Figure B-33: Back Main (BM)
 - Figure B-34: Back Main (BM)-2
 - Figure B-35: Door Side (DS)
 - Figure B-36: Front Main (FM)
 - Figure B-37: Slant Side (SS)
 - Figure B-38: Top Access (TA)

- Primary Stand Drawings
 - Figure B-39: 2” Cradle Plate-900# Mount
 - Figure B-40: Primary Baseplate

- Secondary Stand Drawings
 - Figure B-41: 2” Cradle Plate-150# Mount
 - Figure B-42: Secondary Baseplate

Engineering Drawings

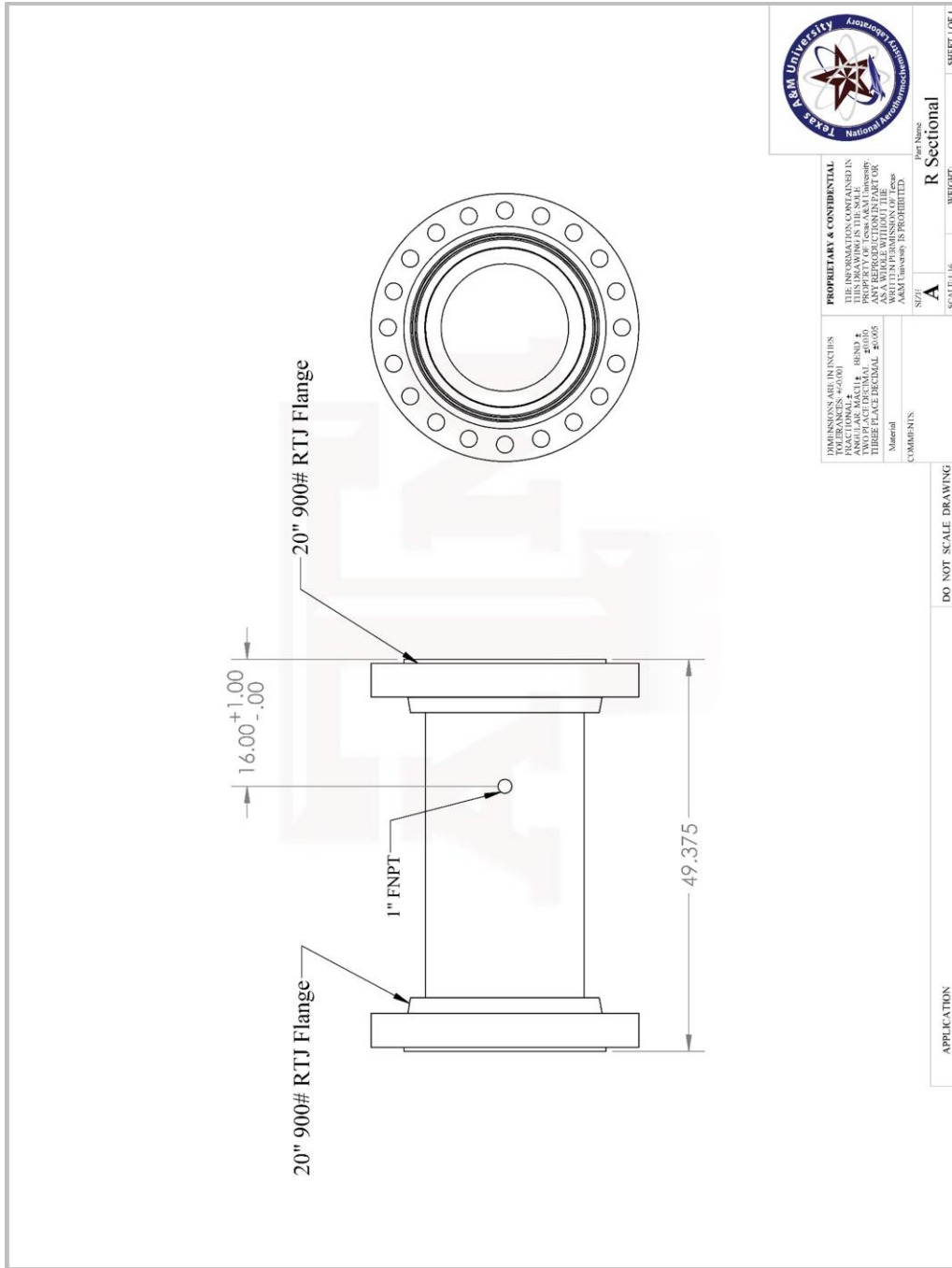


Figure B-107. Driver section drawing submitted to Circle H Manufacturing for ASME certified high pressure welding.

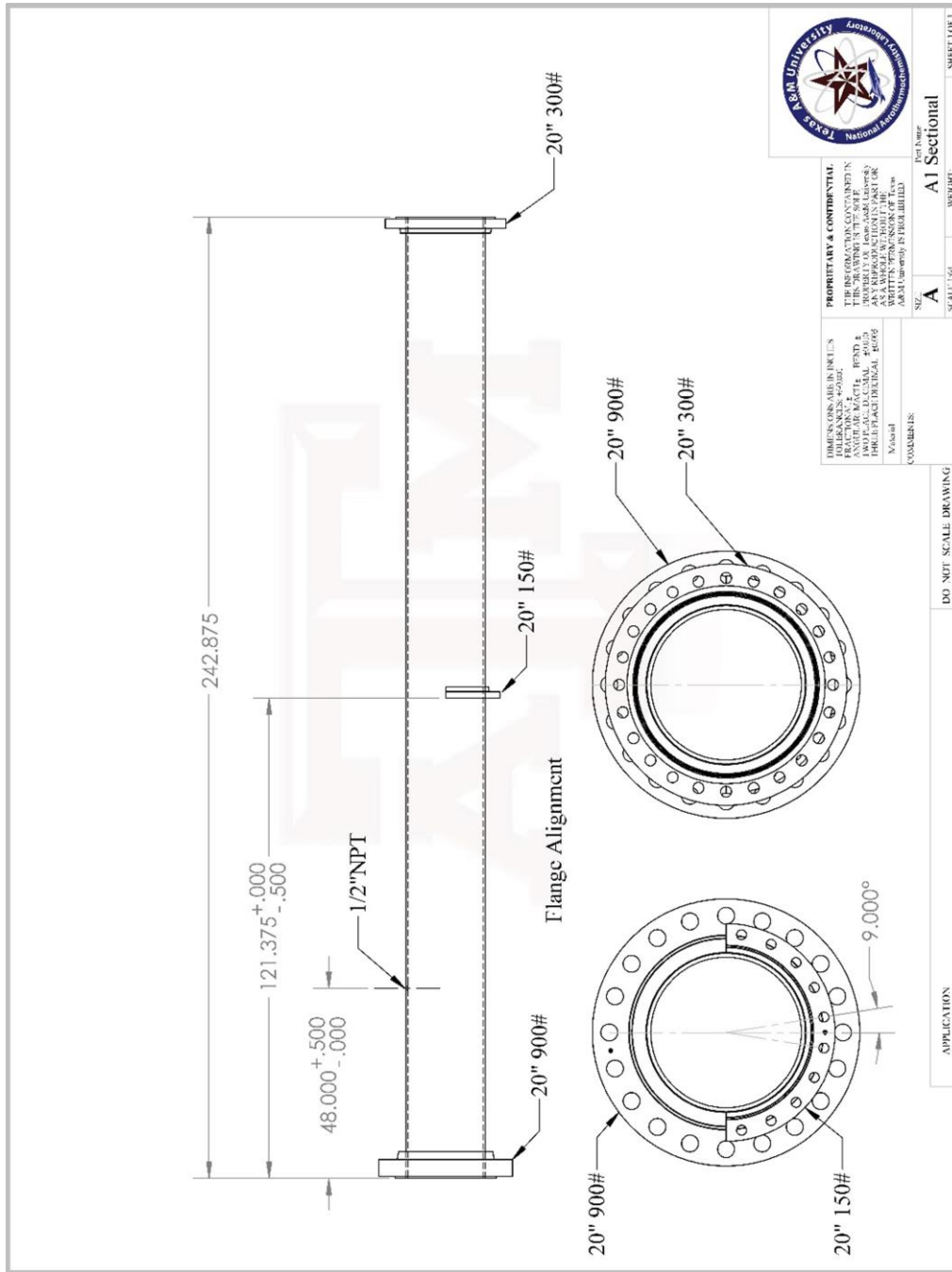


Figure B-3. First accelerator section drawing submitted to Circle H Manufacturing for ASME certified high pressure welding.

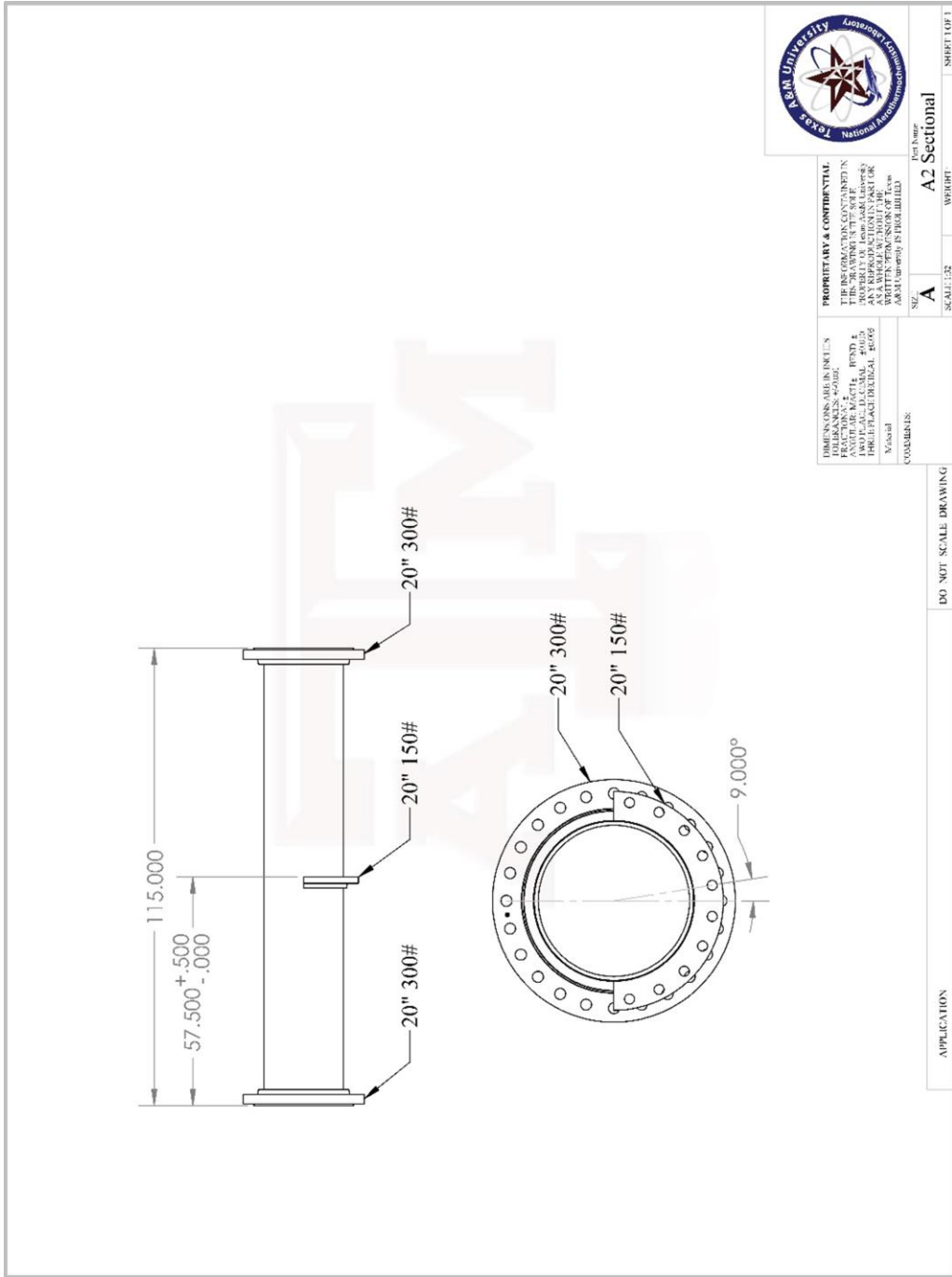


Figure B-4. Second accelerator section drawing submitted to Circle H Manufacturing for ASME certified high pressure welding.

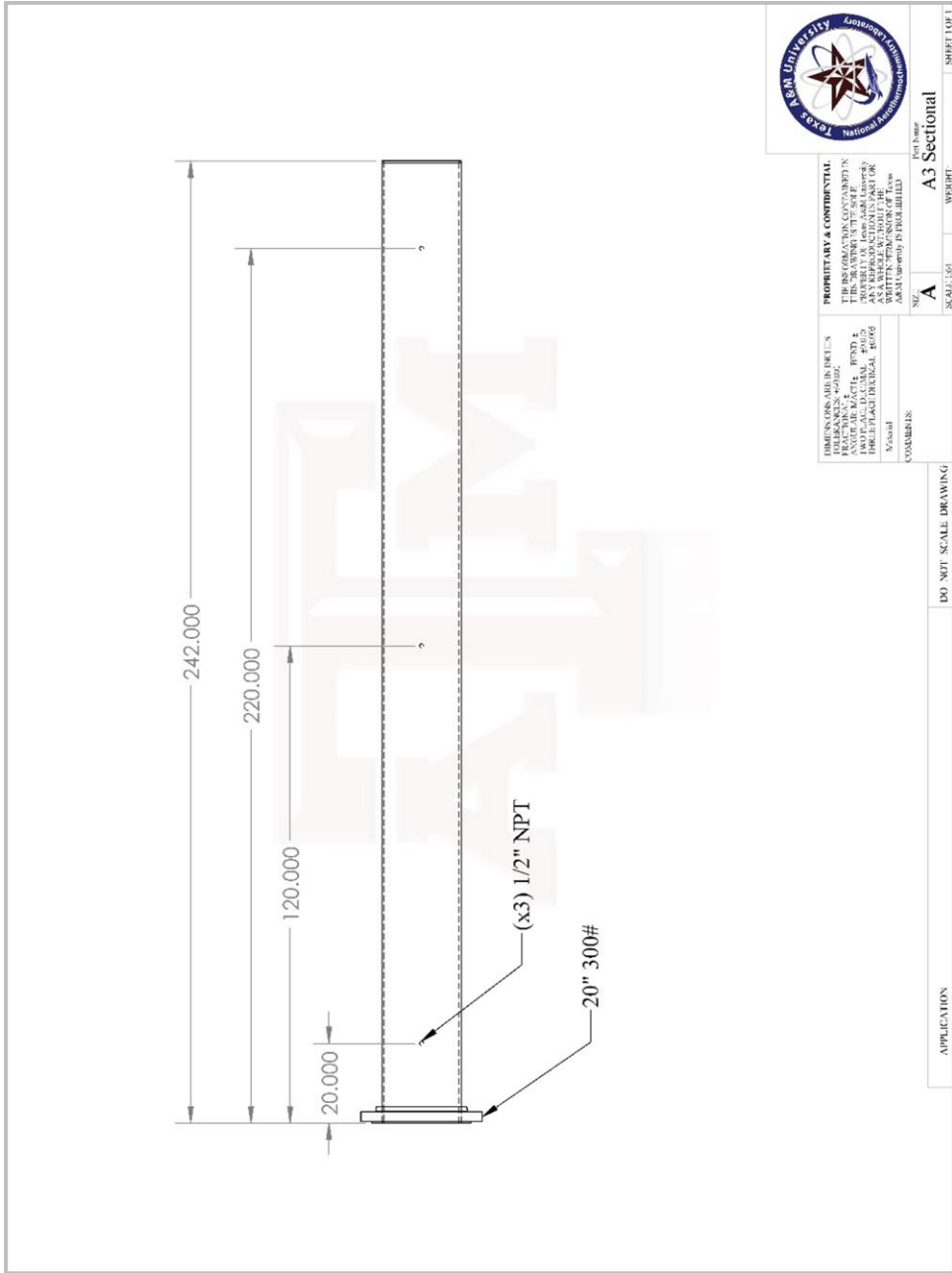


Figure B-5. Third accelerator section drawing submitted to Circle H Manufacturing for ASME certified high pressure welding.

Welder-Approved Drawings

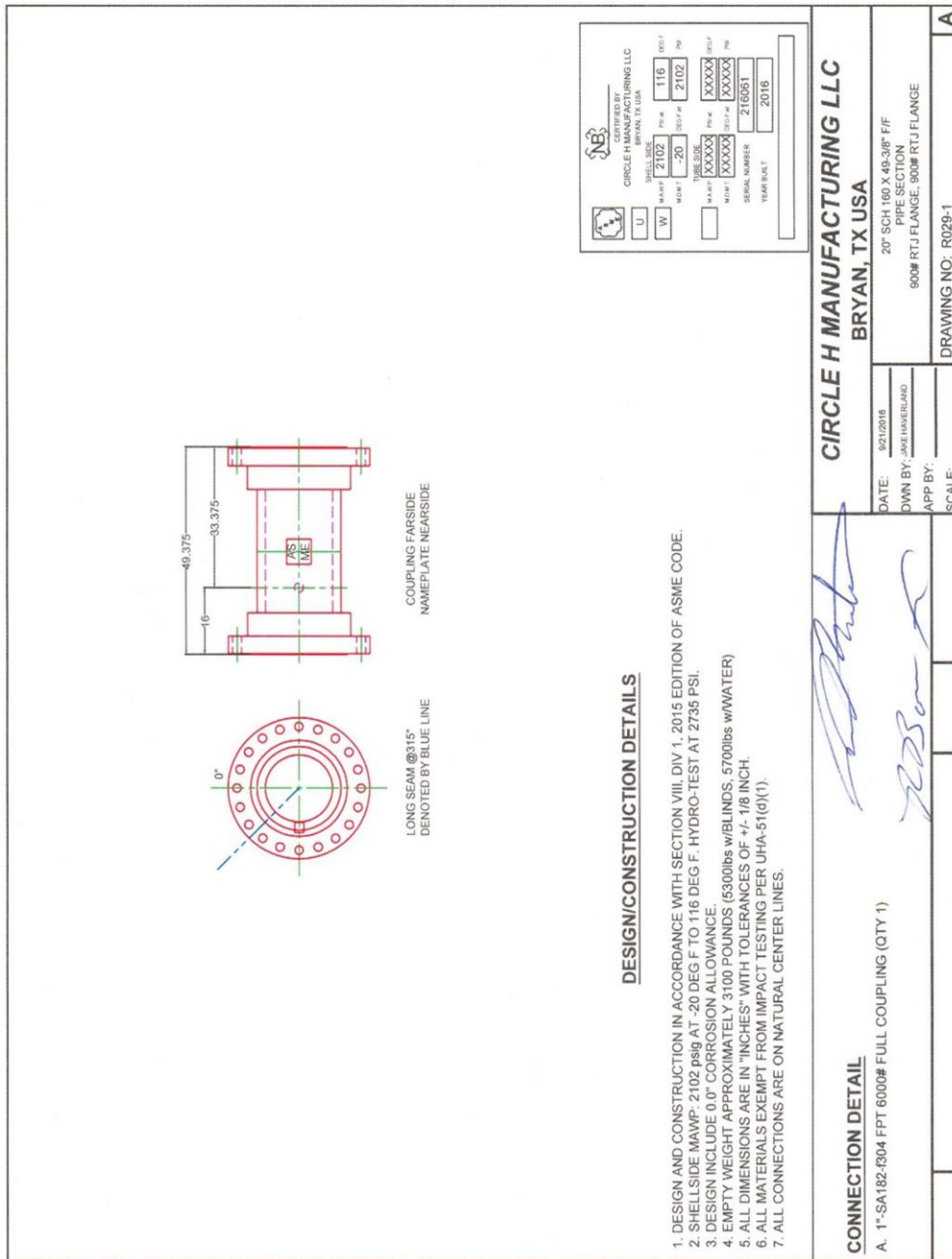


Figure B-6. Circle H Manufacturing drawing of the driver as certified with approval signatures from the responsible engineers.

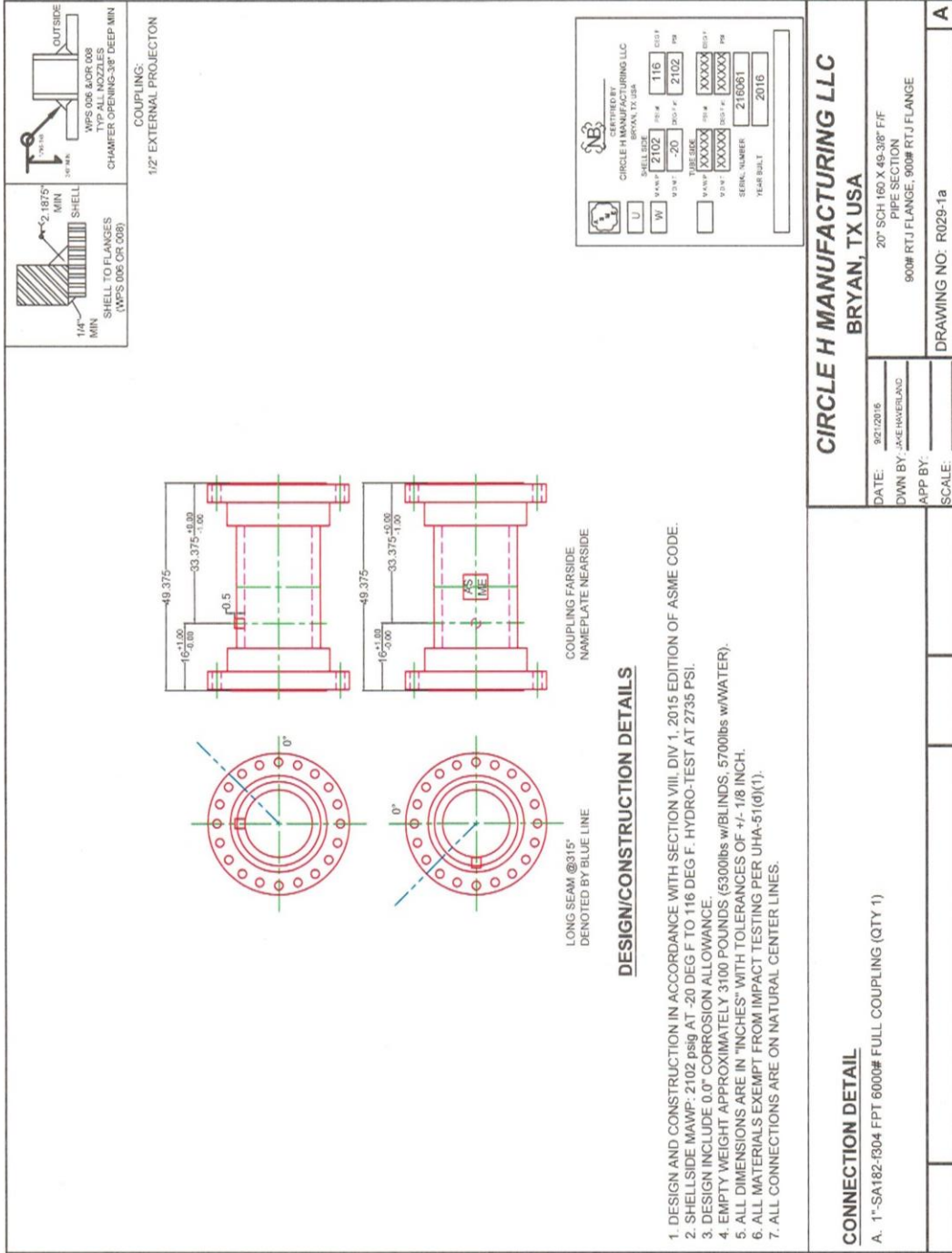


Figure B-7. Circle H Manufacturing drawing of the driver as certified and approved.

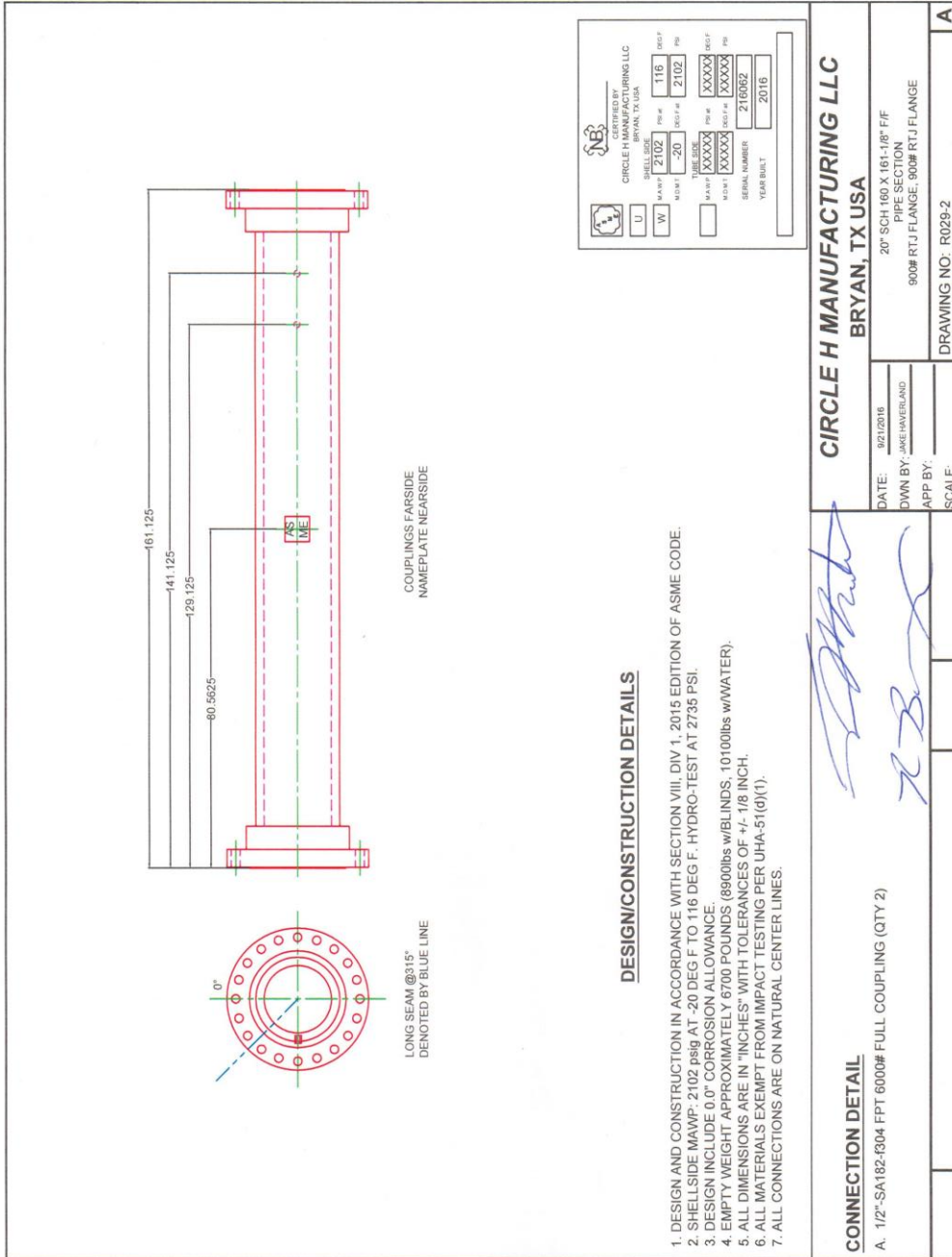


Figure B-8. Circle H Manufacturing drawing of the driven as certified with approval signatures of the responsible engineers.

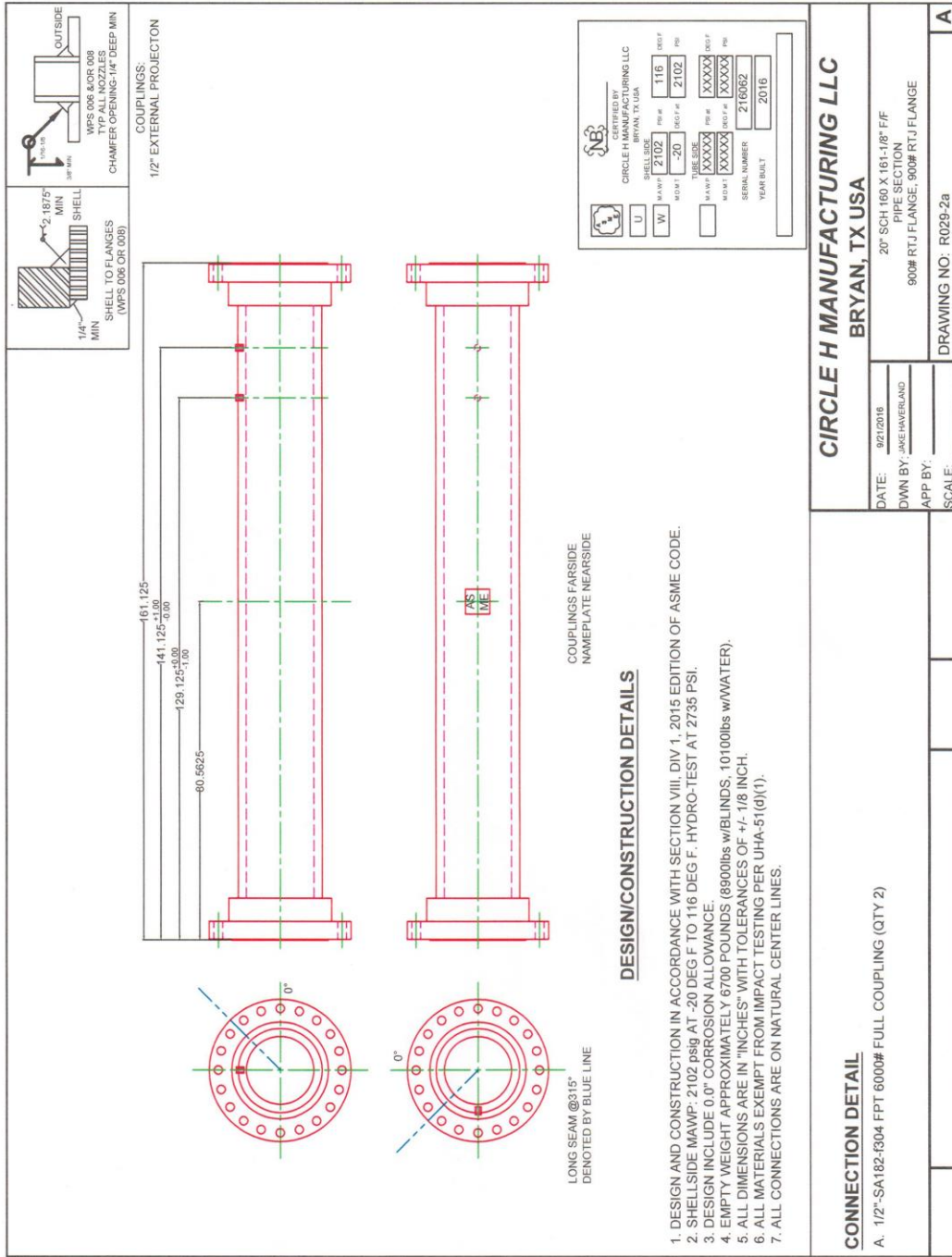


Figure B-9. Circle H Manufacturing drawing of the driven as certified and approved.

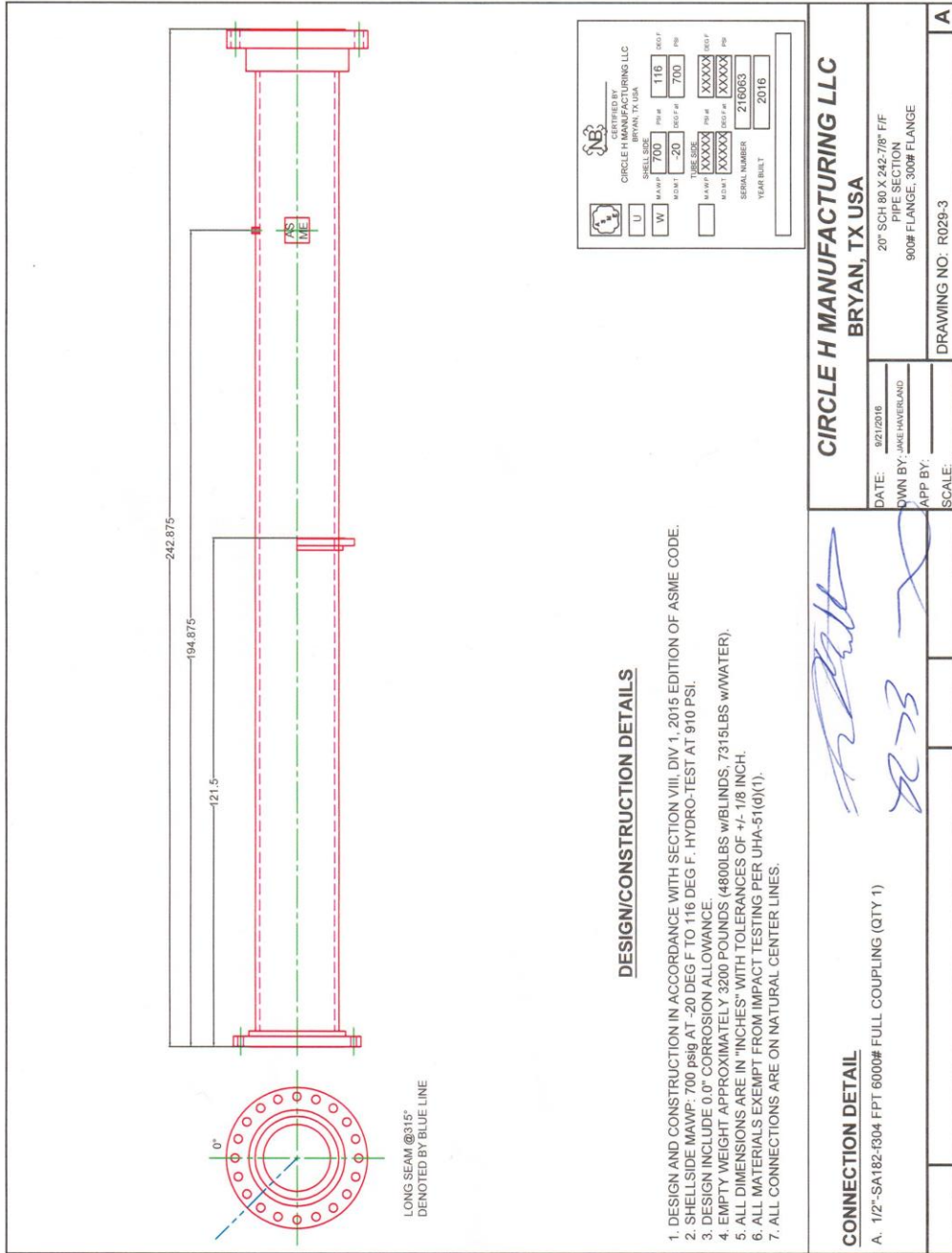


Figure B-10. Circle H Manufacturing drawing of the first accelerator segment as certified with approval signatures of the responsible engineers.

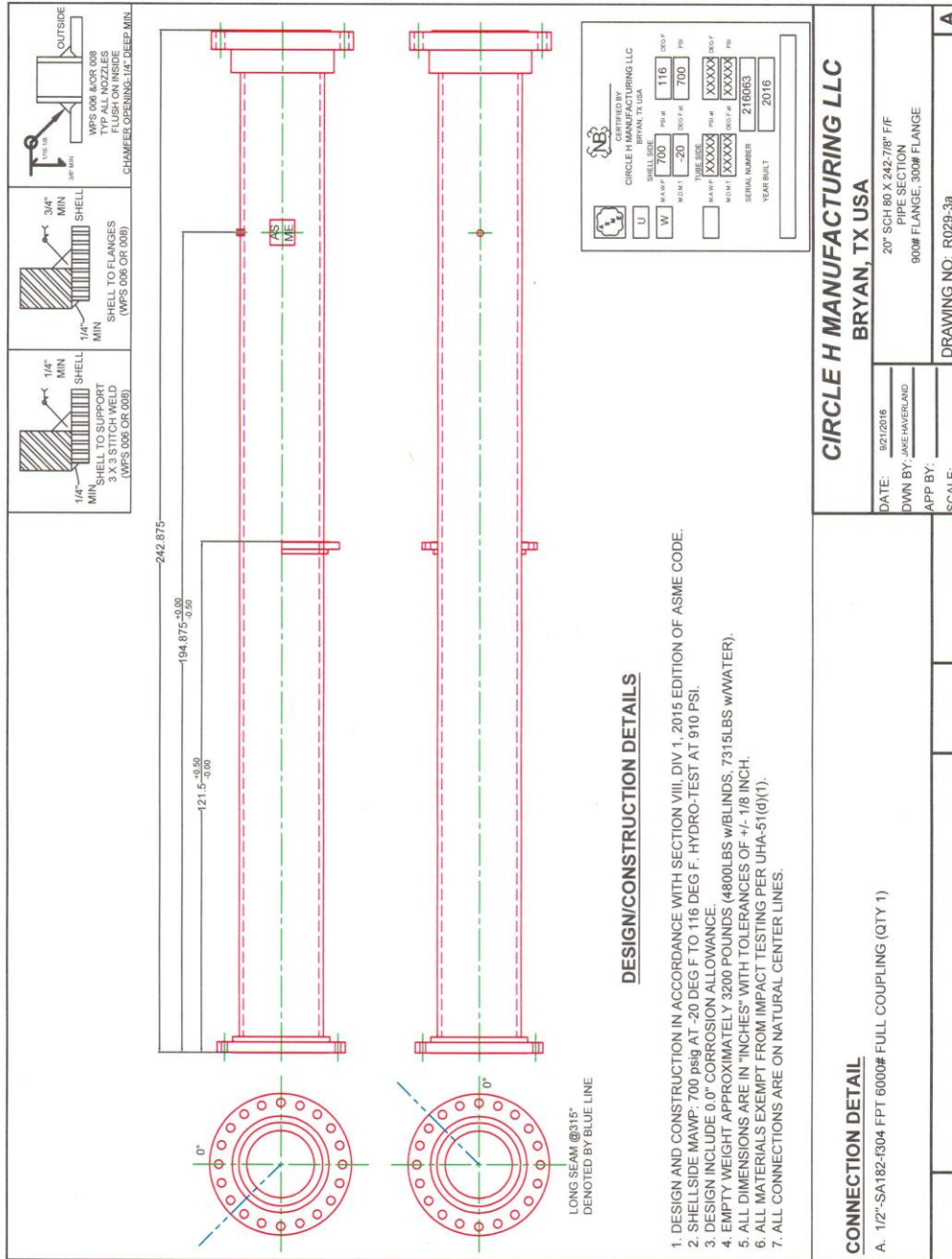


Figure B-11. Circle H Manufacturing drawing of the first accelerator segment as certified and approved.

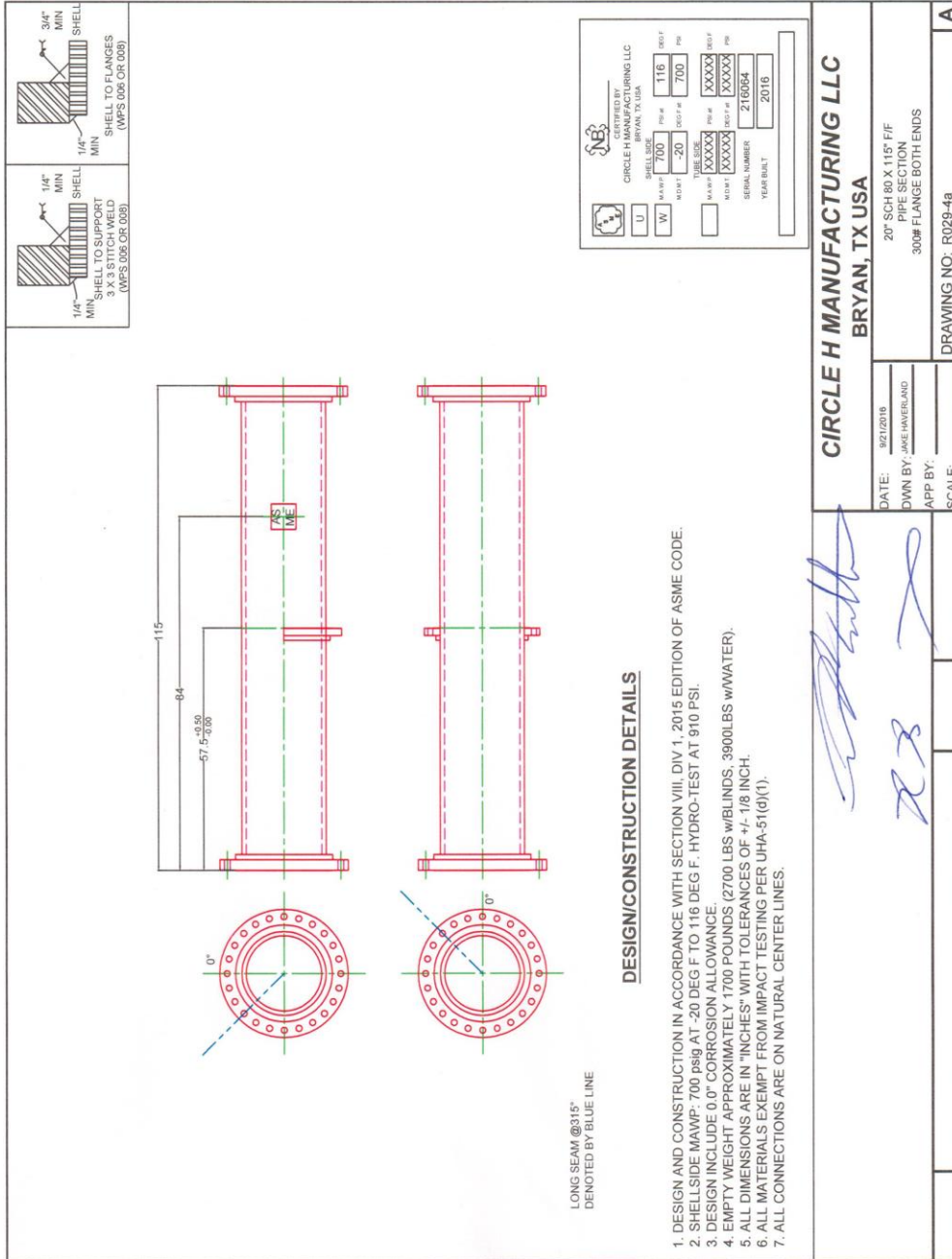


Figure B-12. Circle H Manufacturing drawing of the driven as certified with approval signatures of the responsible engineers.

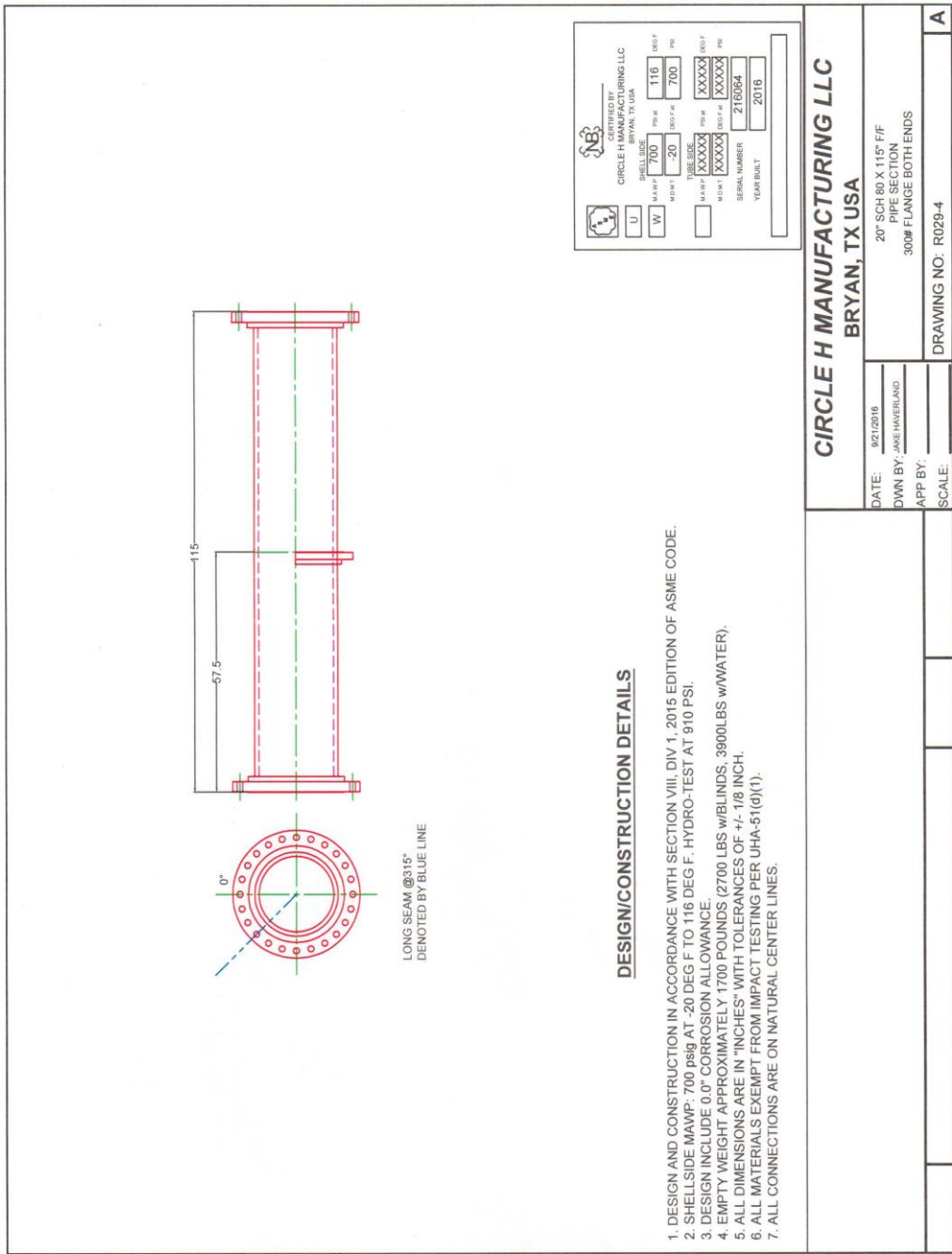


Figure B-13. Circle H Manufacturing drawing of the driven as certified and approved.

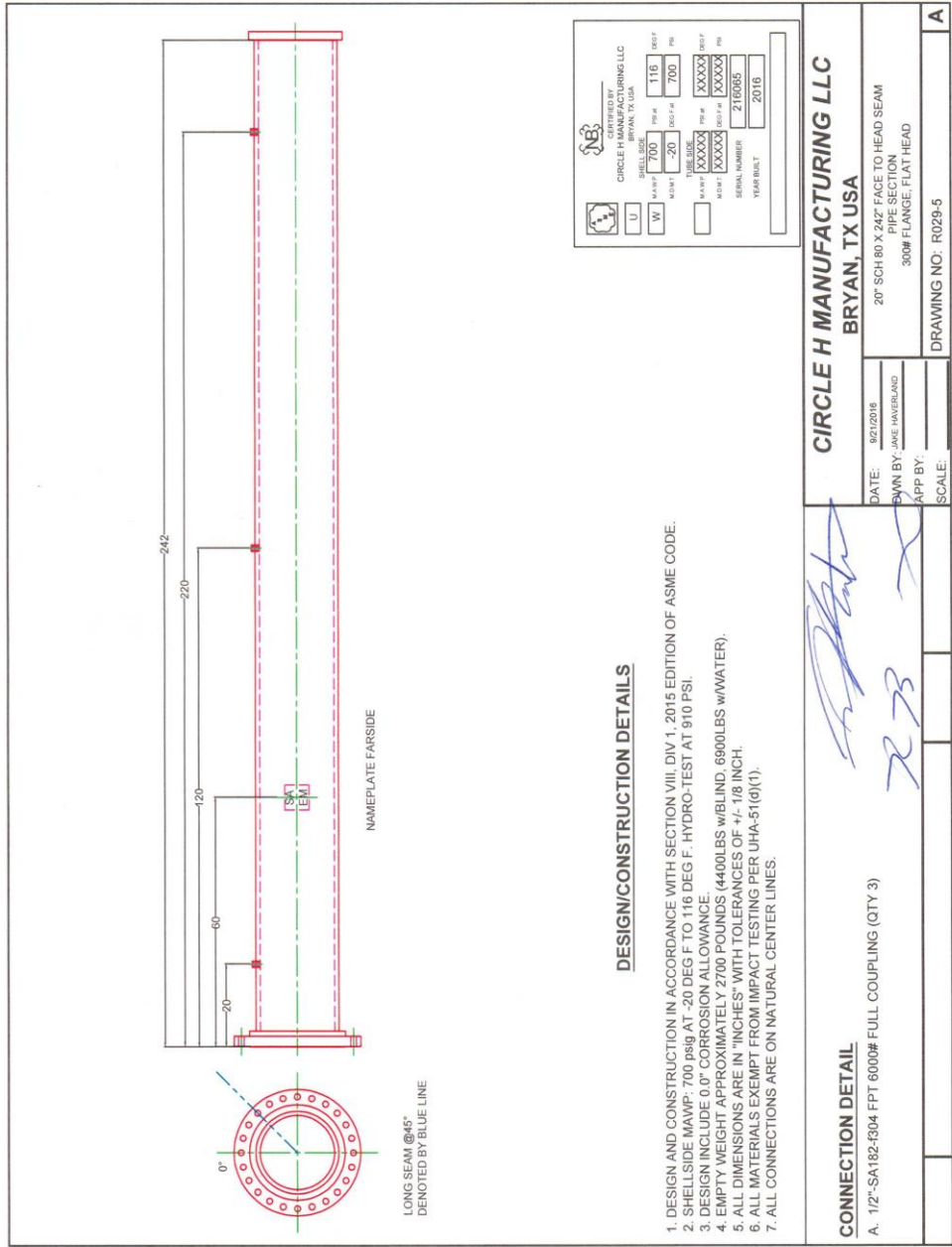


Figure B-14. Circle H Manufacturing drawing of the driven as certified with approval signatures of the responsible engineers.

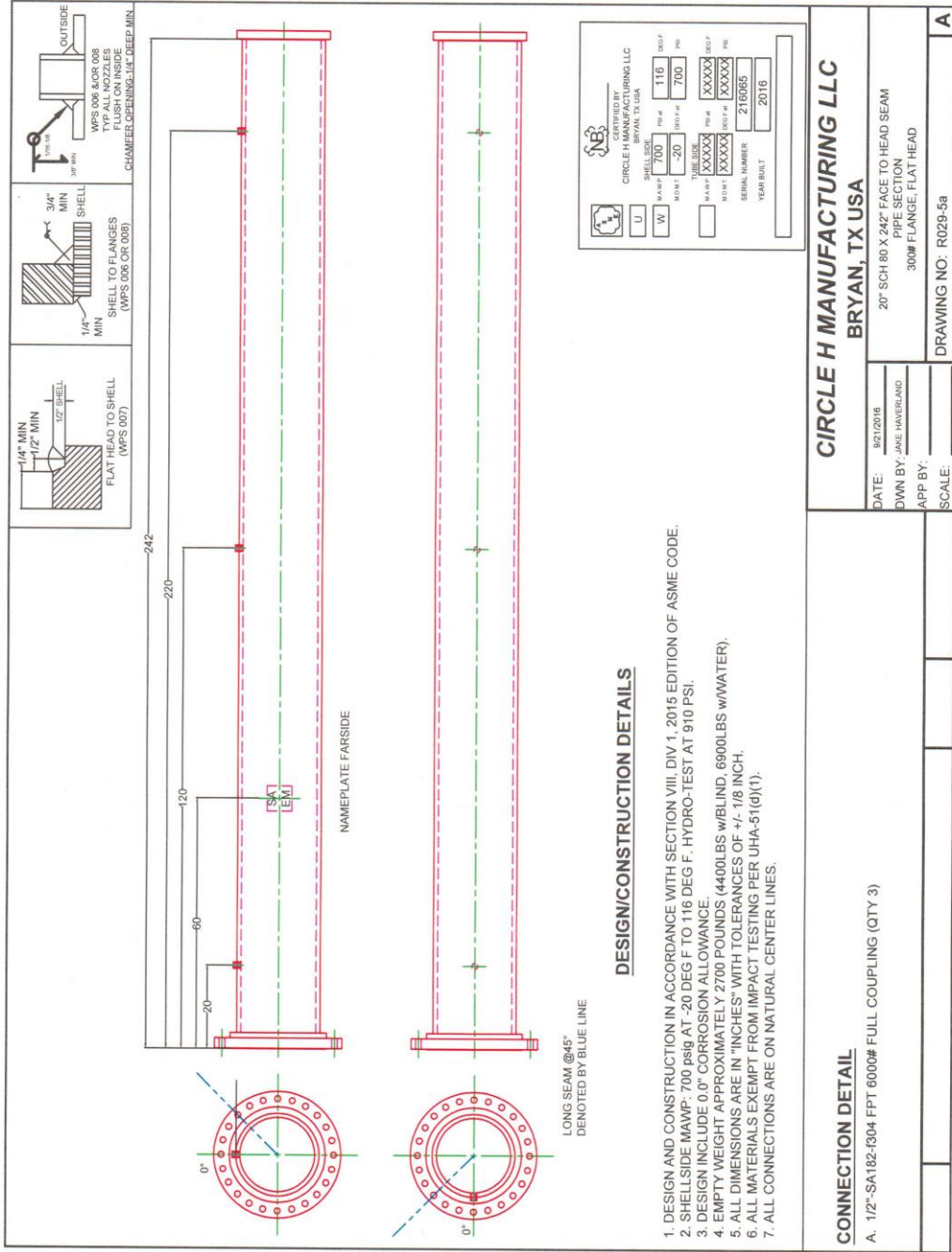


Figure B-15. Circle H Manufacturing drawing of the driven a.s certified and approved.

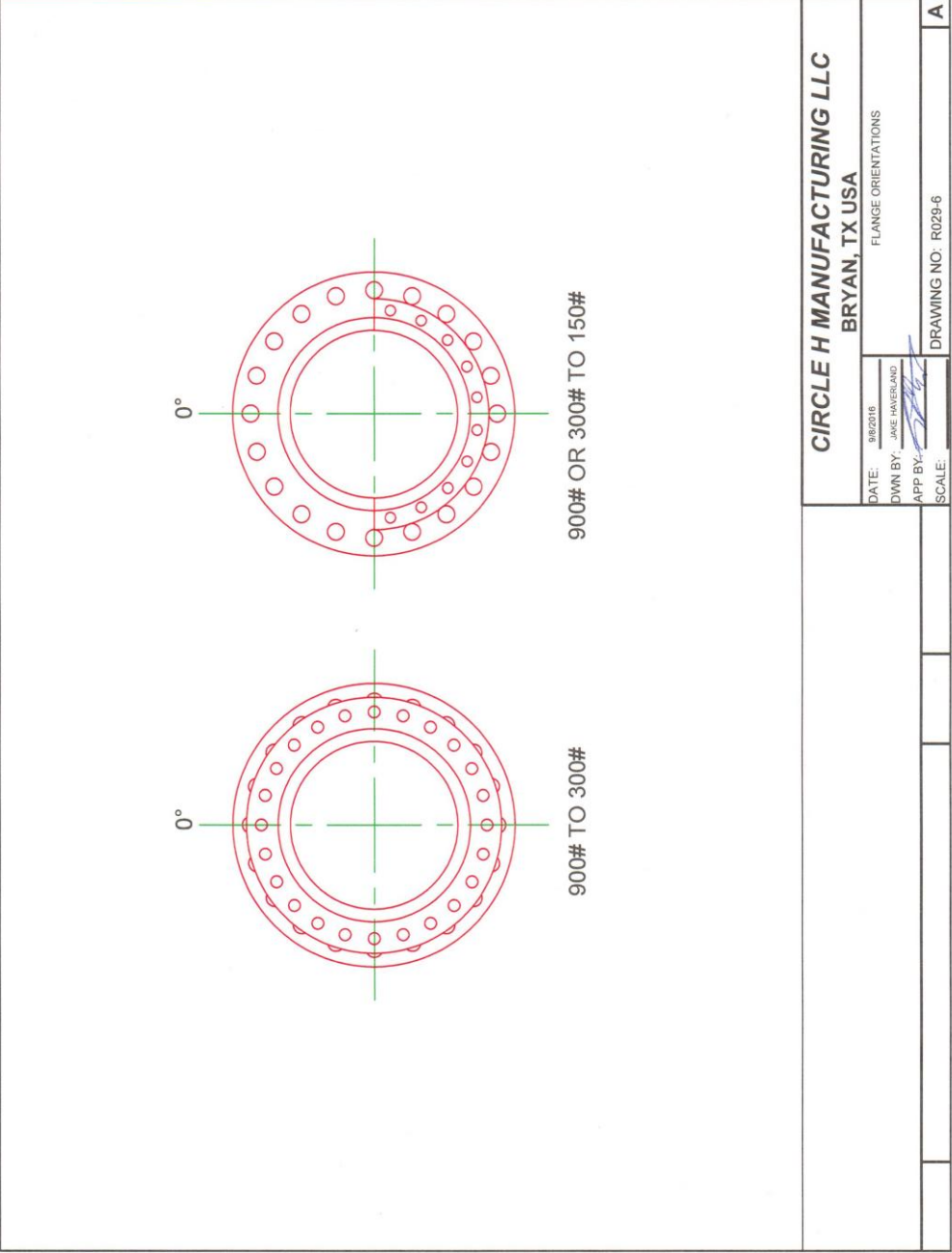


Figure B-16. Circle H Manufacturing drawing detailing the hole alignment of the flanges relative to one another.

R/N/A Components

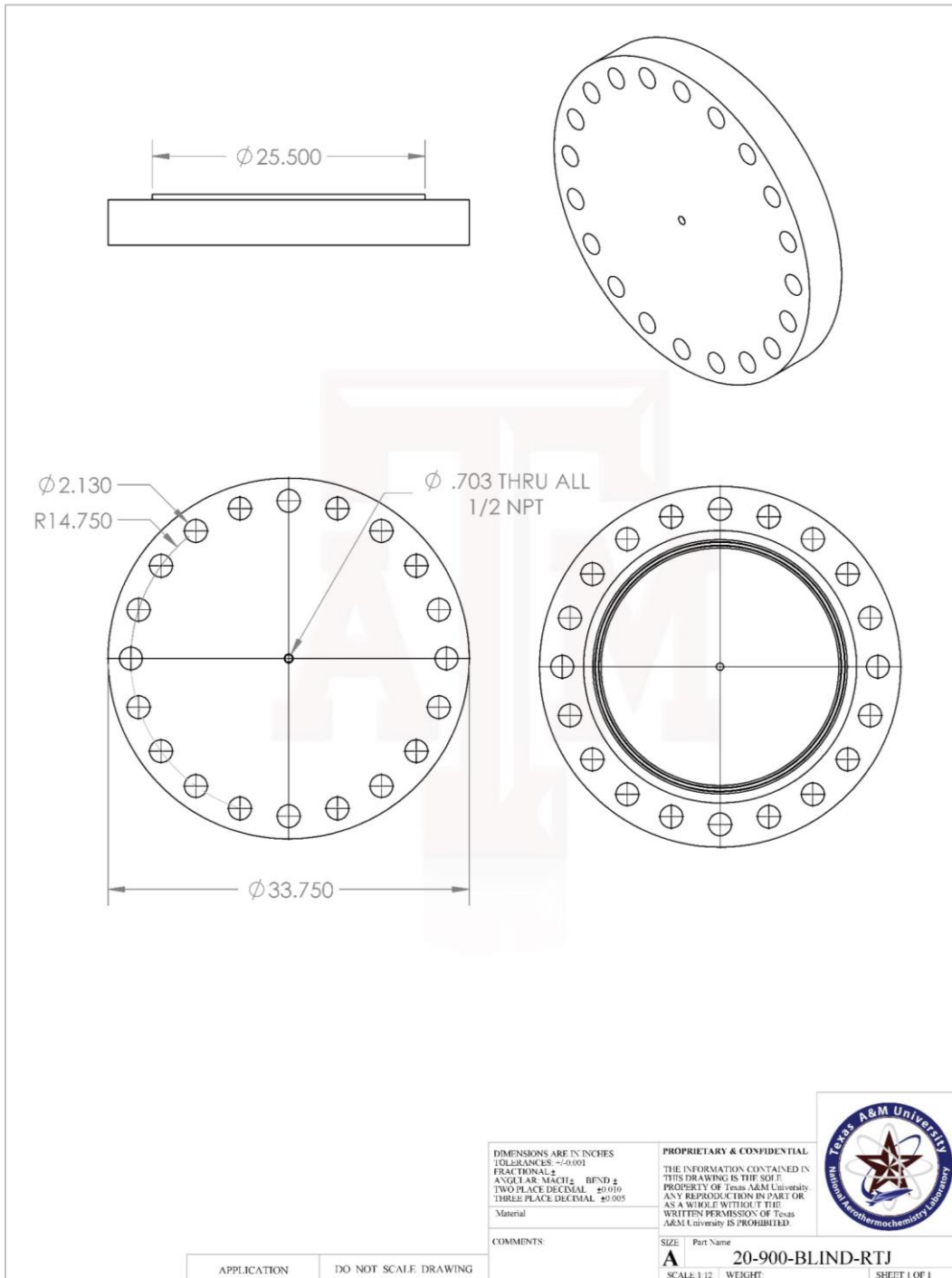


Figure B-18. Dimensional drawing for a 20" class 900 RTJ blind.

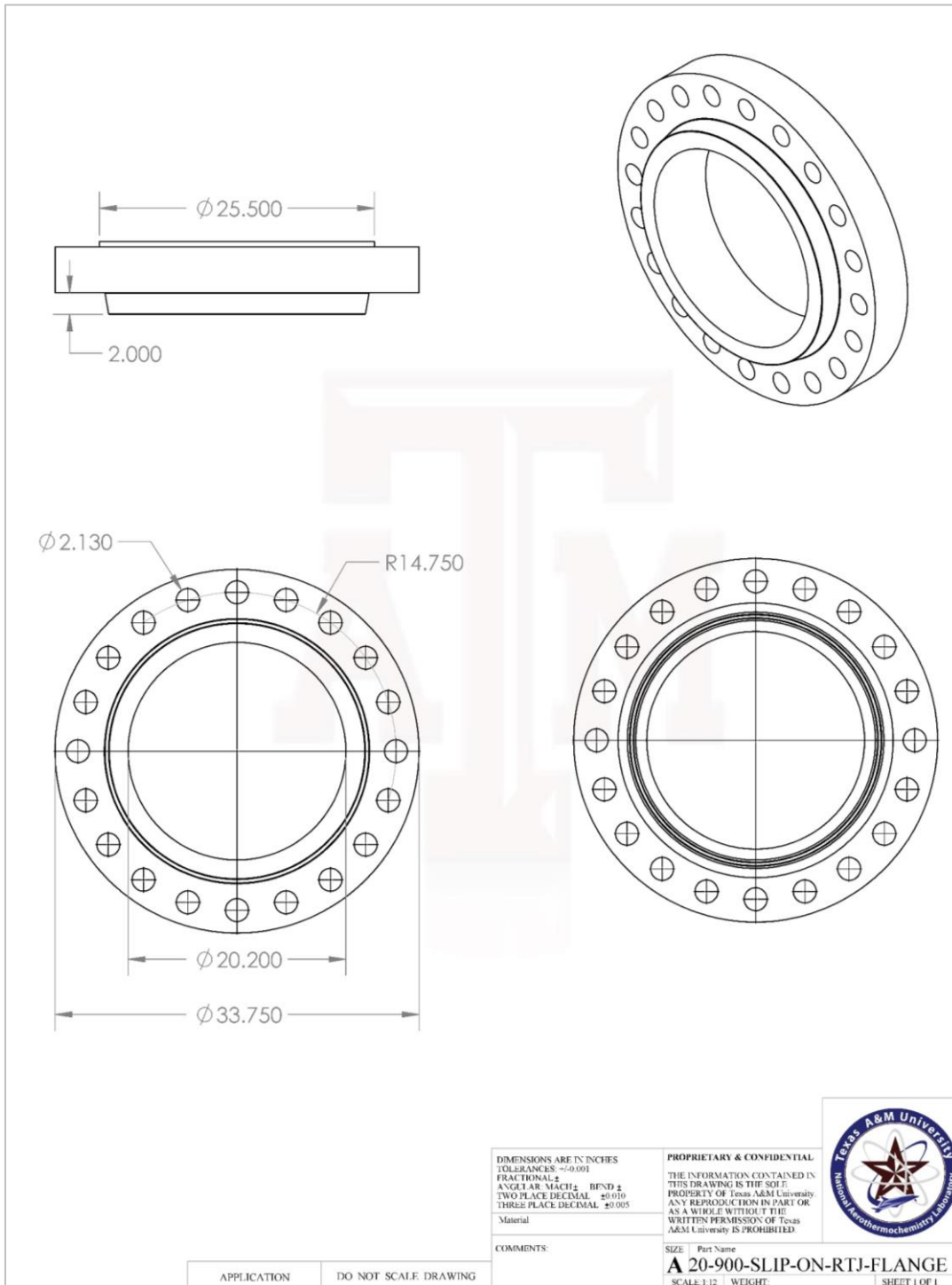


Figure B-19. Dimensional drawing for a 20" class 900 RTJ slip-on flange.

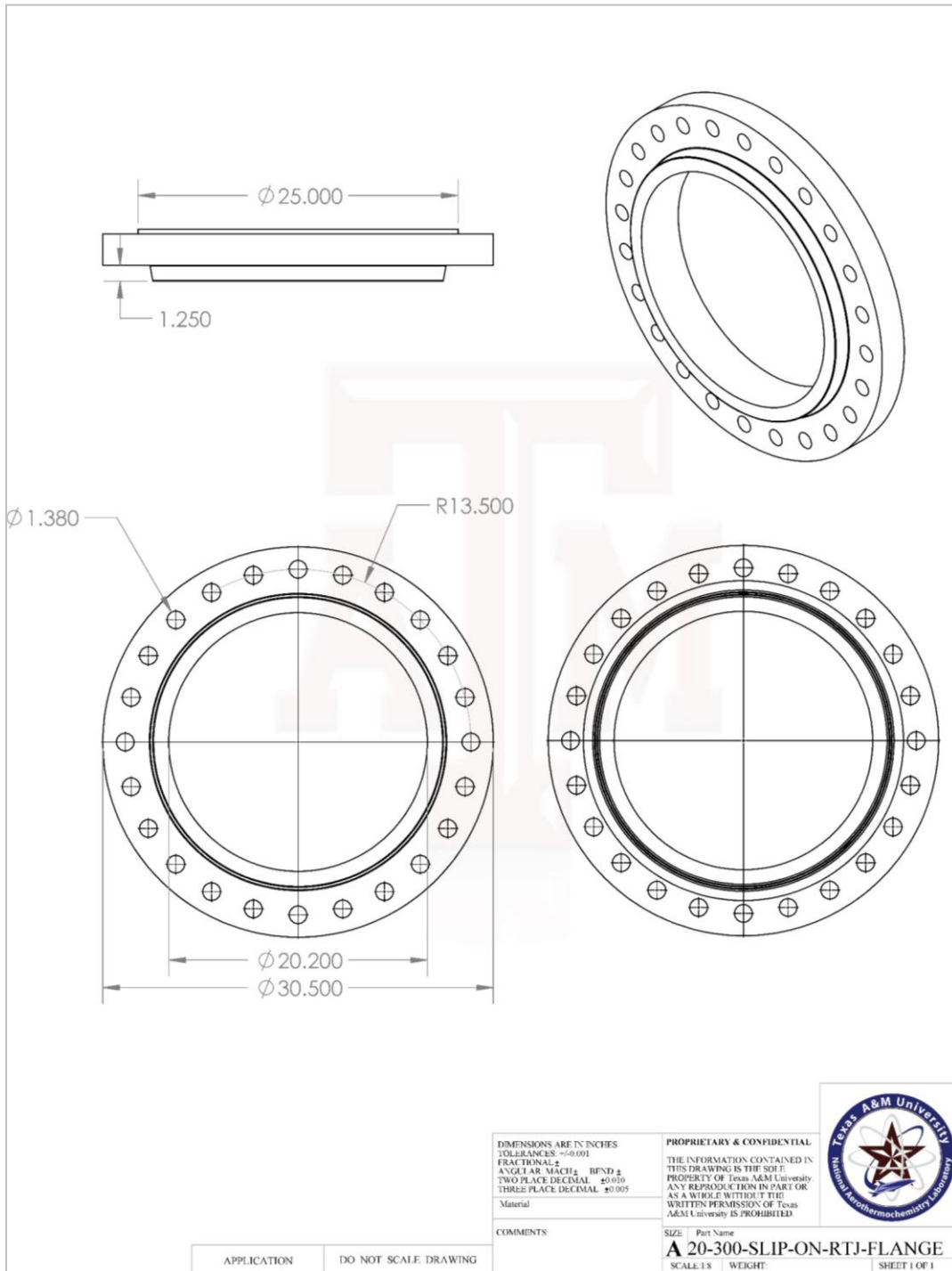


Figure B-20. Dimensional drawing for a 20" class 300 RTJ slip-on flange.

Breech Diaphragm System

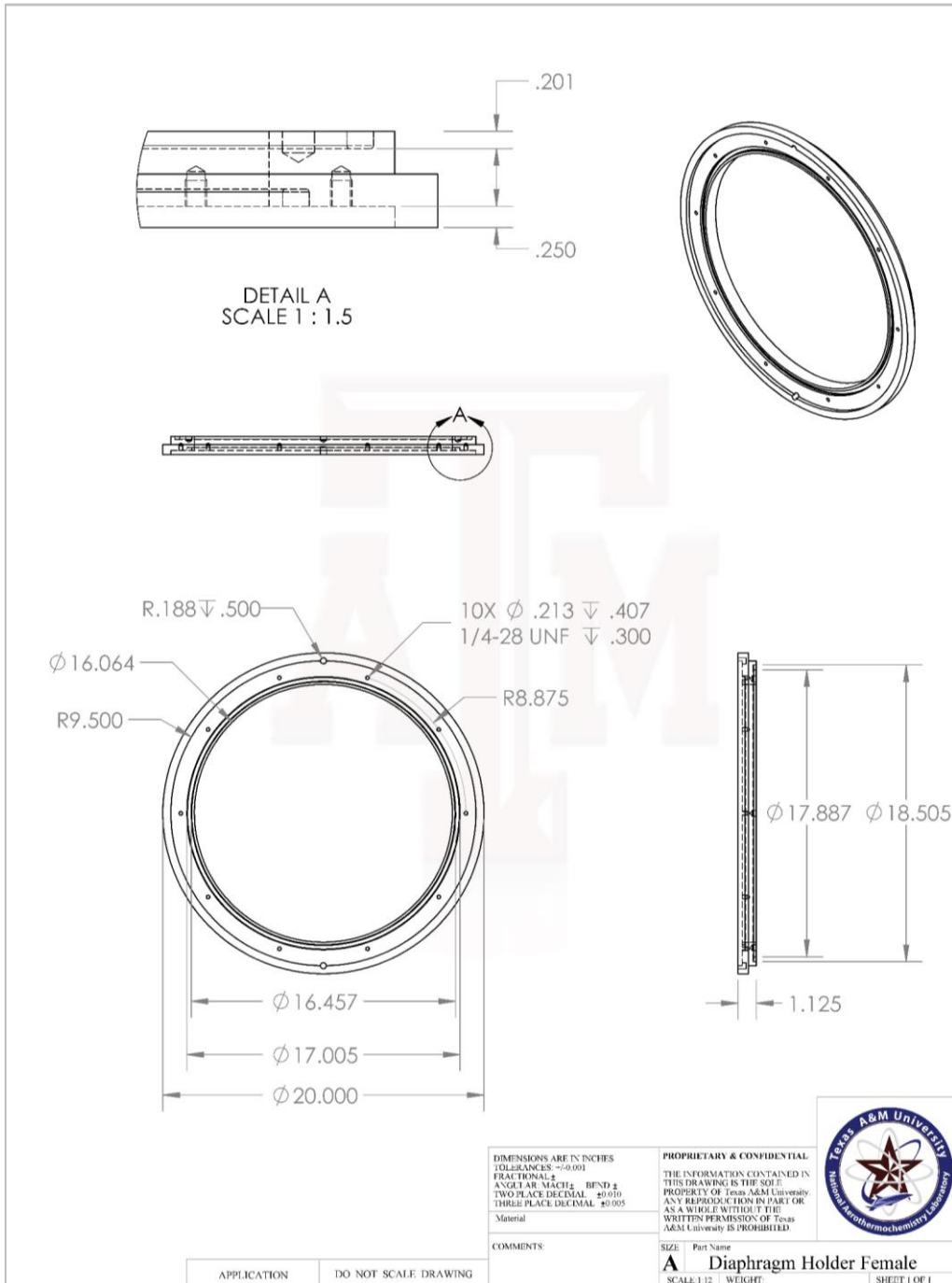


Figure B-21. Dimensional drawing for the female component of the diaphragm holder.

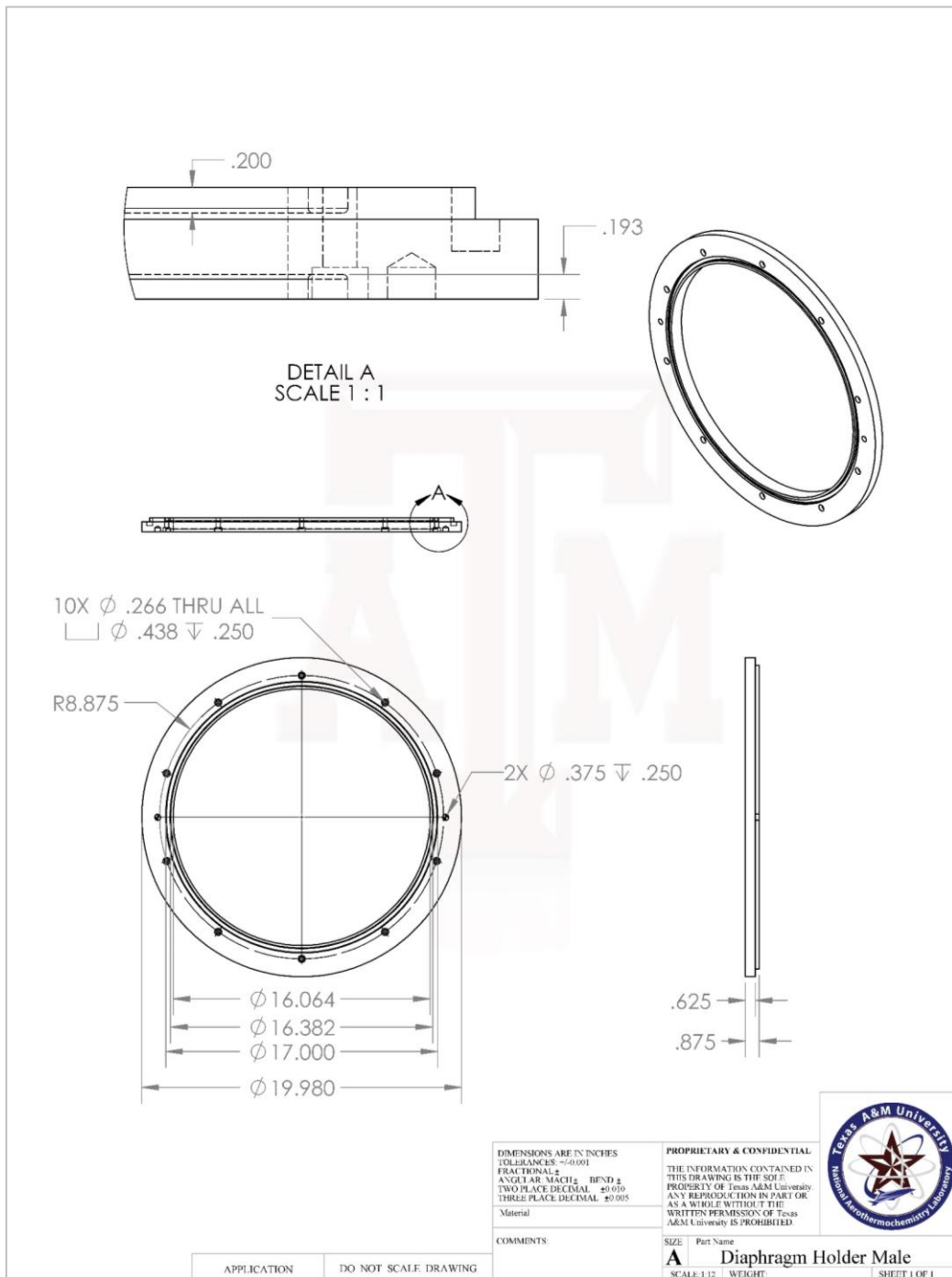


Figure B-22. Dimensional drawing for the male component of the diaphragm holder.

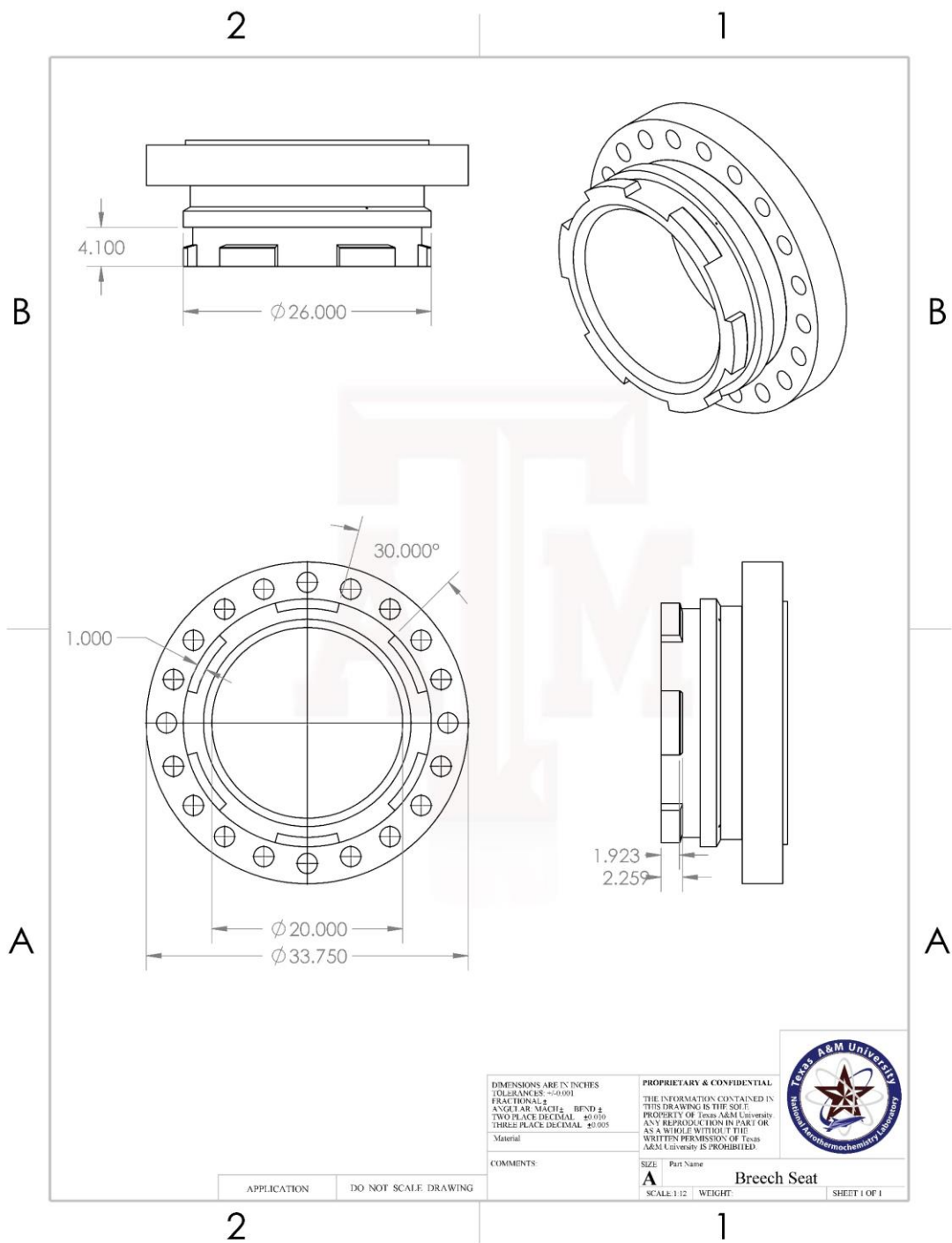


Figure B-23. Dimensional drawing for the breech seat made out of a heavy barrel 20” 900# RTJ slip-on flange.

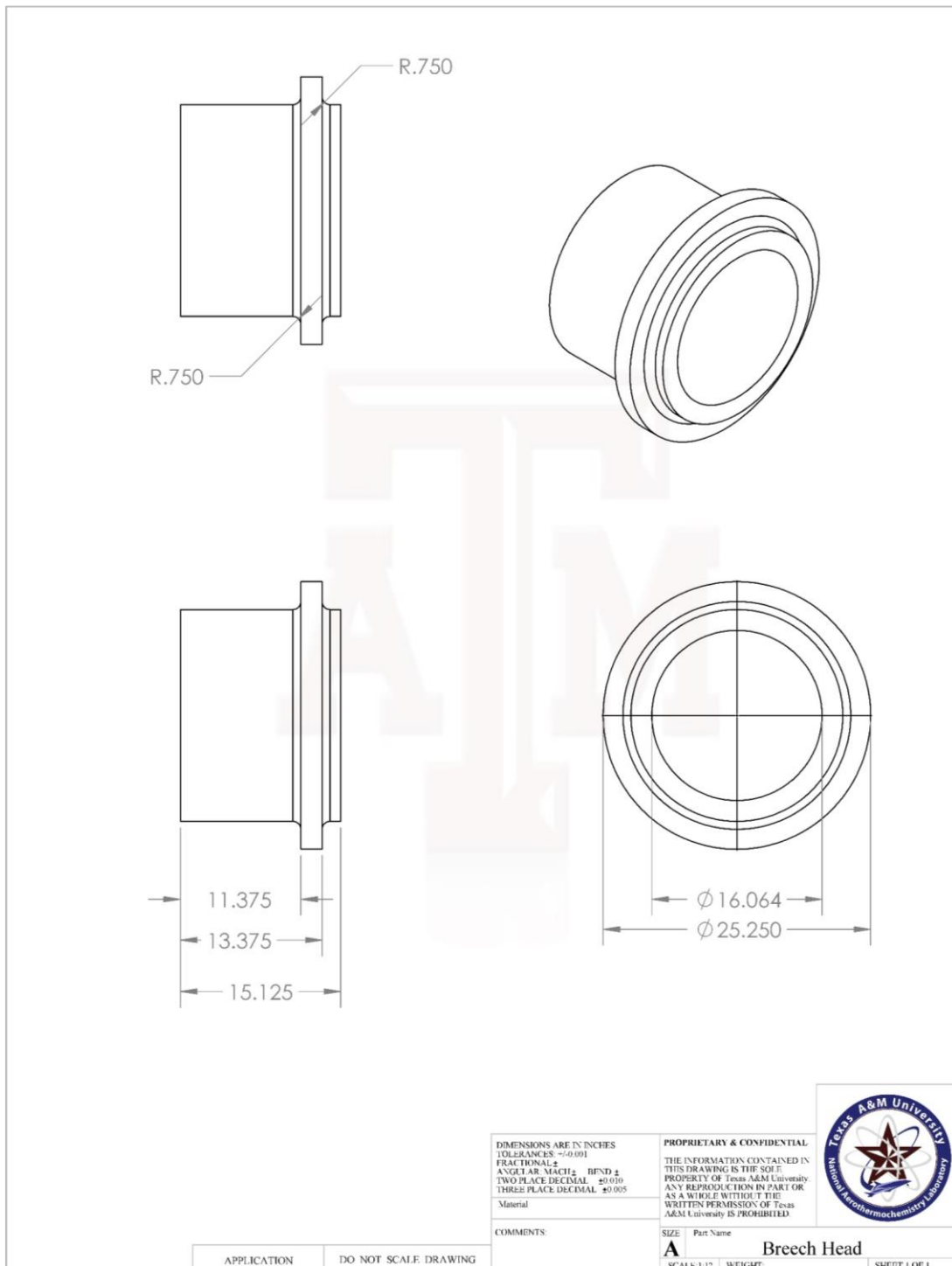


Figure B-24. Dimensional drawing for the breech head made out of a small section of 20" schedule 160 pipe with a custom cut metal collar welded on.

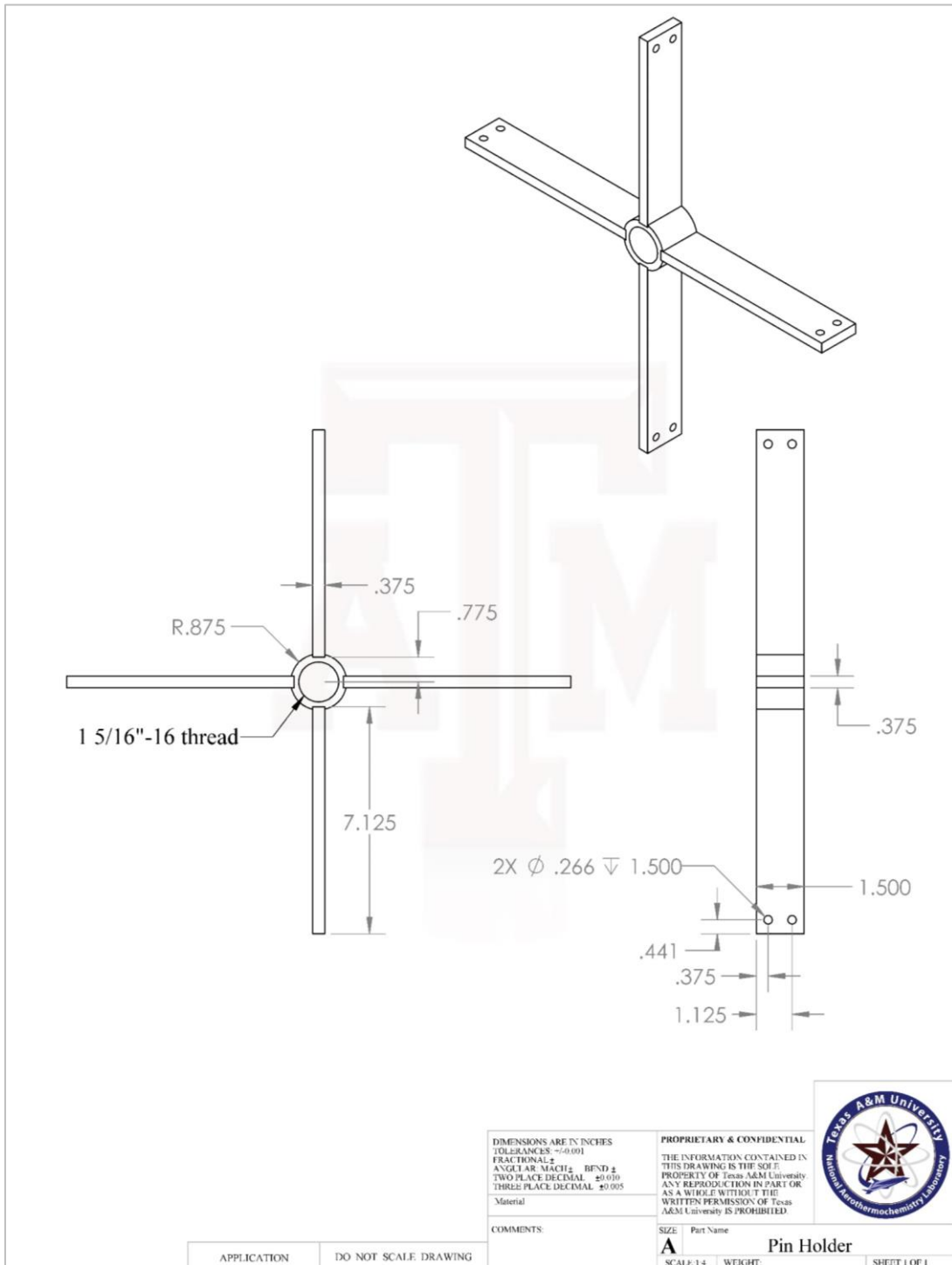


Figure B-25. Dimensional drawing of the insertable pin cross assembly made from four arms and a central circular body.

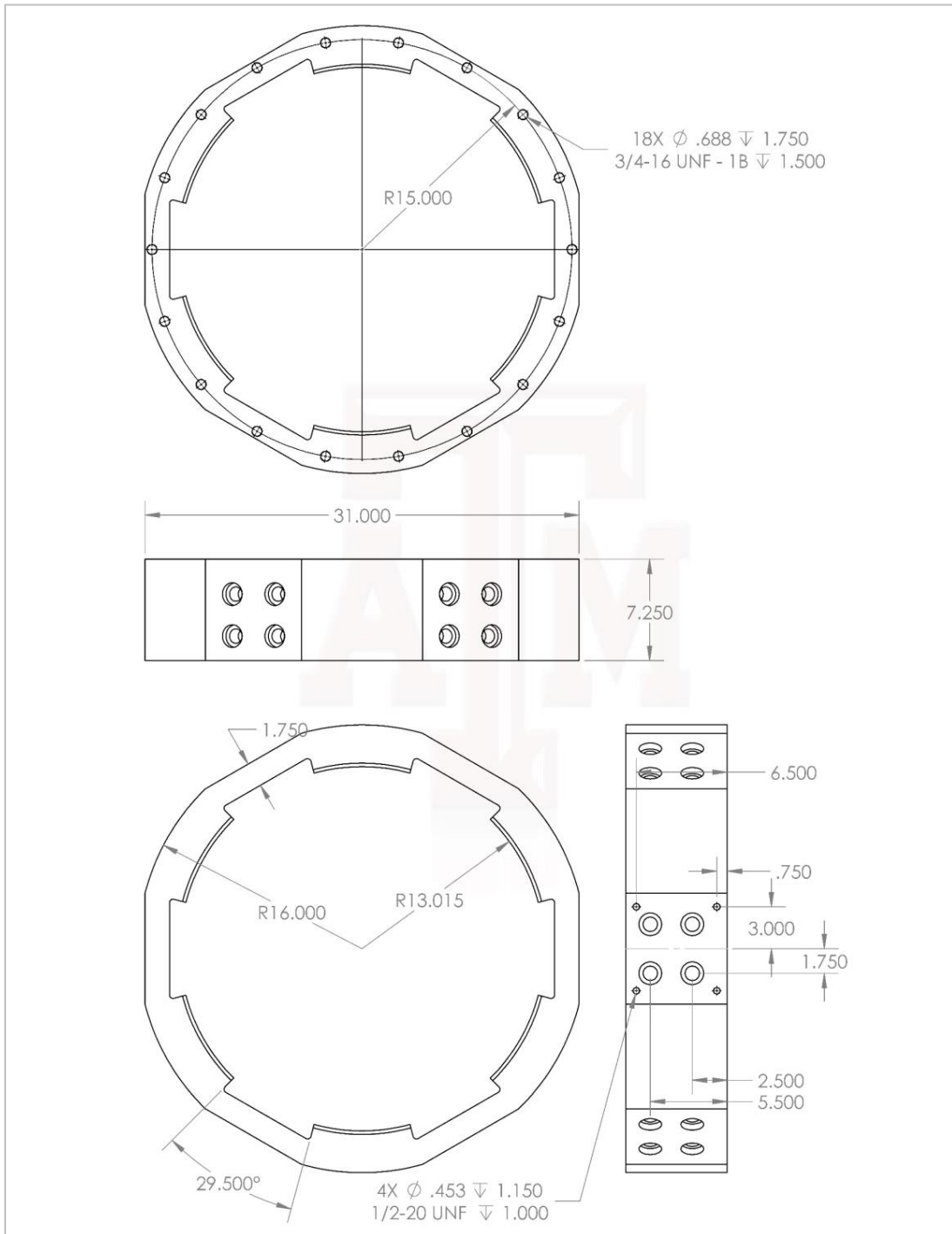


Figure B-26. Dimensional drawing for the breech locking nut made out of a slab of steel cut from an 8" thick A36 plate..

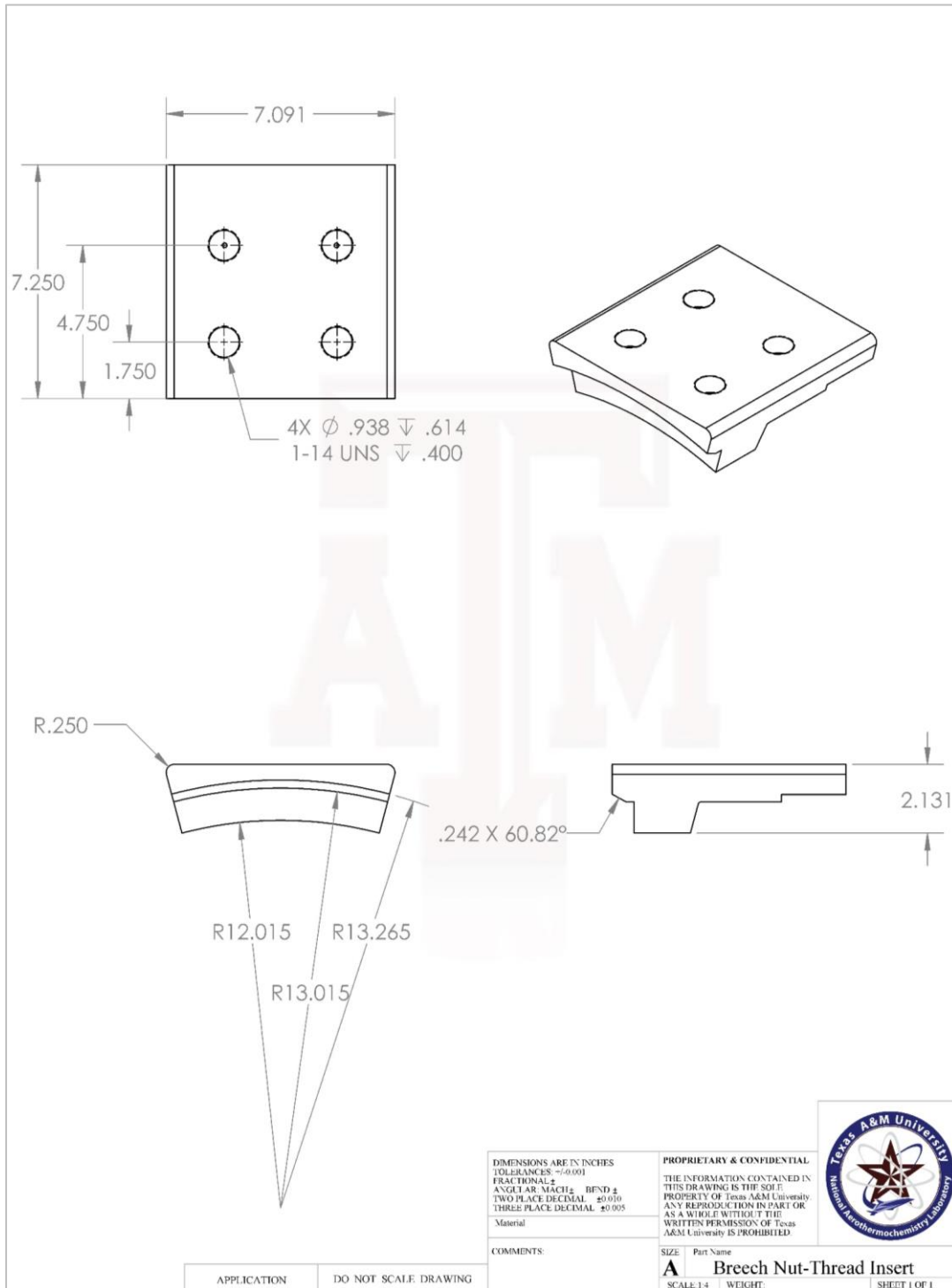


Figure B-27. Dimensional drawing for the insertable tooth for the locking nut.

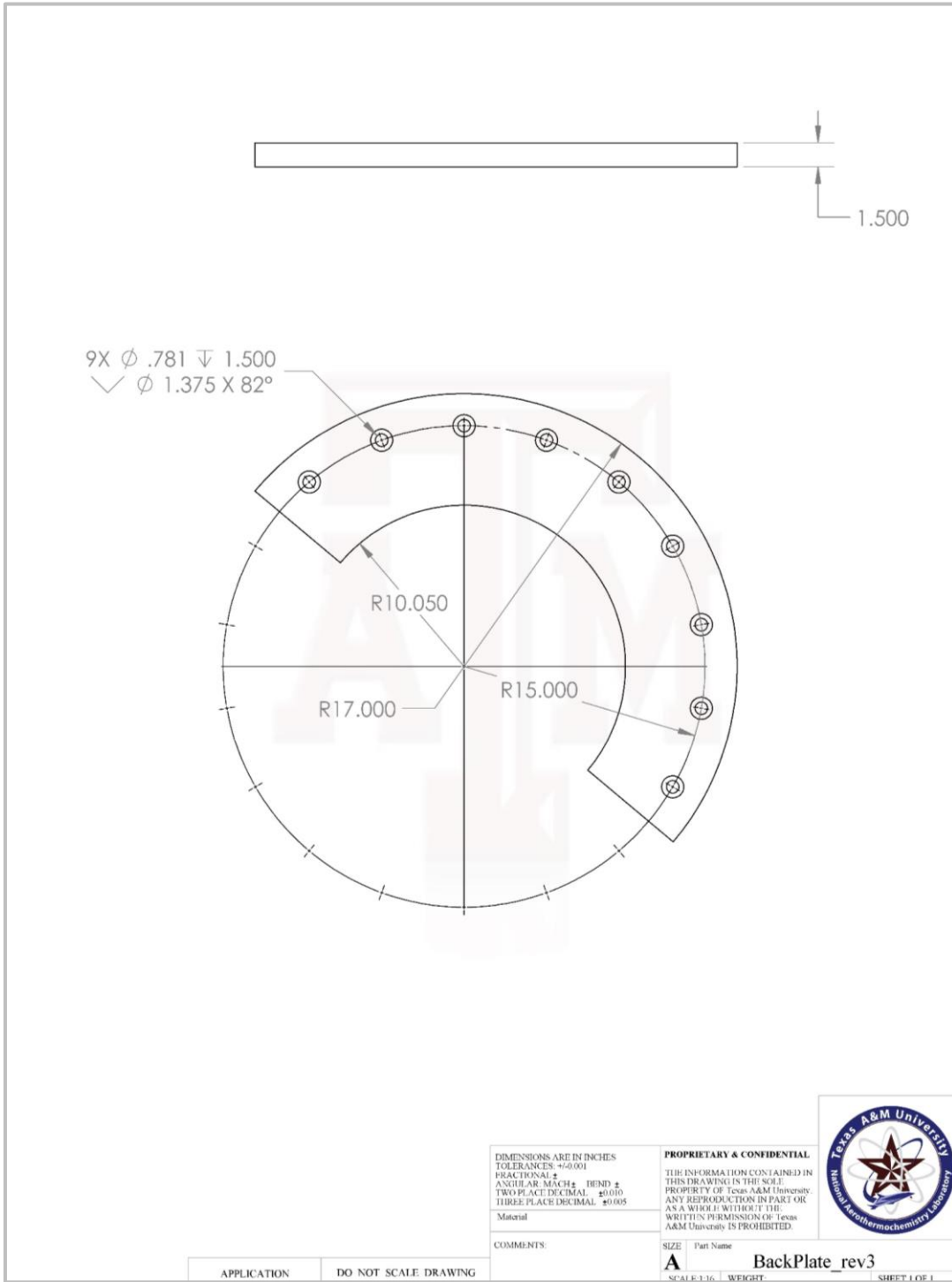


Figure B-28. Dimensional drawing of the semicircular plate that attaches to the back of the locking nut.

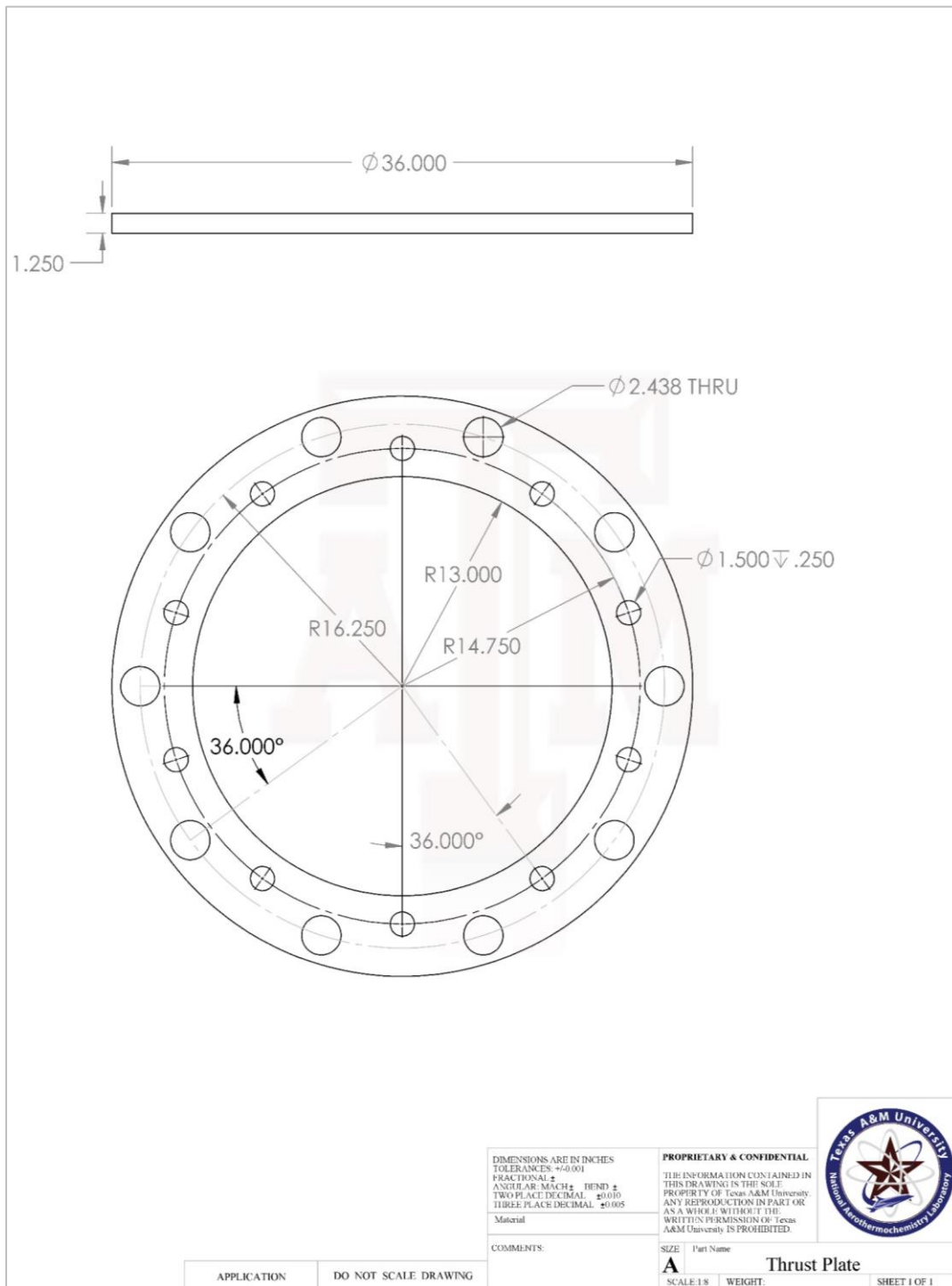


Figure B-29. Dimensional drawing for the breech locking nut made out of a slab of steel cut from an 8" thick A36 plate.

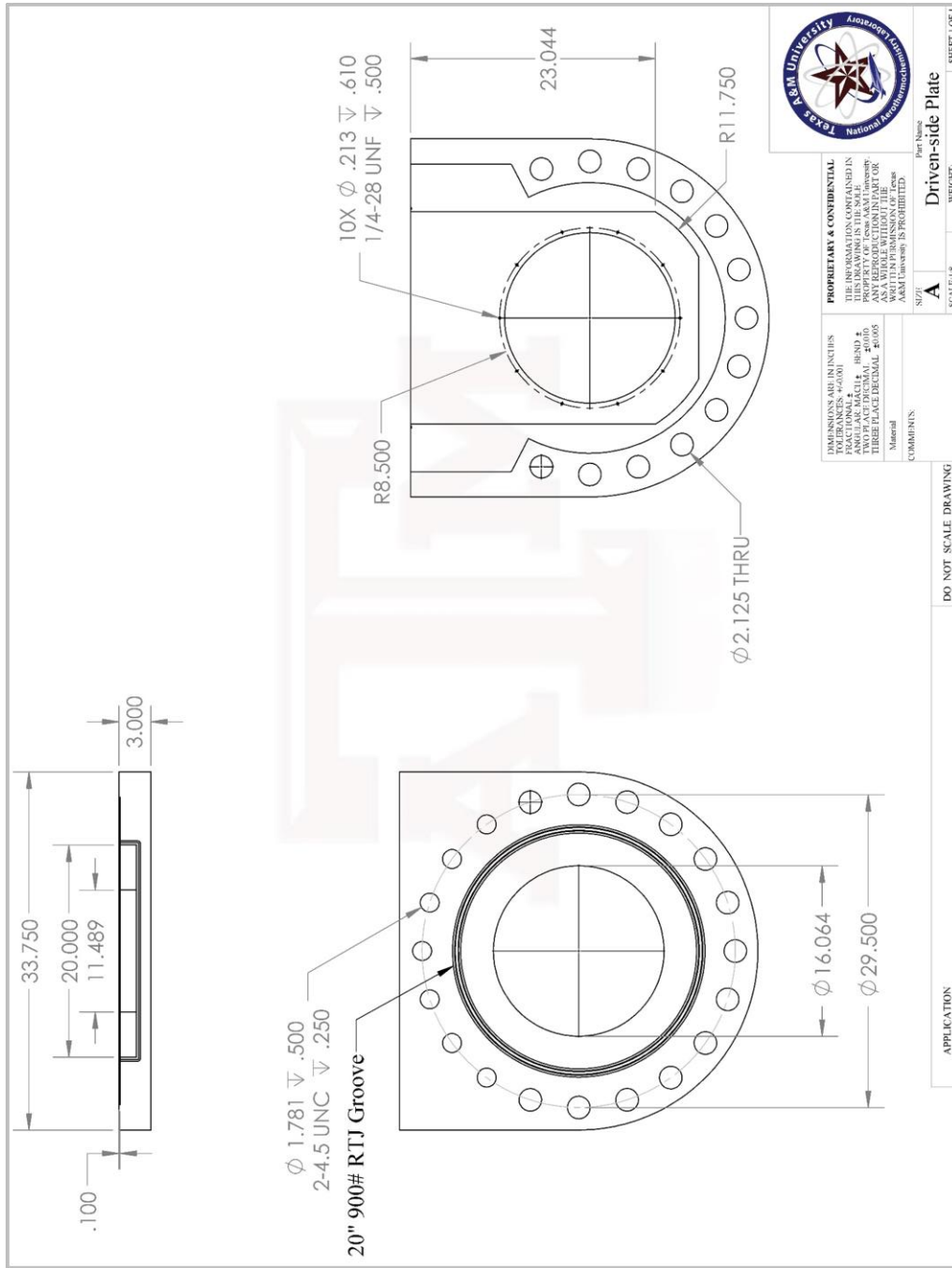


Figure B-30. Dimensional drawing for the larger component of the mylar diaphragm apparatus that attaches to the driven pipe.

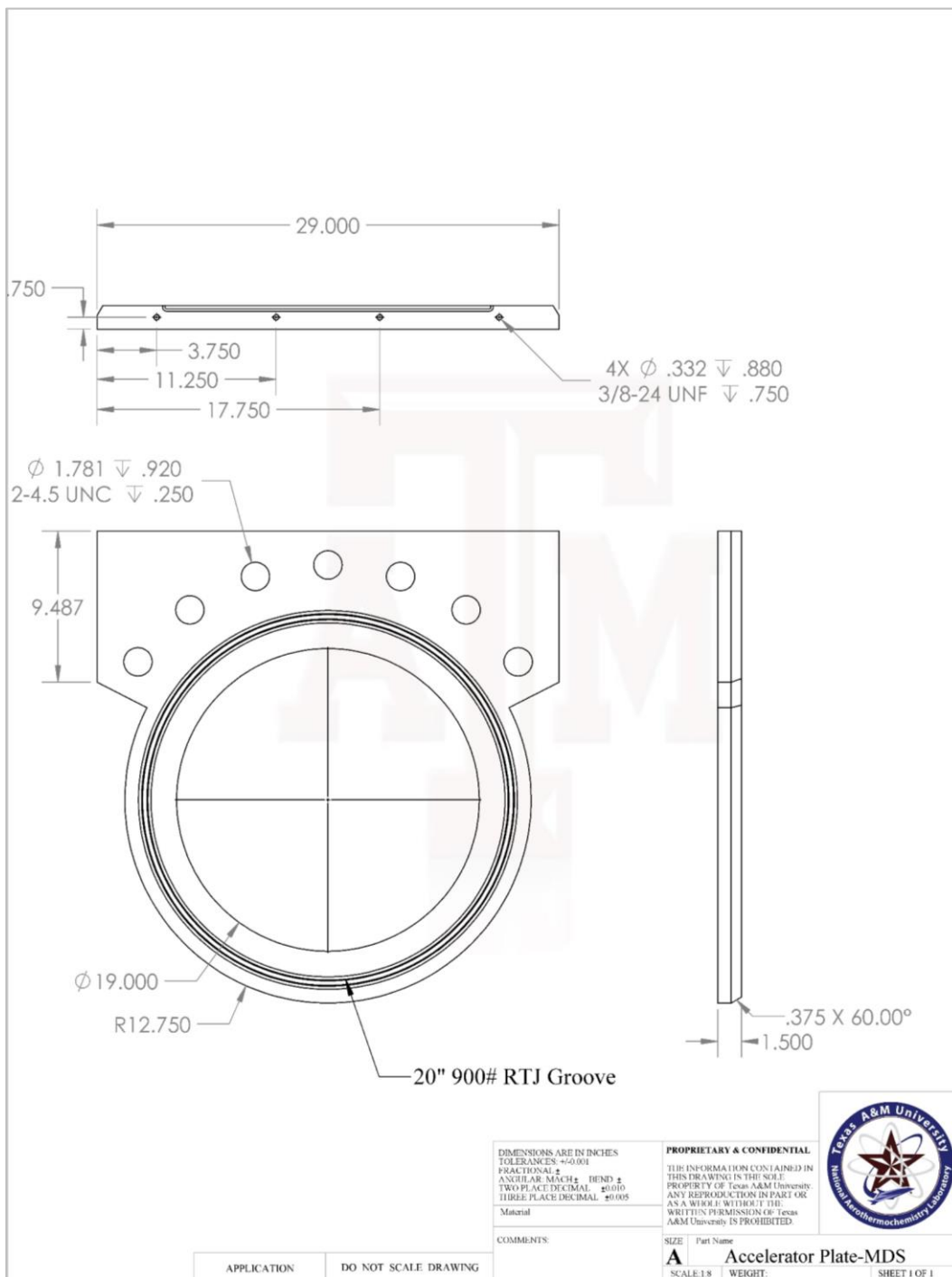


Figure B-31. Dimensional drawing for the smaller component of the mylar diaphragm apparatus that connects to the accelerator pipe.

Test Section

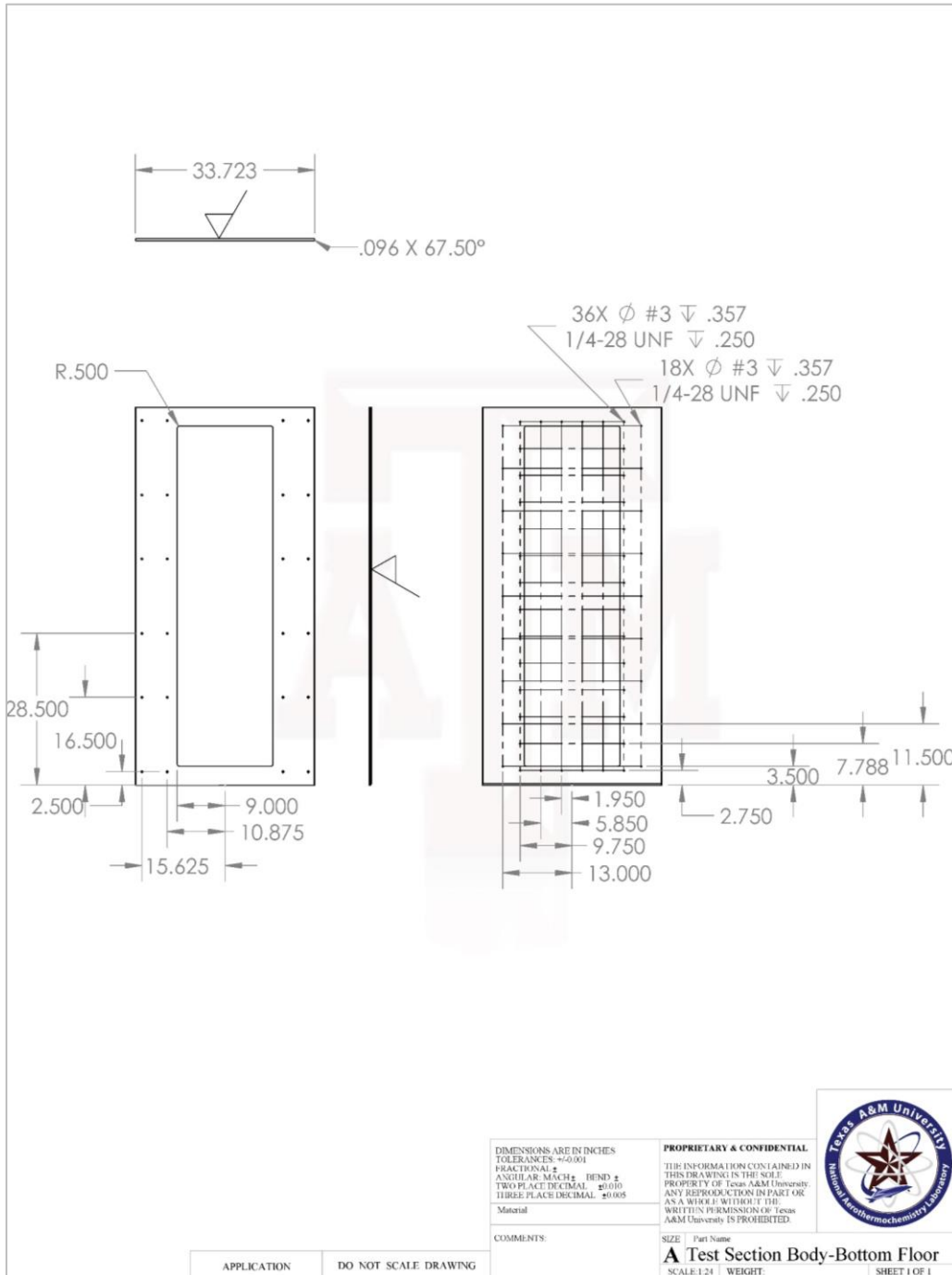


Figure B-32. Dimensional drawing for the floor access plate of the test section skeleton.

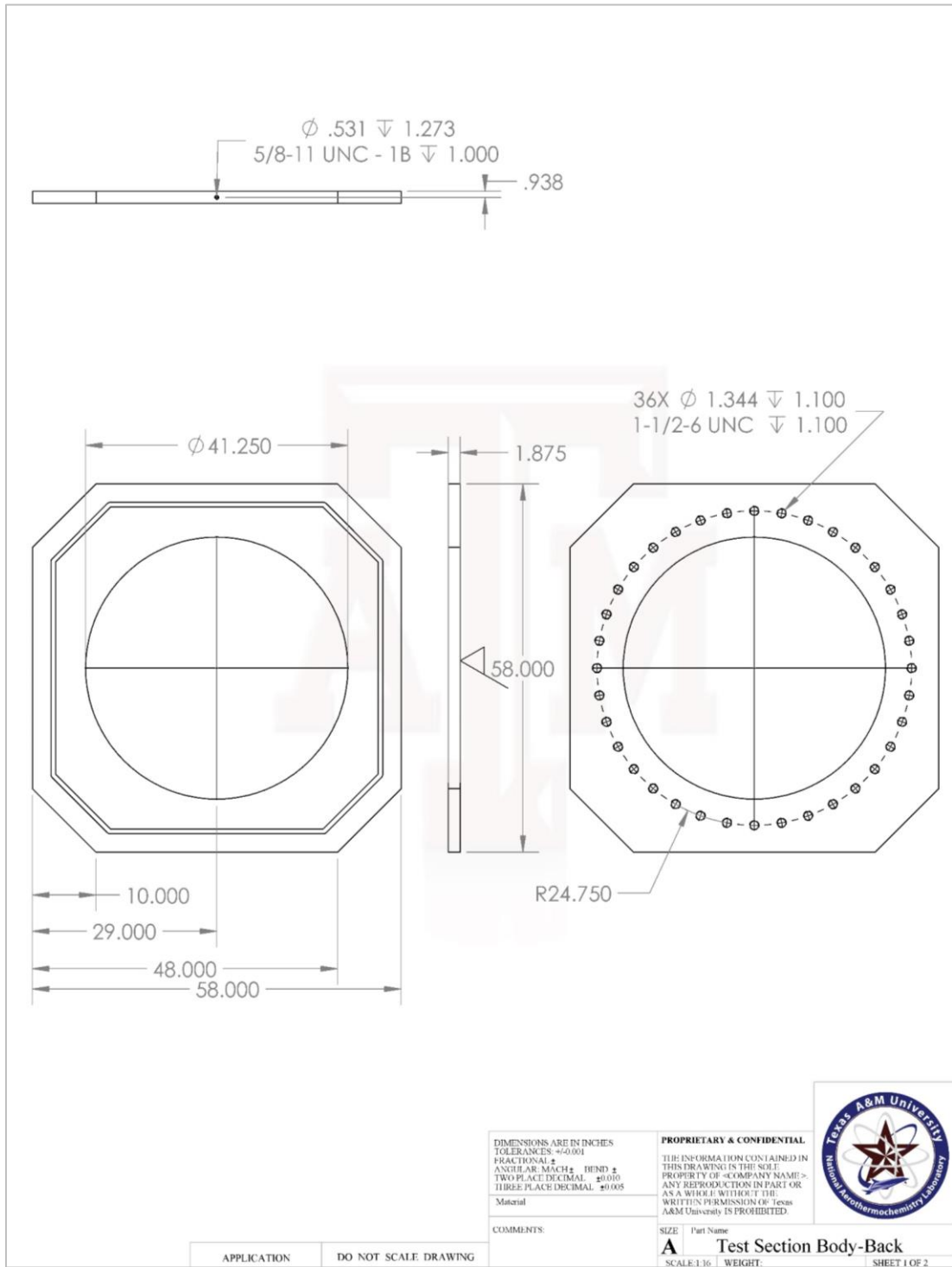


Figure B-33. Dimensional drawing for the back plate of the test section skeleton without dimensions of the alignment groove.

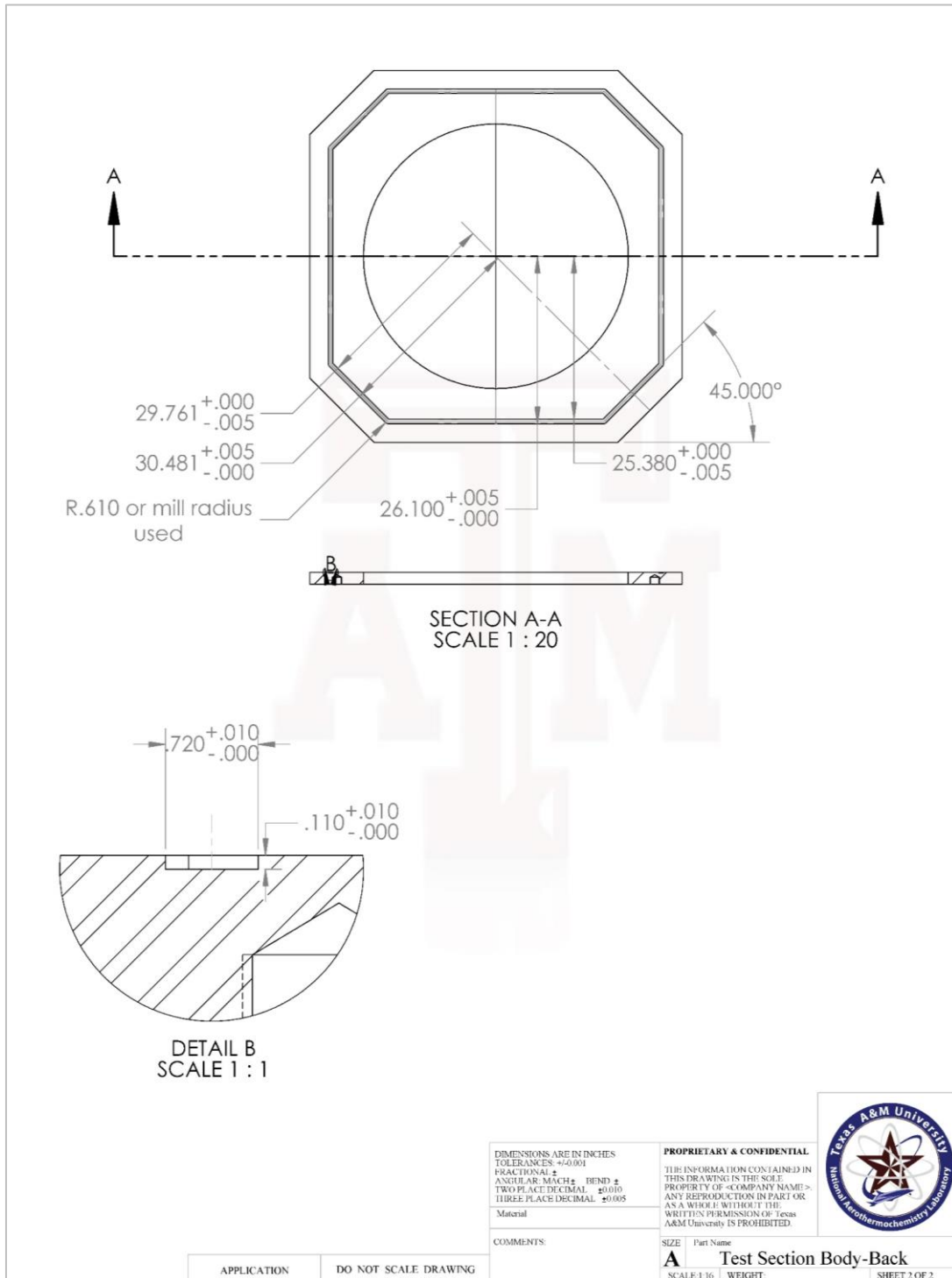


Figure B-34. Dimensional drawing for the back plate of the test section skeleton with dimensions for the alignment groove.

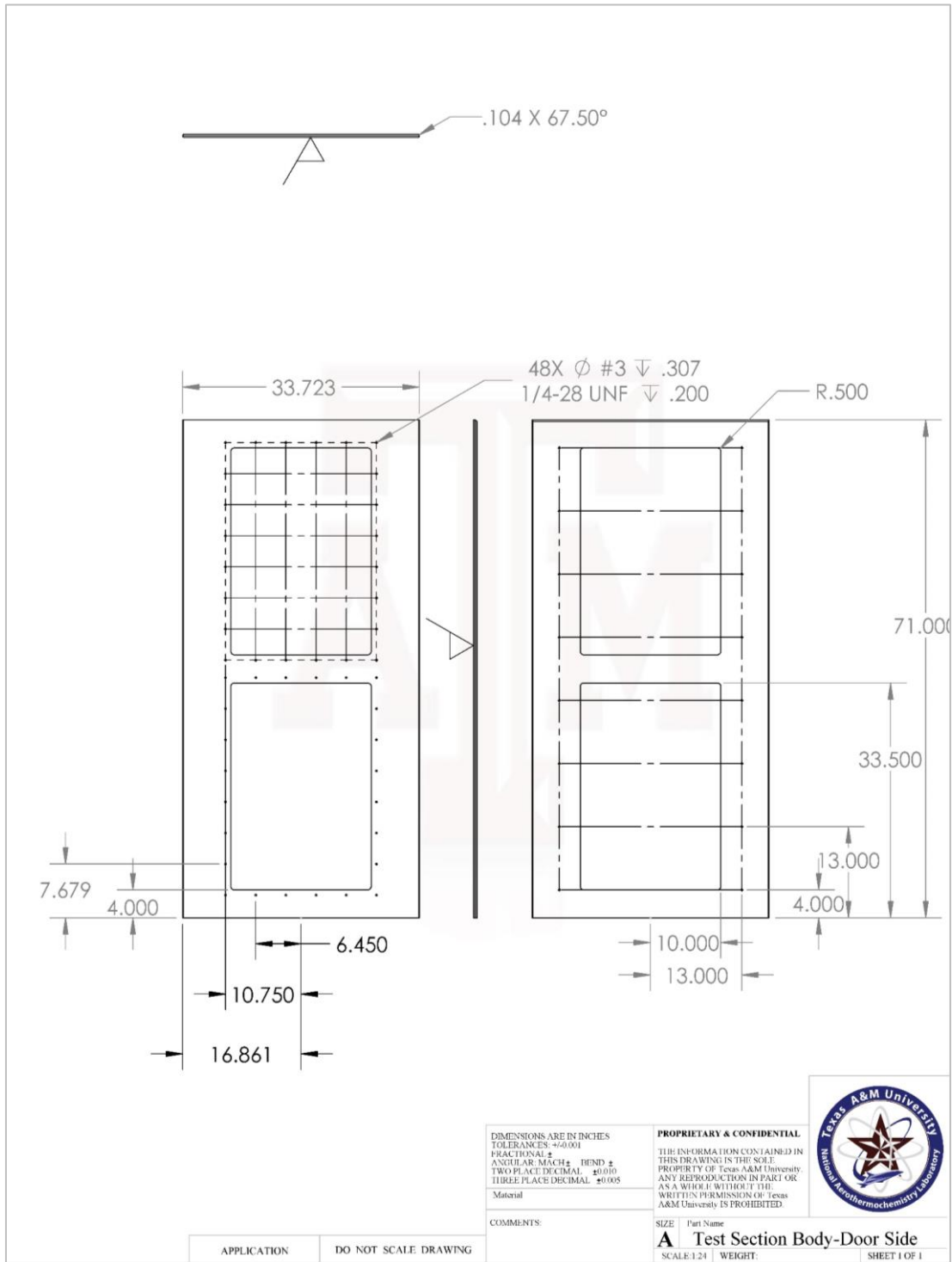


Figure B-35. Dimensional drawing for the door plates of the test section skeleton.

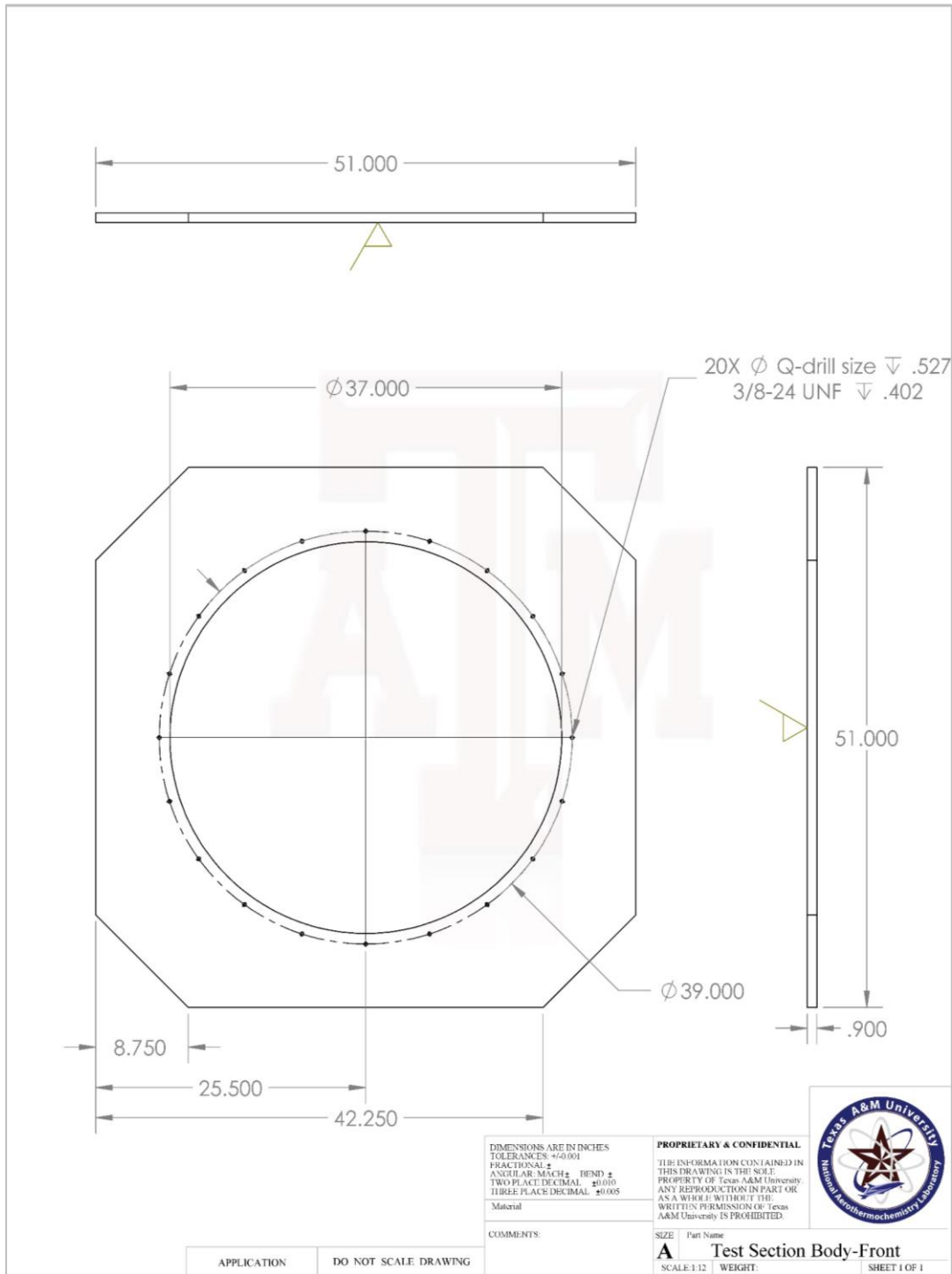


Figure B-36. Dimensional drawing for the front plate of the test section skeleton.

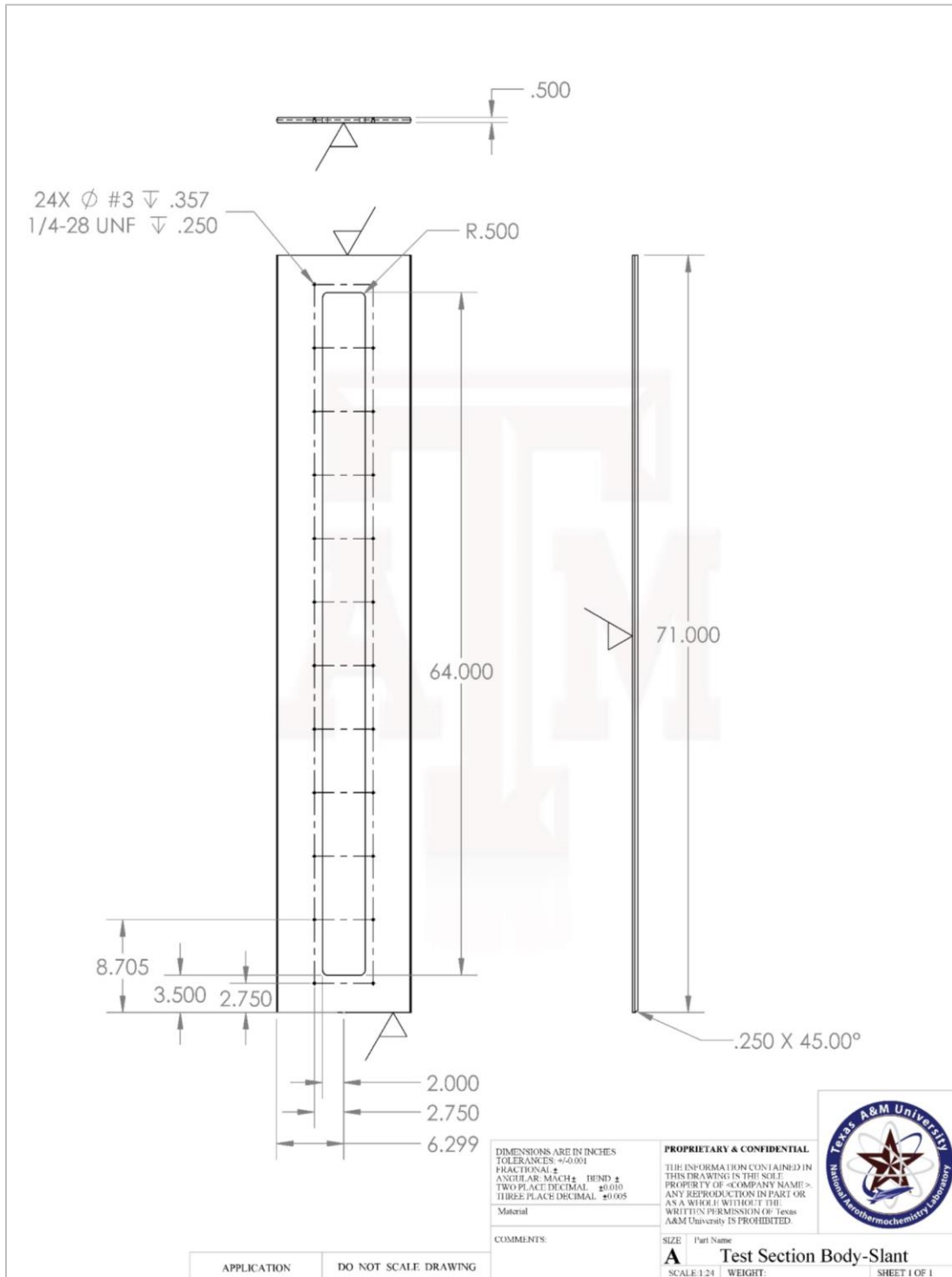


Figure B-37. Dimensional drawing for the diagonal plates of the test section skeleton.

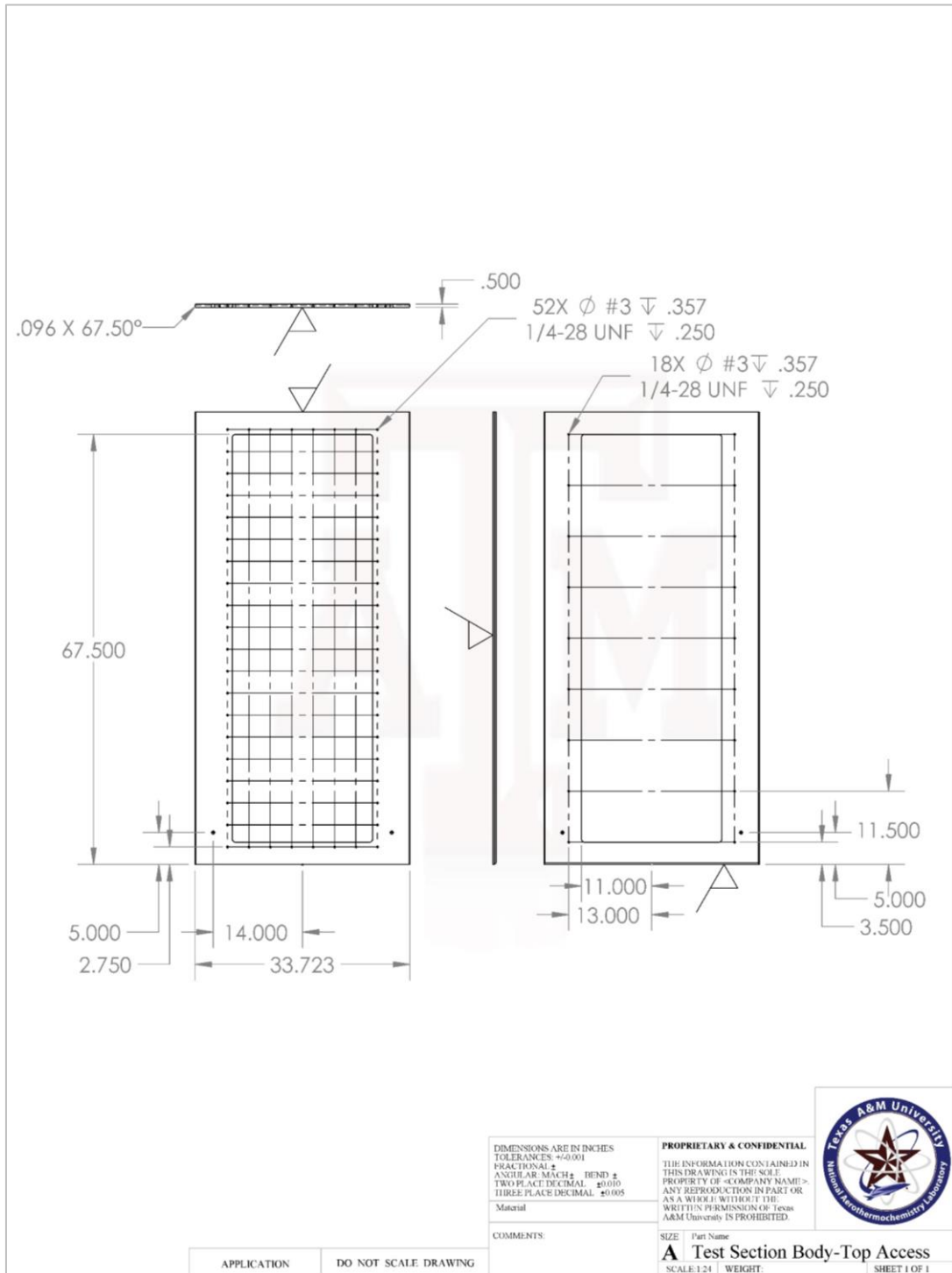


Figure B-38. Dimensional drawing for the roof plate of the test section skeleton.

Primary Support Stands

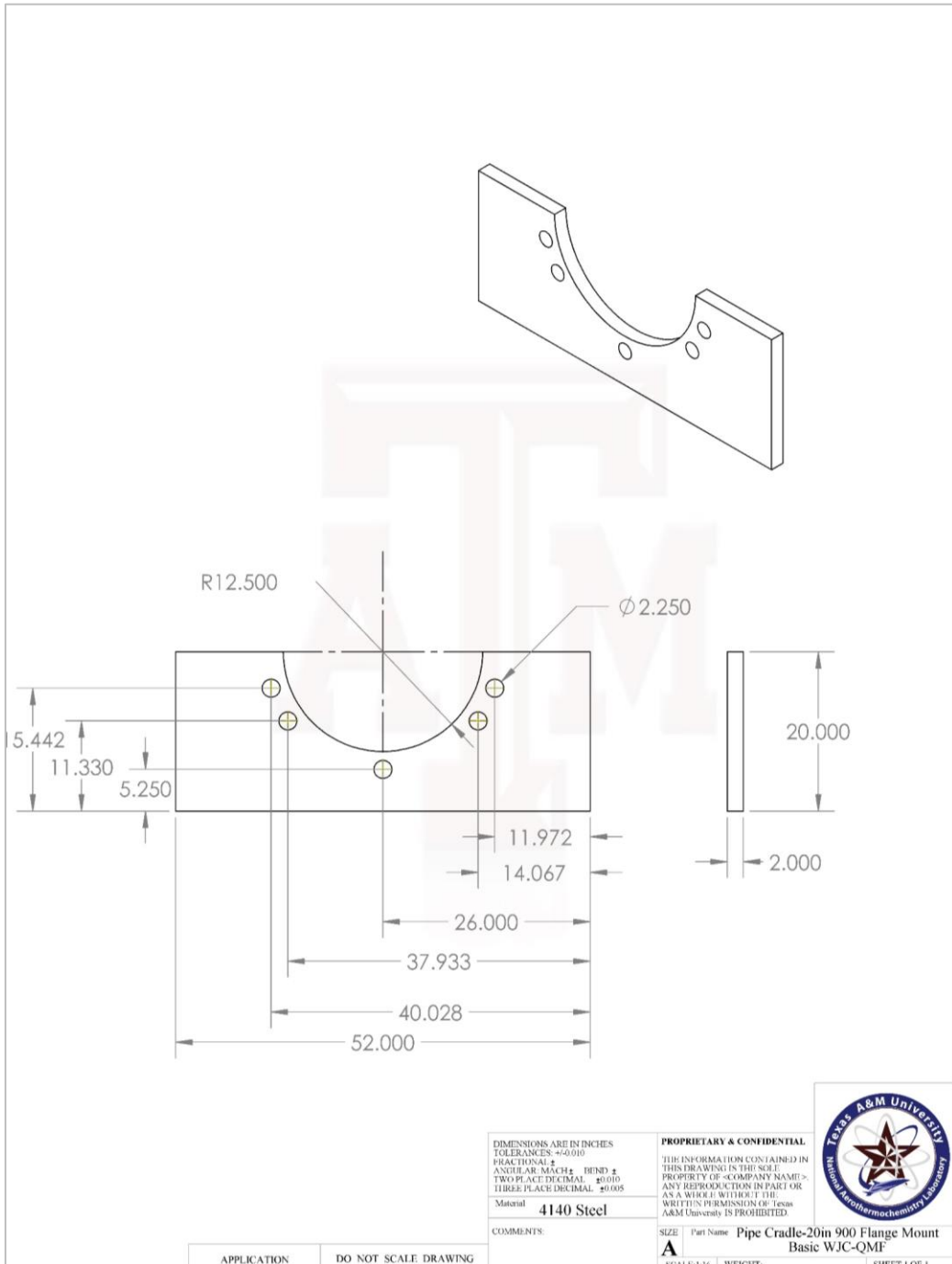


Figure B-39. Dimensional drawing for pipe cradle plate to hold the 20” 900# flanges and 20” schedule 160 pipe.

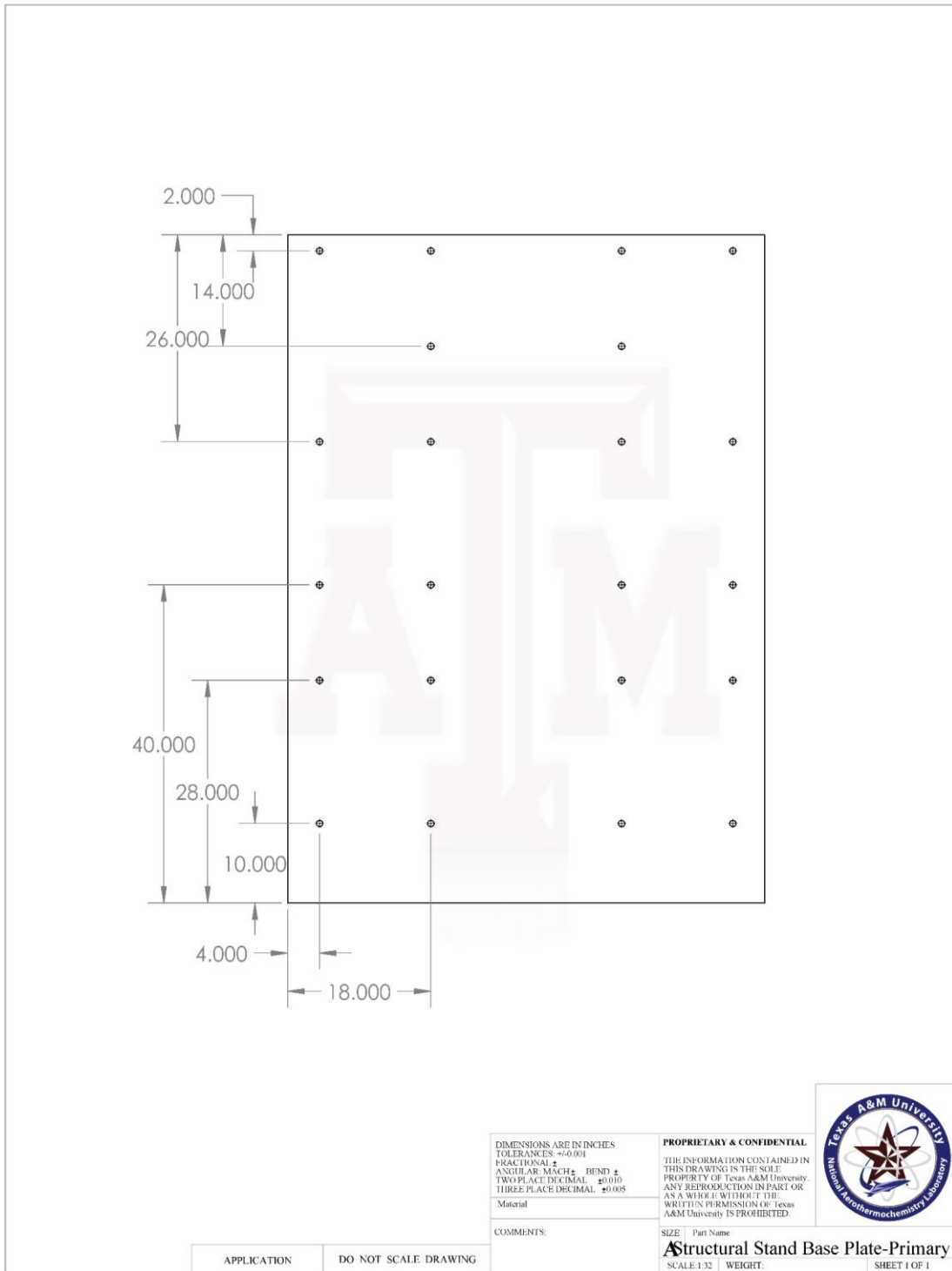


Figure B-40. Dimensional drawing for primary stand baseplate with $\frac{3}{4}$ " free clear holes that are torched into the plate.

Secondary Support Stands

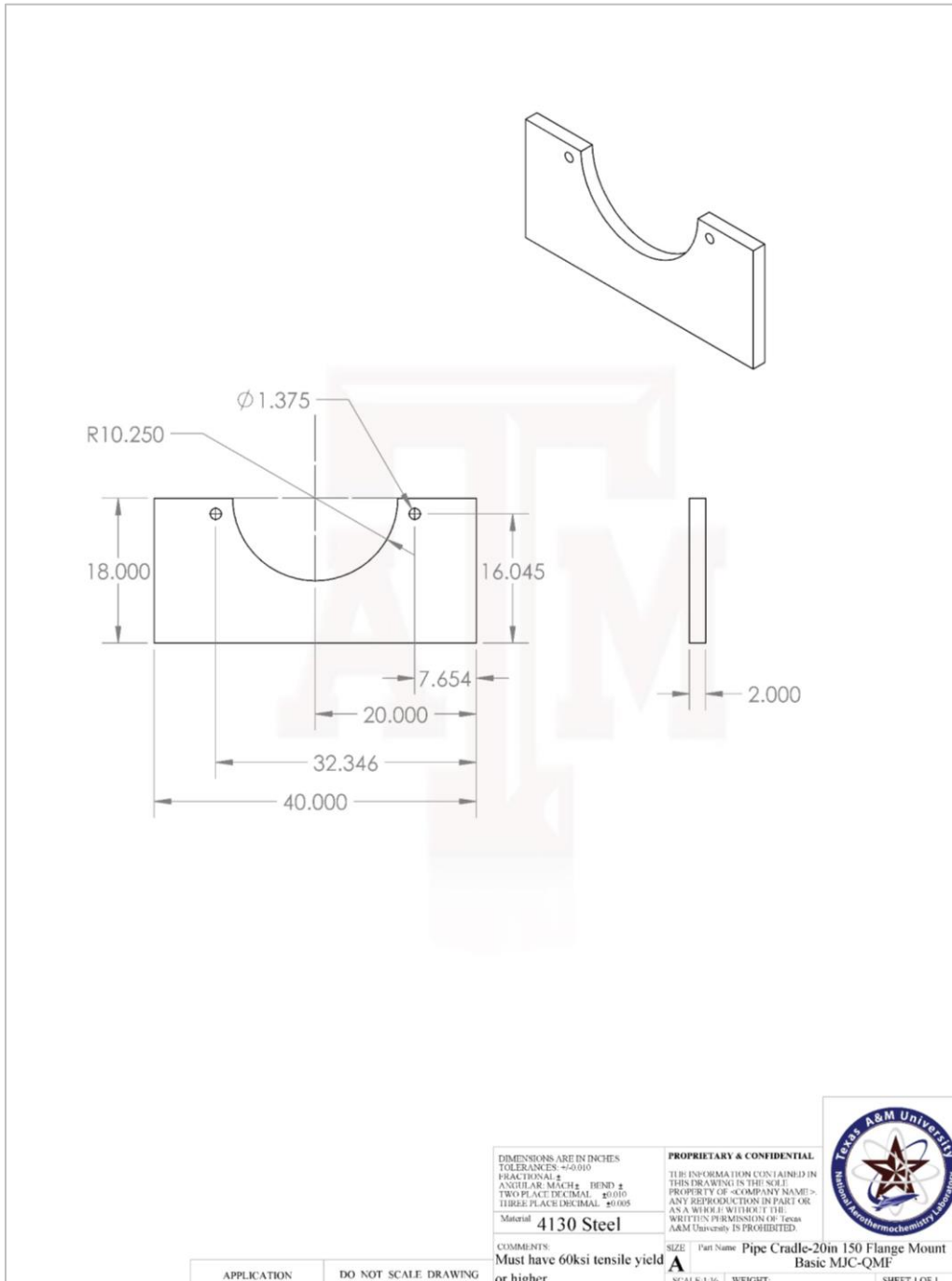


Figure B-41. Dimensional drawing for pipe cradle plate to hold the 20” 150# flanges and 20” schedule 80 pipe.

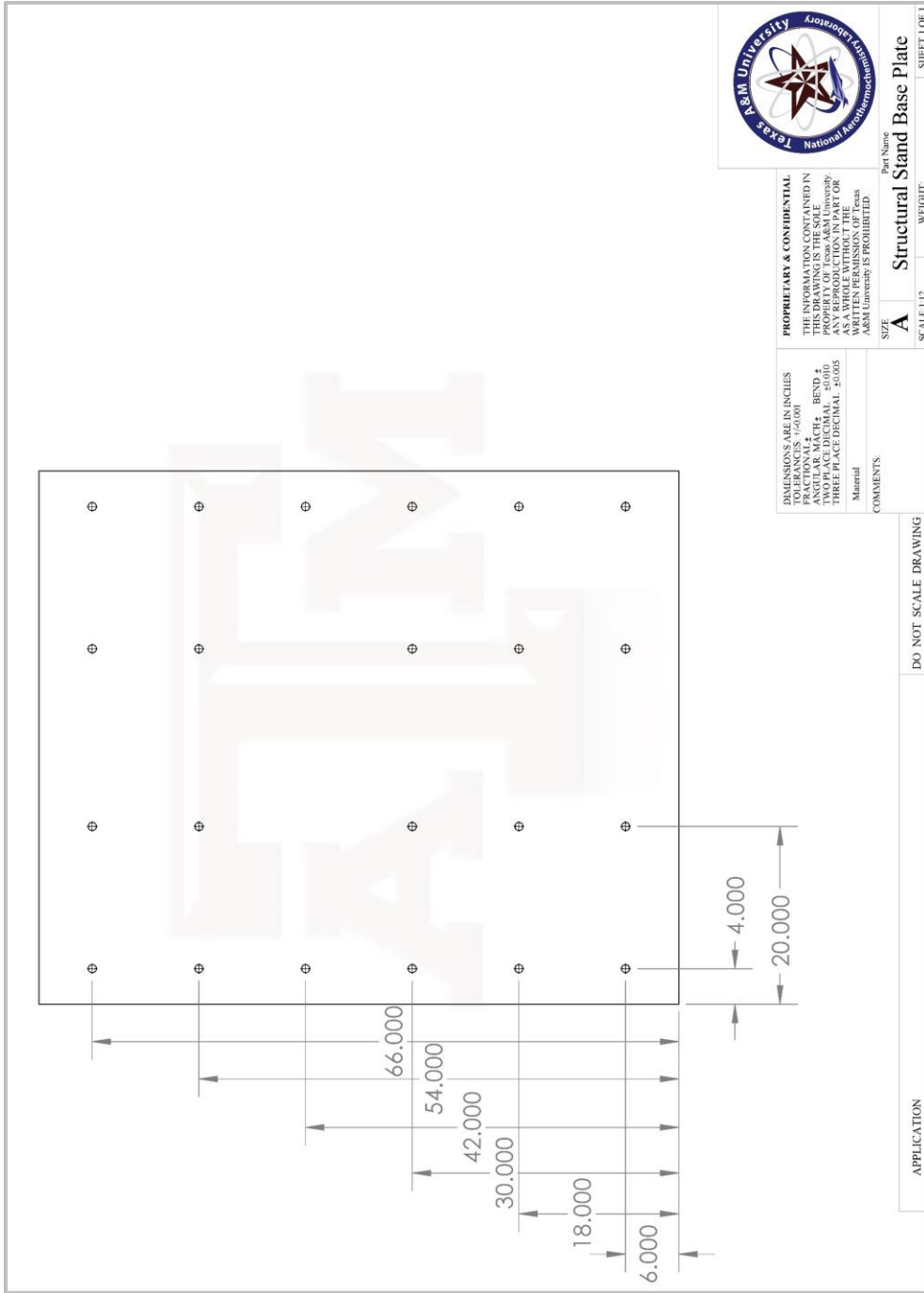


Figure B-42. Dimensional drawing for secondary stand baseplate with 3/4" free clear holes that are torched into the plate.

APPENDIX C

CONTROL DIAGRAMS

This section contains flow schematics for the control of the facility, including ball valves and digital regulators, the electrical diagram for the control box, and the hydraulic diagram to move and lock the beech.

- Hydraulics Flow Diagram
 - Figure C-1: Hydraulic Flow Diagram
- Facility Operation Flow Diagram
 - Figure C-2: Facility Operations Flow Diagram
- Electronics Wiring Diagrams
 - Figure C-3: Current Amplification/Ball Valve Control
 - Figure C-4: Warning Light Circuit Board Layout
 - Figure C-5: Safety Contact Switch Diagram
- Computer Communications Protocol
 - Figure C-6: Computer Operations Protocol

Hydraulics Flow Diagram

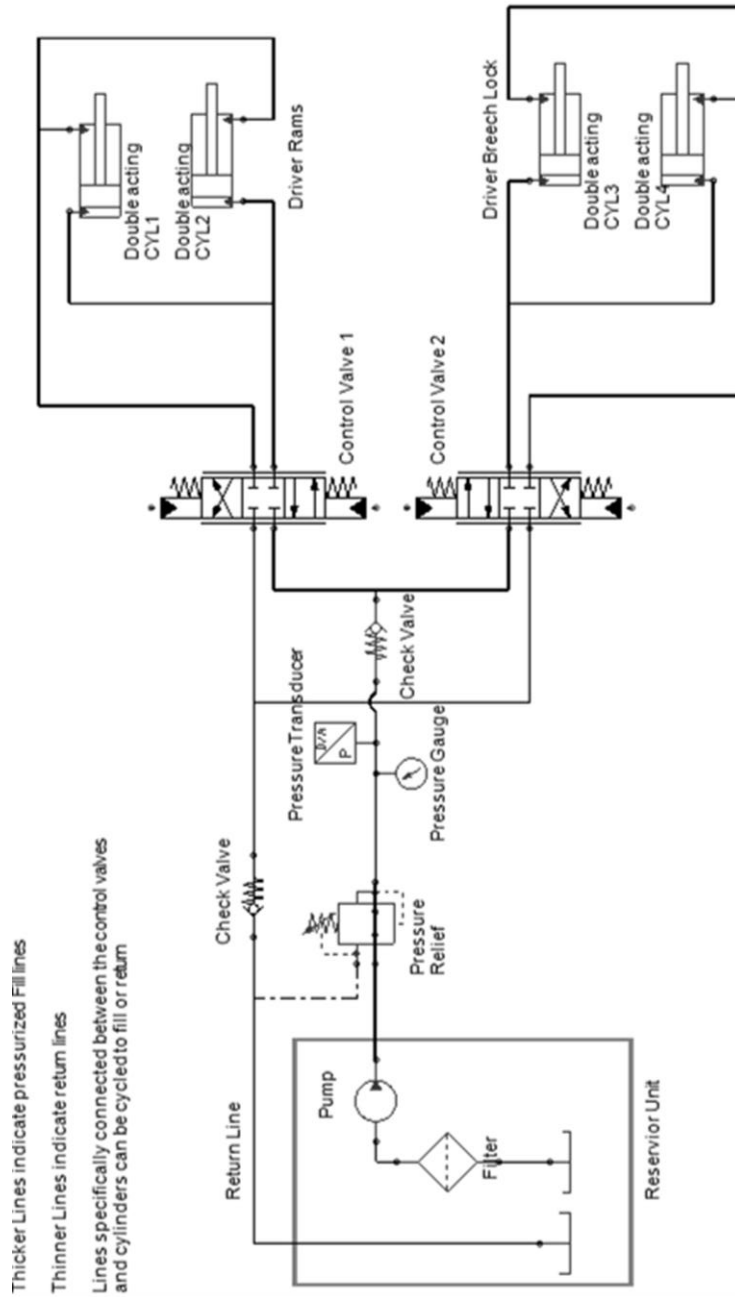


Figure C-1. Hydraulics flow diagram with double-acting cylinders, directional control valves, pressure transducer, check valves, and power unit.

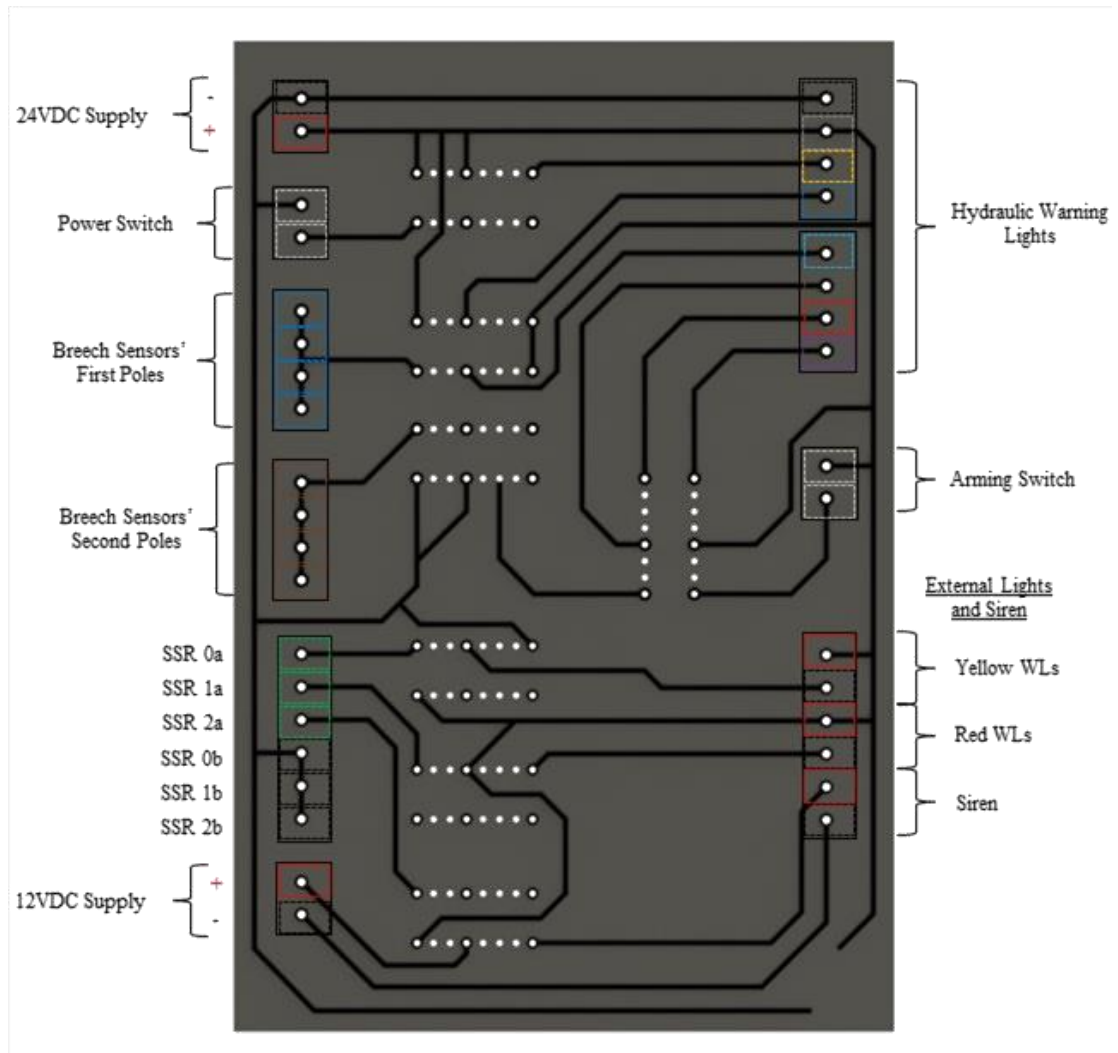


Figure C-4: Circuit layout for the warning system lights and logic switches required to activate at correct time interval.

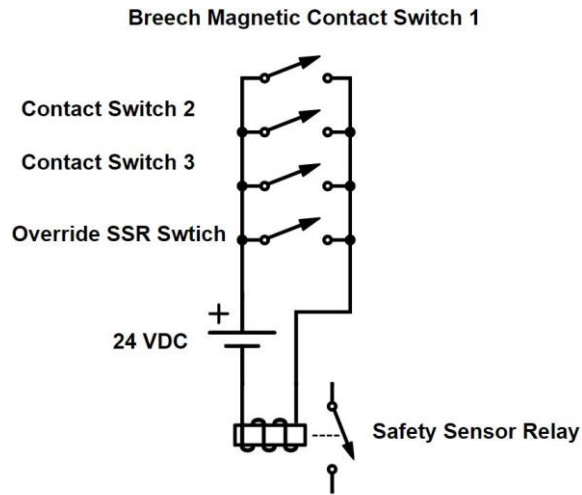


Figure C-5: Circuit diagram for safety contact switches.

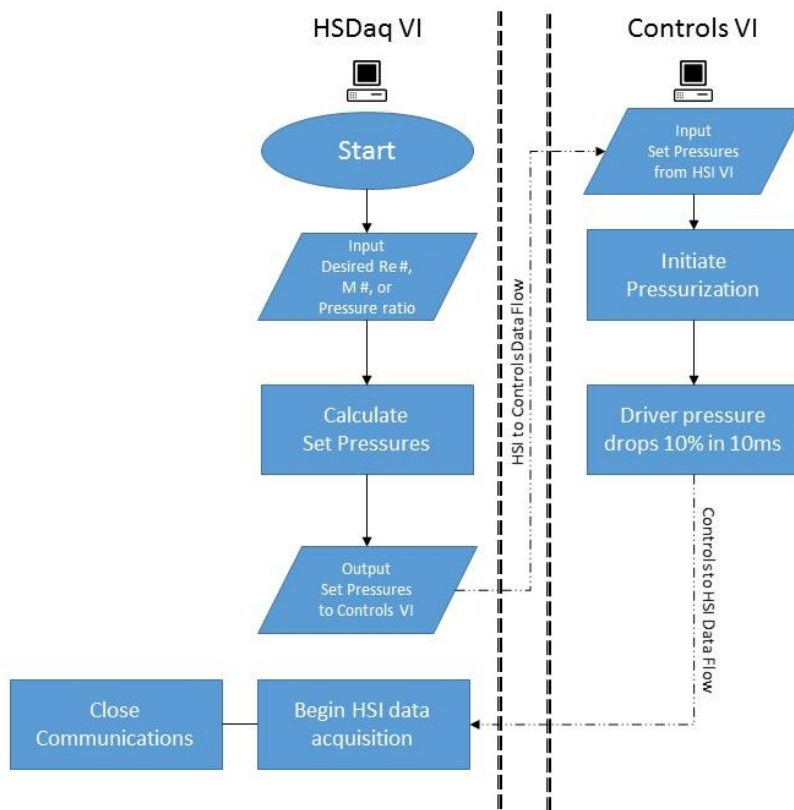


Figure C-6: Data flow diagram of information passed between the controls and HSDaq VI programs.